DEVELOPMENT AND APPLICATION OF MOLECULARLY IMPRINTED POLYMERS FOR SELECTED ANTIDEPRESSANTS AND STUDIES OF THEIR ENVIRONMENTAL FATE

Tjaša Gornik

Doctoral Dissertation
Jožef Stefan International Postgraduate School
Ljubljana, Slovenia

Supervisor: Assoc Prof Dr Tina Kosjek, Department of Environmental Sciences, Jožef Stefan Institute, Ljubljana, Slovenia
Co-Supervisor: Prof Dr Ester Heath, Department of Environmental Sciences, Jožef Stefan Institute, Ljubljana, Slovenia

Evaluation Board:
Prof Dr Milena Horvat, Chair, Department of Environmental Sciences, Jožef Stefan Institute, Ljubljana, Slovenia
Prof Dr Davide Vione, Member, Dipartimento di Chimica, Universitá di Torino, Torino, Italy
Prof Dr Peter Krajnc, Member, Faculty of Chemistry and Chemical Engineering, Maribor, Slovenia

MEDNARODNA PODIPLOMSKA ŠOLA JOŽEFA STEFANA
JOŽEF STEFAN INTERNATIONAL POSTGRADUATE SCHOOL

Tjaša Gornik

DEVELOPMENT AND APPLICATION OF MOLECULARLY IMPRINTED POLYMERS FOR SELECTED ANTIDEPRESSANTS AND STUDIES OF THEIR ENVIRONMENTAL FATE

Doctoral Dissertation

RAZVOJ IN UPORABA MOLEKULARNO VTISNJENIH POLIMEROV ZA IZBRANE ANTIDEPRESIVE TER RAZISKAVE NJIHOVE PRISOTNOSTI IN RAZGRADNJE V OKOLJU

Doktorska disertacija

Supervisor: Assoc Prof Dr Tina Kosjek

Co-Supervisor: Prof Dr Ester Heath

Ljubljana, Slovenia, November 2022

Acknowledgments

First, I would like to thank my supervisor Assoc Prof Dr Tina Kosjek for her guidance, help and support during my PhD at the Department of Environmental Sciences at the Jožef Stefan Institute and Jožef Stefan International Postgraduate School in Ljubljana. I would also like to thank my co-supervisor Prof Dr Ester Heath for her assistance, shared knowledge and time.

Dr Marjeta Česen, Anja Vožič, Taja Verovšek, Dr Ana Kovačič, Dr Žiga Tkalec, Dr Milka Ljoncheva, Dr David Škufca, Tamara Gajšt, Dr Ivona Križman Matasić and Maria Laimou-Geraniou, thank you for sharing ideas, discussions, experiences and especially lunch breaks. Thank you also, Dr Jelena Golubović, for your steadfast encouragement and friendship, even from another country.

I want to thank Dr Dušan Žigon, for the help and great company when sampling and for the lessons in liquid chromatography coupled with mass spectrometry. Dr David Heath, thank you for all the thoughtful writing recommendations and interesting debates. Thank you, Silva Perko, for every additional minute of your time. Your every visit meant a problem got solved.

A part of this work was only realized because of the important contributions of Dr Prof Davide Vione and Dr Luca Carena. Thank you for welcoming me to the University of Torino in Italy and sharing your knowledge on photodegradation. I am grateful to Dr Prof Peter Kranjc and Dr Amadeja Koler for sharing their know-how and the synthesized molecularly imprinted materials. I would like to express my gratitude to Dr Prof Börje Sellergren and Dr Sudhirkumar Shinde from Malmö University for the opportunity to further expand my knowledge on molecularly imprinted polymers in Sweden. Thank you as well to Assist Prof Jurij Trontelj and Prof Robert Roškar form the Faculty of Pharmacy in Slovenia, Prof Dr Karel Jeřabek from the Institute of Chemical Process Fundamentals of the Czech Academy of Sciences, and Prof Dr Juliane Hollender from Eawag, The Swiss Federal Institute of Aquatic Science and Technology in Switzerland for their contributions.

I also want to offer my gratitude to the Slovenian Research Agency (P1-0143, J1-6744, BI-IT-18-20-005), the COST research network (COST NEREUS ES1403) and the Erasmus Plus program for financial support.

I am also grateful to the evaluation board members: Prof Dr Milena Horvat, Prof Dr Davide Vione and Prof Dr Peter Krajnc, for reviewing and evaluating this thesis.

A big thank you goes to my friends Nika, Tina, Aleksandra, Vesna, Jasna, Keli, Erika, Nataša and Sandi for encouraging me, believing in me and keeping my spirits high. Last but not least, a very special thank you goes out to my family for their love and endless support.

Abstract

This thesis focuses on the fate of chosen antidepressants in the environment. Studied compounds belong to the class of selective serotonin reuptake inhibitors. Reportedly they do not completely mineralize by existing water treatment processes and their residues cause unwanted toxic effects in aquatic organisms. However, to date, insufficient information has been gathered to form an action plan for managing their presence in the environment, and especially detailed information on processes they undergo during wastewater treatment and after they enter the environment is missing.

A literature overview revealed that among the commonly used treatment techniques, secondary biological treatment with activated sludge is the most efficient in removing selective serotonin reuptake inhibitors, with some compounds, like sertraline being rarely addressed. Accordingly, the processes involved in its removal and the efficiency of the sludge-based treatment were studied. The results revealed adsorption to sludge as the primary removal process, followed by biodegradation. Removal efficiencies fluctuated between 77% and 81% in conventional wastewater treatment plants with activated sludge and exceeded 90% in laboratory-scale simulations. Structures of ten transformation products were identified and their presence was detected in actual wastewater samples.

Sertraline and paroxetine were chosen for the degradation study during exposure to sunlight in surface waters. Their photochemistry was researched, and the data was modelled to obtain information on their degradation kinetics. Altogether fourteen transformation products were identified, and degradation pathways were proposed. Both compounds were readily photodegradable with half-lives of only a few days in shallower water. In both cases, direct photolysis and reactions with photochemically produced reactive intermediates, more specifically hydroxyl and carbonate radicals, were the main degradation pathways. The presence of three sertraline transformation products was confirmed in surface waters for the first time.

For all the studies mentioned above to be successful, sensitive, robust, and precise analytical methods were developed. Also, specialized materials, *i.e.*, imprinted polymers with sertraline as the template, were developed to improve the sample preparation step by increasing recovery and minimizing matrix effects. Some difficulties were, however, encountered when using them for trace-level analysis. Then again, they were well suited as alternative wastewater treatment sorbents for removing selective serotonin reuptake inhibitors. The materials were also cross-reactive for metabolites and transformation products of selective serotonin reuptake inhibitors.

Altogether, this thesis fills the knowledge gap regarding the behavior of selective serotonin reuptake inhibitors after they leave the human body and is a sound basis for further research. For example, the newly identified transformation products should lead to a more thorough study of the environmental impact of the studied antidepressants. Further, insight is provided into an alternative water purification technique applying molecularly imprinted polymers. Lastly, the experimental designs used in our studies can be applied to other environmental contaminants.

Povzetek

Osrednja tema doktorskega dela je usoda izbranih antidepresivov v okolju. Preučevane spojine spadajo v razred selektivnih zaviralcev ponovnega privzema serotonina. Že obstoječi postopki čiščenja vode niso uspešni pri njihovem odstranjevanju, hkrati pa njihovi ostanki povzročajo neželene toksične učinke pri vodnih organizmih. Na tej točki še vedno nimamo dovolj informacij za oblikovanje akcijskega načrta za obvladovanje njihove prisotnosti v okolju, manjkajo nam predvsem podrobne informacije o procesih, ki so jim podvrženi med čiščenjem odpadne vode in po vstopu v okolje.

Pri pregledu literature smo odkrili, da je bilo od pogosto uporabljenih načinov čiščenja odpadne vode sekundarno biološko čiščenje z aktivnim blatom najučinkovitejše pri odstranjevanju omenjenih antidepresivov, pri čemer so nekatere spojine, kot je sertralin, zelo slabo raziskane. V skladu s temi ugotovitvami smo preučevali postopke njegovega odstranjevanja in učinkovitost čiščenja z uporabo aktivnega blata. Rezultati so pokazali, da je adsorpcija na aktivno blato primarni proces odstranjevanja, ki mu sledi biorazgradnja. Učinkovitost čiščenja je v dejanskih čistilnih napravah nihala med 77 % in 81 %, v laboratorijskih simulacijah pa je presegla 90 %. Identificirali smo strukture desetih produktov transformacije in zaznali njihovo prisotnost v vzorčenih odpadnih vodah.

Sertralin in paroksetin sta bila izbrana za študijo razgradnje med izpostavljenostjo sončni svetlobi v površinskih vodah. Raziskali smo njuno fotokemijo, pridobljene podatke pa modelirali, da smo pridobili informacije o kinetiki njihove razgradnje. Skupaj je bilo identificiranih štirinajst produktov transformacije in predlagali smo tudi dva mehanizma razgradnje. Obe spojini sta lahko fotorazgradljivi z razpolovnima dobama le nekaj dni v plitvejši vodi. V obeh primerih sta bili glavni poti razgradnje direktna fotoliza ter reakcije s fotokemično proizvedenimi reaktivnimi intermediati, natančneje hidroksilnimi in karbonatnimi radikali. Prisotnost treh produktov transformacije sertralina smo tudi prvič potrdili v površinskih vodah.

Da bi bile vse zgoraj omenjene študije uspešne, je bilo potrebno razviti občutljive, robustne in natančne analitske metode. Razviti so bili tudi specializirani materiali, tako imenovani vtisnjeni polimeri s sertralinom kot šablono, z namenom da bi izboljšali korak priprave vzorca s povečanjem izkoristka in zmanjšanjem učinkov matriksa. Vendar smo pri njihovi uporabi za analizo sertralina v sledovih naleteli na določene težave. Po drugi strani pa so bili materiali uporabni kot alternativni sorbenti za odstranjevanje selektivnih zaviralcev ponovnega privzema serotonina iz odpadne vode. Prav tako so navzkrižno vezali metabolite ter produkte transformacije selektivnih zaviralcev ponovnega privzema serotonina.

To doktorsko delo je zapolnilo znanstvene vrzeli, ki se navezujejo na vedenje selektivnih zaviralcev privzema serotonina, potem ko zapustijo človeško telo, ter so dobra osnova za nadaljnje raziskave na tem področju. Na primer, novo identificirani transformacijski produkti bi morali voditi v temeljitejše raziskave vpliva proučevanih antidepresivov na okolje. Poleg tega smo predstavili vpogled v alternativno tehniko čiščenja vode z uporabo molekularno vtisnjenih polimerov. Nazadnje, eksperimentalne načrte, uporabljene v naših študijah, je mogoče uporabiti tudi za druge okoljske onesnaževalce.

Contents

List of Figures

List of Tables

Abbreviations

WW	... Wastewater
SSRI	... Selective serotonin reuptake inhibitor
MIP	... Molecularly imprinted polymer
OECD	... Organization for economic cooperation and development
FVX	... Fluvoxamine
ESC	... Escitalopram
SER	... Sertraline
PXT	... Paroxetine
CIT	... Citalopram
FLU	... Fluoxetine
5-HT	... 5-hydroxytryptamine
OCD	... Obsessive-compulsive disorder
NFLU	... Norfluoxetine
COMT	... Catechol-O-methyltransferase
NCIT	... N-desmethyl citalopram
NS	... Norsertraline
API	... Active pharmaceutical ingredient
WWTP	... Wastewater treatment plants
EU	... European Union
PE	... Population equivalent
COD	... Chemical oxygen demand
BOD	... Biochemical oxygen demand
WFD	... Water Framework Directive
SW	... Surface waters
ERA	... Environmental risk assessment
TP	... Transformation product
$\log K_{ow}$	... Octanol-water partition coefficient
$\log K_{oc}$	... Sorption coefficient
logP	... Partition coefficient
pKa	... Dissociation constant
AOP	... Advanced oxidation processes
UV	... Ultraviolet
USEPA	... US Environmental protection agency
AC	... Activated carbon
H_2O_2	... Hydrogen peroxide
LOQ	... Limit of Quantification
GAC	... Granulated activated carbon
PAC	... Powdered activated carbon
DP	... Direct photolysis
IP	... Indirect photolysis
Φ	... Quantum yield

PPRI ... Photochemically produced reactive intermediate
CDOM ... Chromophoric dissolved organic matter
$HO^{\bullet}$ ... Hydroxyl radicals
$CO_3^{\bullet -}$ ... Carbonate radicals
^{3}CDOM* ... Excited triplet states of the chromophoric dissolved organic matter
$^1O_2$ ... Singlet oxygen
BAF ... Bioaccumulation factors
EC50 ... Median effective concentration
LC50 ... Median lethal concentration
NOEC ... No-observable-effect concentrations
LOEC ... Lowest observable-effect concentrations
SPE ... Solid phase extraction
LSE ... Liquid-solid extraction
PLE ... Pressurized liquid extraction
MS ... Mass spectrometry
LOD ... Limits of detection
HPLC ... High-performance liquid chromatography
UHPLC ... Ultra-high-performance liquid chromatography
LC ... Liquid chromatography
GC ... Gas chromatography
LOD ... Limit of detection
PDA ... Photodiode array
MS/MS ... Tandem mass spectrometer
HRMS ... High-resolution mass spectrometry
SRM ... Selected reaction monitoring
MRM ... Multiple reaction monitoring
Qtof ... Quadrupole time-of-flight
DIA ... Data independent acquisition
DDA ... Data-dependent acquisition
HILIC ... Hydrophilic interaction chromatography
QC ... Quality control
QA ... Quality assurance
VIM ... International Vocabulary of Metrology
F ... Target left free in the solution
B ... Target bound to the polymer
t_R ... Retention time
K_a ... Association constant
K_d ... Dissociation constant
n_{empty} ... Mols of empty binding sites
n_{bound} ... Mols of bound target
D ... Distribution ratio
IF ... Imprinting factor
NIP ... Non-imprinted polymer
α ... Selectivity factor
FTIR ... Fourier-transform infrared spectroscopy
NMR ... Nuclear magnetic resonance
APEX ... Aqueous photochemistry of environmentally occurring xenobiotics

Chapter 1

Introduction

A pharmaceutical is any compound or combination of compounds intended to treat or prevent disease in humans and animals [1]. Rapid economic development, technological advances, increased livestock and aquaculture practices, and a growing global population are increasing pharmaceutical consumption [2]. As a result, the number of confirmed cases (Figure 1) of pharmaceutical residues detected in the environment continues to rise [3].

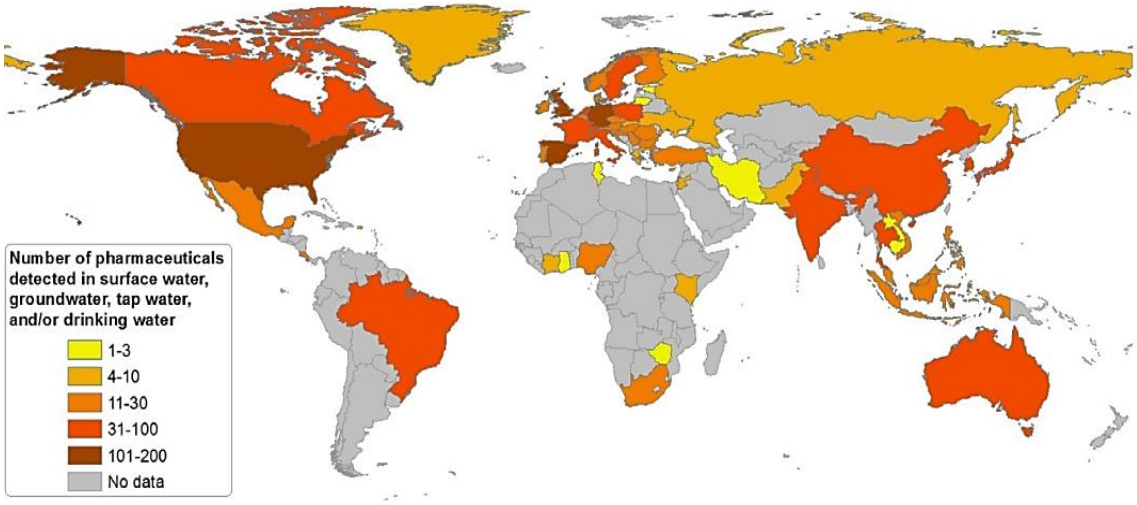

Figure 1: A map showing the number of pharmaceuticals detected in environmental water samples [3].

The pharmaceutical industry, healthcare facilities, agriculture and aquaculture contribute to environmental exposure to pharmaceuticals; however, urban wastewaters (WW) remain the main emission source. While pharmaceuticals are metabolized or degraded in the body, 30-90 % of oral doses are excreted as active substances [2]. Additionally, their removal during WW treatment is still low in most cases, and once in the environment they are very likely to cause harm since they are specifically designed to interact with living organisms and produce pharmacological effects. Wildlife exposure is long-term and includes a cocktail of several substances; hence the outcomes are hard to predict [3], [4]. The research in this area bloomed after 1990 due to the development of available instrumentation that can detect low environmental concentrations (ng L^{-1} or lower). Through the years, more attention has been given to certain classes of pharmaceuticals. Initially, beginning with endocrine disrupting compounds, followed by antibiotics, anti-inflammatory compounds, cytostatics, antihypertensives, cholesterol-

lowering agents, antidiabetics, and lately antidepressants [2], [4], [5]. This thesis focuses on the latter, which aims to fill the observed knowledge gap about the behavior of the most prescribed antidepressant class, the selective serotonin reuptake inhibitor (SSRI) class. This thesis further addressed their treatment and chemical analysis, where molecularly imprinted polymers (MIPs) are employed as a proof-of-concept to demonstrate the versatile possibilities for their application.

1.1 Antidepressants

1.1.1 Classification

Antidepressants form five classes based on the Anatomical Therapeutic Chemical (ATC) classification: non-selective monoamine reuptake inhibitors (N06AA), SSRI (N06AB), non-selective monoamine oxidase inhibitors (N06AF), monoamine oxidase A inhibitors (N06AG) and other antidepressants (N06AX). The group of SSRIs includes nine antidepressants (Table 1). Six of them, sertraline (SER), fluoxetine (FLU), citalopram (CIT), escitalopram (ESC), paroxetine (PXT) and fluvoxamine (FVX), are registered worldwide, and five are also registered in Slovenia [6]. From the remaining three, both zimeldine and alaproclate were discontinued due to adverse effects on the liver [7], while etoperidone was withdrawn because of additional effects on the adrenergic and dopaminergic systems, causing sedative and cardiovascular effects [8]. This thesis focuses on the SSRIs that are still prescribed and hence can potentially contaminate the environment.

1.1.2 SSRI: treatment, administration and consumption

As a result of the growing prevalence of psychiatric disorders and awareness of mental health issues, antidepressant consumption is increasing. The Organization for Economic Co-operation and Development (OECD) report “Health at a glance”, which provides a set of indicators on health system performance and population health, states that the consumption of antidepressants in the OECD countries more than doubled between the years 2000 and 2020 (Figure 2) [2], [9]. This increase in consumption derives mainly from the class of SSRIs [10]–[12]. The high number of prescriptions is due to their high therapeutic efficacy, favorable safety profile, less complex pharmacology and good tolerance in special populations, such as the elderly [13]–[15].

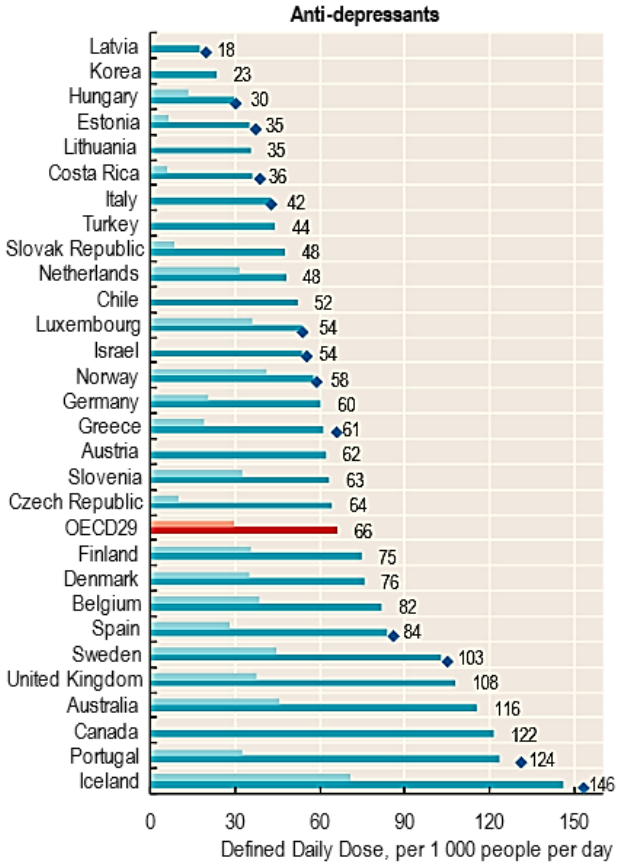

Figure 2: Antidepressant drug consumption in 2000 (light blue line), 2019 (darker blue line) and 2020 (dark blue diamond) [2].

Except for FVX, the registered SSRIs are all in the Top 200 list of Prescribed Drugs in the US (Table 1) and the list of Top 25 psychiatric medications of 2018 in the US [10], [16]. The situation is similar in Europe, including Slovenia, where more than 374,632 prescriptions for SSRIs were given in 2020. ESC or SER are the most commonly prescribed antidepressants in the countries mentioned above. In Slovenia, they are followed by duloxetine, mirtazapine, PXT and CIT [10], [11], [17], [18].

Table 1: Chemical and pharmaceutical classification of SSRIs [10], [17]–[20].

ATC code	SSRI	Abbreviation	CAS	IUPAC name	Trade name	US Top 200 list	Registered (Slovenia)
N06AB02	zimeldine	/	56775-88-3	(Z)-3-(4-bromophenyl)-N,N-dimethyl-3-(pyridin-3-yl)prop-2-en-1-amine	/	/	No
N06AB03	fluoxetine	FLU	54910-89-3	N-methyl-3-phenyl-3-[4-(trifluoromethyl)phenoxy]propan-1-amine	Prozac, Selfemra, Sarafem, Fodiss, Portal	20.	Yes
N06AB04	citalopram	CIT	59729-33-8	(RS)-1-[3-(dimethylamino)propyl]-1-(4-fluorophenyl)-1,3-dihydroisobenzofuran-5-carbonitrile	Celexa, Cipramil, Citalon, Citalox	30.	Yes
N06AB05	paroxetine	PXT	61869-08-7	(3S,4R)-3-[(2H-1,3-benzodioxol-5-yloxy)methyl]-4-(4-fluorophenyl)piperidine	Paxil, Brisdelle, Pexeva, Saroxite, Paluxon, Parogen, Paroxat	78.	Yes
N06AB06	sertraline	SER	79617-96-2	(1S,4S)-4-(3,4-dichlorophenyl)-N-methyl-1,2,3,4-tetrahydronaphthalen-1-amine	Zoloft, Lustral, Asentra, Mapron	12.	Yes
N06AB07	alaproclate	/	60719-82-6	1-(4-chlorophenyl)-2-methylpropan-2-yl 2-aminopropanoate	/	/	No
N06AB08	fluvoxamine	FVX	54739-18-3	2-{[(E)-{5-methoxy-1-[4-(trifluoromethyl)phenyl] pentylidene}amino]oxy}ethanamine	Faverin, Luvox	/	No
N06AB09	etoperidone	/	52942-31-1	2-[3-[4-(3-chlorophenyl)piperazin-1-yl]propyl]-4,5-diethyl-1,2,4-triazol-3-one	Centren, Depraser, Staff	/	No
N06AB10	escitalopram	ESC	128196-01-0	(S)-1-[3-(dimethylamino)propyl]-1-(4-fluorophenyl)-1,3-dihydroisobenzofuran-5-carbonitrile	Lexapro, Cipralex, Citafort, Ecytara, Eqores, Otigem	19.	Yes

1.1.3 SSRI: administration, pharmacokinetics and pharmacodynamics

The SSRI group is structurally heterogeneous; however, the compounds exhibit similar action in the 5-hydroxytryptamine (5-HT) pathway by inhibiting the reuptake of the neurotransmitter serotonin from the synaptic cleft and hence increasing its availability at receptor sites [21]. They have practically no affinity to other receptors (α1-, α2-, and β-adrenergic; serotonergic; dopaminergic; histaminergic 1; muscarinic; and gamma-aminobutyric acid receptors) [13], [15], [22]. They are all prescribed for major depressive and obsessive-compulsive disorder (OCD). Some of them also have additional indications such as panic (CIT, ESC, PXT, SER), social anxiety (ESC, PXT, SER), generalized anxiety (ESC, PXT) and post-traumatic stress disorder (PXT, SER) as well as bulimia nervosa (FLU). Other indications, such as neuropathic pain, are being investigated [22].

All SSRIs are administrated orally and are used in salt form, either maleate (FVX), oxalate (ESC), hydrochloride (SER, FLU, PXT, CIT) or hydrobromide (CIT) [22]. In some cases, a racemic mixture is used (FLU, CIT), while others are sold as optically pure enantiomers (SER, PXT, ESC) or are achiral (FVX). They are readily absorbed from the gastrointestinal tract but have variable bioavailability due to first-pass metabolism. Their volume of distribution is large (5-45 L kg^{-1}), and in plasma, they are bound to proteins to varying degrees (>95 % for FLU, SER, PXT and <80 % for FVX, CIT and ESC). The pharmacokinetic profiles are linear for SER, ESC and CIT and non-linear for FLU, PXT and FVX [13], [15], [22]–[30].

FLU is extensively metabolized by CYP2D6 (Figure 3), and its main metabolite, norfluoxetine (NFLU), retains similar activity and selectivity towards 5-HT reuptake inhibition. Elimination half-life is four to six days for FLU and four to 16 days for NFLU. Both are predominantly excreted in the urine, and around 11 % of the initial dose is excreted as FLU, 7 % as NFLU, 7-8 % as their glucuronides and more than 20 % as hippuric acid [23], [31].

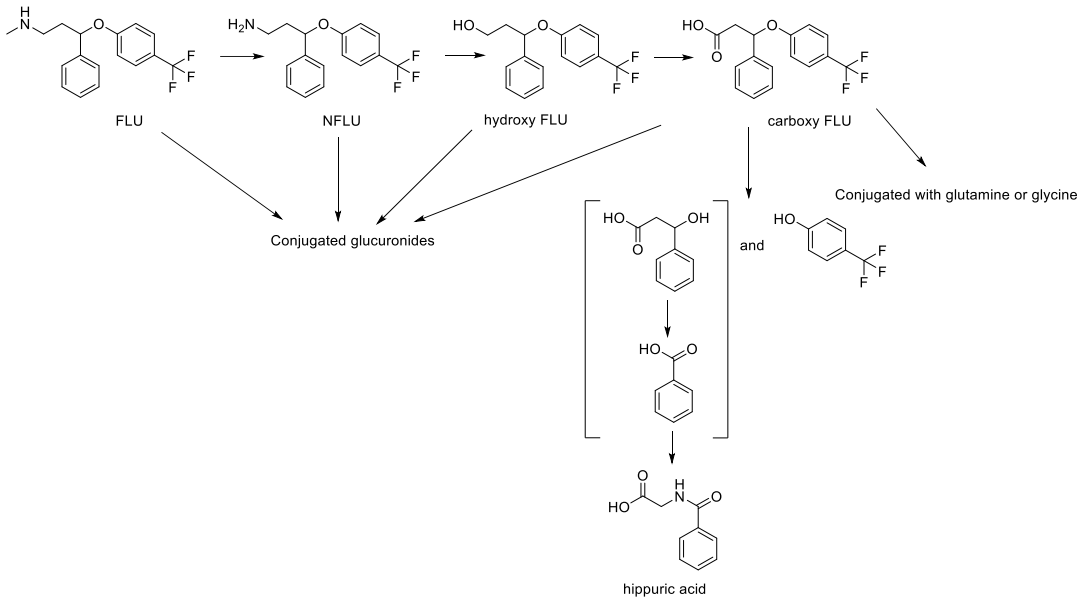

Figure 3: Metabolic pathway of FLU (adapted from [23]).

The enzymes CYP3A4, CYP2C19, CYP2D6, monoamine oxidase (MAO) A, MAO-B and aldehyde oxidase are all involved in CIT metabolism. The formed metabolites, N-desmethyl (NCIT; 30-50 % of the initial CIT dose), N,N-didesmethyl (5-10 % of CIT dose) and N-oxide CIT retain activity, while the deaminated propionic acid derivative is inactive (Figure 4). The elimination time of CIT is about 1.5 days. CIT and metabolites are excreted *via* the liver and kidney. 12-23 % of the daily dose of CIT is excreted in the urine unchanged [28], [29], [32], [33]. While CIT is a racemic mixture, the S-enantiomer is responsible for most of its pharmacological effects [29]. Hence ESC, the S-enantiomer is twice as potent and sold separately [29], [34]. Absorption, protein binding, the volume of distribution, metabolism and elimination are similar to CIT [27], [34], [35].

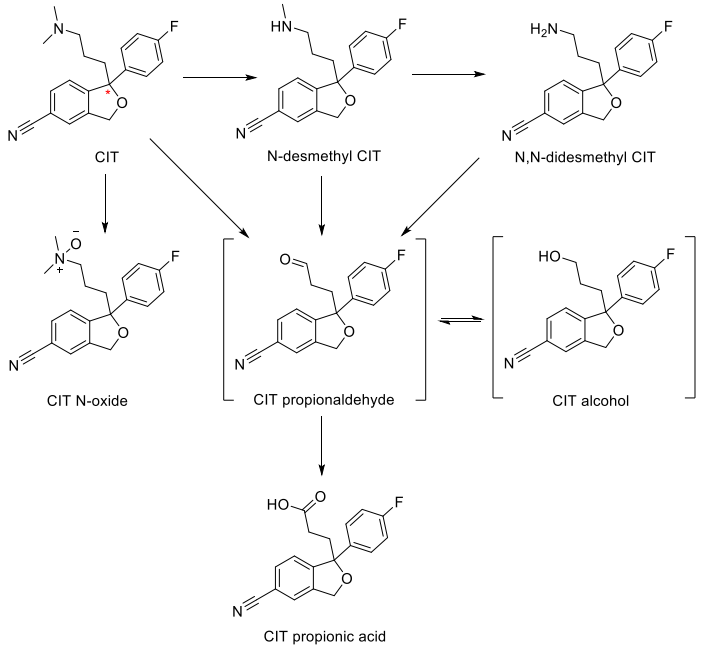

Figure 4: Metabolic pathway of CIT (adapted from [24], [28], *-chiral center).

The enzymes involved in PXT metabolism are CYP2D6, CYP1A2, CYP3A5, CYP3A4 and catechol-O-methyltransferase (COMT). Its metabolites (Figure 5) are inactive. PXT and its metabolites are excreted in urine and feces, with only around 5 % of PXT excreted in unchanged form. The elimination time is approximately 24 h [13], [15], [36], [37].

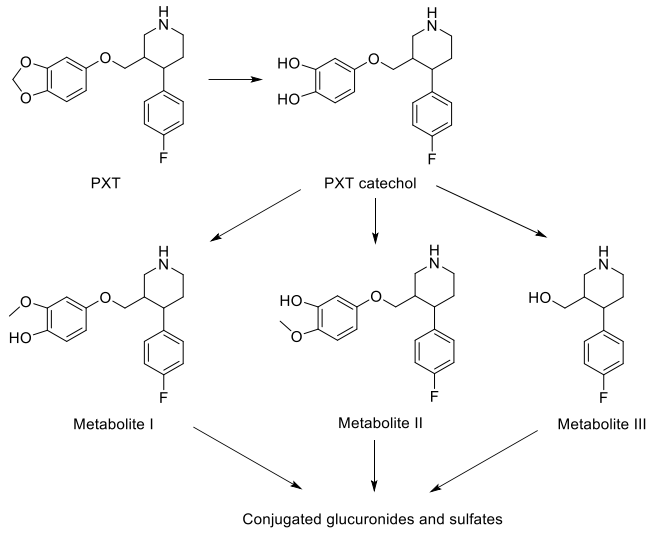

Figure 5: PXT metabolic pathway (adapted from [15], [37]).

SER undergoes extensive first-pass hepatic metabolism following different pathways (CYP3A4, CYP2C19, CYP2B6; Figure 6). Its primary metabolite, norsertraline (NS), is modestly pharmacologically active (5-10 % compared to SER). Both metabolite and parent compound are excreted in urine and feces in equal amounts, with a half-life of approximately 26 hours and 62-104 hours, respectively. Only 0.2 % of unchanged SER is excreted in the urine [15], [25], [38].

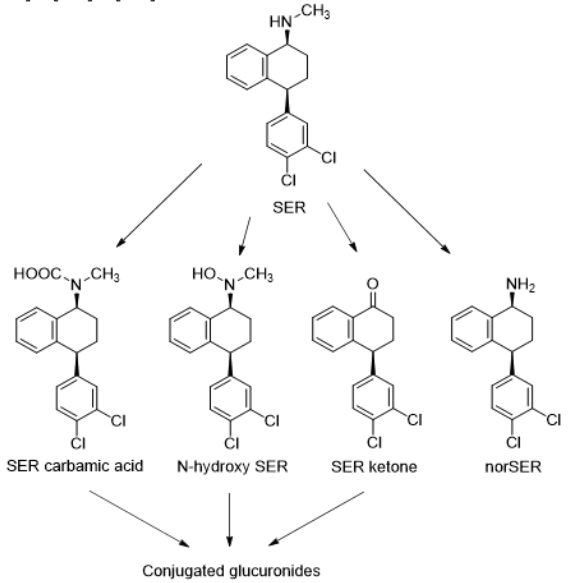

Figure 6: SER metabolic pathway (adapted from [25]).

FVX is extensively metabolized by the CYP2D6, CYP1A2, amine oxidase and N-acetyltransferase (Figure 7). The structures of nine metabolites, the result of oxidative

demethylation, have been suggested. None of the metabolites shows any significant activity. [26], [39], [40].

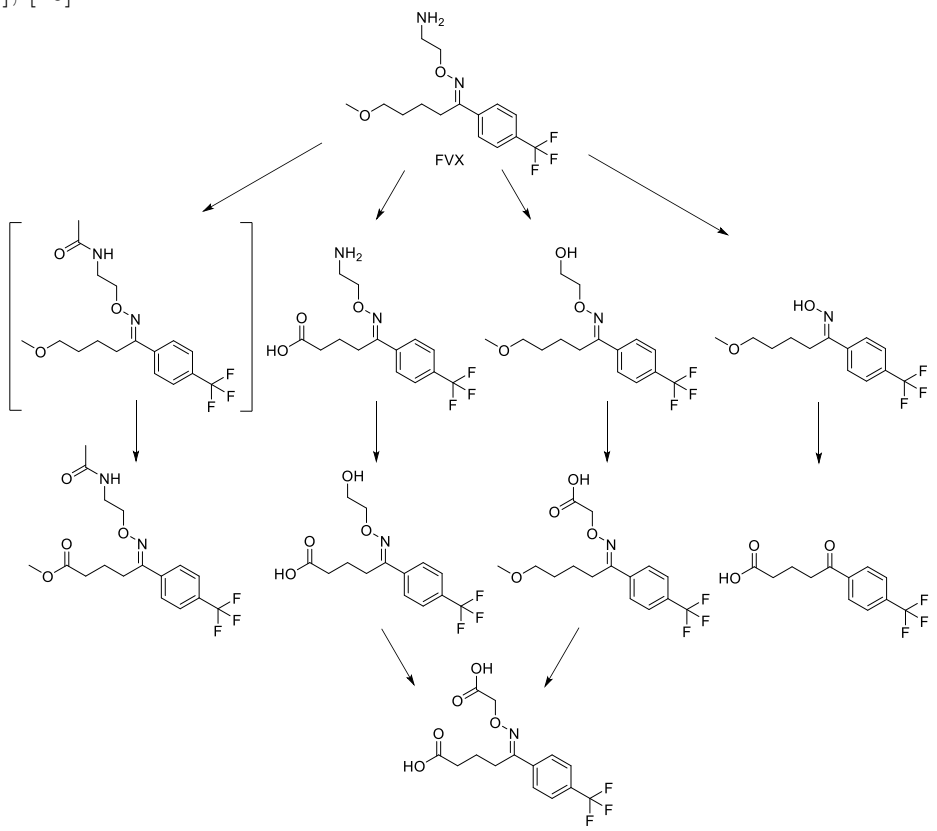

Figure 7: FVX metabolic pathway (adapted from [26]).

Drug-drug interactions are important when an active pharmaceutical ingredient (API) inhibits any enzymes involved in SSRI metabolism. At the same time, PXT, FLU and NFLU are inhibitors of CYP2D6, while FVX is a potent inhibitor of CYP1A2, CYP2C19 and a moderate inhibitor of CYP2C9, CYP2D6 and CYP3A4 [15], [26].

1.2 Antidepressants in the Environment

1.2.1 Sources

The pharmaceutical industry, agriculture, aquaculture, healthcare facilities and households are the sources of pharmaceuticals in the environment (Figure 8). While pharmaceuticals in agriculture or aquaculture seep directly into the surface or groundwater, pharmaceuticals for human use, such as SSRI, are excreted and sometimes even discarded into the toilet, where they end up in the sewage system and undergo treatment in wastewater treatment plants (WWTPs). The SSRIs are only partially removed during treatment; therefore, WW effluents represent the primary emission source. Based on reports of SSRI adsorption to solid material, other byproducts of WW treatment, such as biosolids and sludge, could also contribute to their presence in the environment [4], [9], [41]. According to Langford and Thomas (2009), the contribution from hospital effluents is small compared to municipal areas. For example, SER and PXT originating from hospital effluents contributed only 0.5

% and 0.1 % of the total PXT and SER from Oslo's WWTPs, respectively. The potential contribution of the pharmaceutical industry has yet to be determined [9], [42].

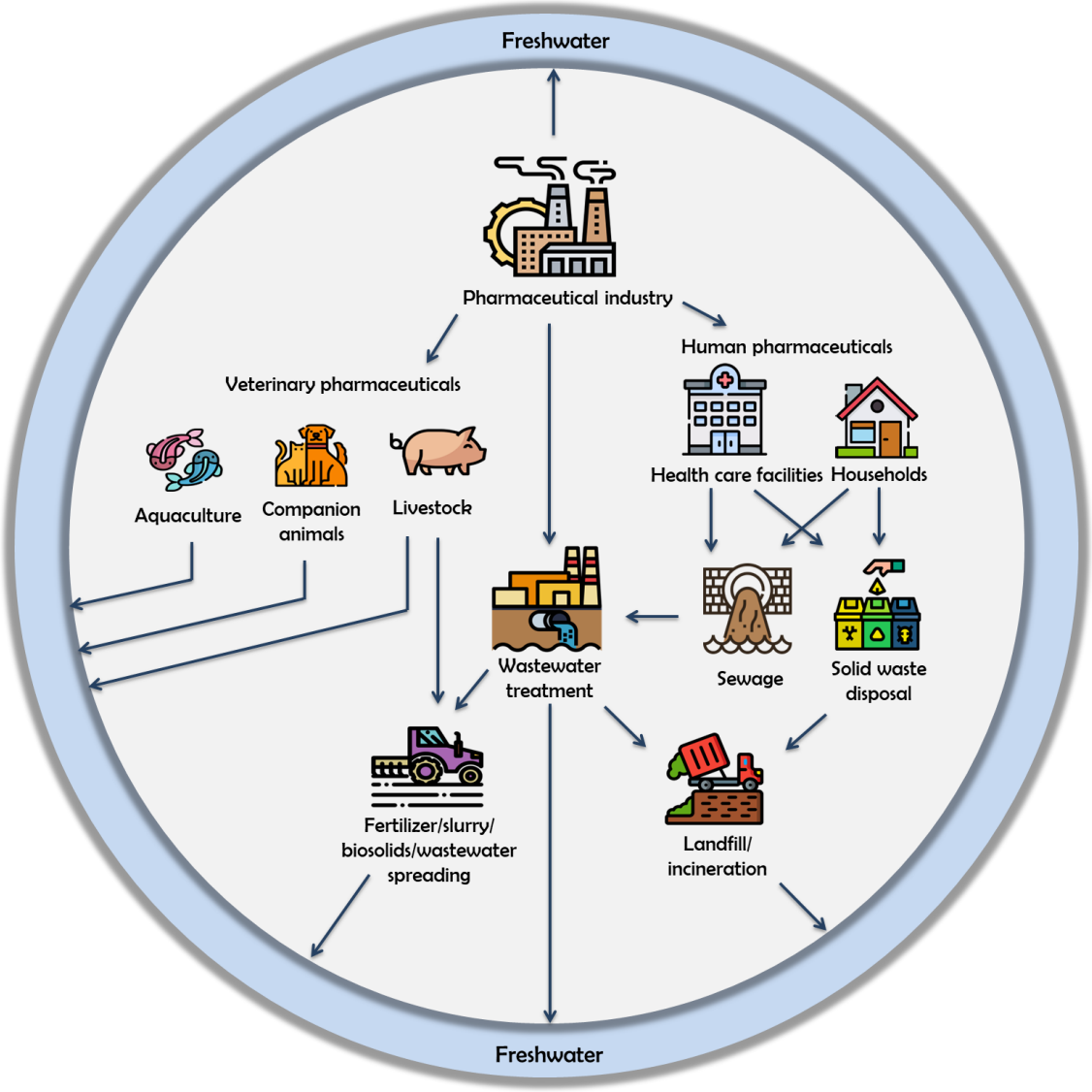

Figure 8: Sources and pathways of pharmaceuticals in the environment (adapted from [43], [44]). Icon source: Flaticon, Freepik.

1.2.2 Legislation

Legislation regulating the presence of organic contaminants of emerging concern in the environment, especially pharmaceuticals, is still under development. In the European Union (EU), the first regulation concerning the collection, treatment and discharge of urban and specific industrial WW was established in 1991 to protect the environment from the adverse effects of WW discharges [45]. Initially, it prescribed the WW collection and treatment in urban agglomerations based on population equivalents (PE). In 1998 and 2003, additional requirements for WW effluents were added, limiting chemical oxygen demand (COD), biochemical oxygen demand (BOD), total suspended solids, total phosphorus and total nitrogen [46]. In 2000, the Water Framework Directive (WFD) was established in order to protect inland surface waters (SW), transitional waters, coastal waters and groundwater

[47]. In Slovenia, two additional decrees were established based on the existing legislation: (1) Decree on the emission of substances in WW discharged from urban WWTPs (2005), and (2) Decree on the emission of substances and heat when discharging WW into waters and the public sewage system (2012). Since 2015 the former has no longer been in force. Also, the regulations do not specifically discuss the presence of pharmaceuticals in the environment. However, an Environmental risk assessment (ERA) has been a mandatory part of every application for marketing authorization for a medicinal product for human use since 2006 [48]. A Watch List for emerging water pollutants was also established in 2015 as part of the WFD. The substances on the list are monitored in SW or another more appropriate matrix (*e.g.*, biota, sediment) across the EU to obtain data for an EU-wide risk assessment and to set Environmental Quality Standards when needed. The main inclusion criteria are a suspected significant risk to the aquatic environment and a lack of sufficient monitoring or modelled exposure data. The frequency of monitoring is no less than once per year, and the list of substances is updated every two years. Although diclofenac, estrone, 17-beta-estradiol, 17-alpha-ethinylestradiol, erythromycin, clarithromycin and azithromycin were included in the first version of the watch list [49], [50], in the second review, diclofenac was removed from the watch list, since satisfactory monitoring data were collected. While with other candidates, such as 17-alpha-ethinylestradiol, the extremely low LOQs needed to provide data of adequate quality still pose a problem. Ciprofloxacin and amoxicillin were added in 2018 [51]–[53]. In the future third installment of the Watch List, the first antidepressant, venlafaxine and its metabolite O-desmethylvenlafaxine are likely to be added [54]. While antidepressants from the SSRI class have not yet been included in the WFD Watch List, their consumption information is included in OECD reports, and their environmental concentrations are part of several monitoring prioritization lists [2], [5].

1.2.3 Occurrence

The number of studies reporting the presence of SSRIs in different compartments of the environment has been increasing [55]. Their behavior is highly dependent on their physicochemical properties. The properties reported for SSRIs are gathered in Table 2. Following the reported properties, the SSRIs in the environment are mainly present in their salt form and are readily soluble hence their continuous presence in water compartments. However, the reported low octanol-water partition coefficients ($logK_{ow}$) of their salt forms do not coincide with their sorption and bioaccumulation properties in the environment. Occurrence data and experimentally obtained high sorption coefficients for soil and sediment ($logK_{oc}$) indicate that they are likely affected by the characteristics of the sorbent [55]–[58]. Kwon et al. (2008) established that the sorption capacity negatively correlated with the soil and sediment pH and was influenced by organic matter contents. A cation exchange mechanism was also suggested as a possible reason behind the observed higher sorption [57].

Table 2: SSRI physicochemical properties. [1] – calculated in ChemAxon or ACD/Labs Percepta Platform, [2] – salt form [56], [57], [59], [3] – based on experiments using two types of sediment and three types of soil [57].

SSRI	CAS number	MW ($g\ mol^{-1}$)	pKa[2]	logP[1]	$logK_{ow}$[2]	$logK_{oc}$[3]	Solubility ($mg\ L^{-1}$)[2]
FLU	54910-89-3	309.13	10.05	4.17	1.22±0.10	4.09-5.49	38.4
CIT	59729-33-8	324.16	9.59	3.76	1.39±0.10	5.32-6.02	31.1
PXT	61869-08-7	329.14	10.32	3.15	1.37±0.10	3.91-5.46	61.4

SER	79617-96-2	305.07	9.47	5.15	1.37±0.10	3.80-4.85	3.5
FVX	54739-18-3	318.33	9.39	2.80	1.12±0.10	3.35-4.28	22.2
ESC	128196-01-0	324.16	9.50	3.76	/	/	/
NS	87857-41-8	292.20	9.52	4.72	/	/	/
NFLU	57226-68-3	295.30	9.10	3.25	/	/	/
NCIT	62498-67-3	310.37	10.5	/	/	/	/

Mole and Brooks (2019) reviewed all published literature reporting on the global occurrence of SSRIs in water matrices. They included 152 relevant publications, predominately from Europe and North America. Only fifteen papers covered the Asia-Pacific, and three were found for South America. There is no literature discussing the presence of SSRI residues in Africa or Antarctica. As expected from the low numbers of prescriptions for FVX, it was only detected in WW and not in SW. FLU and CIT were the most researched, followed by SER and PXT. While, in general, the determined concentrations fall into the lower ng L^{-1} range, the highest detected levels are worrisome and reach µg L^{-1}, as reported in Table 3. Even their metabolites and transformation products (TPs), including NS, NFLU, NCIT and didesmethyl CIT, have been detected on several occasions [55], [58].

Table 3: The maximum concentrations of the SSRI detected in different aqueous matrices [55], [58], [60]–[62].

SSRI	WW influent [µg L^{-1}]	WW effluent [µg L^{-1}]	SW [µg L^{-1}]
SER	1.00	1.93	0.22
ESC	32.3	1.14	0.52
PXT	39.7	0.74	0.27
CIT	17.1	9.20	0.43
FLU	3.47	2.70	0.33

Reports of SSRIs adsorbing to sewage sludge are supported by concentrations reported at a few hundred ng g^{-1} and, in extreme cases, > 3 µg g^{-1} (SER and CIT) [63]. Additionally, although the loss of a methyl group in SSRI metabolites increases polarity, the presence of NS, NCIT and NFLU in sewage sludge has also been confirmed [63]–[65]. Domestic sludge was reported to be more contaminated than industrial or mixed sewage sludge [65]. This tendency of SSRIs to adsorb is also observed in sediment. SER, FLU, PXT, CIT, FVX and the metabolites NS and NFLU were detected at low ng g^{-1} levels. SER had the highest detection frequency [66]–[68].

The SSRIs have also been determined in aquatic organisms. Most occurrence studies sampled fish tissue and predominately determined SER, FLU and CIT [55], [69]. The reported concentrations are mostly in the low ng g^{-1} range [58], [67], [70]–[75]. The TPs NFLU and NS have also been detected in aquatic organisms. While in most cases, NFLU is reported at slightly higher concentrations than FLU, the ratio between NS and SER is much higher. This finding indicates that the parent compound is metabolized or excreted faster than the metabolite. The highest detected levels of NS (647.3 ± 111.5 ng g^{-1}) were in fish livers [58], [69].

1.2.4 Fate and transformation

As mentioned, the pathway of a pharmaceutical after it leaves the human body or when it is inappropriately disposed of most commonly starts in WWTPs and continues into the

environment. During this time, it undergoes several processes, such as hydrolysis, bio/photodegradation, sorption and uptake by plants and animals. These processes represent the possible pathways of contaminant removal from the environment and the potential formation of TPs. TPs can either be more, less or similarly active and toxic than the parent compound [76], [77]. The following chapters include all available data on the environmental fate of SSRIs.

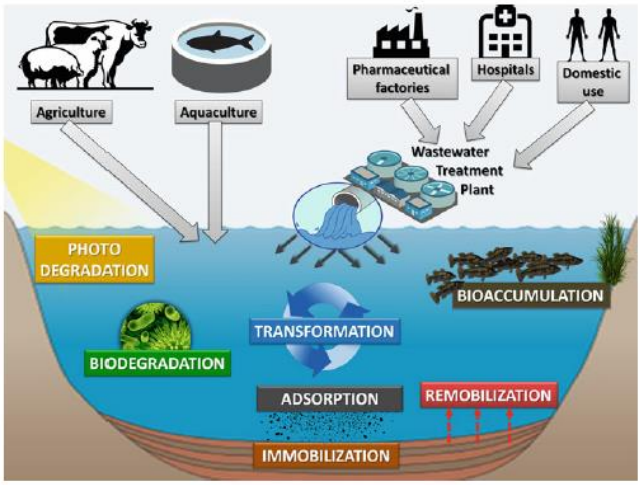

Figure 9: Potential pharmaceutical transformation pathways [78].

1.2.4.1 Wastewater treatment

The processes occurring during WW treatment are an important part of understanding the fate of the SSRIs in the environment and the risks they present. There are three stages of WW treatment primary, secondary and tertiary. During primary treatment, coarse solids and large materials are removed, making adsorption the main removal pathway. This process is followed by secondary biological treatment. WW is predominantly purified in bioreactors containing activated sludge designed to remove dissolved biodegradable or colloidal organic matter. The OECD report states that secondary biological treatment is, on average, 30% more efficient than primary treatments in removing pharmaceuticals [44]. Tertiary treatments are added in some cases to enhance the removal efficiency of the WWTP. However, their implementation is generally expensive. The primary removal mechanism depends on the type of treatment used, ranging from advanced membrane filtration and carbon adsorption to advanced oxidation processes (AOP) [79]. Since conventional WWTPs were not designed to remove micropollutants such as pharmaceuticals, most treatments are not sufficiently effective for removing these compounds [44].

Cao et al. (2020) researched the contributions of different treatment processes to SSRI removal in two WWTPs in China. They found that pretreatment processes, such as grit removal and hydrolysis acidification, could partially remove SER and PXT. The SSRIs were, however, primarily removed during sludge-based secondary treatment. Among them, the segmented anaerobic, anoxic and aerobic membrane reactor was the most efficient type of treatment. Adsorption to sludge was the leading removal mechanism of SSRIs, followed by biodegradation, which corresponds with the high $\log K_{oc}$ values that Kwon and Armbrust (2008) reported (Table 2). Positive correlations between the removal and the presence of specific microbial communities were identified, varying between compounds. Tertiary ultraviolet (UV) radiation treatment removed 1.3 % to 27 %, while chlorination was efficient in cases of PXT and FLU (6.9 % and 12 %). The removal of SER by chlorination

treatment was not reported though Huerta-Fontela et al. (2011) observed significant removal (>99 %) after chlorination was used as the pretreatment [80], [81]. The removal efficiencies of several WWTPs are given in Table 4. Only studies with 24-hour composite samples were included to allow comparison, and removal efficiencies for SSRIs varied considerably between the WWTPs studied. These differences may be due to varying conditions (*e.g.*, inflows) and treatments applied. However, we can generally conclude that at least secondary treatment is needed for removal efficiencies above 50 %. Including tertiary treatment additionally improved the removal of SSRIs. Angeles et al. (2020) highlighted the efficiency of using activated carbon (AC). However, no data has been reported on FVX removal during WW treatment.

Biological treatment plays an important role in removing SSRIs, and many studies have tried to elucidate the mechanisms behind their removal. For instance, the biotransformation of FLU in a batch experiment using activated sludge was researched by Gulde et al. (2016) at an initial concentration of 120 µg L^{-1}. The experiment lasted four days, and FLU removal was >90 %. High adsorption to sludge was observed, and an additional slight decrease of the initial concentration during the first 24 h, most likely due to other abiotic processes. The observed transformations included possible FLU demethylation into NFLU, N-acetylation, N-propionylation and N-succinylation (Figure 10). The latter three reactions were also observed for the demethylated NFLU [82]. High adsorption has also been observed by Cao et al. (2020) and Salgado et al. (2012), while less adsorption to sludge and more biodegradation were reported during other studies. For example, in experiments performed by Velázques and Nacheva (2017), 84.7 % of FLU was removed by biodegradation and 8.8±1.9 % by adsorption. In these studies, the authors used different microbial consortiums, which might have influenced the final results [80], [83], [84].

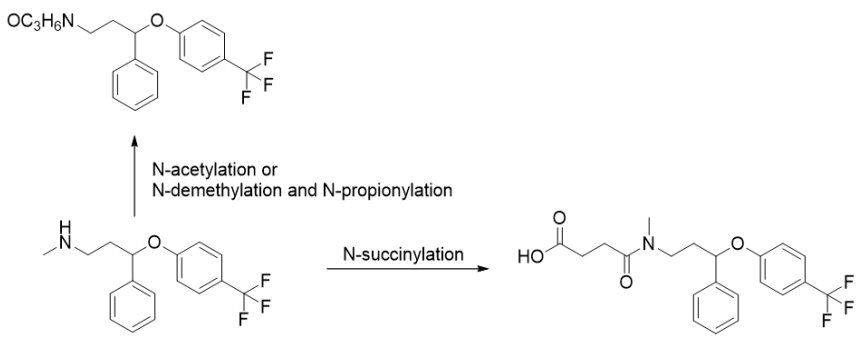

Figure 10: Proposed biodegradation mechanism of FLU during batch degradation experiments (adapted from [82]).

Beretsou et al. (2016) studied the biotransformation of CIT in batch experiments performed in aerated activated sludge at 2 mg L^{-1}. CIT was not completely removed in six days. Forty % and 70 % of CIT were removed during the first nine hours and three days %, respectively, and then stayed stable for the next three days. The high removal in the batch experiment agreed with the batch experiment performed by Casas et al. (2015), who reported removal of almost 80 %. A 13 % decrease in CIT concentration was due to adsorption to sludge. Fourteen TPs were detected, and for 13 of them, tentative structures were suggested (Figure 11). Four of them also formed during abiotic conditions [85]. Most of the TPs underwent hydroxylation, oxidation, hydrolysis or N-demethylation. Five of the identified TPs were detected in the tested WW effluent: N-desmethylcitalopram (NCIT, CTR 311), 3-oxo-CIT (CTR 339A), CIT N-oxide (CTR341), amide CIT (CTR343) and CIT carboxylic acid (CTR 344) [85], [86]. Removal in the first nine hours of the batch

experiment performed by Beretsou et al. (2016) is in the same range as most removals reported in WWTPs (Table 4). This lower removal in actual WW was also observed by Casas et al. (2015). While Beretsou et al. (2016) suggest the lower hydraulic retention time (HRT) to be the main reason, Casas et al. (2015) propose de-conjugation or formation of the parent compound from other metabolites to be the reason behind their lower removal [85]–[87].

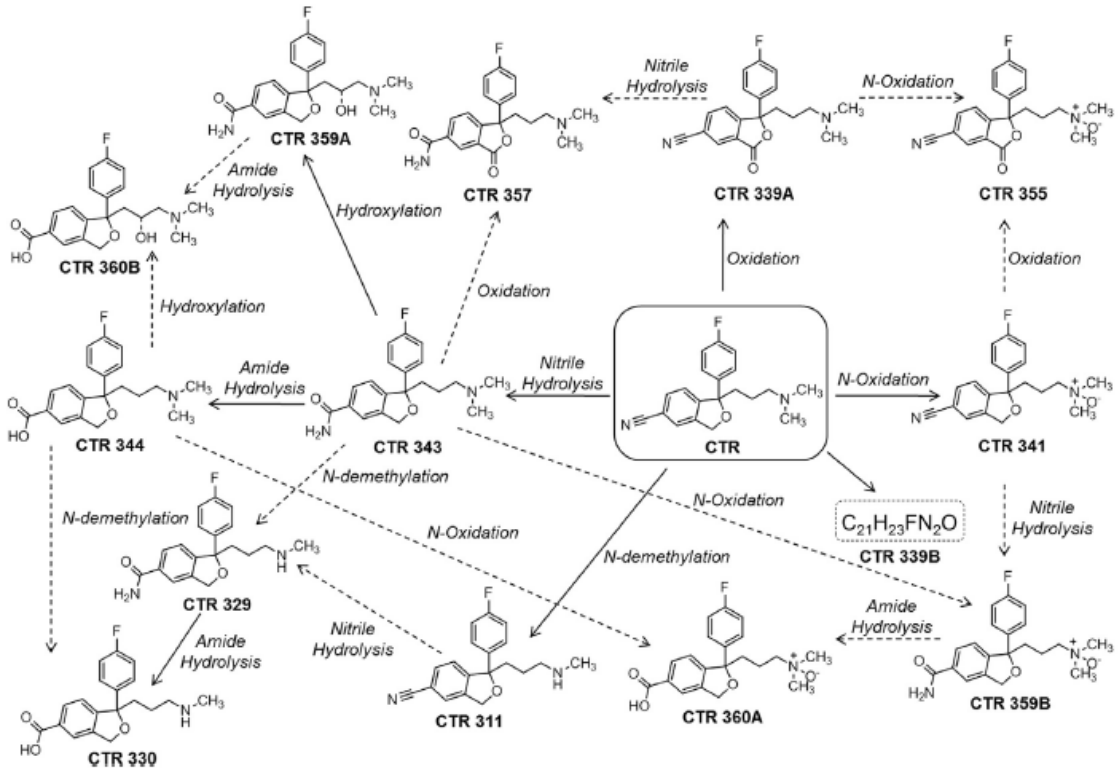

Figure 11: Proposed biodegradation pathway of CIT in batch degradation experiments [85].

Cunningham et al. (2004) performed adsorption and biodegradation studies as part of the ERA of PXT. PXT was partially adsorbed to activated sludge during the first day of the experiment, with no further decrease of concentration observed in the following 31 days. It was poorly biodegradable during aerobic biodegradability studies, including various inocula originating from domestic and industrial WWTPs and soils. Its biodegradability did not improve even when PXT was present as the single carbon source. As such, no PXT biodegradation products were identified [88].

Except for the US Environmental protection Agency (USEPA) report, which shortly evaluated all the SSRIs in an activated sludge experiment, determining all of them as poorly biodegradable, no data was available on SER and FVX removal mechanisms and biotransformation [68]. Since the secondary treatment does not entirely mineralize the SSRIs from WW, different tertiary treatments have already been examined [79]. Considering that they sorb to activated sludge to a high extent, AC, with its large surface area, was one of the first investigated treatments. Ek et al. (2014) confirmed its efficiency (90-98 %) in studies where CIT and SER were translocated to AC from WW during a pilot AC treatment procedure [89]. Guillossou et al. (2019) also observed a 40 % increase in removal efficiency when AC treatment was added to an existing WWTP, including secondary biological treatment [90]. There are two types of AC used, granulated (GAC) and powdered (PAC). The advantage of using PAC is that it can be added when needed; however, another filtration unit must be installed to remove it from the treated WW. As

a regular treatment, GAC packed in bed filters or columns is used. This method has a faster breakthrough for more hydrophilic compounds and has higher initial costs than PAC, but GAC is easier and cheaper to regenerate in the long run. Nevertheless, the material's performance decreases with every regeneration cycle and must be disposed of eventually [79], [91]. Greener and more cost-effective alternatives, such as products of pyrolysis of primary and secondary paper mill sludge, spent coffee grounds, pine bark and cork waste, have also been considered for the removal of SSRIs with varying success but have yet to outperform commercial AC [92]–[95].

Advanced membrane filtration was the second type of tertiary treatment considered. In membrane filtration, the membrane acts as a barrier retaining the particles, microorganisms and, in some cases, micropollutants. The mechanisms behind the removal process include size exclusion, charge repulsion and adsorption, with the main categories including microfiltration, ultrafiltration, nanofiltration, and reverse osmosis [79]. Unfortunately, the removal of SSRIs during tertiary membrane processes has not yet been investigated.

Lastly, several studies investigate the efficiency of AOPs in removing SSRIs. These processes involve the production of reactive intermediate radicals, mostly hydroxyl radicals, which indiscriminately attack organic compounds degrading them in the process. There are many types of AOP, including UV radiation, oxygen, ozone, hydrogen peroxide (H_2O_2) and their combinations. AOP can be chemical, sonochemical, thermochemical or electrochemical, depending on the method used to produce the reactive oxygen species. Solid catalysts, such as TiO_2, can also be part of the AOP system. The main advantage of the process is high efficiency and even the possibility of complete mineralization for recalcitrant compounds. The drawbacks are the cost of maintaining such systems, high energy consumption and safety issues [79], [96]. In the case of SSRI, ozonation with or without additives (H_2O_2, TiO_2, UV radiation, iron) is the most commonly researched process [96]–[105], followed by Fenton or photo-Fenton oxidation [100], [106]–[108]. The removal of the SSRIs depend on their initial concentration, steric hindrance in tertiary amines, the dosage of ozone, iron or other additives, treatment duration, matrix pH and the presence of other carbon sources due to the matrix scavenging effect [98], [106]. AOPs are promising techniques for SSRI removal. However, on top of the aforementioned disadvantages, there are also reports of the formation of potential toxic TPs including aldehydes and N-oxides [101], [104]. In this context, the study by Li et al. (2019) directly evaluated and compared the potential environmental and toxicity impacts of these three aforementioned types of WW tertiary treatments by comparing ozonation, GAC and reverse osmosis. The SSRI FLU, SER and PXT were also among the studied micropollutants. They highlighted reverse osmosis as the greatest environmental burden due to high energy and material consumption during treatment. Ozonation was suggested for local water environments with low eutrophication and ecotoxicity, since it had the best removal efficiency, while GAC was suggested to be more appropriate for long term regional scale WW treatment, due to lower electricity consumption, despite the high regeneration costs [109].

Table 4: Overview of the removal efficiencies reported for SSRI at different WWTPs. 100 % removal indicates the presence below limit of quantification (LOQ). ND – not defined.

SSRI	Removal	Type of treatment	Reference
FLU	8-54 %	Primary (mechanical sieves)	[110], [111]
	16 %	Primary (chemically enhanced with alum and $FeCl_3$)	[64]
	32-47 %	Secondary (biological nutrient removal)	
	27-50 %	Secondary (aerated filter)	

	24 %	Secondary (trickling filter/solid contact)	
	42 %	Secondary (activated sludge)	
	100 %	Secondary (activated sludge with extended aeration); tertiary (with UV)	[112]
	100 %	Secondary (activated sludge); tertiary (with UV)	
	65±4 %	Secondary (aerated COD removal and activated sludge)	[59]
	79-84 %	Secondary (fixed bed reactor)	[113]
	68 %	Secondary (trickling filter)	
	10-70 %	Secondary (fluidized bed biological reactor)	
	2.4 %	Primary (hydrolysis-acidification)	[80]
	3 %	Primary (grit chamber)	
	25 %	Secondary (cyclic activated sludge system aeration)	
	10 %	Secondary (cyclic activated sludge system sinking)	
	18 %	Secondary (sequencing batch reactor aeration)	
	12 %	Secondary (sequencing batch reactor sinking)	
	8 %	Secondary (anaerobic biologic reactor)	
	8.7 %	Secondary (anoxic biologic reactor)	
	34 %	Secondary (aerobic biologic reactor)	
	-1 %	Secondary (sedimentation tank)	
	6.9 %	Tertiary (Chlorination)	
	5.2 %	Tertiary (UV)	
CIT	29-57 %	Primary (mechanical sieves)	[110], [111]
	3.5 %	Primary (chemically enhanced with alum and $FeCl_3$)	[64]
	27-32 %	Secondary (biological nutrient removal)	
	25-37 %	Secondary (aerated filter)	
	3.8 %	Secondary (trickling filter/solid contact)	
	41 %	Secondary (activated sludge)	
	18 %	Secondary (activated sludge)	[114]
	35.5-100 %	Secondary (activated sludge with extended aeration); tertiary (with UV)	[112]
	34.6 %	Secondary (activated sludge with conventional and extended aeration); tertiary (with UV)	
	100 %	Secondary (trickling filters)	
	100 %	Secondary (activated sludge)	
	44.6 %	Secondary (activated sludge); tertiary (with UV)	
	100 %	Secondary (biofiltration); tertiary (with UV)	
	36±7 %, 33±7 %	Secondary (aerated COD removal and activated sludge)	[59]
	20 %	Primary (hydrolysis-acidification)	[80]
	-114 %	Primary (grit chamber)	
	53%	Secondary (cyclic activated sludge system aeration)	
	-20 %	Secondary (cyclic activated sludge system sinking)	
	31 %	Secondary (sequencing batch reactor aeration)	
	11 %	Secondary (sequencing batch reactor sinking)	
	27 %	Secondary (anaerobic biologic reactor)	
	19 %	Secondary (anoxic biologic reactor)	

	49 %	Secondary (aerobic biologic reactor)	
	4.8 %	Secondary (sedimentation tank)	
	-39 %	Tertiary (Chlorination)	
	1.3 %	Tertiary (UV)	
	85-93 %	Secondary (fixed bed reactor)	[113]
	45-61 %	Secondary (trickling filter)	
	57-62 %	Secondary (fluidized bed biological reactor)	
	100 %	Secondary (ND); tertiary (GAC and UV radiation)	[115]
	100 %	Secondary (ND); tertiary (moving bed biofilm reactor, tertiary clarifiers, conventional filtration)	
	100 %	Secondary (ND); tertiary (flocculation sediment, ozonation, biologically activated filtration, GAC, UV)	
	11 %	Primary; secondary (sequential batch reactor), tertiary (UV)	
	15 %	Secondary (aerobic/anaerobic batch reactor, membrane bioreactor); tertiary (UV)	
	35 %	Primary (ND); secondary (sequential batch reactor), tertiary (chlorination)	
	11 %	Primary (ND); secondary (activated sludge); tertiary (chlorination)	
SER	11-55 %	Primary (mechanical sieves)	[110], [111]
	26 %	Primary (chemically enhanced with alum and $FeCl_3$)	[64]
	25-34 %	Secondary (biological nutrient removal)	
	37-46 %	Secondary (aerated filter)	
	33 %	Secondary (trickling filter/solid contact)	
	48 %	Secondary (activated sludge)	
	81 %	Secondary (activated sludge)	[114]
	100 %	Secondary (activated sludge with extended aeration); tertiary (with UV)	[112]
	82±2 %	Secondary (aerated COD removal and activated sludge)	[59]
	82-86 %	Secondary (fixed bed reactor)	[113]
	16-67 %	Secondary (trickling filter)	
	28-76 %	Secondary (fluidized bed biological reactor)	
	12.5 %	Primary (grit chamber)	[80]
	14 %	Secondary (anaerobic biologic reactor)	
	10 %	Secondary (anoxic biologic reactor)	
	27 %	Secondary (aerobic biologic reactor)	
	6%	Secondary (sedimentation tank)	
	11 %	Tertiary (UV)	
	100 %	Secondary (ND); tertiary (GAC and UV radiation)	[115]
	99 %	Secondary (ND); tertiary (moving bed biofilm reactor, tertiary clarifiers, conventional filtration)	
	100 %	Secondary (ND); tertiary (flocculation sediment, ozonation, biologically activated filtration, GAC, UV)	
PXT	17-94 %	Primary (mechanical sieves)	[110], [111]
	7.5 %	Primary (chemically enhanced with alum and $FeCl_3$)	[64]

	24-27 %	Secondary (biological nutrient removal)	
	27-29 %	Secondary (aerated filter)	
	26 %	Secondary (trickling filter/solid contact)	
	35 %	Secondary (activated sludge)	
	100 %	Secondary (activated sludge with extended aeration); tertiary (with UV)	[112]
	41.1 %	Secondary (activated sludge); tertiary (with UV)	
	76±2 %, 76±3 %	Secondary (aerated COD removal and activated sludge)	[59]
	7 %	Primary (hydrolysis-acidification)	[80]
	13 %	Primary (grit chamber)	
	38 %	Secondary (cyclic activated sludge system aeration)	
	-11 %	Secondary (cyclic activated sludge system sinking)	
	29 %	Secondary (sequencing batch reactor aeration)	
	-2 %	Secondary (sequencing batch reactor sinking)	
	-4.3 %	Secondary (anaerobic biologic reactor)	
	8.8 %	Secondary (anoxic biologic reactor)	
	21 %	Secondary (aerobic biologic reactor)	
	0.4 %	Secondary (sedimentation tank)	
	12 %	Tertiary (Chlorination)	
	27 %	Tertiary (UV)	

In addition to WW effluent, sewage sludge is another byproduct of WW treatment that introduces contaminants into the environment. In Europe, most of the sludge is incinerated. Nevertheless, in certain countries, it is used as fertilizer for agriculture (Ireland - 89 %), composting (Czechia – 42 %), or landfill (Malta – 100 %) [116], [117]. On the other hand, USEPA reports land application (*e.g.*, agricultural, home garden, landscaping, golf course) as the main sludge disposal route (43 %), closely followed by landfilling (42 %) and incineration (14 %) [118]. Although sludge used for landfilling and land application has to fulfill strict requirements, there remains a possibility of contamination of ground waters and crops. SSRIs are a problematic group of compounds because most of them adsorb to sludge. Additionally, studies researching plant uptake from contaminated soils found that SSRIs can accumulate in plant tissue, with SER being the main compound accumulated [119]. The treatment of sludge is suggested as a possible solution. Vasskog et al. (2009), Bergersen et al. (2015), and Bergersen et al. (2012) researched both aerobic and anaerobic treatments, both of which proved to be successful in reducing the initial concentrations of SSRI in sewage sludge. PXT was most easily removed, while SER was the most persistent under both conditions. The presence of metabolites was also observed (NS, NCIT, NFLU) [120]–[122].

1.2.4.2 Environmental transformation

Once pharmaceuticals are released into the environment, they undergo the same processes as other organic contaminants. Their main difference is that they have passed through the human digestive system and possibly WW treatment. Therefore, they often enter the aquatic environment partly transformed or, when intact, remain resistant to further hydrolytic and biological degradation [123]. Therefore, abiotic degradation is considered the leading transformation process [124].

Hydrolysis and photodegradation

Once they reach the environment, photodegradation has been considered one of the main transformation mechanisms of SSRIs. Two main types occur in aquatic systems: direct photolysis (DP) and indirect photolysis (IP). In DP, the transformation of the observed compound occurs because it absorbs solar irradiation (100 nm-1mm); hence it is an important degradation process for sunlight-absorbing compounds. The extent of the photodegradation will depend on the extent to which the compound absorbs sunlight, the irradiation intensity of sunlight and the quantum yield (Φ). The latter represents the probability that the absorption of a photon induces photolysis [124]–[126]. IP results from the reaction between the compound in question and photochemically produced reactive intermediates (PPRIs) formed by light absorption by natural photosenzitizers. These include chromophoric dissolved organic matter (CDOM), bicarbonate, carbonate, nitrate, and nitrite. The most important PPRIs formed are hydroxyl ($HO^{\bullet}$), carbonate radicals ($CO_3^{\bullet-}$), the excited triplet states of CDOM (^{3}CDOM*) and singlet oxygen ($^1O_2$). In some cases, other radical species, such as $^{\bullet}NO_2$, $Cl_2^{\bullet-}$ and $Br_2^{\bullet-}$, can also be involved [124]–[127].

FLU is the most studied SSRI in the group, which is not surprising since it was the first SSRI approved in 1986 [128]. The quantum yield of DP was determined by both Kwon and Armbrust (2006) and Lam et al. (2005) under a Xenon lamp with a filter cutting off wavelengths under 290 nm, while Wols et al. (2014) performed their experiments under a monochromatic lamp at 254 nm commonly used in WW treatment (Table 5). The determined quantum yields in the first two reports are in a similar range, although pH-dependent. However, at 254 nm, the quantum yield is much higher. Although many polyatomic organic molecules follow Kasha's rule and have a similar Φ at all wavelengths, FLU seems to be an exception. Its photodegradation is fastest at alkaline pH [123], [129], [130]. The compound also undergoes IP in the presence of different PPRIs. It is susceptible to photodegradation in the presence of CDOM and $HO^{\bullet}$, while it is not sensitive to $CO_3^{\bullet-}$ [129], [130]. The determined second-order rate constants are stated in Table 5. The TPs formed during both DP and IP can be found in Figure 12 and were formed by O-demethylation, hydroxylation, demethylation and hydrolysis to carboxylic acid [123], [129], [131].

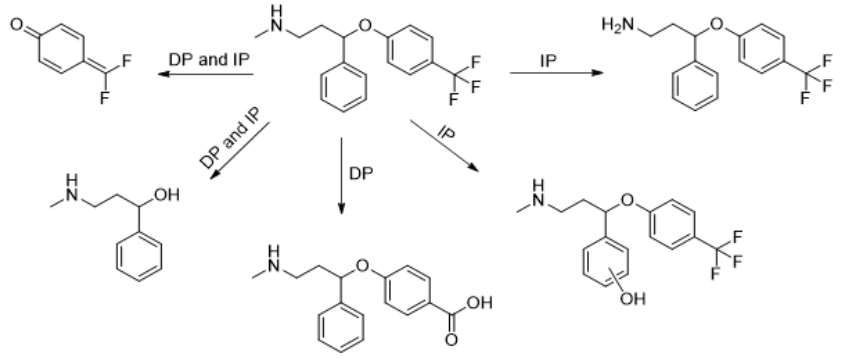

Figure 12: FLU TPs identified during DP and IP (adapted from [123], [129], [131]).

Similarly to FLU, Kwon and Armbrust (2005) consider CIT hydrolytically stable. On the contrary, a small percentage of CIT hydrolyzed during the experiments performed by Osawa et al. (2019) and Sharma et al. (2011). During photodegradation experiments, CIT was also observed to degrade faster under alkaline conditions, actual SW and in humic water, which is an artificial approximation of dissolved organic matter found in SW [132]. The latter indicates that PPRIs play an important role in CIT photodegradation. The Φ

can be found in Table 5, while no data on the influence of particular PPRI has been provided in the literature. Nevertheless, several TPs formed during photodegradation in distilled, humic and SW have been identified (Figure 13). Reactions of oxidation, N-oxidation, dehalogenation, hydroxylation, N-demethylation and N-hydrolysis were observed [133]–[135].

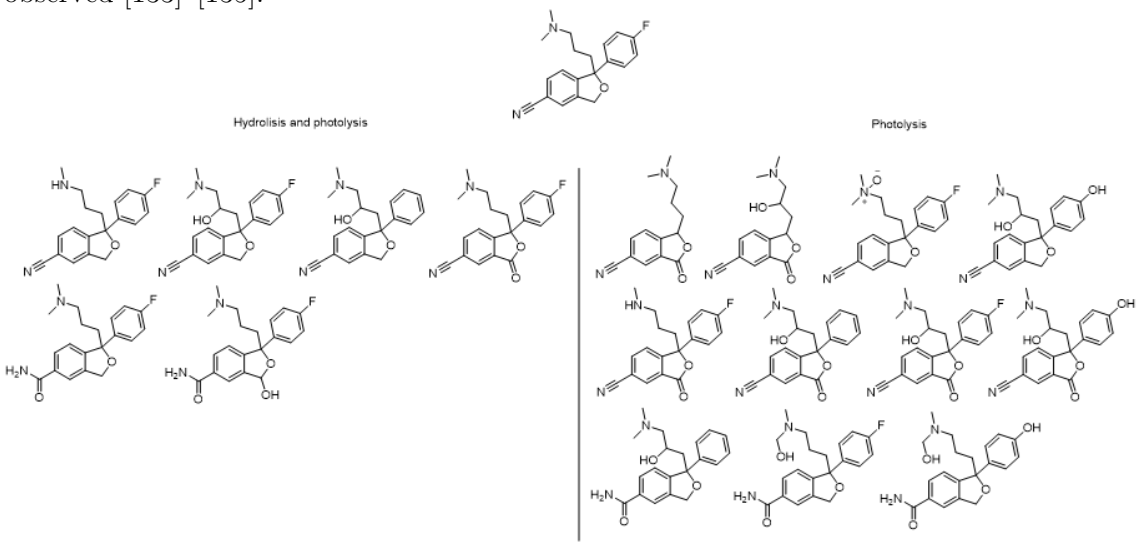

Figure 13: CIT TPs identified during hydrolysis and photolysis (adapted from [133]–[135]).

So far, no significant PXT hydrolysis has been observed. However, PXT undergoes photodegradation at pH 5 to 9 [136], [137]. Again, the higher the pH, the faster the photodegradation. Contrary to other SSRIs, the degradation rate of PXT was lower in humic, lake, and river water than in distilled or ultrapure water. This lower rate might result from the scavenging effect of the water matrix. The Φ and secondary rate constants for the reactions with $HO^{\bullet}$, $CO_3^{\bullet -}$ and $^1O_2$ are stated in Table 5 [130], [136], [137]. Figure 14 shows the structure of two tentatively suggested TPs, with the tricyclic TP resistant to further photodegradation [136], [138].

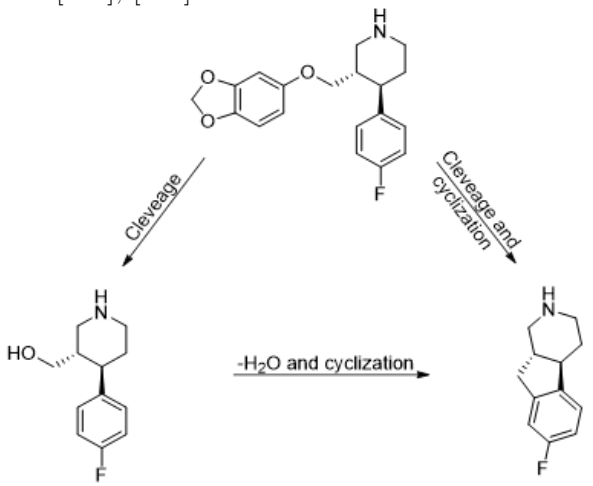

Figure 14: PXT proposed photodegradation (adapted from [136]).

SER was found to be hydrolytically stable [68]. Its photostability was investigated by Jakimska et al. (2014). Again they observed that a higher pH resulted in accelerated photodegradation, as did irradiation in river water, WW influent and effluent compared to ultrapure water, indicating that SER undergoes reactions with the formed PPRIs [139],

[140]. Seven TPs were identified in irradiated river water samples (Figure 15). The transformations included hydroxylation, dehalogenation, dehydrogenation and oxidation [140].

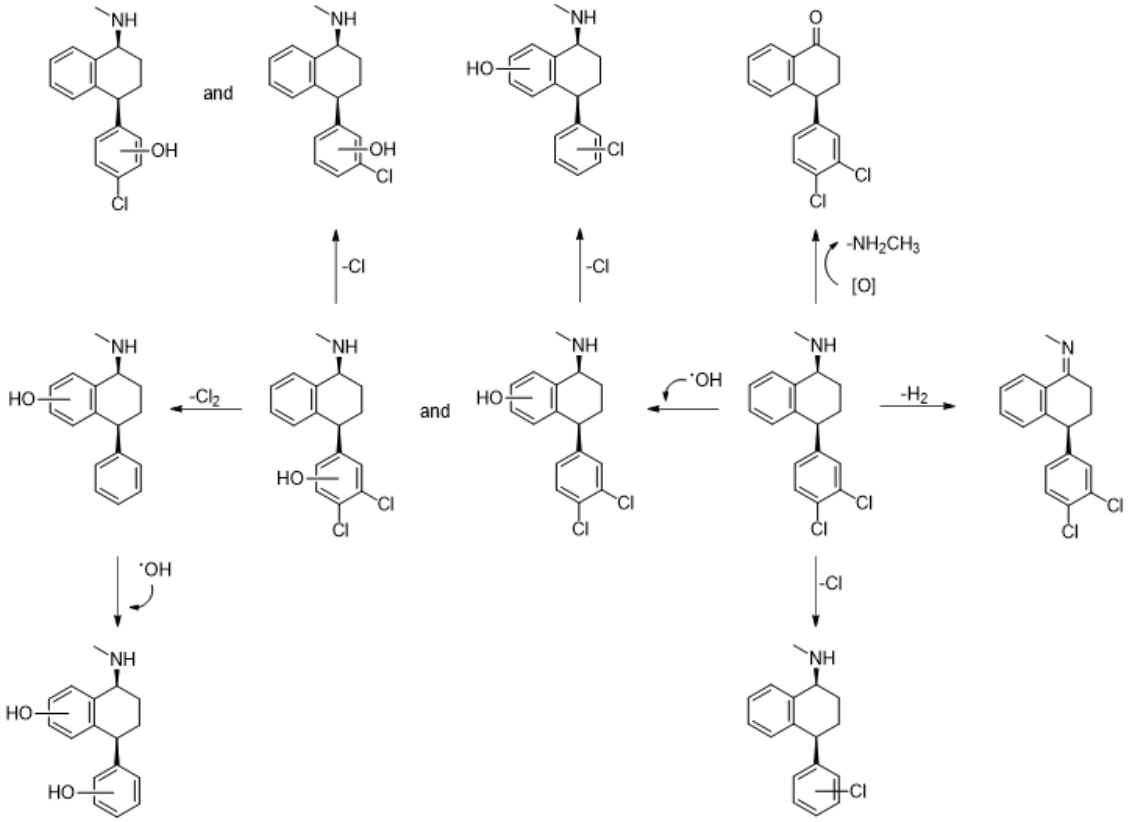

Figure 15: Proposed photodegradation pathway of SER (adapted from [140]).

In the case of FVX, Kwon and Armbrust (2005b) did not observe any notable hydrolysis. They did, however, observe photoisomerisation of the (E)-isomer to the (Z)-isomer under simulated sunlight (Figure 16). It occurred at all tested pH (5, 7 and 9) in two stages, where a slower second stage followed a faster first stage. The Φ for both stages at each pH can be found in Table 5. The isomerization was six- to seven times faster in humic and lake water than at pH 9. No other TPs were observed during the irradiation of FVX [141].

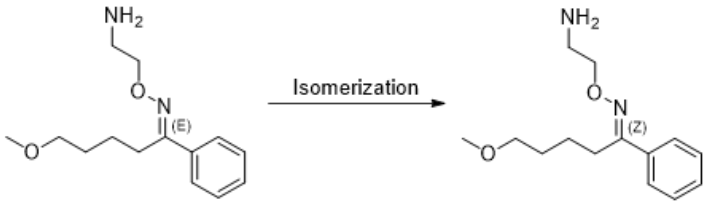

Figure 16: Photo-isomerization of FVX (adapted from [141]).

Table 5: Secondary rate constants and quantum yields of SSRI reported in the literature.

SSRI	Φ	k(SSRI + PPRI), L mol^{-1} s^{-1}		
		$HO^{\bullet}$	$CO_3^{\bullet-}$	$^1O_2$
FLU	a (4.2±1.5)x10^{-5} b (2.3/3.1/8.5)x10^{-5} c 0.41±0.042	a (8.4±0.5)x10^9 a (9.6±0.8)x10^9 c (9±1.8)x10^9	-	/
CIT	d 2.6x10^{-4}	/	/	/
PXT	e (2.71/3.26/3.77)x10^{-4} c 0.21±0.14	c (9.6±3.6)x10^9 f (8.65±0.12)x10^9	c (4.2±0.9)x10^8	f (1.18±0.13)x10^8
SER	/	/	/	/
FVX	g 1st stage: (5.51/5.16/8.55)x10^{-3} g 2nd stage: (1.91/2.19/1.87)x10^{-3}	/	/	/

[a] Lam et al., 2005

[b] Kwon and Armbrust, 2006 (at pH 5/7/9)

[c] Wols et al., 2014 (monochromatic lamp at 254 nm)

[d] Kwon and Armbrust, 2005a (at pH 9)

[e] Kwon and Armbrust, 2004 (at pH 5/7/9)

[f] Santoke and Cooper, 2017

[g] Kwon and Armbrust, 2005b (at pH 5/7/9)

Biodegradation

In the environment, pharmaceuticals can be further degraded by microbes. Although the biodegradability of contaminants has been thoroughly studied during WW treatment, few studies report biodegradation in SW specifically. The concentration of microorganisms capable of biodegradation is much lower than biological treatments in WWTPs. Additionally, most pharmaceuticals are not expected to undergo extensive biodegradation after entering the environment, especially after demonstrating recalcitrance to human metabolism and WW treatment [123]. In the class of SSRI, FLU is the only compound where aerobic biodegradation was explicitly studied in SW, estuarine water and seawater. Both Baena-Nogueras et al. (2017) and Benotti and Brownawell (2009) reported FLU as relatively labile, reporting half-lives of a few days and up to two weeks, depending on the conditions [142], [143].

Adsorption and stability in sediment

The sediment is an important reservoir for most SSRIs since their concentrations remain stable. Only PXT was shown to be sensitive to light even when adsorbed to sediment [67], [68], [123].

Bioaccumulation

SSRIs were one of the first human pharmaceutical classes found to bioaccumulate in fish tissue [55], [69], [70], [144]. Parent compounds and metabolites accumulate predominately in fish brains and liver but have been shown to accumulate also in other organisms such as crabs [58], [69], [144]. The reported bioaccumulation factors (BAFs) of SSRIs differ between species and are influenced by the pH of the water. The higher the pH, the less

ionized the SSRI, and the higher the BAF. From the SSRIs and their monitored metabolites, NS has the highest reported BAFs for brain, gonad, liver and muscle fish tissue in different species [58], [69], [70], [145], [146]. However, Boström et al. (2017) did not observe any biomagnification through the food chain for SER or FLU [147].

1.2.5 Ecotoxicity

SSRIs modulate the function of the neurotransmitter serotonin in the human body, which explains why aquatic organisms with a physiological system that also includes the serotonergic pathway can be affected by their presence [9], [148], [149]. Although the specific physiological role of serotonin in many species is unknown, it controls several biological functions, such as reproduction, metabolism and behavior. Thus, influencing this pathway is expected to manifest in many various effects.

As mentioned in Chapter 1.2.3, SSRIs have been detected in aquatic organisms. Acute and chronic toxicity has been studied on cell lines: PLHC-1 (Poeciliopsis lucidahepatoma cell), RTG-2 (rainbow trout gonadal cell line) [150] and several organisms ranging from bacteria (*Vibrio fischeri*), algae (*Pseudokirchneriella subcapitata, Scendesmus acutus, Scendesmus quadricauda, Chlorella vulgaris, Dunaliella tertiolecta, Scendesmus vacuolatus*), protista/protozoa (*Spirostomum ambiguum*), crustacean (*Daphnia magna, Ceriodaphnia dubia, Gammarus pulex, Thamnocephalus platyurus, Hyalella azteca*), gastropods (*Chlorostoma funebralis, Lithopoma americanum, Tegula fasciatus, Nucella ostrina, Potamopyrgus antipodarum*), mussels (*Lampsilis siliquoidea, Ligumia recta*), amphibians (*Xenopus laevis*) to fish (*Pimephales promelas, Gambusia affinis, Oryzias latipes, Oncorhynchus mykiss, Carassius auratus)*. SER and FLU are the most researched SSRI in this field, followed by CIT, PXT and FVX. These studies identified SER or FLU as the most ecotoxic compounds from the SSRI class. The endpoints observed in the studies were lethality, survival, growth inhibition, immobilization, adhesion to substrate, deformity, reproduction, number of offspring, foot movement, heartbeat, mobility, predator-prey behavior, feeding behavior, immunity, gene expression and endocrine responses. The determined median effective concentration (EC50) and median lethal concentration (LC50) determined for the estimation of acute toxicity of SSRIs were all in the range of a few 100 μg L^{-1} or even mg L^{-1}. Conversely, studies researching chronic toxicity reported no-observable-effect concentrations (NOEC) and lowest observable-effect concentrations (LOEC) at levels lower than 1 μg L^{-1}. Along with the findings from Christensen et al. (2007) and Minguez et al. (2018) that the toxicity of the SSRI is additive, this suggests that chronic toxic effects may already be observed at current environmental concentrations [56], [69], [145], [148], [151]–[165].

1.3 Analysis of SSRI in the Environment

As seen in the analysis of pharmaceuticals and other similar polar organic compounds, the analysis of SSRIs and their TPs in environmental samples considers sampling, storage, sample preparation and instrumental analysis.

1.3.1 Sampling

The most common types of sampling used for SSRI analysis were grab samples and composite samples. The simplest type, the grab sample, gives us information on the state of the environment at a specific time. However, this type of sampling does not account for environmental fluctuations and is hence not very representable. The alternative is to sample several grab samples over time and test them separately or take composite samples,

where the samples are combined before analysis. They can be either time or flow-proportional. Unfortunately, when taking composite samples, data on concentration variability is lost [166].

Although not widely used in SSRI analysis, passive sampling is also viable. It is based on the free flow of the analyte from the sample matrix to the receiving phase. The advantages of this type of sampling include a more representative result and *in situ* application with less sample preparation, such as filtration or centrifugation. However, it includes more initial optimization of the process [166], [167]. Biota can also be seen as a passive sampler in water matrices. However, by using a living organism, we must consider its metabolism, excretion, target tissue and movement patterns [166].

1.3.2 Storage

Storage generally depends on the analyte's stability (if known) and the analysis timeframe. For SSRI analysis, stabilization techniques are applied if the samples are not prepared immediately. Samples are either frozen at -80°C or -20°C or refrigerated and prepared in the next 12 to 72 hours [65], [168]–[176]. As an alternative, López-Serna et al. (2011) also suggested freezing samples loaded onto solid phase extraction (SPE) cartridges [177]. Stability testing was only performed on filtered (0.7 µm pores) spiked WW containing SSRI and their metabolites (PXT, CIT, FLU, NFLU, SER, NS) by Lajeunesse et al. (2008). The experiment confirmed their stability at 4°C in the dark for seven days, with losses $<$ 82 %.

1.3.3 Sample preparation

While in some recent studies, the preparation of aqueous samples only involves mixing and filtering the sample to decrease the time of analysis and sample manipulations, analysis of SSRIs still mostly includes an extraction step. Their environmental concentration is generally in the ng L^{-1} or ng g^{-1} range, which is difficult to detect without preconcentrating. In addition, extraction also reduces the effects of matrix [178]–[180]. Before extraction, some pre-preparation steps might be included. For example, additives are sometimes added (*e.g.*, EDTA), or pH is adjusted for better extraction recovery. Aqueous samples are commonly filtered to avoid clogging the cartridges, and solid samples are homogenized [63], [170], [171], [173], [174], [181]–[183].

The sample preparation of choice for aqueous samples is SPE, either in online or offline mode [180], [181], [184]. Commercially available cartridges of different chemistries are most commonly utilized. Cation-exchange sorbents are used when only SSRIs are determined since the molecules have an amino group that can be ionized. Mixed mode or reverse phase polymeric sorbents are used when other differently charged compounds are also targeted. Cases of mixing a range of different sorbents have also been reported [63], [67], [170], [171], [173], [180], [181], [183]–[188]. Other alternative extraction techniques that were applied include solid-phase microextraction [189], traditional liquid-liquid extraction [175], hollow-fiber liquid-phase microextraction [176] and gel electromembrane extraction combined with switchable hydrophilicity solvent-based homogeneous liquid-liquid microextraction [190]. These former techniques are based on non-specific binding. In cases where less matrix effect and better sensitivity are needed, specially tailored materials were also applied as SPE sorbents (*e.g.*, MIPs) [180], [191].

Liquid-solid extraction (LSE) and pressurized liquid extraction (PLE) were used to extract SSRIs from solid matrices. PLE, in general, results in higher recoveries and faster extraction rates and requires less extraction solvent [172], [180], [181], [184], [192]–[195].

1.3.4 Instrumental analysis

1.3.4.1 Analysis of SSRI in environmental samples

When analyzing SSRIs, reference standards of the compounds are readily available; therefore, the analysis performed is targeted. The current instruments of choice for targeted analysis of environmental contaminants are high-performance liquid chromatography (HPLC) or ultra-high-performance liquid chromatography (UHPLC) for compound separation coupled with a triple quadrupole (QQQ) or quadrupole-linear ion trap (Qtrap) for detection [55], [172], [173], [180], [181], [183], [187], [196]–[198].

In the case of SSRIs, liquid chromatography (LC) is favored over gas chromatography (GC) since GC-based methods require an additional derivatization step in order to make the compounds sufficiently volatile to ensure a good chromatographic response and relevant LOQ and limits of detection (LOD). Common silylating agents are inappropriate for SSRIs since they generally lack the appropriate functional group. Alternatively, pentafluoropropionic anhydride, heptafluorobutyric acid, acetic anhydride and (S)-(-)-trifluoroacetylprolyl chloride are viable options [184], [199]. LC separation of SSRI is usually performed on reverse phase C18 columns. Notable in later studies is the use of modified particles, particularly ethylene crosslinking, which provides greater stability at extreme pH of the mobile phase [169], [171], [173], [175], [185], [187], [195], [200]–[206]. Although the use of phenyl C18 columns has reportedly provided better chromatographic separation of the SSRI due to the additional influence of π-π interactions between the phenyl moiety on the column surface and the benzene rings present in their structure, they have seldom been applied in existing studies [170], [207].

For SSRI detection, the trend has shifted from using detectors, such fluorescence, UV/Vis and photodiode array (PDA) detectors, to single quadrupole mass analyzers, tandem mass spectrometers (MS/MS) and more recently to high-resolution MS (HRMS) [180], [193], [194]. MS detectors offer better sensitivity and selectivity, which are crucial in environmental samples that contain trace amounts of targeted analytes in complex matrices [180], [193]. MS/MS detection possible with QQQ and Qtrap is favored over MS detection because it enables an additional fragmentation step and, with it, even higher selectivity and usually higher sensitivity [198], [208]. Current guidelines also state that when a reference standard is available, the identity of a compound in a sample is confirmed based on matching retention times and at least two transitions per target, which cannot be achieved with MS-only detection [198], [209]. The acquisition mode generally used on QQQ and Qtrap instruments is the selected reaction monitoring (SRM) or multiple reaction monitoring (MRM), where precursor-product ion transitions are being monitored [198], [208]. In most cases, electrospray ionization (ESI) in positive mode is employed. The $[M+H]^+$ ion formed is most likely the result of protonation of the amino group that all of the SSRIs have in common [180], [184], [207]. This type of ionization is very susceptible to matrix effects, which can be modified by appropriate sample preparation or using atmospheric-pressure chemical ionization (APCI) that is less prone to ion-signal suppression [172], [175], [180], [184], [192], [210].

Although using instruments that enable MS/MS detection with a unit resolving power is still prevalent in target analysis, the use of HRMS instruments, such as quadrupole time-of-flight (Qtof) and Orbitrap, brings a specific set of advantages. The newer instruments have high enough sensitivity in full-scan acquisition mode to detect trace amounts of contaminants without the initial preselection of transition ions. They also enable additional advanced acquisition mode combinations (*e.g.*, data-dependent acquisition (DDA) and data-independent acquisition (DIA)) and offer the option of using accurate mass for additional identity confirmation [198], [211]. Examples of HRMS instruments used for

targeted SSRI determination include the studies by Gago-Ferrero et al. (2020) and Baduel et al. (2015), where emerging contaminants were analyzed in WW and fish tissue, including FLU, SER, CIT and NCIT. The authors based their findings on MS and MS/MS spectra obtained during DIA and DDA on LC-Qtof instruments [212], [213]. However, HRMS instruments are more commonly applied to the identification of compounds with no available reference standards [51], [198], [214].

1.3.4.2 Identification of TPs

SSRIs and their previously identified metabolites often have available reference standards and are predominately determined by targeted analysis, and there are only a few cases reported in the literature where their presence was detected during suspect or non-target analysis [202], [215]. These types of analysis are more commonly applied to TPs structure elucidation. In suspect screening, we have some initial information about the compounds we wish to determine, most commonly molecular formula and structure. Hence, prior to analyzing samples from existing literature, compound databases and knowledge-based pathway prediction software tools can be used to form a suspect list. In non-target or unknown screening, we have no prior information about the compounds to be detected [198]. In both types of screening, the high resolving power and mass accuracy of the HRMS is needed for the reliable identification of a compound [51], [198], [214].

Table 6 includes data on identifying SSRI TPs discussed in Chapter 1.2.4, formed during photo- or biodegradation studies. All TPs were identified in laboratory-scale experiments. For LC separation, either reverse phase or hydrophilic interaction chromatography (HILIC) columns were used, and in newer references, they were hyphenated with HRMS, which provides more reliable identifications. HRMS detection was performed in DDA when Orbitrap systems were used and in broadband collision-induced dissociation (bbCID) mode in Qtof instruments [82], [85], [134]. In both acquisition types, full-scan MS and MS/MS data are obtained within the same acquisition. Due to the data's complexity, commercial software was used in addition to manual processing by Gulde et al. (2016) and Beretsou et al. (2016). The software applied for the structure elucidation of SSRI TPs were Compound Discoverer, Sieve and Metabolite Detect.

The processing steps for HRMS data included exact mass filtering (differences in monoisotopic mass ≤ 5 ppm), peak detection (based on blank-subtraction, noise filtering, signal intensity, peak shape), isotopic pattern matching, MS/MS fragmentation matching and structure-retention relationships prediction modelling. Additionally, the formation profile of the potential TPs was observed. Information on the increase and decrease of a TP during the experiment helps to determine if we are dealing with a TP and what the possible degradation mechanism could be. Where standards were available, the TPs were confirmed by reference standard matching. The remaining unknown and suspect peaks were tentatively identified based on the obtained data using a confidence level system (Figure 17) proposed by Schymanski et al. (2014) [82], [85], [209].

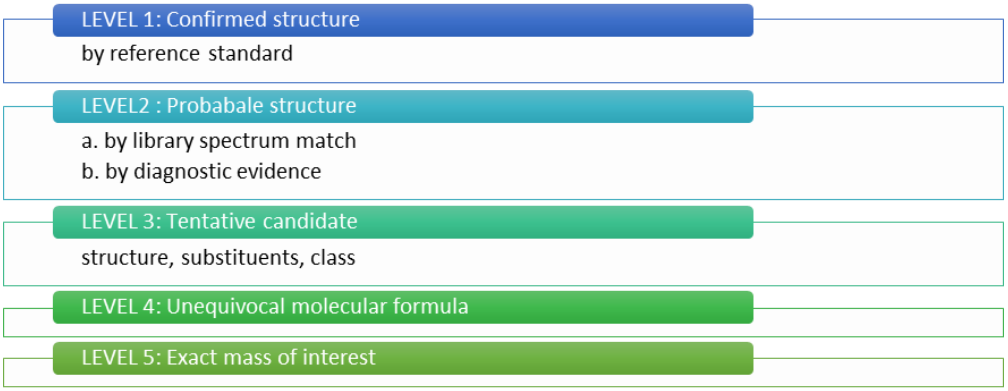

Figure 17: Confidence levels for HRMS compound identification as proposed by Schymanski et al. (adapted from Schymanski et al., 2014).

Jakimska et al. (2014) also used HRMS for TP identification; however, their report does not explain the details of their identification process [140]. Studies performed earlier when HRMS instruments were not widely available are typically based on identifying TPs using MS/MS or even just MS data. When reference standards of the TP were used for identification, the suggested structure still has a high confidence level, while in some cases, additional confirmation is needed. Alternative methods for additional confirmation were also applied in certain studies. For example, Sharma et al. (2011) confirmed the identities of the TPs with orthogonal techniques such as NMR and FTIR, while Lam et al. (2005) verified the structures of their defluorinated TPs and the one hydroxylated TP by irradiating standards of two other trifluoromethylated compounds, by performing the experiment in $H_2{}^{18}O$ [129], [135].

The next step after confirming the identity of a detected contaminant is its quantification. Determination of environmental exposure is crucial for toxicity risk assessment and monitoring prioritization [202], [216]. In order to determine the concentration of a contaminant, an available reference standard is necessary because the matrix effect and ionization efficiency vary between each compound. Hence, the measured height or area of the signals of different compounds are not comparable. Quantifying compounds in target analysis is, therefore, not a problem, while quantifying previously unknown TPs can only be achieved if standards are obtained. Instead, a semi-quantitative approach is often applied, where a structurally similar standard is used based on the assumption that the response of the target compound and the chosen standard is similar, as seen in the study of CIT TP formation by Beretsou et al. (2016). Typically the standard of the parent compound is used since it is, in general, readily available [51], [85], [198], [202], [216]. Other approaches include using a standard with a similar retention time or computational predictions based on ionization efficiencies and structural information [51], [216].

Table 6: Details on the identification procedure of SSRI TPs during biodegradation and photodegradation. ND - not defined, Photo - photodegradation, Bio – biodegradation.

SSRI/ degradation	Suspect list	Detection	Data analysis software	Identified TPs	Identification based on	Reference
FLU/Bio	EAWAG-PPS	HPLC-Orbitrap, DDA	Compound Discoverer 1.0; Sieve 2.2; MassFrontier 7.0	7	Ref. standard, exact mass, fragmentation pattern, isotopic pattern	[82]
CIT/Bio	EAWAG-PPS MetabolitePredict	UHPLC-Qtof, full scan, MS/MS	Metabolite Tools 2.0	14	Ref. standard, exact mass, fragmentation pattern, isotopic pattern	[85]
FLU/Photo	/	LC-QQQ-ESI, MS	ND	1	Ref. standard	[123]
FLU/Photo	/	LC-QQQ-ESI, MS/MS	ND	4	Parent mass, fragmentation pattern, retention time	[129]
FLU/Photo	/	LC-QQQ-ESI, MS/MS	ND	1	Ref. standard	[131]
CIT/Photo	/	LC-QQQ-ESI, MS	ND	2	Parent mass; Fragmentation pattern	[133]
CIT/Photo	EAWAG-PPS MetabolitePredict	UHPLC-Qtof, MS/MS	DataAnalysis 4.1	17	Exact mass, fragmentation pattern, isotopic pattern	[134]
CIT/Photo	/	LC-microTOF, MS/MS; NMR; FTIR	ND	3	Parent mass, fragmentation pattern	[135]
PXT/Photo	/	LC-QQQ-ESI, MS	ND	2	Parent mass, fragmentation pattern	[136]
SER/Photo	/	UHPLC-Qtof, MS/MS	Mass Hunter	10	Exact mass, fragmentation pattern (data not provided)	[140]

1.3.5 QA/QC

In order to guarantee the quality of produced data, a quality control (QC) and quality assurance (QA) system must be in place. Validation of the developed analytical method is one of the first levels of QA in a laboratory. In the International Vocabulary of Metrology (VIM), validation is defined as a "*provision of objective evidence that a given item fulfils specified requirements, where the specified requirements are adequate for an intended use*", *i.e.*, proving that our analytical procedure, applicable to a specified type of test material and chosen concentration range is fit for its intended purpose [217]–[219].

The extent of validation depends on the type of method. Different guidelines exist depending on the purpose of the method. However, the main characteristics that need to be addressed stay the same (Table 7). Validation of a method can be done in-house, for only one laboratory or expanded into a collaborative or interlaboratory study, comparing the validation parameters between different laboratories [219].

Table 7: Validation performance characteristics [217]–[221]. Definitions are cited from VIM. CRM – certified reference material.

Parameter	Definition	Expression
Accuracy	The closeness of agreement between a measured quantity value and a true quantity value of a measurand	Expressed with precision and trueness parameters
Precision	The closeness of agreement between indications or measured quantity values obtained by replicate measurements on the same or similar objects under specified conditions; is defined on three levels: (1) Repeatability or inter-assay precision: variability over a short time interval under the same conditions (2) Intermediate precision or within-lab variation due to random effects: variability over a longer period, under different conditions (3) Reproducibility or inter-laboratory variation: tested by collaborative studies.	- standard deviation (SD) - relative standard deviation (RSD) or % coefficient of variation (% CV) - confidence interval
Trueness	The closeness of agreement between the average of an infinite number of replicates measured quantity values and a reference quantity value	If CRMs are used: bias - an estimate of a systematic measurement error If CRMs are not available: % recovery of a known, spiked amount of analyte
Recovery	The proportion of analyte present in or added to the analytical portion of	% Recovery of a known, spiked amount of analyte

	the test material, which is extracted and presented for measurement	
Specificity	The ability to assess the analyte unequivocally in the presence of components which may be expected to be present, typically impurities, degradants, and matrix	Must be demonstrated: - for identification tests as % correct classification of negative and positive results - for quantitative tests as % recovery of samples, spiked with possible interferences
LOD	The lowest amount of analyte in a sample which can be detected but not necessarily quantitated as an exact value	3-times the SD of the baseline in the blank samples divided by the slope of the calibration curve or signal-to-noise ratio 3/1
LOQ	The lowest amount of analyte in a sample which can be quantitatively determined with suitable precision and accuracy	10-times the SD of the blank baseline divided by the slope of the calibration curve or signal-to-noise ratio 10/1
Linearity	The ability (within a given range) to obtain test results which are directly proportional to the concentration (amount) of analyte in the sample	Must be demonstrated, R^2 of the calibration curve, homoscedasticity test (weighting when necessary)
Robustness	A measure of its capacity to remain unaffected by small but deliberate variations in method parameters and indicates its reliability during normal usage	The measure of variability and reproducibility obtained under different conditions
Measurement uncertainty	Non-negative parameter characterizing the dispersion of the quantity values being attributed to a measurand, based on the information used	It comprises many components that can be evaluated based on their SD, from assumed probability distributions, based on experience or other information. Covariance between components needs to be established.

1.4 Molecularly Imprinted Polymers

Molecular recognition, the ability to differentiate between molecules, which is best represented by antibodies, enzymes and receptors, is the principle exploited in MIPs. MIPs are tailor-made polymers where a chosen template is imprinted during the polymerization process. After the template is removed from the polymer, we are left with selective recognition sites that roughly follow the “lock and key principle” (Figure 18) [222], [223]. The obtained MIPs are generally thermally and chemically much more stable compared to their biological counterparts. The extensive development in the preparation of MIPs, from specially designed ingredients and complex polymerization procedures to surface post-modifications, also enables us to tailor the MIPs according to the chosen application's specifications [224], [225].

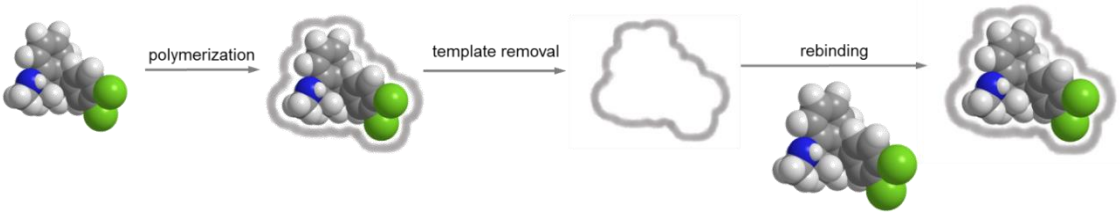

Figure 18: The schematic representation of imprinting (adapted from [225]).

1.4.1 Imprinting approaches

Depending on the type of interactions applied to bind the template, there are two main types of molecular imprinting: (1) non-covalent and (2) covalent. A third approach combines both types of interactions, known as the semi-covalent approach [223].

1.4.1.1 The non-covalent approach

In the non-covalent binding (established by van der Waals forces, hydrophobic, ionic, and hydrogen interactions), the binding sites are formed by self-assembly between the template and monomers, followed by cross-linked co-polymerization. After the removal of the template, the formed interactions between the target and monomer are again non-covalent. This strategy is utilized more often since the synthetic procedures and template removal is less complex. However, the interactions are weaker than covalent bonds; hence, we need several interactions at multiple docking points. Larger complex molecules are also harder to imprint because they are less rigid, and their secondary or tertiary structures might be affected during polymerization.

Additionally, their size might prevent their penetration into the polymer matrix in order to rebind. MIPs produced by this approach are more prone to non-specific interactions due to the excess monomer needed for the efficient formation of the pre-polymerization complex. Template leaching or bleeding is also a commonly reported problem [222], [223], [225], [226].

1.4.1.2 The covalent approach

The reversible covalent bond between the template and monomer is usually formed before the polymerization step and should withstand polymerization. Ideally, we should be able to cleave the template in mild conditions, and rebinding should be a fast process. A great deal of optimization is needed to achieve this. Nevertheless, in covalent bonding, the reported imprinting yields are better defined and the binding sites formed are more homogenous than non-covalent binding sites [223], [225].

1.4.1.3 The semi-covalent approach

The semi-covalent approach combines the previously mentioned advantage of having a reversible covalent linkage between the template and monomer during polymerization with the non-covalent binding of the target in the rebinding step. This combination should solve the problems of non-specific interactions, template leaching, non-homogenous binding sites and slow rebinding [223].

1.4.2 The building blocks

In order to succeed with MIP synthesis, the appropriate building blocks must be chosen. This choice can be made by studying the existing literature, by studying the non-polymeric

mode systems with analytical and spectroscopic methods or by applying *in silico* methods, *e.g.*, electronic structure methods and molecular dynamics simulations [222], [223]. The structure of the chosen template dictates what functional elements should be present in the ingredients, for example, a hydrogen donor/hydrogen acceptor complementary pair. The template must also be chemically inert and stable during polymerization [223], [227]. The functional monomers are the building blocks interacting and binding the template during the polymerization or later recognition. In contrast, the structural monomers form the polymeric network that shapes the recognition sites, supports the functional monomers and defines the mechanical stability of the polymer. For this reason, the latter are also referred to as cross-linkers [223], [227]. The solvent brings all the ingredients into one phase and is responsible for forming the porous structure; hence the name porogen is often applied. It also influences the stability of the pre-polymerization complex between the functional monomers and the template [227]–[229]. The most common procedure for the synthesis of MIPs is free radical polymerization. In order to start the reaction, we need to add radical initiators. The polymerization can be triggered and controlled by either heat, light, chemical or electrochemical means.

1.4.3 Types of polymerizations

The application of a MIP dictates the type of polymerization applied. The simplest MIPs are bulk and in-solvent polymers synthesized in confined spaces. There is a downside to the simplicity of its synthesis. After the polymerization, the polymer must be washed, dried, ground, sieved and sometimes even sedimented. These processes are time-consuming and yield irregularly shaped and sized particles. The binding sites are often hard to access, meaning the time to reach an equilibrium state can be long [222], [223], [227]. In order to get spherical particles and skip all the grinding and sieving, the MIPs are made by precipitation or emulsion polymerization. In both cases, the polymer is formed inside droplets of monomer. In the former, an emulsion between water and hydrophobic monomer is formed first; therefore, a surface-active agent is needed to stabilize the droplets and form micelles. In the latter, the droplets are formed during mechanical dispersion [222], [230]. The problem of slow mass transfer can be addressed with surface imprinting, such as grafting layers of MIP onto beads by retaining the radical polymerization at the surface [227], [230], [231]. The polymers can also be synthesized *in situ* to avoid additional handling of MIPs after polymerization, for example, in a column ready to be used right after the template removal [227], [232].

1.4.4 Characterization techniques

1.4.4.1 Evaluation of the binding characteristics

A few established methods are applied to evaluate the recognition characteristics of the synthesized MIP. The two most prevalent methods are batch rebinding and chromatography studies, while radioligand studies, calorimetry and solid phase extraction studies have also been applied [222], [223]. In batch rebinding studies, a known amount of material is incubated in solutions with known concentrations of the target. The target concentration left free in the solution (F) is often determined by spectroscopic techniques or HPLC. The amount of target bound to the polymer (B) is calculated from the data [222], [233]. When using chromatography for evaluation, the material must be packed into chromatography columns, considering particle shape and size. The parameter used to evaluate the material is the injected target's retention factor (k), calculated from the retention time (t_R). If the target exhibits a longer t_R, this stands as evidence of selectivity

[222], [223], [234]. Other studies apply the principles of frontal chromatography by continuously running a specific target concentration through the column and determining the breakthrough time or volume when the target appears in the eluent [222].

The MIPs' selectivity, affinity and capacity can be determined from the experimental data obtained. The first step is the construction of binding isotherms. They present the concentration-dependent recognition behavior typically plotted as B vs F (Figure 19).

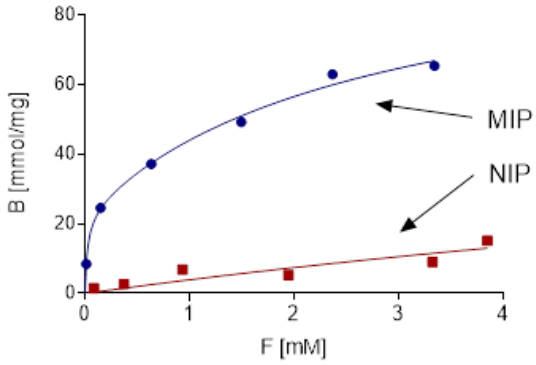

Figure 19: An example of a binding isotherm of the imprinted (MIP) and non-imprinted polymer (NIP).

The binding affinity can be evaluated by calculating the association constant (K_a) in L mol^{-1} or dissociation constant K_d (mol L^{-1}). If all the binding sites are identical the K_a can be expressed as $K_a = \frac{n_{bound}}{n_{empty}\, x\, F}$; where n_{empty} is the mols of empty binding sites and n_{bound} the mols of the bound target. Since n_{empty} is hard to determine, the affinity is more often expressed as n_{bound} or % of the bound target or as distribution ratio $D = \frac{B}{F}$ in L g^{-1} [222], [223], [229]. Binding capacity is similarly calculated in different ways; however, it is mainly reported as the equilibrium n_{bound} at a certain concentration [222], [235]. Selectivity can be reported as the imprinting factor (IF), comparing the MIP to its non-imprinted polymer (NIP) or a polymer imprinted with a different template. Alternatively, it can be evaluated by binding a competitor and expressed as the selectivity factor (α) [222], [223], [229]. The IF is the ratio between MIP and NIP's distribution ratios (D), while α is the ratio between the target D and competitor D. When we have sufficient data points, a binding model can be fitted. The fitting can be done either empirically or based on the number of binding sites and their affinities. The models are classified either as homogenous or heterogeneous. The former assumes that there is only one type of binding site, while the latter assumes the polymer has two or more types of binding sites [223]. The Langmuir isotherm (Eq. 1) is a homogenous model most often applied to homogenous systems such as enzymes and monoclonal antibodies (Table 8). In order to linearize the Langmuir equation, the Scatchard plots have been used, where $\frac{B}{F}$ is plotted against B and the Langmuir equation is rearranged into: $\frac{B}{F} = \frac{N}{K_d} - \frac{B}{K_d}$, where N is the number of binding sites [222], [223], [233]. Unfortunately, most MIPs do not fit into a homogenous model since they have different types of binding sites. Hence bi- or tri-Langmuir equations (Eq. 2-3) are applied to the data, taking into account two or three types of binding sites. However, the MIP could have a continuous range of binding sites. In that case the Freundlich isotherm (Eq. 4) is fitted to the data, where A [cm^{-3} mg^{-1}] and m (dimensionless) are empirical constants. Although it fits the data of several synthesized MIPs, its main disadvantage is that it

does not allow for saturation. A combination of both equations, a Langmuir-Freundlich equation (Eq. 5) has also been fitted to several MIP binding data [222], [223].

Table 8: Binding models of adsorption isotherms [222].

Model	Equation
Langmuir	$B = \frac{F\,x\,n}{K_d+F}$ (Eq. 1)
Bi-Langmuir	$B = \frac{F\,x\,n_1}{K_{d1}+F} + \frac{F\,x\,n_2}{K_{d2}+F}$ (Eq.2)
Tri-Langmuir	$B = \frac{F\,x\,n_1}{K_{d1}+F} + \frac{F\,x\,n_2}{K_{d2}+F} + \frac{F\,x\,n_3}{K_{d3}+F}$ (Eq. 3)
Freundlich	$B = A\,x\,F^m$ (Eq. 4)
Langmuir-Freundlich	$B = \frac{N\,x\,A\,x\,F^m}{1+A\,x\,F^m}$ (Eq.5)

The same experiments can also be applied to determine other parameters, *e.g.,* binding kinetics and the influences of temperature, pH, salt ions or other parameters on binding [222], [236], [237].

1.4.4.2 Evaluation of chemical characteristics

MIPs can be characterized by methods that can be applied to solid samples. For example, the percentage by mass of carbon, hydrogen and nitrogen can be obtained using elemental analysis. Similarly, Fourier-transform infrared spectroscopy (FTIR) and solid-state ^{13}C nuclear magnetic resonance (NMR) can be used to garner information on the composition of the polymer (distinctive functional groups) from characteristic diagnostic signals. The degree of polymerization can also be estimated with both techniques from peaks corresponding to unreacted double bonds [228], [233], [238].

1.4.4.3 Evaluation of physical characteristics

Surface area and porosity can be measured using nitrogen sorption or mercury intrusion porosimetry. The former is used more often since it is better at probing smaller pores. The information obtainable with these measurements are surface area ($m^2\ g^{-1}$), specific pore volume ($mL\ g^{-1}$), average pore diameter and pore size distribution [228]. Solvent uptake or swelling experiments are often performed to gain an estimation of the specific pore volume [228], [233], [234]. Lastly, scanning electron microscopy can be used to understand the macroporous morphology of MIPs better [228], [233].

1.4.5 Applications in environmental sciences

The advantages of MIPs have been exploited in many fields, from chemistry, biotechnology, pharmacy and environmental sciences. In the latter, the main researched applications are chromatographic stationary phases, sample preparation, sensor technology and water purification [239]–[243]. The main problems encountered in the environmental application of MIPs are water compatibility and bleeding of the template.

MIPs can be packed into HPLC columns as the stationary phase and used for analytical or preparative separations [223]. They are commonly used for separating chiral compounds [241]. There have been a few drawbacks reported, such as poor column efficiencies, severe tailing and peak broadening because of the slow mass transfer; nevertheless, these deficiencies are being overcome by the continuous advancements in MIP production [223], [241], [244], [245].

MIPs can also be used as the recognition element of a sensor, which is responsible for recognizing and binding the target. It is connected to the interrogative transducer that translates the chemical signal into a quantifiable signal. They can be optical, electrochemical or mass sensitive [223], [246]. The research in this area is already quite extensive, especially for cases where MIP-based sensors can be used as an alternative to biosensors, which rely on antibodies, enzymes or receptors as recognition elements, with obvious drawbacks [223], [239], [247].

The most researched area for MIP application is the use in sample preparation, more specifically in SPE. The main principle and procedure of MIP-packed cartridges are the same as with other SPE sorbents. They are already commercially available for specific analytes or groups of analytes [41], [248], [249]. The main advantages of using MIPs should be the reduced matrix effect and the possibility of reusing the material. One major drawback, especially in the field of environmental analytical chemistry, where analytes are found in trace concentrations, is the bleeding of the template leftover from the imprinting, although this can sometimes be avoided by imprinting a dummy template [223], [242], [250].

MIPs have also been included in the search for more effective WW treatment techniques. For example, they have been used as adsorbents that bind problematic molecules, such as endocrine-disrupting chemicals, pharmaceuticals, metal ions and pesticides [222], [238], [243], [251]. There has not yet been a large-scale application of MIPs for water clean-up, although Le Noir et al. (2009) coated Kaldness carriers in an imprinted cryogel for removing 17b-estradiol, 2-nonylphenol and atrazine. These carriers usually are used for cultivating microorganisms as a part of biological treatment [222], [252].

1.4.6 MIPs for SSRI recognition

MIP technology has also been studied for SSRI recognition. Table 9 lists the templates used, the intended targets, the tested matrix and their application. Most studies used FLU as the template and target since it was the most frequently prescribed SSRI in the past. In the case of ESC, most MIPs were synthesized to separate ESC from (R)-citalopram, successfully imprinting only one optical isomer. A few studies also imprinted SER; however, PXT has not yet been used as a template. The produced MIPs were used as sensors for SPE or other types of extractions (*e.g.*, stir bar) and chromatographic separation. Except for Demeestere et al. (2010), the MIPs were applied to biological samples or pharmaceutical formulations [41]. They have not yet been used for trace-level analysis in environmental matrices or water purification. The only MIPs used for SPE of river water and WW are part of the SupelMIP trademark of Sigma Aldrich, and therefore data on the synthetic procedure, format and template are not available. Demeestere et al. (2010) reported superior SPE recoveries for SSRI extractions compared to other tested antidepressants. Nevertheless, compared to commercially available Oasis HLB cartridges, the LODs, extraction recoveries and matrix ion suppression were similar when the washing step of the extraction was optimized. Unfortunately, the cartridges can no longer be purchased [249].

Table 9: List of SSRI imprinted polymers. VEN – venlafaxine, DUL – duloxetine, ND – not defined.

Template	Target	Format	Matrix	Application	Reference
ND	PXT, FLU, CIT	SupelMIP antidepressant commercial SPE cartridges	river water, WW effluent, influent	SPE	[41]
FLU	FLU, CIT, FVX, SER, VEN, DUL	precipitation polymerization with modifications	plasma	on-line SPE	[253]
FLU	FLU	precipitation polymerization	plasma, capsules	sensor	[254]
FLU	FLU	coprecipitation onto magnetic chitosan/graphene oxide	water, urine, capsules	SPE	[255]
FLU	FLU	precipitation polymerization	capsules, plasma, urine	SPE	[256]
FLU, DUL	FLU, DUL	bulk polymerization	phosphate buffer	extraction	[257]
FLU	FLU	precipitation polymerization	pharmaceutical formulations	sensor	[258]
CIT	CIT	bulk polymerization	water (varied pH)	controlled release	[259]
CIT	CIT	precipitation polymerization	serum, urine	SPE	[260]
ESC	ESC	coating, bulk polymerization	water (varied pH, ionic strength)	stir bar extraction	[261]
ESC	ESC, desmethyl-ESC	coating, bulk polymerization	urine	stir bar extraction	[262]
ESC	ESC	grafting	/	chromatographic separation	[241]
ESC	ESC	precipitation polymerization	urine	sensor	[263]
carboxy- ESC	ESC	grafting	urine	SPE	[264]
SER	SER	precipitation polymerization	tablets, urine, serum	sensor	[265]
SER	SER	grafting	urine, plasma	SPE	[266]
SER	SER	precipitation polymerization	tablet, serum	sensor	[267]
FVX	FVX	bulk polymerization	serum	sensor	[268]
FVX	FVX	bulk polymerization	urine, plasma	SPE	[269]

Chapter 2

Aims and Hypotheses

The surge in the number of reports detecting antidepressants in environmental matrices combined with data indicating serious sublethal toxic effects has highlighted the need to investigate their behavior in the environment after they leave the human body. The work focuses on a class of antidepressants called SSRIs. This class includes the most prescribed antidepressants and some of the most prescribed pharmaceuticals in Europe and the USA. Excluded from this study are unregistered compounds. Additional research into FVX was also deemed less pressing than other SSRIs since environmental concentrations have not yet reached concerning levels. Although the fate of FLU and CIT (and consequently ESC) has been researched, information is lacking on the fate of SER and PXT. However, they were all included in MIP application studies as model compounds. This thesis also investigated MIPs as tools to improve existing analytical methods and as a form of WW treatment. The former application included implementing MIPs in sample preparation, taking advantage of their molecular recognition ability, potentially lowering the matrix effect and increasing the extraction recoveries. Taking advantage of the fact that SSRIs are prone to adsorb to solid particles, we also studied the possibility of using the MIPs as part of WW treatment, comparing it to the existing non-specific tertiary treatment with AC.

In order to fill the discovered knowledge gap on SSRI behavior and to determine the benefits of different MIP applications, the aims of this thesis were:

1) development, optimization and validation of analytical methods for quantification of selected SSRI and identification of their TPs in aqueous samples;

2) determination of SSRI levels in Slovenian WW and receiving SW;

3) investigation of the least studied SSRIs, namely SER and PXT breakdown during photodegradation and identification of their TPs;

4) investigation of SER breakdown during biodegradation and identification of TPs and assessment of removal efficiency of SER during biological treatment;

5) synthesis and performance evaluation of MIPs, when used as SPE sorbents;

6) synthesis and performance evaluation of MIPs used as WW treatment technique.

In this frame, the following hypotheses were tested:

H1: Photodegradation is the main degradation pathway of SER and PXT in SW. During sunlight irradiation, TPs are formed.

H2: SER is only partially biodegradable. TPs are formed during SER biodegradation.

H3: SER and PXT and their residues are present in Slovenian SW and WW.

H4: Besides the original template compound, MIPs can rebind structurally related analogues, metabolites and TPs.

H5: MIPs can be used as sorbents for SPE of SER and its residues.

H6: MIPs can be utilized to remove SSRI and its residues from WW.

Chapter 3

Publications

The outcomes of this thesis are included in five scientific publications and divided into two fields:

1) Chapter 3.1: Environmental fate of SSRIs
   - I. Determination and photodegradation of sertraline residues in aqueous environment.
   - II. Phototransformation study of the antidepressant paroxetine in surface waters.
   - III. Biotransformation study of antidepressant sertraline and its removal during biological wastewater treatment.
2) Chapter 3.2: Application of MIPs in SSRI environmental analysis and water treatment
   - I. Preparation of molecularly imprinted copoly(acrylic acid-divinylbenzene) for extraction of environmentally relevant sertraline residues.
   - II. Molecularly imprinted polymers for the removal of antidepressants from contaminated wastewater.

3.1 Environmental Fate of Selected SSRI

3.1.1 Determination and photodegradation of sertraline residues in aqueous environment

The paper "Determination and photodegradation of sertraline residues in aqueous environment" by T. Gornik, A. Vožič, E. Heath, J. Trontelj, R. Roškar, D. Žigon, D. Vione and T. Kosjek was published in *Environmental Pollution* in January 2020. Together with Assoc Prof Dr T. Kosjek and Prof Dr D. Vione, I prepared the experimental design. I was responsible for the experimental work, method optimization and validation, data analysis and writing of the majority of the manuscript with assistance from A. Vožič in sample preparation and from Assist Prof J. Trontelj, Prof R. Roškar and Dr D. Žigon in sample analysis. The processing of the laboratory scale data with the "Aqueous Photochemistry of Environmentally occurring Xenobiotics" (APEX) software and the TP toxicity prediction was performed by D. Vione. The work was supervised and guided by Assoc Dr T. Kosjek and Prof Dr E. Heath.

Based on the number of prescriptions, occurrence and ecotoxicology data for different SSRIs, SER is the compound that should be investigated more in-depth [55], [69], [182], [200]. Hence, this study focused on the transformations of SER in SW under sunlight and the mechanisms behind it. Rate constants between SER and different photosensitizers and reaction quenchers were determined in laboratory-scale irradiation experiments, which enabled us to predict SER phototransformation kinetics using the APEX software. SER photodegradation followed pseudo-first-order kinetics dominated by direct photolysis with a quantum yield of 0.95. Indirect photolysis occurring in the presence of certain reactive species (e.g., $OH^{\bullet}$, $CO_3^{-\bullet}$, $^3CDOM^*$) additionally accelerated its degradation rate. The findings were validated by irradiating SER-spiked SW with sunlight. Structures of five TPs were suggested, and three were also detected in the sampled Slovenian SW. The ECOSAR toxicity prediction software indicated that these TPs would either be comparably or less toxic than the parent compound.

This work fulfils the following thesis aims 1) develop, optimize and validate analytical methods for quantifying target SSRIs and identifying their TPs in aqueous samples with different analytical techniques (GC-MS, LC-UV, LC-MS/MS); 2) to investigate SER breakdown during photodegradation and identify its TPs and 3) determine SER residues in SW.

The work is unique because it studies in-depth SER photodegradation, including laboratory scale experiments, photochemical modeling, and even sunlight-irradiated SW experiments. Additionally, the TPs formed during these experiments were identified. Three were previously detected during photodegradation experiments, while two were observed during biodegradation experiments in soil enriched with biosolids. The results also confirm the presence of three identified TPs in actual SW samples. The paper thus provides essential insights into SER behavior after entering the environment and establishes photodegradation as an important SER transformation pathway.

Environmental Pollution 256 (2020) 113431

Contents lists available at ScienceDirect

Environmental Pollution

journal homepage: www.elsevier.com/locate/envpol

Determination and photodegradation of sertraline residues in aqueous environment☆

Tjasa Gornik [a, b], Anja Vozic [c], Ester Heath [a, b], Jurij Trontelj [c], Robert Roskar [c], Dusan Zigon [a], Davide Vione [d], Tina Kosjek [a, b, *]

[a] Jozef Stefan Institute, Department of Environmental Sciences, Jamova 39, Ljubljana, Slovenia
[b] Jozef Stefan International Postgraduate School, Jamova 39, Ljubljana, Slovenia
[c] University of Ljubljana, Faculty of Pharmacy, Department of Biopharmacy and Pharmacokinetics, Askerceva 7, Ljubljana, Slovenia
[d] University of Turin, Department of Chemistry, Via Pietro Giuria 5, Torino, Italy

ARTICLE INFO

Article history:
Received 7 August 2019
Received in revised form
15 October 2019
Accepted 17 October 2019
Available online 23 October 2019

Keywords:
Sertraline
Environment
Water
Photodegradation
Transformation product

ABSTRACT

Sertraline is an antidepressant drug that has been frequently reported in the aquatic environment and biota. While the research has mostly dealt with its occurrence and toxicity, there is a lack of information pertaining to its environmental transformation. The present study aimed to fill in these gaps by giving an insight into mechanisms of sertraline phototransformation in surface waters, which was recognized as the main transformation pathway for this contaminant.

We performed photodegradation experiments in presence of photosensitizers or reaction quenchers to determine rate constants and used them to predict sertraline phototransformation kinetics by "Aqueous Photochemistry of Environmentally occurring Xenobiotics" (APEX) software. It was established that sertraline degrades by pseudo-first order kinetics mostly dominated by direct photolysis, while the presence of certain reactive species including $^{\bullet}OH$, $CO_3^{\bullet-}$ and $^3CDOM^*$ further accelerate the compound's breakdown rate. To validate the predicted results, sertraline-spiked surface water was irradiated by sunlight, where the half-life of sertraline at around 1.4 days was estimated. While following the photodegradation kinetics, we also identified five transformation products, of which three were determined in Slovenian surface waters. According to the ECOSAR toxicity prediction, these transformation products will either have comparable or lower toxicity than their parent compound.

1. Introduction

The presence of pharmaceutical residues in environmental waters has become an established phenomenon all over the world. These compounds enter wastewater (WW) through human excretion and inappropriate disposal (Vasskog et al., 2006), especially since their removal in WW treatment plants is often incomplete (Lajeunesse et al., 2012; Vasskog et al., 2006).

The focus of our study is the antidepressant sertraline (SER), (1S, 4S)-4-(3,4-dichlorophenyl)-N-methyl-1,2,3,4-tetrahydronaphthalen-1-amine. Before entering the environment, the drug is metabolized in the liver. N-desmethylsertraline or norsertraline (norSER), is the major metabolite. *In vitro* studies also report on the formation of sertraline ketone (SEK), N-hydroxy-sertraline and sertraline carbamic acid in the Phase I metabolic reactions. Glucoronidation is the main reaction of its Phase II metabolism (De Vane et al., 2002). Both the parent drug and norSER have already been detected in the range of ng L^{-1} in surface waters (SW) and WW (Golovko et al., 2014; Lajeunesse et al., 2012; Schultz et al., 2010). SER reportedly also accumulates both in sediments and aquatic organisms, affecting locomotor activity, feeding behavior, predator-prey interactions and reproduction (Hedgespeth et al., 2014; Kwon and Armbrust, 2008; Minguez et al., 2015). The groups of Kuzmanović et al. (2016) and Osorio et al. (2016) determined SER to be one of the main emerging contaminants contributing to chronic toxic effects in four river basins in Spain (Kuzmanović et al., 2016; Osorio et al., 2016).

In the environment, organic pollutants are subjected to biotic and abiotic degradation processes, among which hydrolysis, photodegradation and microbiological degradation are most common. SER is known to be hydrolytically stable and poorly biodegradable, thus photodegradation is potentially its main natural removal

☆ This paper has been recommended for acceptance by Charles Wong.

* Corresponding author. Jozef Stefan Institute, Jamova 39, 1000, Ljubljana, Slovenia.
E-mail address: tina.kosjek@ijs.si (T. Kosjek).

https://doi.org/10.1016/j.envpol.2019.113431
0269-7491/

process (Lam et al., 2004; US Environmental Protection Agency, 2016). During degradation processes structural changes of the parent compound can occur, resulting in the formation of transformation products (TPs). The chemical structures of TPs are not necessarily identical to metabolites formed in the human body therefore exposure and risks related to their occurrence in the environment should be assessed, starting with the definition of their exact structures and the assessment of their formation kinetics, which are amongst the principal aims of this study.

Jakimska et al. (2014) have carried out photodegradation experiments of SER under natural solar irradiation and using a xenon lamp. The impacts of matrix and pH on degradation kinetics were followed, but except for the finding that autocatalytic reactions occurred in the photodegradation mixture, there were no solid conclusions made in regards to the effects of different water matrices (Jakimska et al., 2014). To improve the lacking knowledge in this field, we aimed to assess the effect of direct (DP) and indirect photolysis on SER phototransformation kinetics and TP formation by measurements of photochemical reactivity on adopted laboratory systems, which were intended to measure the kinetic parameters rather than to mimic the environment. The rationale is that it is not possible to perform laboratory experiments that are representative of the environmental conditions even if natural water samples are irradiated, since there are several variables that are difficult to include in the experimental design (e.g., depth of the water column) (Bianco et al., 2015). Instead, to improve the understanding of the photochemical behavior of natural waters, one has to model photoreactivity in deep waters and, to do so, DP quantum yields and second-order reaction rate constants are needed. With the partial exception of the processes mediated by the excited triplet states of chromophoric dissolved organic matter (^{3}CDOM*) (Wenk and Canonica, 2012), these parameters are almost independent of the experimental conditions. Therefore, the laboratory photodegradation experiments should focus on accuracy rather than on similarity to SW chemistry (Bodrato and Vione, 2014). For these reasons, we accomplished our research by the following steps: (*i*) laboratory measurements of SER photoreactivity parameters under UV lamps; (*ii*) photochemical modelling of SER photo-fate in shallow solutions; (*iii*) validation of our photochemical model by comparing its prediction results with the behavior of SER in river water under natural sunlight, and (*iv*) prediction of the photochemical behavior of SER in sunlit natural water bodies. In all breakdown experiments we also followed the formation of TPs and investigated their presence in Slovene rivers.

2. Materials and methods

2.1. Standards, chemicals and materials

The list of standards, reagents and chemicals can be found in the Supplementary material (SM), Chapter 1.1. and the preparation of standard and working solutions in Chapter 1.2.

2.2. Analytical method

2.2.1. Method development and validation

Samples for the preliminary study of SER degradation kinetics (initial concentration of 10 $\mu g\,L^{-1}$) were analyzed by gas chromatography coupled to mass spectrometry (GC-MS; Table 1, Method 1) after appropriate sample preparation with solid phase extraction (SPE) reported in Table 1. In cases where no SPE preconcentration was needed (initial concentrations of 1 $mg\,L^{-1}$ and 10 $mg\,L^{-1}$), the sample was withdrawn, transferred into LC sample vial, diluted if appropriate and analyzed by an ultra-high performance liquid chromatograph coupled to a hybrid quadrupole-linear ion trap mass spectrometry analyzer (UHPLC-QqLIT-MS/MS, Table 1, Method 2). The structural characterization of TPs in these samples was performed by an UHPLC-hybrid quadruple time-of-flight mass spectrometer (UHPLC-QToF MS).

SW samples were analyzed by UHPLC-QqLIT-MS/MS after SPE cleaning (Table 1, Method 3).

Internal standard (IS) deuterated SER (SER-D_3) was added to samples before undergoing SPE at the concentration of 2.5 $\mu g\,L^{-1}$ (Method 1) or 20 $ng\,L^{-1}$ (Method 3), and deuterated bupropion (BUP-D_9) was added to the first fraction of eluate (4 × 0.6 mL of methanol) from SW samples in Method 3 at the concentration of 10 $ng\,L^{-1}$ to cover for SEK instrumental analysis. Eluates were nitrogen dried at 40 °C before redissolving them in the injection solvent. More details on the instrumental operation are given in SM, Chapter 1.3.

The method performance was evaluated by estimating linearity, trueness, repeatability, sensitivity, matrix effect and recovery. The information on the exact determination of each parameter can be found in SM, Chapter 1.4.

2.3. Photodegradation experiments

2.3.1. Laboratory scale measurements for parameter modelling

Laboratory scale experiments were performed in a cylindrical glass reactor by exposing 760 mL of MQ aqueous solutions of SER to UV irradiation, at initial SER concentrations of approximately 10 $\mu g\,L^{-1}$ and 1 $mg\,L^{-1}$ (Fig. S-1). A medium pressure mercury lamp (MP, 125 W, 3010/PX0686 Photochemical Reactors Ltd, London, UK) was used as the source of UV radiation. A filter of borosilicate glass was used to cut off transmission below 300 nm. The intensity of the lamp was determined with ferrioxalate actinometry as 1.41×10^{-6} E s^{-1}, according to the procedure adapted from Kete (2008) and Murov et al. (1993) (Kete, 2008; Murov et al., 1993). The spectra of SER absorbance and the relative intensity spectra of the MP lamp equipped with the filter are provided in the SM (Fig. S-2).

Degradation kinetics was described with the pseudo-first order

Table 1
Specifications of sample preparation and analysis for Methods 1, 2 and 3. MeOH – methanol, EtAc – ethyl acetate, TEA – trimethylamine, FA – formic acid, Ac_2O – acetahydride.

Method	Instrumental analysis	Matrix	Cartridges	Sample volume [mL]	Flow rate [mL min^{-1}]	Conditioning	Equilibration	Washing	Elution	Derivatization	Injection solvent
Method 1	GC-MS	MQ	Oasis HLB	200	1–2	3 mL EtAc 3 mL MeOH	3 mL MQ water	3 mL MQ	3 × 0.6 mL 2% TEA in MeOH	15 µL of Ac_2O 5 µL of pyridine	500 µL EtAc
Method 2	LC-MS/MS	MQ	/	1	/	/	/	/	/	/	MQ W
Method 3	LC-MS/MS	SW	Strata XC	250	6–7	3 mL MeOH	3 mL acidified W (pH 2)	4 mL 0.1 M HCl; 2 mL 20% MeOH in W	4 × 0.6 mL MeOH; 3 × 0.6 mL 5% NH_4OH in MeOH	/	100 µL 20% MeOH in 0.1% aqueous FA

degradation rate constant (k'_{SER}) and half-life ($t_{1/2}$) of SER at specified concentrations. The exposure times were adapted on the basis of the observed degradation rate. In case of UHPLC-MS/MS analysis 1-mL sub-samples were withdrawn from the same photodegradation experiment, whereas in case of the GC-MS analysis a 200-mL sample for each time point was withdrawn from an individual photodegradation experiment. Analyses were performed in duplicates. Repeatability of the photodegradation experiments was determined as the relative standard deviation (RSD) between three replicate experiments at the initial concentration of 1 mg L^{-1} and with the addition of 1 mM $NaNO_3$. The RSD is reported for three time points (0, 30, 120 min).

In the experiments, we investigated the influence of pH and of radical sources or scavengers: $NaNO_3$ (1.0 mM), 2-propanol (2-P; 0.3 μM, 3.0 μM, 30 μM), $NaHCO_3$ (0.50, 1.0, 10 mM), NaH_2PO_4 (1.0, 10 mM), Rose Bengal (RB; 10 μM), anthraquinone-2-sulfonic acid sodium salt monohydrate (AQ2S; 3.0 μM) on degradation kinetics. The additives were chosen based on the requirements of the modelling software (see segment 2.4 Photochemical modelling). In direct photolysis experiments, for the pH 5.0 adjustment we used acetate buffer (4 mM) and for pH 12.0 the 4 mM phosphate buffer. Along with the degradation kinetics study, we followed the formation of TPs. The potential toxicity of SER and the formed TPs has been predicted with ECOSAR software and can be found in SM, Chapter 6.

2.3.2. Photodegradation in surface waters

The SW solar irradiation experiments were performed in 1000 mL of SW sampled from river Gradaščica (46°02′29.4″N 14°29′16.0″E), spiked at SER initial concentrations of 50 ng L^{-1} and 1000 ng L^{-1}. The chemical parameters of the SW were monitored before starting the experiment. The concentration of nitrite and nitrate ions, dissolved organic carbon (DOC) and chemical oxygen demand (COD) were determined using Hach reagents for water analysis (see Table S–4 for details). pH was measured with a pH meter from WTW, Wissenschaftlich-Technische Werkstätten GmbH (Weilheim, Germany) and dissolved oxygen (DO) with a HQ30d probe from Hach (Düsseldorf, Germany). The irradiation lasted for 504 h, of which 148.2 were sun hours. The experiment was executed at 45°58′10.6″N 14°41′53.7″E. The irradiation data was collected at the closest weather station, 25 km away, where the solar hours were determined with a heliograph with a threshold between 100 and 150 W/m^2 of direct irradiation.

Along with the solar irradiation experiments the same matrix spiked with the same amount of SER was irradiated using UV/VIS MP lamp as described in 2.3.1.

2.4. Photochemical modelling

The model assessment of SER photodegradation was carried out with the APEX software (Aqueous Photochemistry of Environmentally-occurring Xenobiotics), available for free as Electronic Supplementary Information of Bodrato and Vione (2014). The specific requirements are reported in SM, Chapter 3.1.

3. Results and discussion

3.1. Development and validation of the analytical method for SER determination in aqueous environment

Table S–1 reports the validation parameters for the three developed methods described in Chapter 2.2.1. The LOQ of Method 1 was too high to tackle environmental levels of SER, while the UHPLC-QqLIT-MS/MS method was favored due to its simplicity and sufficient sensitivity. Method 3 is the environmentally applicable one; it showed satisfactory repeatability and trueness and was validated in the relevant concentration range (Table S–1). The trueness error and RSDs at the HC and LC standard additions in SW samples were both below 15% confirming that Method 3 can be successfully applied for quantifying SER and its TPs in SW matrices (Table S–1).

3.2. SER laboratory scale photodegradation for parameter modelling

Photodegradation of SER followed pseudo-first order kinetics. The degradation constants and half-lives for different photodegradation experiments are listed in Table 2. Half-lives ranged from less than an hour to more than 2 days, depending on the reaction conditions, such as the addition of photosensitizers or quenchers, pH and SER concentration. As shown in Table 2 and Fig. S-3, higher SER concentration yielded a decrease in the photodegradation rate. The experiment repeatability (RSD) was <6.6% for all three time points.

3.2.1. Direct photolysis and impact of pH on the degradation constant

In order to evaluate the influence of pH on SER direct photodegradation, we performed the experiments at different pH values, e.g., at pH 5.0, pH 7.0 and pH 12.0. The pH 7.0 was chosen to reflect natural conditions, while the pH 5 and 12 were chosen to observe if the ionization of the compound influences the degradation time and kinetics. Because of the presence of an amino group and pKa of 9.47, at chosen pH the compound is either fully protonated (pH 5 and 7) or in neutral form (pH 12) (Bergersen et al., 2015). The results (Table 2 and Fig. S-4) proved that photodegradation is pH-dependent, resulting in fastest degradation at the alkaline pH, which is in agreement with the findings for the other selective serotonin reuptake inhibitors (Kwon and Armbrust, 2006, 2005a; 2005b, 2004). We chose to perform the remaining experiments at pH 7.0 as an approximation of natural pH. At pH 7, the calculation of the DP quantum yield of SER (see SM, Chapter 3.2) gave $\Phi_{SER} = 0.95$. This value is quite high, for example the reported quantum yields of carbamazepine and atrazine are $7.8 \cdot 10^{-4}$ and $1.58 \cdot 10^{-2}$, respectively. When the Φ_{SER} value is combined with the absorption of radiation by SER that is extended up to around 450 nm (Fig. S-2), it suggests that the DP is likely to be a very important phototransformation process for SER in natural waters (Bodrato and Vione, 2014).

3.2.2. Reaction with •OH

Amongst the sources of •OH we selected nitrate. The reason is that it gives better estimations of the •OH reaction rate constant

Table 2
Pseudo-first order degradation constant (k'_{SER}) and $t_{1/2}$ of SER in the irradiated MQ solution with different additives.

Concentration	10 μg L^{-1}		1 mg L^{-1}	
Conditions	k'_{SER} [s^{-1}]	$t_{1/2}$ [h]	k'_{SER} [s^{-1}]	$t_{1/2}$ [h]
pH 5.0 ± 0.1	$<1.7\times10^{-6}$	>60	$<1.7\times10^{-6}$	>60
pH 7.0 ± 0.1	1.7×10^{-5}	11.6	6.7×10^{-6}	28.9
pH 12.0 ± 0.1	3.3×10^{-5}	5.78	1.7×10^{-5}	11.6
1 mM $NaNO_3$	1.0×10^{-4}	1.93	1.7×10^{-5}	11.6
1 mM $NaNO_3$ + 0.5 mM $NaHCO_3$	1.2×10^{-4}	1.65	6.7×10^{-5}	2.89
1 mM $NaNO_3$ + 1.0 mM $NaHCO_3$	2.7×10^{-4}	0.72	1.0×10^{-4}	1.93
1 mM $NaNO_3$ + 10 mM $NaHCO_3$	8.3×10^{-4}	0.23	1.5×10^{-4}	1.28
10 μM RB	3.5×10^{-4}	0.55	2.7×10^{-4}	0.72
3.0 μM AQ2S: 1st stage	5.7×10^{-4}	0.34	8.3×10^{-4}	0.23
3.0 μM AQ2S: 2nd stage	1.3×10^{-4}	1.44	1.7×10^{-5}	11.6

than nitrite, whose quantum yield of $^{\bullet}OH$ formation varies in the solar UV range, which is not the case with nitrate. In the experimental setup we added 1.0 mM of NO_3^-, which induced a degradation kinetics that was ideal for SER degradation monitoring. As expected, the degradation rate in the presence of $^{\bullet}OH$ radicals was notably higher as compared to the DP (Table 2). 2-P was added at final concentrations of 0.3 μM, 3.0 μM, 30 μM to the reaction mixture for determining the second-order reaction rate constant between SER and the formed $^{\bullet}OH$. 2-P works as $^{\bullet}OH$ scavenger and competes with SER for $^{\bullet}OH$ reaction, resulting in a decrease in the SER degradation rate (Fig. S-7). The kinetic model used to describe $^{\bullet}OH$ degradation took into account the occurrence of acetonitrile in the system, which derived from the dilution of the SER stock solution in this solvent. The exact mechanism and calculations can be found in SM, Chapter 3.3 (reactions S1−S5) (Vione et al., 2011). The calculated reaction rate constant between SER and $^{\bullet}OH$ was $k_{SER+^{\bullet}OH} = 2 \times 10^{10}\ M^{-1}\ s^{-1}$. The value of $k_{SER+^{\bullet}OH}$ indicates that the reaction between SER and $^{\bullet}OH$ is near diffusive control in aqueous solution.

3.2.3. Reaction with $CO_3^{\bullet-}$

The concentrations of carbonate and bicarbonate ions in the environmental waters depend on the composition of rock and soil that water flows through ("USGS Water-Quality Information: Water Hardness and Alkalinity," 2017). During irradiation of natural water samples, carbonate radicals $CO_3^{\bullet-}$ are formed upon oxidation of HCO_3^-/CO_3^{2-} present by $^{\bullet}OH$, and of CO_3^{2-} by $^3CDOM^*$ (Canonica et al., 2005). These radicals may also affect photodegradation, but they are less reactive than $^{\bullet}OH$ (Vione et al., 2011). To observe the effect of $CO_3^{\bullet-}$ on SER photodegradation, we added $NaHCO_3$ at final concentrations of 0.50 mM, 1.0 mM and 10 mM to the mixture containing NO_3^- and SER (Fig. S-5, S-8). The nitrate photolysis yields $^{\bullet}OH$, which in turn produces $CO_3^{\bullet-}$ upon reaction with bicarbonate and carbonate. The proposed mechanism of reaction with SER includes reactions between all three components ($^{\bullet}OH$, $CO_3^{\bullet-}$ and SER) (Bouillon and Miller, 2005; Vione et al., 2011). It should however be noted, that the enhancement of SER photodegradation by $NaHCO_3$ could also be affected by the change of pH, depending on the fraction of undissociated compound. Namely, the pH of the solutions increased from 6.5 to 8.2 with the increasing concentration of $NaHCO_3$ additions. To measure how this change influenced the reaction rate, and in agreement with Vione et al. (2009a), we conducted experiments with phosphate ions (NaH_2PO_4 and Na_2HPO_4), at the same concentrations and pH as in the $NaHCO_3$ experiments. There were no significant changes observed with the phosphate, which confirms that $CO_3^{\bullet-}$ radicals drive the degradation of SER. Thus, by being sufficiently reactive towards $CO_3^{\bullet-}$, SER will most likely undergo a similar transformation in environmental waters (Vione et al., 2009a, 2009b).

The acceleration of SER photodegradation in the presence of $NaHCO_3$ could be reproduced reasonably well by assuming $k_{SER+CO_3^{\bullet-}} = 2 \times 10^8\ M^{-1}\ s^{-1}$ (see SM, Chapter 3.4 for additional details).

3.2.4. Reaction with $^1O_2$

$^1O_2$ is another of the reactive transient species formed in environmental waters. As the source of $^1O_2$ we used the sensitizer molecule RB. The optimal pH values for this xantene derivative range between 5 and 12, where it occurs in the dianion form and absorbs radiation at wavelengths from 450 to 600 nm, with a maximum at 548 nm. The RB reaction mechanism under irradiation enabled us to study SER degradation induced by $^1O_2$ alone. (Vione et al., 2011). In agreement with our expectations, $^1O_2$ accelerated the degradation of SER as shown in Table 2. The second-order rate constant for the reaction between SER and $^1O_2$ was calculated on the basis of additional experiments with furfuryl alcohol, whose reactivity with RB has previously been established (Vione et al., 2011). The calculated second-order reaction rate constant was $k_{SER+^1O_2} = (1.3 \pm 0.2) \times 10^6\ L\ mol^{-1}\ s^{-1}$. This reaction rate constant is relatively low (e.g., one order of magnitude lower than that of diclofenac, which reacts negligibly with $^1O_2$ in the natural environment) (Avetta et al., 2016). This means that the reaction between SER and $^1O_2$ may be important in laboratory experiments of RB irradiation but it is unlikely to play an important role in sunlit natural SW. The information on the exact calculations can be found in SM, Chapter 3.5.

3.2.5. Reaction with irradiated AQ2S

AQ2S was chosen because it forms a reactive triplet state ($^3AQ2S^*$) under irradiation, but does not yield $^1O_2$ or $^{\bullet}OH$. AQ2S is here used as the CDOM proxy, since the quinones are a part of CDOM and they form reactive triplet states. The schematic of the process can be found in SM (Fig. S-9). AQ2S is usually more reactive than CDOM, and thus represents an upper limit of $^3CDOM^*$ reactivity (Bianco et al., 2016; Vione et al., 2011). Solutions containing 3.0 μM of AQ2S yielded a sufficiently high reaction rate for SER degradation. Calculation details for the second-order rate constant ($k_{SER+^3AQ2S^*} = 7 \times 10^9\ L\ mol^{-1}\ s^{-1}$) are provided in SM, Chapter 3.6.

3.3. Photochemical modelling

Based on the calculated photoreactivity parameters of SER, namely the photolysis quantum yield ($\Phi_{SER} = 0.95$) and the second order rate constants with $^{\bullet}OH$ ($k_{SER+^{\bullet}OH} = 2 \times 10^{10}\ L\ mol^{-1}\ s^{-1}$), $CO_3^{\bullet-}$ ($k_{SER+CO_3^{\bullet-}} = 2 \times 10^8\ L\ mol^{-1}\ s^{-1}$), $^1O_2$ ($k_{SER+^1O_2} = (1.3 \pm 0.2) \times 10^6\ L\ mol^{-1}\ s^{-1}$) and the AQ2S triplet state, $^3AQ2S^*$ ($k_{SER+^3AQ2S^*} = 7 \times 10^9\ L\ mol^{-1}\ s^{-1}$), it was possible to model the SER phototransformation kinetics under conditions that are significant for SW. Note that $k_{SER+^3AQ2S^*}$ can be considered as an upper limit for the reaction rate constant between SER and $^3CDOM^*$, $k_{SER+^3CDOM^*}$, because $^3AQ2S^*$ is generally more reactive than average $^3CDOM^*$ (Avetta et al., 2016).

Fig. 1 reports the modeled first-order decay constants of SER, as well as the corresponding half-lives, as a function of the dissolved organic carbon (DOC) that is a measure of the DOM in a water body. The different processes that contribute to SER photodegradation are also highlighted.

The figure shows that, for a water depth of 5 m, the photodegradation of SER would be dominated by the DP. The reactions with $^{\bullet}OH$ and $CO_3^{\bullet-}$ would play a secondary role. The highlighted role of $^3CDOM^*$ is referred to $k_{SER+^3CDOM^*} = k_{SER+^3AQ2S^*}$, and it constitutes an upper limit for the importance of the process. The lower limit is obtained under the hypothesis that the $^3CDOM^*$ process is unimportant. To get an insight into the relevant range of variation, the half-life of SER with DOC = 10 mg C L^{-1} would vary from 3 days with $k_{SER+^3CDOM^*} = k_{SER+^3AQ2S^*}$, to 5 days by excluding the $^3CDOM^*$ process. Note that an increase of the DOC is expected to inhibit the reactions with $^{\bullet}OH$ and $CO_3^{\bullet-}$, because DOM is a key scavenger of both radical species. Increasing DOC also inhibits the DP, because the CDOM would compete with SER for sunlight irradiance. In contrast, the $^3CDOM^*$ reactions would be enhanced at high DOC because of elevated levels of CDOM that is the immediate $^3CDOM^*$ precursor (Avetta et al., 2016).

3.4. Identification of TPs and their formation profiles

3.4.1. Peak detection, identity confirmation and formation profiles

Fig. S-10 in the SM shows the extracted ion chromatograms of a

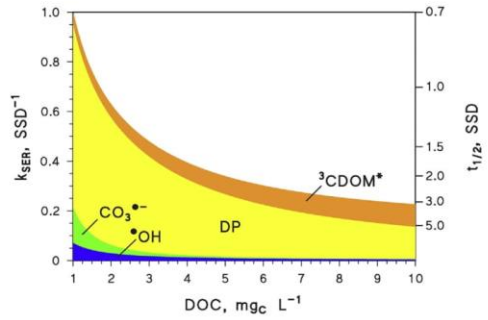

Fig. 1. Modeled pseudo-first order rate constant of SER phototransformation (k_{SER}) as a function of the water DOC. The right-hand Y-axis also reports the SER half-lives. Other water conditions: 5 m depth, 0.1 mM nitrate, 1 μM nitrite, 1 mM bicarbonate, 10 μM carbonate. The steady-state $CO_3^{\bullet-}$ concentration in the modeled conditions (DOC = 1–10 mg C L^{-1}) was in the range of 10^{-16}–10^{-14} M. The different photochemical processes that account for SER photodegradation are highlighted with different colours. The time unit is the SSD (summer sunny days equivalent to 15 July at 45°N latitude). (For interpretation of the references to colour in this figure legend, the reader is referred to the Web version of this article.)

sample treated with RB and irradiated for 105 min. There are evident chromatographic peaks of the residual SER at 3.80 min, and of three TPs, i.e. nor-SER at 3.84 min, SEI at 3.54 min and SEK at 5.14 min. Each TP was defined by three MRM transitions (Tables S–2) and the retention time matching with standards. Furthermore, we detected two additional compounds with chromatographic peaks at t_R 3.29 min and t_R 3.53 min that underwent the same transition as SEK (MRM 291 > 238), as shown in Fig. S-10 (D) and Fig. 2. These two compounds (TP1 at t_R 3.29 min and TP2 at t_R 3.53 min) were absent in the control samples, thus we presumed them to be TPs of SER. The enhanced product ion spectra reported in Fig. 2 were collected at declustering potentials (DP) reported.

The formation of SEI, norSER, SEK, TP1 and TP2 was monitored over time in photodegradation experiments (direct photolysis, $NaNO_3$, $NaNO_3$ + $NaHCO_3$, RB, AQ2S, see section 2.3.1.) at SER initial concentration of 1 mg L^{-1}. The graphs showing TP formation are presented in the SM, Figs. S-11 to S-19. The formation of SEI has already been proposed in the photodegradation study by Jakimska et al. (2014), and by Shen et al. (2011) in the reaction with the TetraAmido Macrocyclic Ligand (TAML) activator. In our experiments the formation of SEI took place instantly, i.e., at the very beginning of the irradiation experiments, though it was shown that the compound did not occur as a product of simple hydrolysis and there was no SEI observed in non-irradiated samples. The abundance of SEI generally decreased during the course of the experiments, except in the case of the reaction with AQ2S, which suggests that SEI may also be a product of triplet-sensitized SER degradation. SEI showed instability in water solutions, even degrading during the SPE sample preparation, which might explain its absence in real SW samples. Along with the fact that SEI clearly underwent fast degradation during the irradiation experiments (Figs. S-11 to S-19),

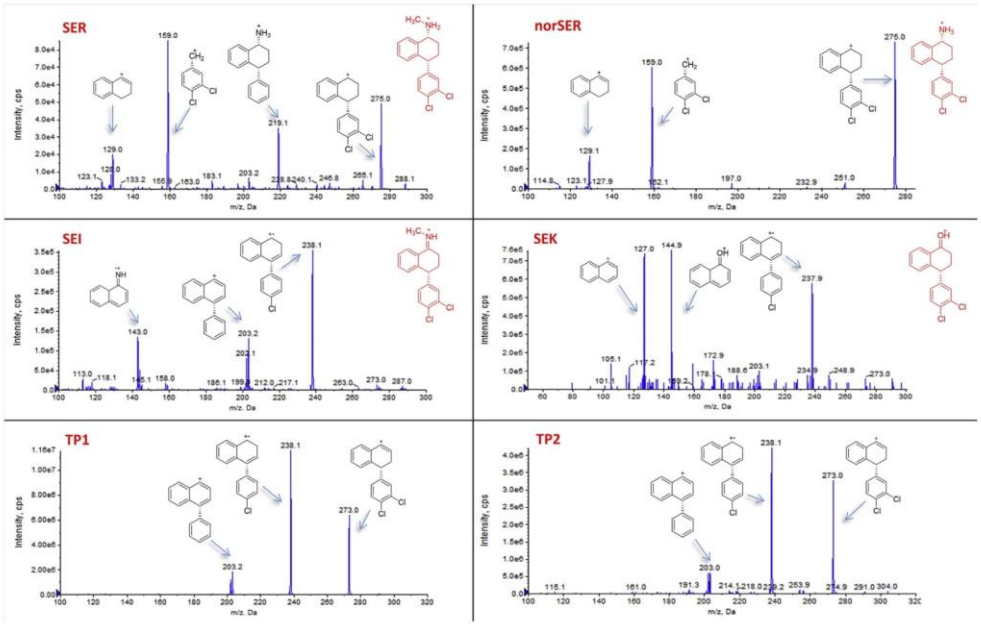

Fig. 2. Enhanced product ion MS spectra of SER (top left), nor-SER (top right), SEI (middle left), SEK (middle right), TP1 (bottom left), and TP2 (bottom right) and the proposed chemical structures assigned to the fragment ions. The spectra were collected at collision energies (CE) 35 V for SER, SEI, TP1 and TP2, 20 V for norSER and 10 V for SEK, with the collision energy spread of 15 V.

it is believed that SEI is unlikely to be a persistent TP of SER. NorSER is a metabolite of SER, but it has also been found in the reaction of SER with the TAML activator (Shen et al., 2011), whereas Jakimska et al. (2014) have not reported its formation in their photodegradation study (Jakimska, A. et al., 2014). In our experiments, norSER was formed in all cases, except when only $NaNO_3$ ($^{\bullet}OH$ reaction) was added. SEK formation was observed in most cases, except for reactions with $NaNO_3$, AQ2S or upon direct photolysis at pH 5.0. Its formation was already reported by Jakimska et al. (2014) and by Shen et al. (2011) (Jakimska et al., 2014; Shen et al., 2011). We detected TP2 only in the photodegradation reactions with triplet states (AQ2S) and $^1O_2$ (RB), while TP1 was observed during all of the experiments. The peak area of TP1 showed a gradual increase in the irradiation experiments, except in the case of AQ2S, where it reached a plateau after 15 min irradiation. In any case, the AQ2S kinetics of TP formation is very specific (Fig. S-19) and is probably the result of two-stage degradation kinetics of SER (Fig. S-6).

3.4.2. Identification of TP1 and TP2

Structural elucidation of TP1 and TP2 was performed by the UHPLC-QToF MS analysis with main results gathered in Tables S−3 and Fig. S-20 in SM. Three main peaks were detected at 3.06 min (TP1), 3.22 min (TP2) and 3.56 min (SER), showing the same elution order on the C-18 column as in case of the UHPLC-QqLIT-MS/MS analysis. SER showed its protonated molecular ion at $[M+H]^+$ 306.0816, from which its elemental formula $C_{17}H_{17}NCl_2$ was calculated. An isotope signal at *m/z* 308.0810 at about 30% of the parent mass height confirmed the presence of two Cl ions in the structure. The fragment ion observed at *m/z* 275 resulted from the loss of CH_3NH_2 and *m/z* 159 from the further loss of the tetralin ring.

For the compounds TP1 and TP2 the protonated molecule was observed at $[M+H]^+$ 322.0765, corresponding to the elemental formula $C_{17}H_{18}NOCl_2$. This means than an additional oxygen atom is incorporated into SER structure. In TP1 the most prominent fragment ion observed was *m/z* 304 formed after the loss of H_2O, while in TP2 smaller fragments at *m/z* 304 and *m/z* 291 were detected corresponding to the subsequent cleavages of H_2O and CH_3NH_2. Both TPs showed *m/z* 273, which is 2 Da less than the analogous fragment ion of SER (*m/z* 275), suggesting a double bond formed during the fragmentation of the TPs. Corresponding fragmentation was previously suggested by Li et al. (2013) for TPs formed during incubation of SER in three types of agricultural soil with and without the addition of biosolids (Li et al., 2013). In agreement with this report we propose the formation of hydroxysertraline with three possible placements of the OH group, making TP1 and TP2 constitutional isomers.

3.5. SW water irradiation

The lab scale photodegradation of SER in SW was carried out under both the MP lamp and natural sunlight. The photodegradation due to solar irradiation was two to three times slower (in solar hours) than the lab scale experiments, which was expected due to the difference in the overall irradiation energy that the samples received (Table 3).

The predicted half-time for SER photodegradation, following our model at DOC concentration 4.14 mg L^{-1} as per the irradiated SW sample should be around 2 SSD. From our experimental data, the degradation lifetime is estimated at around 1.3−1.4 days (31.8−34.7 h), in good agreement with model predictions. The main reasons for the relatively small discrepancy are probably the difference in the irradiation energy received, pH, the column-depth bias and the fact that the SW collected was not sterile. Therefore, some biodegradation could have occurred, which is suspected based on the 37% decrease of SER within the 1-month control study (Fig. S-21).

We observed that four TPs (norSER, SEK, TP1, TP2) were formed during the SW irradiation experiments. Based on the trend in the MP lamp experiments and the observed maximum in the solar irradiated samples (Fig. 3), we may have missed the peak concentrations of norSER and SEK during the first week of irradiation. In addition to norSER and SEK, TP1 and TP2 were formed in both solar and lab scale experiments, but since there is no reference standard available for this compound, we cannot report its concentration in the figures.

3.6. Real surface water samples

As can be seen in Table 4, SER was detected in SW A and C. Additionally, we determined norSER and SEK in SW C. In the same sample also TP1 was identified, but not quantified due to the absence of its reference standard. TP2 was not detected, whereas possible reasoning for the absence of SEI (instability) is given in the previous segment. Altogether, we confirmed the presence of three out of five identified TPs in the environment. To the best of our knowledge, the environmental occurrence of TP1 and SEK is reported herein for the first time. The highest concentrations of SER and peak areas of TPs were detected in SW C. This finding is not surprising when taking into account that SW C flows in the region of Slovenia having the highest reported percentage of patients prescribed with SER (Nacionalni inštitut za javno zdravje, 2018), while its flow is smaller when compared to those of the rivers SW A and SW B. Overall, while norSER and SEK may also be SER metabolites, TP1 should be significantly produced by photochemical processes, both direct and indirect.

4. Conclusions

- Both DP and indirect photodegradation contribute to SER photoinduced degradation, with indirect photodegradation playing a role at higher concentrations of senzitizers present.
- The degradation kinetics of SER is pseudo-first order. The rate of degradation is influenced by pH, where the protonated SER is more photochemically stable than its neutral form.
- This is the first report on formation of norSER during photodegradation under conditions that are significant for SW. While the formation of TP1 and TP2 was before suggested in soil

Table 3
Degradation k'_{SER} and $t_{1/2}$ of solar and laboratory scale irradiation experiments in SW.

SER concentration [ng L^{-1}]	Type of irradiation	Units	k'_{SER} [s^{-1}]	$t_{1/2}$ [h]
50	MP lamp	hours	8.2×10^{-5}	2.36
	solar	hours	5.0×10^{-6}	34.7
	solar	solar hours	2.0×10^{-5}	9.33
1000	MP lamp	hours	5.3×10^{-5}	3.58
	solar	hours	8.3×10^{-6}	31.8
	solar	solar hours	3.2×10^{-5}	5.94

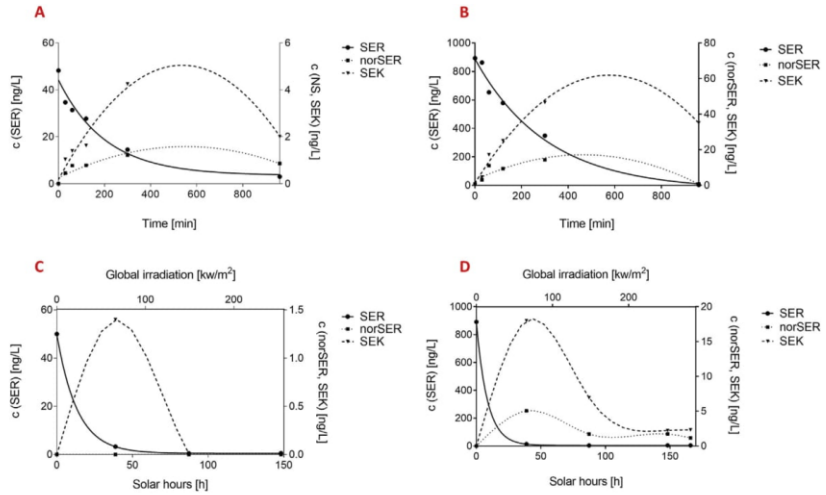

Fig. 3. Photodegradation of SER and TP formation in SW at 50 ng L^{-1} (A) and 1 mg L^{-1} (B) under the MP lamp and at 50 ng L^{-1} (C) and 1 mg L^{-1} (D) under sunlight.

Table 4
Sampling details, determined concentrations of SER, norSER and SEK, and qualitative determination of TP1 and TP2 in SW A, B and C. ND – not detected.

	Sampling data				c [ng L^{-1}]			Screening	
SW	Sampling location	Sampling date	pH	DO [mg L^{-1}]	SER	norSER	SEK	TP 1	TP 2
A	46°04′10.7″N 14°37′58.6″E	October 16, 2018	7.22	10.04	0.51 ± 0.16	< LOQ	< LOQ	ND	ND
B	46°06′31.7″N 14°36′41.8″E	October 17, 2018	7.84	8.91	< LOQ	< LOQ	< LOQ	ND	ND
C	46°07′49.5″N 15°02′07.7″E	October 18, 2018	7.82	9.10	9.28 ± 0.69	1.77 ± 0.14	1.43 ± 0.26	identified	ND

samples, we proved that they form also in the aqueous environment.

- Solar degradation experiments confirmed the results obtained by photochemical modelling, which suggested that the SER half-life might range from <1 day to about 3–5 days, depending on water conditions.
- The presence of SER and three of its TPs in the aqueous environment was confirmed and their potential toxicity evaluated as comparable or lower than SER toxicity.

Overall, this study brings a substantial insight into the photochemical fate of the antidepressant SER in the aquatic environment, but there remain several knowledge gaps on its environmental fate. One example is its unrecognized biological breakdown; yet even more far-reaching is the general issue on how to improve the determination of the compound's unknown TPs in the environment, i.e., how to make the "nontarget analysis more targeted".

Acknowledgements

The authors acknowledge the financial support from the Slovenian Research Agency (research core funding No. P1-0143) and project J1-6744 (Development of Molecularly Imprinted Polymers and their application in environmental and bio-analysis) and also acknowledge the help of Tjaša Brcar and Žiga Šmidhofer from the University of Ljubljana Faculty of Pharmacy and the Chair of Buildings and Constructional Complexes from the University of Ljubljana Faculty of Civil and Geodetic Engineering. Financial support from the Scientific and Technological Cooperation Agreement between Italy and Slovenia (Slovenian Research Agency & Italian Ministry of Foreign Affairs) is also acknowledged.

Appendix A. Supplementary data

Supplementary data to this article can be found online at https://doi.org/10.1016/j.envpol.2019.113431.

References

Avetta, P., Fabbri, D., Minella, M., Brigante, M., Maurino, V., Minero, C., Pazzi, M., Vione, D., 2016. Assessing the phototransformation of diclofenac, clofibric acid and naproxen in surface waters: model predictions and comparison with field data. Water Res. 105, 383–394. https://doi.org/10.1016/j.watres.2016.08.058.

Bergersen, O., Hanssen, K.Ø., Vasskog, T., 2015. Aerobic treatment of selective serotonin reuptake inhibitors in landfill leachate. Environ. Sci. Eur. 27, 6. https://doi.org/10.1186/s12302-014-0035-0.

Bianco, A., Fabbri, D., Minella, M., Brigante, M., Mailhot, G., Maurino, V., Minero, C., Vione, D., 2016. Photochemical transformation of benzotriazole, relevant to sunlit surface waters: assessing the possible role of triplet-sensitised processes. Sci. Total Environ. 566 (567), 712–721. https://doi.org/10.1016/j.scitotenv.2016.05.119.

Bianco, A., Fabbri, D., Minella, M., Brigante, M., Mailhot, G., Maurino, V., Minero, C., Vione, D., 2015. New insights into the environmental photochemistry of 5-chloro-2-(2,4-dichlorophenoxy)phenol (triclosan): reconsidering the importance of indirect photoreactions. Water Res. 72, 271–280. https://doi.org/10.1016/j.watres.2014.07.036.

Bodrato, M., Vione, D., 2014. APEX (Aqueous Photochemistry of Environmentally occurring Xenobiotics): a free software tool to predict the kinetics of photochemical processes in surface waters. Env. Sci Process. Impacts 16, 732–740. https://doi.org/10.1039/C3EM00541K.

Bouillon, R.-C., Miller, W.L., 2005. Photodegradation of dimethyl sulfide (DMS) in natural waters: laboratory assessment of the nitrate-photolysis-induced DMS oxidation. Environ. Sci. Technol. 39, 9471–9477. https://doi.org/10.1021/es048022z.

Canonica, S., Kohn, T., Mac, M., Real, F.J., Wirz, J., von Gunten, U., 2005. Photosensitizer method to determine rate constants for the reaction of carbonate radical with organic compounds. Environ. Sci. Technol. 39, 9182–9188. https://doi.org/10.1021/es051236b.

De Vane, C.L., Liston, H.L., Markowitz, J.S., 2002. Clinical pharmacokinetics of sertraline. Clin. Pharmacokinet. 41, 1247–1266.

Golovko, O., Kumar, V., Fedorova, G., Randak, T., Grabic, R., 2014. Seasonal changes in antibiotics, antidepressants/psychiatric drugs, antihistamines and lipid regulators in a wastewater treatment plant. Chemosphere 111, 418–426. https://doi.org/10.1016/j.chemosphere.2014.03.132.

Hedgespeth, M.L., Nilsson, P.A., Berglund, O., 2014. Ecological implications of altered fish foraging after exposure to an antidepressant pharmaceutical. Aquat. Toxicol. 151, 84–87. https://doi.org/10.1016/j.aquatox.2013.12.011.

Jakimska, A., Kaszynska, M., Nagórski, P., Kot Wasik, A., Namieśnik, J., 2014. Environmental fate of two psychiatric drugs, diazepam and sertraline: phototransformation and investigation of their photoproducts in natural waters. J. Chromatogr. Sep. Tech. 5 https://doi.org/10.4172/2157-7064.1000253.

Kete, M., 2008. Razvoj Pilotnega Sistema Za Čiščenje Vode Na Principu TiO2 Fotokatalize. Univerza v Novi Gorici.

Kuzmanović, M., López-Doval, J.C., De Castro-Català, N., Guasch, H., Petrović, M., Muñoz, I., Ginebreda, A., Barceló, D., 2016. Ecotoxicological risk assessment of chemical pollution in four Iberian river basins and its relationship with the aquatic macroinvertebrate community status. Sci. Total Environ. 540, 324–333. https://doi.org/10.1016/j.scitotenv.2015.06.112.

Kwon, J.-W., Armbrust, K.L., 2008. Aqueous solubility, n-octanol–water partition coefficient, and sorption of five selective serotonin reuptake inhibitors to sediments and soils. Bull. Environ. Contam. Toxicol. 81, 128–135. https://doi.org/10.1007/s00128-008-9401-1.

Kwon, J.-W., Armbrust, K.L., 2006. Laboratory persistence and fate of fluoxetine in aquatic environments. Environ. Toxicol. Chem. 25, 2561–2568.

Kwon, J.-W., Armbrust, K.L., 2005a. Degradation of citalopram by simulated sunlight. Environ. Toxicol. Chem. 24, 1618–1623.

Kwon, J.-W., Armbrust, K.L., 2005b. Photo-isomerization of fluvoxamine in aqueous solutions. J. Pharm. Biomed. Anal. 37, 643–648. https://doi.org/10.1016/j.jpba.2004.09.057.

Kwon, J.-W., Armbrust, K.L., 2004. Hydrolysis and photolysis of paroxetine, a selective serotonin reuptake inhibitor, in aqueous solutions. Environ. Toxicol. Chem. 23, 1394–1399.

Lajeunesse, A., Smyth, S.A., Barclay, K., Sauvé, S., Gagnon, C., 2012. Distribution of antidepressant residues in wastewater and biosolids following different treatment processes by municipal wastewater treatment plants in Canada. Water Res. 46, 5600–5612. https://doi.org/10.1016/j.watres.2012.07.042.

Lam, M.W., Young, C.J., Brain, R.A., Johnson, D.J., Hanson, M.A., Wilson, C.J., Richards, S.M., Solomon, K.R., Mabury, S.A., 2004. Aquatic persistence of eight pharmaceuticals in a microcosm study. Environ. Toxicol. Chem. 23, 1431–1440.

Li, H., Sumarah, M.W., Topp, E., 2013. Persistence and dissipation pathways of the antidepressant sertraline in agricultural soils. Sci. Total Environ 296–301. https://doi.org/10.1016/j.scitotenv.2013.02.080, 452–453.

Minguez, L., Ballandonne, C., Rakotomalala, C., Dubreule, C., Kientz-Bouchart, V., Halm-Lemeille, M.-P., 2015. Transgenerational effects of two antidepressants (sertraline and venlafaxine) on *Daphnia magna* life history traits. Environ. Sci. Technol. 49, 1148–1155. https://doi.org/10.1021/es504808g.

Murov, S.L., Carmichael, I., Hug, G.L., 1993. Handbook of Photochemistry, second ed. CRC Press.

Nacionalni inštitut za javno zdravje, 2018. Poraba Ambulantno Predpisanih Zdravil V Sloveniji V Letu 2017 (Ljubljana).

Osorio, V., Larrañaga, A., Aceña, J., Pérez, S., Barceló, D., 2016. Concentration and risk of pharmaceuticals in freshwater systems are related to the population density and the livestock units in Iberian Rivers. Sci. Total Environ. 540, 267–277. https://doi.org/10.1016/j.scitotenv.2015.06.143.

Schultz, M.M., Furlong, E.T., Kolpin, D.W., Werner, S.L., Schoenfuss, H.L., Barber, L.B., Blazer, V.S., Norris, D.O., Vajda, A.M., 2010. Antidepressant pharmaceuticals in two US effluent-impacted streams: occurrence and fate in water and sediment, and selective uptake in fish neural tissue. Environ. Sci. Technol. 44, 1918–1925.

Shen, L.Q., Beach, E.S., Xiang, Y., Tshudy, D.J., Khanina, N., Horwitz, C.P., Bier, M.E., Collins, T.J., 2011. Rapid, biomimetic degradation in water of the persistent drug sertraline by TAML catalysts and hydrogen peroxide. Environ. Sci. Technol. 45, 7882–7887. https://doi.org/10.1021/es201392k.

US Environmental Protection Agency, 2016. Final Report, the Environmental Occurrence, Fate, and Ecotoxicity of Selective Serotonin Reuptake Inhibitors (SSRIs) in Aquatic Environments, Research Project Database. NCER | ORD | US EPA [WWW Document]. https://cfpub.epa.gov/ncer_abstracts/index.cfm/fuseaction/display.highlight/abstract/1755/report/F (accessed 3.7.16).

USGS Water-Quality Information, 2017. Water Hardness and Alkalinity [WWW Document]. https://water.usgs.gov/owq/hardness-alkalinity.html (accessed 7.5.17).

Vasskog, T., Berger, U., Samuelsen, P.-J., Kallenborn, R., Jensen, E., 2006. Selective serotonin reuptake inhibitors in sewage influents and effluents from Tromsø, Norway. J. Chromatogr. A 1115, 187–195. https://doi.org/10.1016/j.chroma.2006.02.091.

Vione, D., Khanra, S., Man, S.C., Maddigapu, P.R., Das, R., Arsene, C., Olariu, R.-I., Maurino, V., Minero, C., 2009a. Inhibition vs. enhancement of the nitrate-induced phototransformation of organic substrates by the •OH scavengers bicarbonate and carbonate. Water Res. 43, 4718–4728. https://doi.org/10.1016/j.watres.2009.07.032.

Vione, D., Maddigapu, P.R., De Laurentiis, E., Minella, M., Pazzi, M., Maurino, V., Minero, C., Kouras, S., Richard, C., 2011. Modelling the photochemical fate of ibuprofen in surface waters. Water Res. 45, 6725–6736. https://doi.org/10.1016/j.watres.2011.10.014.

Vione, D., Maurino, V., Minero, C., Carlotti, M.E., Chiron, S., Barbati, S., 2009b. Modelling the occurrence and reactivity of the carbonate radical in surface freshwater. Compt. Rendus Chem. 12, 865–871. https://doi.org/10.1016/j.crci.2008.09.024.

Wenk, J., Canonica, S., 2012. Phenolic antioxidants inhibit the triplet-induced transformation of anilines and sulfonamide antibiotics in aqueous solution. Environ. Sci. Technol. 46, 5455–5462. https://doi.org/10.1021/es300485u.

3.1.2 Phototransformation study of the antidepressant paroxetine in surface waters

The paper "Phototransformation study of the antidepressant paroxetine in surface waters" by T. Gornik, L. Carena, T. Kosjek and D. Vione was published in *Science of the Total Environment* in June 2021. This paper resulted from the collaboration between the Department of Chemistry at the University of Torino, Italy and the Department of Environmental Sciences at the Jožef Stefan Institute, Slovenia. Conceptualizing the experimental work, laboratory experimental work and writing of the manuscript was performed by myself and Dr L. Carena. My work emphasized analytical method development and validation, environmental sampling, sample analysis, TP identification, and data interpretation, while Dr L. Carena performed modelling and interpretation of photochemical data obtained during the laboratory scale experiments. The work was performed under the supervision of Assoc Prof T. Kosjek and Prof Dr D. Vione.

Similarly to SER, PXT has also been determined in WW and SW around the globe. The growing number of reports and its potential toxicity for aquatic organisms makes researching its behavior in the environment a necessity. In this study, its phototransformation in SW and the photochemistry behind it were studied in-depth. Steady-state laboratory scale irradiation experiments were performed to determine the direct photolysis quantum yield and second-order rate constants of the reactions between PXT and PPRI (i.e., $HO^{\bullet}$, $^{3}CDOM^{*}$ and $^{1}O_{2}$). The obtained information was used to model PXT behavior (pseudo-first order photodegradation rate constant and half-life time) in a SW scenario by varying the depth and chemical composition. Results suggest that direct photolysis ($\Phi = (4.03 \pm 0.25) \times 10^{-2}$) in combination with reactions with $HO^{\bullet}$ and $CO_3^{\bullet -}$ radicals are the main photodegradation pathways in SW. The structures of nine PXT TPs were tentatively identified, and a photodegradation pathway was suggested. Seven of the nine identified TPs were detected for the first time. The occurrence of PXT and its TPs in three Slovenian SW was also investigated. Neither PXT nor TPs were detected in the collected samples, and the developed photochemical model for PXT corroborated the results.

This paper addresses the following thesis aims: 1) development, optimization and validation of analytical methods for quantifying chosen SSRI and identifying their TPs in aqueous samples with different analytical techniques (LC-UV, LC-MS/MS); 2) investigation of PXT breakdown during photodegradation and identification of their TPs and 3) determination of PXT residues in SW.

The findings contribute to a better understanding of the persistence of PXT and its TPs in SW. It provides new information on photodegradation kinetics and a potential degradation pathway, including identifying new TPs with high-resolution MS. It also suggests that the chemical composition and abundance of SW in Slovenia are essential in keeping the burden of pharmaceuticals released in the environment lower than expected, highlighting the additional parameters influencing a contaminants persistence in an environment.

Science of the Total Environment 774 (2021) 145380

Contents lists available at ScienceDirect

Science of the Total Environment

journal homepage: www.elsevier.com/locate/scitotenv

Phototransformation study of the antidepressant paroxetine in surface waters

Tjasa Gornik [a,b,1], Luca Carena [c,1], Tina Kosjek [a,b,*], Davide Vione [c,**]

[a] Jozef Stefan Institute, Department of Environmental Sciences, Jamova 39, Ljubljana, Slovenia
[b] Jozef Stefan International Postgraduate School, Jamova 39, Ljubljana, Slovenia
[c] Department of Chemistry, University of Torino, Via Pietro Giuria 5, 10125 Torino, Italy

HIGHLIGHTS

- The fate of paroxetine in surface waters is largely influenced by photodegradation.
- Direct photolysis and reactions with $HO^{\bullet}$ and $CO_3^{\bullet-}$ are key degradation pathways.
- Nine potential phototransformation products were identified.
- Paroxetine and transformation products were not present in Slovenian water bodies.
- In the majority of Slovenian surface waters paroxetine lifetime was <2 days.

GRAPHICAL ABSTRACT

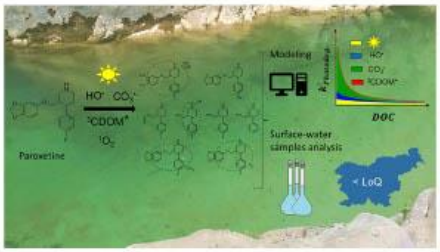

ARTICLE INFO

Article history:
Received 9 November 2020
Received in revised form 3 January 2021
Accepted 19 January 2021
Available online 2 February 2021

Editor: Dimitra A Lambropoulou

Keywords:
Direct photolysis
Hydroxyl radical
Transformation product
Photochemical modelling
Piperidine
Back-reduction

ABSTRACT

In this work, the photochemistry of the antidepressant paroxetine (PXT) and its photochemical fate in surface waters were investigated. The direct photolysis quantum yield, as well as the second-order rate constants of the reactions between PXT and the photochemically produced reactive intermediates (i.e., $HO^{\bullet}$, $^3CDOM^*$ and $^1O_2$) were assessed with steady-state irradiation experiments, while the reaction rate constant with $CO_3^{\bullet-}$ was known from the literature. Using these results, the PXT photochemical fate (i.e., pseudo-first order photodegradation rate constant and half-life time) was modelled in a surface-water scenario by varying the chemical composition of water and its depth. Nine transformation products were identified, formed upon PXT direct and indirect photolysis, and a photodegradation pathway was proposed that is initiated by photohydrolysis of PXT to 4-(4-fluorophenyl)-3-(hydroxymethyl)piperidine.

The results showed that PXT reacts with $HO^{\bullet}$ radicals approaching a diffusion-controlled kinetics, while the direct photolysis quantum yield is $\Phi_{PXT} = (4.03 \pm 0.25) \times 10^{-2}$. Direct photolysis, together with reactions with $HO^{\bullet}$ and $CO_3^{\bullet-}$ radicals would be the main photodegradation pathways for PXT in surface waters. Reaction with $CO_3^{\bullet-}$ is particularly important for low amounts of dissolved organic matter (DOM), high pH and high inorganic carbon, which are for instance typical of surface waters in Slovenia. Finally, PXT reaction with $^3CDOM^*$ is little important because it is significantly inhibited in the presence of antioxidant compounds, which reduce the partially oxidized intermediates back to the parent PXT.

* Correspondence to: Jozef Stefan Institute, Jamova 39, 1000, Ljubljana, Slovenia.
** Correspondence to: Department of Chemistry, University of Torino, Via Pietro Giuria 5, 10125 Torino, Italy.
E-mail addresses: tina.kosjek@ijs.si (T. Kosjek), davide.vione@unito.it (D. Vione).
[1] Joint first authors.

https://doi.org/10.1016/j.scitotenv.2021.145380
0048-9697/

1. Introduction

Paroxetine (hereafter PXT) is an antidepressant of the selective serotonin reuptake inhibitors (SSRI) class. It is the 57th on the list of the Top 200 prescribed drugs in the US (Fuentes et al., 2018), and the 17th on the list of most prescribed psychiatric drugs in the US (McDermott, 2018). PXT is the third most commonly prescribed SSRI in Slovenia, behind escitalopram and sertraline, the presence of which has already been confirmed in Slovenian surface waters (SW). Escitalopram has been reported once at a concentration of 0.42 ng L^{-1} (Klančar et al., 2018), while sertraline has been reported in three cases at concentrations of 0.24 ng L^{-1} (Klančar et al., 2018), 1.77 and 9.28 ng L^{-1} (Gornik et al., 2020).

The main PXT source to the environment is human excretion. In the human body, PXT undergoes extensive phase I and II metabolism, including oxidation to its catechol (PC), followed by formation of the methyl intermediate (PM), and by conjugation (glucuronidation, sulfation). Therefore, less than 1% of the ingested PXT is excreted as the parent compound (Hiemke and Härtter, 2000; Matsunaga et al., 2013).

Cunningham et al. (2004) discussed the hydrolysis of PXT conjugates back to the parent compound or PM in wastewater (WW) treatment systems, suggesting that PXT and PM are the main candidates for monitoring after they enter the aqueous environment. The group then studied the PXT and PM behavior in activated sludge (AS) biodegradation experiments, where PM was extensively removed by both sorption and biodegradation. They also reported that PXT was only removed by sorption to AS. Nevertheless, Radjenović et al. (2007a,b) showed high removal of PXT in both, the conventional AS process (90.6%) and in membrane bioreactors (89.7%) irrespective of the removal mechanism. Despite this, PXT has repeatedly been detected in different environmental compartments (e.g., WW, surface waters (SW), sediment, and fish tissue) (Arnnok et al., 2017; Mole and Brooks, 2019; Schultz et al., 2010; Vasskog et al., 2008, 2006). The reported concentration in SW is generally a few ng L^{-1}. The highest concentrations up to date were reported in the western Lake Erie basin (90 ng L^{-1}) and the Niagara river (270 ng L^{-1}) (Arnnok et al., 2017; Wu et al., 2009). Until now, no data exist on the occurrence of PXT metabolites or transformation products (TPs) in environmental matrices.

Once in the environment, PXT causes neurohormone-like adverse effects in aquatic organisms (e.g. changes in reproduction), similarly as other antidepressants from the SSRI class. Its acute toxicity has been studied on model aquatic organisms of lower trophic levels, where the effects are expected to be the most pronounced (e.g., *C. dubia*, *D. magna*, *D. polymorpha*, *S. striatiunum*, *P. elliptica*, *H. tuberculate*, *X. laevis*) (Fong, 2001; Silva et al., 2015). In comparison, the acute toxicity of PM for aquatic organisms has also been estimated based on tests on *D. magna*, indicating a low risk of any adverse effects arising from the exposure to PM (Cunningham et al., 2004). Hence, the reason for choosing PXT as our focus compound lies in the processes occurring during WW treatment and the results of toxicity tests.

The available literature on the breakdown of PXT after it has reached the environment is quite limited. However, authors agree on photodegradation being one of the main processes of PXT elimination (Cunningham et al., 2004; Henry et al., 2004; Kwon and Armbrust, 2004; Santoke and Cooper, 2017; US Environmental Protection Agency, 2016). In general, photodegradation of a water pollutant can occur through two main pathways, namely direct and indirect photolysis. Direct phototransformation takes place when the compound absorbs solar radiation and gets transformed because of the obtained extra-energy. In contrast, indirect photochemistry involves the reactions between the xenobiotic and the *Photochemically Produced Reactive Intermediates* (PPRIs), which are formed upon sunlight absorption by natural photosensitizers such as the chromophoric dissolved organic matter (CDOM), nitrate and nitrite (Vione et al., 2014). The main PPRIs in SW are hydroxyl and carbonate radicals ($HO^{\bullet}$ and $CO_3^{\bullet-}$, respectively), the excited triplet states of CDOM ($^3CDOM^*$) and singlet oxygen ($^1O_2$). Kwon and Armbrust (2004) have previously performed PXT irradiation experiments in both synthetic buffer-solutions and lake water with a fluorescent light. Santoke and Cooper (2017) have found that $HO^{\bullet}$ and $^1O_2$ play a role in PXT photodegradation in irradiated Suwannee river water samples. Reportedly, photodegradation occurs fast and in a large percentage (Kwon and Armbrust, 2004; Santoke and Cooper, 2017), which implies that TPs could be responsible for the majority of toxic effects and might be better suited as markers of PXT environmental presence (Cunningham et al., 2004; Kwon and Armbrust, 2004). Nonetheless, it is clear from the available literature that there is still a lack of information concerning the relative importance of direct and indirect photochemistry on the environmental fate of PXT, including the formation of other TPs and the relevance of different transformation pathways. The roles of direct photolysis and the reactions with $^3CDOM^*$ and $CO_3^{\bullet-}$, which are known to be important transformation pathways for xenobiotics (Canonica, 2007; Wojnárovits et al., 2020), have still to be determined in the case of PXT. In particular, $^3CDOM^*$ is produced upon absorption of sunlight by CDOM chromophores (e.g., aromatic carbonyls and quinones), following electron excitation to the first excited singlet state ($^1CDOM^*$) and inter-system crossing (McNeill and Canonica, 2016). The carbonate radical $CO_3^{\bullet-}$ is produced upon oxidation of HCO_3^- and CO_3^{2-} by $HO^{\bullet}$ and, usually to a lesser extent, upon oxidation of CO_3^{2-} by $^3CDOM^*$ (Canonica et al., 2005). The $CO_3^{\bullet-}$ transient plays a more important role as the pH is higher (HCO_3^- is less reactive than CO_3^{2-} towards oxidation) and the DOC is lower (organic matter directly scavenges $CO_3^{\bullet-}$ and inhibits its formation) (Vione et al., 2014). See SM, Fig. S-1 for a plot of $[CO_3^{\bullet-}]$ vs. DOC and pH.

To fill in this knowledge gap our research involved: (a) laboratory-scale irradiation experiments to determine the PXT photoreactivity parameters (i.e., direct photolysis quantum yield and second-order reaction rate constants between PXT and the main PPRIs); (b) modelling of PXT photochemical fate in surface water; (c) identification of the TPs formed upon PXT direct and indirect phototransformation, by means of high resolution/accurate mass-mass spectrometry (HR/AM MS); (d) determination of PXT TPs in actual SW samples.

2. Materials and methods

2.1. Standards, chemicals and materials

The data on the standards, chemicals and materials we used can be found in the Supplementary material (SM), Chapter 1.1. The preparation procedure of the stock solutions is reported in SM, Chapter 1.2.

2.2. Irradiation experiments

Irradiation runs were performed with different lamps, depending on the aim of the experiment:

1) A Philips narrow band TL 20 W/01 lamp, which mainly emits in the UVB range of the light spectrum (emission maximum at 313 nm).
2) A UVA black lamp (Philips TL-D 18 W), with emission maximum at 369 nm.
3) A Philips TL D 18 W/16 Yellow lamp, the emission spectrum of which is reported elsewhere (Carena et al., 2017; Vione, 2020).

Chemical actinometry with 2-nitrobenzaldeheyde (Carena et al., 2019; Galbavy et al., 2010; Willett and Hites, 2000) was used to determine the spectral photon flux density occurring in the irradiated solutions.

In general, aqueous solutions (5 or 20 mL) contained (*i*) PXT (usually at 20 μmol L^{-1}, but varied down to 5 μmol L^{-1} in some series of experiments. The latter value is practically the lower limit at which it is still possible to monitor the PXT time trend by HPLC-UV; we avoided sample

concentration procedures because they introduce too much variability, thereby spoiling kinetic data), (*ii*) a suitable photosensitiser (which selectively produces a given PPRI) and (when relevant) (*iii*) a PPRI scavenger. These solutions were put in Pyrex glass cells and magnetically stirred under steady irradiation. The solution pH ranged between 6 and 7, which is quite near typical surface-water conditions (PXT has $pK_a = 9.6$; Cunningham et al., 2004). After scheduled irradiation times, solutions were withdrawn and analysed for PXT with a high-performance liquid chromatograph, equipped with a diode-array detector (HPLC-DAD, Hitachi LaChrom Elite® series).

In general, the time trends of PXT concentration followed pseudo-first order kinetics, namely $[PXT] = [PXT]_0 \times e^{-k' \times t}$, where $[PXT]_0$ is the initial concentration of PXT (vide infra for its values), k' the pseudo-first order rate constant of PXT degradation, and t the irradiation time. After assessing k' from the data fit of $[PXT]$ vs. t, the initial PXT degradation rate was calculated as $R = k' \times [PXT]_0$. An exception was the kinetics of PXT degradation by $^1O_2$, which followed a (pseudo-first order) exponential decay with a small residual (the details about rate calculations are reported in the caption of Fig. S-2).

Irradiation experiments aimed at identifying the TPs were carried out in aqueous solutions (20 mL) containing PXT (100 μmol L^{-1}) and a selective photosensitiser. In particular, hydrogen peroxide (5 mmol L^{-1}) and $NaNO_3$ (10 mmol L^{-1}) were separately used for $HO^•$-induced reactions, benzophenone-4-carboxylate (CBBP, 70 μmol L^{-1}) for transformation by $^3CDOM^*$, and Rose Bengal (RB, 10 μmol L^{-1}) for transformation by $^1O_2$. Finally, a mixture of $NaNO_3$ (10 mmol L^{-1}) and $NaHCO_3$ (0.8 mol L^{-1}) was used as photosensitiser to produce $CO_3^{•-}$ radicals. After collection, samples were analysed for TP identification by means of a ultra-high-performance liquid chromatograph coupled to a hybrid quadruple time-of-flight mass spectrometer (UHPLC-QTof, Waters Quatro Permier series).

2.3. Sample preparation and instrumental analysis

Samples obtained from the irradiation experiments (Section 2.2) were injected into HPLC-DAD or UHPLC-QTof without additional preparation.

The determination of PXT concentration in SW samples (Section 2.5) was carried out using a ultra-high performance liquid chromatograph UHPLC (Shimadzu Nexera X2) - hybrid quadrupole-linear ion trap mass spectrometry analyser (Sciex Qtrap 4500). Before injection, samples were pre-concentrated and cleaned by solid phase extraction (SPE) on Strata XC cartridges. The 250-mL aliquots of each sample were first spiked with PXT-D_6 as an internal standard at the final concentration of 30 ng L^{-1}, and then filtered through Whatman GF/C filters. The pH value was adjusted to 2 with 37% HCl and the samples were loaded onto cartridges preconditioned with 3 mL of MeOH, and equilibrated with 3 mL of HCl-acidified ultrapure water (pH 2) at a flow rate of 6–7 mL min^{-1}. Matrix interferences were washed off with 10% methanol (MeOH) in ultrapure water. PXT was eluted with 3 × 0.6 mL of 5% NH_4OH in MeOH. The extracts were dried at 30 °C under nitrogen flow, and then reconstituted in 100 μL of 20% MeOH in 0.1% formic acid. Samples were prepared in duplicates. The occurrence of TPs was checked in the same extracts.

The exact operating conditions for each instrumental analysis can be found in SM, Chapter 1.3. Information on the analytical method validation is reported in SM, Chapter 1.4.

2.4. Identification of TPs formed by PXT photodegradation experiments

The identification was performed with UHPLC-QTof. The screening approaches were accomplished in the targeted way, where the TPs reported in the literature and candidates predicted from potential phototransformation reactions were manually screened for ("suspect list") (Kwon and Armbrust, 2004; Matsunaga et al., 2013; Vay et al., 2018; Zhao et al., 2007). In addition, we screened for potential TPs using the non-targeted approach with the open-source package MZmine (version 2.53). The analysis of data obtained with liquid chromatography coupled to mass spectrometry (LC-MS) was performed similarly as in Gornik et al. (2020). Data were transformed from raw files into mzML format using Proteowizard (version 3.0.20075) software, before being processed in MZmine. The peaks were detected by first using the centroid mass algorithm, followed by chromatogram building. For the deconvolution of the obtained chromatograms, wavelet (Automated Data Analysis Pipeline (ADAP)) algorithm was utilized (Myers et al., 2017). Deisotoping was done by applying the isotopic peaks grouper algorithm with the RT tolerance of 0.2 min, a m/z tolerance of 25 ppm, and the lowest m/z value as the representative isotope. The peak list alignment algorithm Random Sample Consensus (RANSAC) was applied to the list and gap filling was performed based on the m/z tolerance of 25 ppm. The list of features was filtered and the obtained list of candidates was further evaluated to exclude the compounds present in blanks or control samples. The remaining candidates were tentatively identified based on their MS/MS spectra using Mass Lynx v 4.1. The criteria for TP identification included: 1) a maximum error of 15 ppm between the measured and theoretical mass of the protonated parent molecule, and 40 ppm for its productions; 2) isotopic pattern score over 80%, where available; 3) reasonable ring double bond equivalents (RDBE) value. The chemical structures and transformations were drawn in ChemDraw Ultra 12.0.2 (Perkin Elmer).

2.5. Occurrence of PXT and its TPs in Slovenian SW

We collected six-hour composite samples of three Slovenian rivers (A, B and C) in order to investigate the occurrence of PXT and its TPs. The exact sampling locations and dates can be found in Table S-4 (SM). The values of pH and dissolved oxygen (DO) of the river water at each sampling point were measured with a multi-parameter portable meter MultiLine® Multi 3630 IDS (WTW, Weilheim, Germany).

3. Results and discussion

3.1. Irradiation experiments

3.1.1. PXT direct photolysis

The direct photolyis of PXT was assessed under UVB irradiation (see Fig. 1a for the lamp spectrum, i.e., the spectral photon flux density in the irradiated solutions). Although sunlight has relatively low irradiance in the UVB region, UVB radiation should account for the vast majority of PXT direct photolysis in the environment. Indeed, PXT efficiently absorbs sunlight at $\lambda < 320$ nm (Fig. 1a), while negligible radiation absorption occurs in the UVA and visible regions. This issue, together with the fact that the direct photolysis quantum yields are measured more accurately under narrow-band radiation, justified the choice of the UVB lamp.

PXT (20 μmol L^{-1}) was irradiated in ultrapure water (5 mL) under UVB light for up to 150 min (Fig. 1b). In such conditions, the rate of PXT direct photolysis is expressed as $R_{d.p.} = \Phi_{PXT} \times \int_{\lambda} p^°(\lambda) \times [1 - 10^{-\varepsilon_{PXT}(\lambda) \times b \times [PXT]}] d\lambda$, where $p^°(\lambda)$ is the lamp spectral photon flux density (Fig. 1a), $\varepsilon_{PXT}(\lambda)$ is the molar absorption coefficient of PXT (Fig. 1a), b is the light optical path in solution (0.4 cm), and Φ_{PXT} is the apparent quantum yield of PXT direct photolysis. It was $R_{d.p.} = 2.41 \pm 0.10$ nmol L^{-1} s^{-1}, and the photon flux absorbed by PXT was $P_a = \int_{\lambda} p^°(\lambda) \times [1 - 10^{-\varepsilon_{PXT}(\lambda) \times b \times [PXT]}] d\lambda = (5.97 \pm 0.36) \times 10^{-8}$ Einstein L^{-1} s^{-1}. As a consequence, one gets $\Phi_{PXT} = R_{d.p.} (P_a)^{-1} = (4.03 \pm 0.25) \times 10^{-2}$.

The obtained value of Φ_{PXT} is ~5 times lower than that measured at $\lambda = 254$ nm in previous work, although with high uncertainty (Φ_{PXT} (254 nm) = 0.21 ± 0.14; Wols et al., 2014). Such a difference in the photolysis quantum yield values measured for a certain pharmaceutical (Challis et al., 2014) could be accounted for by the use of dissimilar irradiation wavelengths. Indeed, although the phototransformation

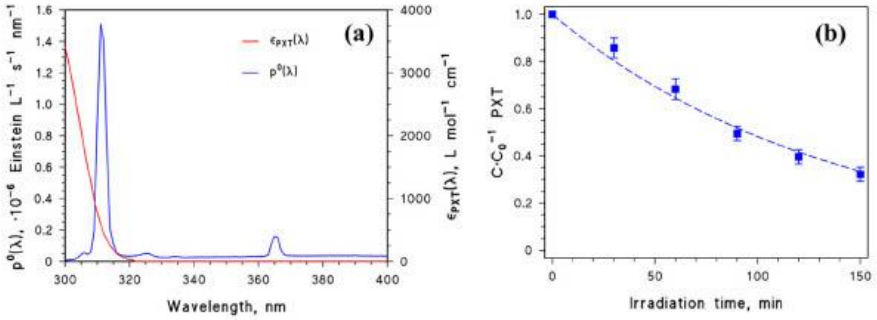

Fig. 1. (a) Molar absorption coefficient of paroxetine ($\epsilon_{PXT}(\lambda)$) and spectral photon flux density ($p^0(\lambda)$) of the Philips narrow band TL 20 W/01 (UVB) lamp. The irradiance of the lamp was 3.7 ± 0.2 W m^{-2}. (b) Degradation profile of PXT by direct photolysis under UVB irradiation. Error bars represent the standard deviation of duplicate runs, while the dashed curve shows the fit of the experimental data with an exponential function.

quantum yields of polyatomic organic molecules often follow Kasha's rule (Turro et al., 1978), it is not uncommon to find a wavelength dependence in the quantum yields of photochemical reactions (Demchenko et al., 2017). In the case of PXT, the UVB quantum yield would be representative of phototransformation under sunlight (also because PXT only absorbs sunlight in the UVB region), differently from the 254-nm quantum yield.

3.1.2. Reaction with HO• radicals

The second-order rate constant of the reaction between PXT and HO• radical ($k_{(HO^\bullet+PXT)}$) was assessed by exploiting the competition between PXT and isopropanol (2-propanol, hereinafter iPr) for reaction with HO• (Carena et al., 2018). iPr is a well-known HO• scavenger, which reacts with HO• radicals mainly through hydrogen abstraction, with a rate constant $k_{(HO^\bullet+iPr)} = 1.9\times10^9$ L mol^{-1} s^{-1} (Buxton et al., 1988).

Aqueous solutions (5 mL) containing H_2O_2 (5 mmol L^{-1}), PXT (20.2 μmol L^{-1}) and iPr (from 0 to 3 mmol L^{-1}) were irradiated under UVB light, in which conditions H_2O_2 is an efficient HO• photosensitiser. The potential reactions taking place during irradiation of these solutions are the formation of HO• radicals upon H_2O_2 photolysis (Eq. (1)), the concurrent scavenging of HO• by H_2O_2, PXT and iPr (Eqs. (2), (3), (4)), as well as the direct photolysis of PXT (Eq. (5)). Actually, these reactions are not the only ones that occur in the system, but they are the most important in the assessment of $k_{(HO^\bullet+iPr)}$. Additionally, the reaction between HO• and iPr mainly forms the α-hydroxyalkyl radical $(CH_3)_2C^\bullet OH$, which can react with dissolved O_2 to produce superoxide radical, $HO_2^\bullet$, acetone and other small organic compounds (von Sonntag and Schuchmann, 1991). Because the degradation of iPr by HO• produces several radical species (here generally defined as X•), the possible reactions between PXT and X• (Eq. (6)) should not be ruled out a priori.

$$H_2O_2 + h\nu \rightarrow 2\ HO^\bullet \quad (1)$$

$$HO^\bullet + H_2O_2 \rightarrow H_2O + HO_2^\bullet \quad k_{(HO^\bullet+H_2O_2)} = 2.7\times10^7\ L\ mol^{-1}s^{-1}\ (Buxton\ et\ al.,\ 1988) \quad (2)$$

$$HO^\bullet + PXT \rightarrow products \quad k_{(HO^\bullet+PXT)}\ (to\ be\ determined) \quad (3)$$

$$HO^\bullet + iPr \rightarrow H_2O + (CH_3)_2C^\bullet OH \quad k_{(HO^\bullet+iPr)} = 1.9\times10^9\ L\ mol^{-1}s^{-1}\ (Buxton\ et\ al.,\ 1988) \quad (4)$$

$$PXT + h\nu \rightarrow products\ \Phi_{PXT} = (4.03\pm0.25)\times10^{-2} \quad (5)$$

$$PXT + X^\bullet \rightarrow products \quad (6)$$

The overall degradation rate of PXT (R_{tot}) can be described as the sum $R_{tot} = R_{(PXT+HO^\bullet)} + R_{d.p.} + R_{add}$, where $R_{(PXT+HO^\bullet)}$, $R_{d.p.}$ and R_{add} are the rates of Eqs. (3), (5) and (6), respectively. $R_{d.p.}$ was measured as 2.7 ± 0.3 nmol L^{-1} s^{-1} (Fig. 2a), in good agreement with the value of 2.4 ± 0.1 nmol L^{-1} s^{-1} reported in the previous section. This is due to the fact that UVB radiation absorption by H_2O_2 is low enough, not to interfere significantly with the direct photolysis of PXT (note, however, that low radiation absorption by H_2O_2 is offset by its high quantum yield of HO• generation, i.e., $\Phi_{HO^\bullet}^{H_2O_2} \sim 1$; Wols et al., 2014).

R_{tot} was measured at different iPr concentrations, and then corrected for $R_{d.p.}$ (i.e., $R_{tot} - R_{d.p.} = R_{(PXT+HO^\bullet)} + R_{add}$). The sum $R_{(PXT+HO^\bullet)} + R_{add}$ decreased with increasing alcohol concentration (Fig. 2b), because of the competition between iPr and PXT for reaction with HO•. Competition kinetics can be modelled by considering that $R_{(PXT+HO^\bullet)} = k_{(HO^\bullet+PXT)} \times [HO^\bullet] \times [PXT]$, and by reasonably adopting the steady-state approximation for the hydroxyl radicals concentration ($[HO^\bullet]$). By taking into account the formation of HO• and its consumption by H_2O_2, PXT and iPr, one gets $R_{f,HO^\bullet} = [HO^\bullet] \times (k_{(HO^\bullet+H2O2)} \times [H_2O_2] + k_{(HO^\bullet+PXT)} \times [PXT] + k_{(HO^\bullet+iPr)} \times [iPr])$, where $R_{f,HO^\bullet}$ is the formation rate of HO• radicals upon H_2O_2 photolysis (Eq. (1)). By replacing the value of $[HO^\bullet]$ thus obtained in the expression for $R_{(PXT+HO^\bullet)}$, one gets the following:

$$R_{(PXT+HO^\bullet)} + R_{add} = \frac{R_{f,HO^\bullet} \times k_{(HO^\bullet+PXT)} \times [PXT]}{k_{(HO^\bullet+H_2O_2)} \times [H_2O_2] + k_{(HO^\bullet+PXT)} \times [PXT] + k_{(HO^\bullet+iPr)} \times [iPr]} + R_{add} \quad (7)$$

Eq. (7) was used to fit the experimental data reported in Fig. 2b, with $R_{f,HO^\bullet}$, $k_{(HO^\bullet+PXT)}$ and R_{add} as fit variables, yielding $k_{(HO^\bullet+PXT)} = (1.7\pm0.5)\times10^{10}$ L mol^{-1} s^{-1}. Although slightly higher, this value of $k_{(HO^\bullet+PXT)}$ is in good agreement with the findings of previous works, where Wols et al. (2014) and Santoke and Cooper (2017) report $k_{(HO^\bullet+PXT)} = (9.6\pm3.6)\times10^9$ L mol^{-1} s^{-1} and $k_{(HO^\bullet+PXT)} = (8.7\pm0.1)\times10^9$ L mol^{-1} s^{-1}, respectively. Indeed, the difference between these values is well within the variability that is usually found during the determination of second-order kinetic constants with different experimental procedures (see, for instance, Berto et al., 2018). Also consider, however, that the method we used here to determine $k_{(HO^\bullet+PXT)}$ (substrate + quencher) is more time-consuming than the alternative method based on substrate + probe molecule, but it is more robust because it is less prone to interferences by unwanted additional processes (Minella et al. 2017). Indeed, while it is possible to take substrate direct photolysis into account in the substrate + probe method, there is no way at all to account for reactions like Eq. (6) (PXT + X•).

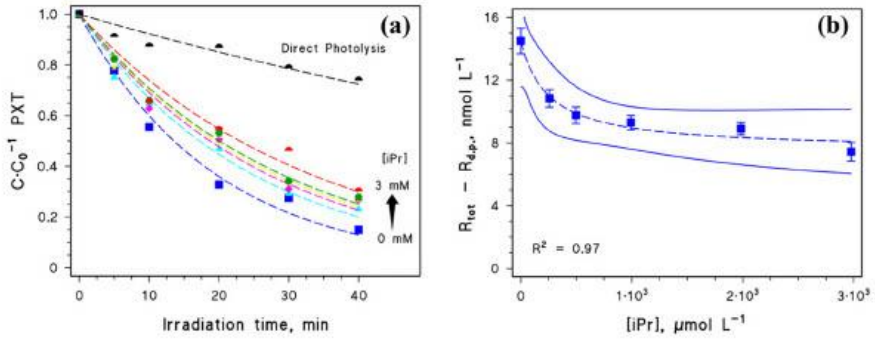

Fig. 2. (a) Degradation profiles of PXT under UVB, measured in the presence of H_2O_2 (5 mmol L^{-1}) and different concentrations of iPr. The direct photolysis was assessed in the absence of both H_2O_2 and iPr. (b) Experimental data of $R_{tot} - R_{d,p.}$ as a function of the added iPr concentration. The errors bars represent the standard errors related to the fit of the curves reported in (a). The dashed line shows the data fit with Eq. (7), with the associated 95% confidence bands (solid lines) and $R^2 = 0.97$, which both represent the goodness of the fit.

Data fit also yielded $R_{f,HO^\bullet} = 9.6 \pm 1.5$ nmol L^{-1} s^{-1} and $R_{add} = 7.6 \pm 0.6$ nmol L^{-1} s^{-1}. Note that R_{add} was quite high, thereby suggesting that the reactivity of PXT with $X^\bullet$ would not be negligible.

3.1.3. PXT reactivity towards singlet oxygen ($^1O_2$)

Aqueous solutions (5 mL) containing PXT (from 5 to 20 μmol L^{-1}) and the dye Rose Bengal (10 μmol L^{-1}) were irradiated under a lamp Philips TL D 18 W/16 Yellow to assess the second-order rate constant $k_{(^1O2+PXT)}$ of the reaction PXT + $^1O_2$ (Vione, 2020). The yellow lamp was chosen because its long-wavelength emission excites Rose Bengal selectively, without unwanted excitation of additional species like PXT. The excited triplet state of RB ($^3RB^*$), which is generated following light absorption by RB, is able to efficiently react with dissolved oxygen in its ground triplet state to produce $^1O_2$. The majority of $^1O_2$ undergoes deactivation by collision with the surrounding water molecules, with a quenching rate constant $k_{q,^1O2} = 2.5 \times 10^5$ s^{-1} (Wilkinson et al., 1995). The remaining fraction of $^1O_2$ can react with PXT (Scheme 1).

The rate of PXT transformation by $^1O_2$, which is assessed from the measured degradation profiles of PXT (Fig. S-2: a), is $R = k_{(^1O2+PXT)} \times [^1O_2] \times [PXT]$, where $[^1O_2]$ is the steady-state concentration of singlet oxygen. The steady-state condition was here provided by (*i*) steady irradiation; (*ii*) partitioning of dioxygen between the irradiated solution and the headspace of the glass cell; (*iii*) regeneration of the RB ground-state after $^3RB^*$ quenching; (*iv*) continuous formation of $^1O_2$ upon RB irradiation, and (*v*) fast quenching of $^1O_2$ by water (Scheme 1). By considering the formation rate of $^1O_2$ by irradiated RB ($R_{f,^1O2}$), one has $[^1O_2] = R_{f,^1O2}(k_{q,^1O2} + k_{(^1O2+PXT)} \times [PXT])^{-1}$. In our case it was determined $R_{f,^1O2} = (6.5 \pm 0.6) \times 10^{-7}$ mol L^{-1} s^{-1} by measuring the degradation rate of furfuryl alcohol (FFA, 100 μmol L^{-1}) upon reaction with $^1O_2$. The use of FFA as $^1O_2$ probe to measure $R_{f,^1O2}$ has been widely adopted and described in previous works (Carena et al., 2017; Rosario-Ortiz and Canonica, 2016; Vione, 2020).

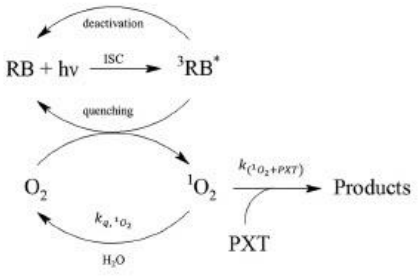

Scheme 1. Simplified scheme showing the potential reactions taking place in the irradiated solutions, used for the determination of the second-order rate constant of the reaction between PXT and singlet oxygen.

Note that the rate constants for the reactions between organic pollutants and $^1O_2$ in water often range between 10^6 and 10^7 L mol^{-1} s^{-1} (Arnold et al., 2017; Wilkinson et al., 1995). If this is our case as well, it should be $k_{(^1O2+PXT)} \times [PXT] \ll k_{q,^1O2}$ in the adopted range of [PXT] = 5–20 μmol L^{-1}. Therefore, the PXT degradation rate by $^1O_2$ can be linearly related to [PXT] as in Eq. (8):

$$R = \frac{R_{f,^1O_2} \times k_{(^1O_2+PXT)}}{k_{q,^1O_2}} \times [PXT] \quad (8)$$

A linear trend was actually found experimentally for *R* vs. [PXT] (Fig. S-2: b), which allows for the assessment of $k_{(^1O2+PXT)}$ from the line slope, $m = (3.29 \pm 0.21) \times 10^{-4}$ s^{-1}. By so doing, one finally gets $k_{(^1O2+PXT)} = m \times k_{q,^1O2} \times (R_{f,^1O2})^{-1} = (1.26 \pm 0.20) \times 10^8$ L mol^{-1} s^{-1}. This value is in very good agreement with that of $(1.18 \pm 0.13) \times 10^8$ L mol^{-1} s^{-1} obtained by Santoke and Cooper (2017) with a competition kinetics approach.

3.1.4. Reaction of PXT with the excited triplet states of CDOM ($^3CDOM^*$)

CBBP was here used as proxy molecule for CDOM. CBBP has been widely adopted as CDOM proxy in previous works (Carena et al., 2019; Li et al., 2015; McNeill and Canonica, 2016; Wenk and Canonica, 2012). A protocol has been recently proposed based on steady irradiation experiments, to assess the reactivity of organic pollutants with the excited triplet state of CBBP ($^3CBBP^*$) (Minella et al., 2018). This protocol involves the irradiation of aqueous solutions (5 mL) containing CBBP (~70 μmol L^{-1}) and different concentrations of the organic substrate S (S = PXT in our case). By studying the dependence of the PXT degradation rate (*R*) on the added PXT concentration ([PXT]), the value of the second-order rate constant of the reaction PXT + $^3CBBP^*$ can be obtained with the following equation (Carena et al., 2019; Minella et al., 2018):

$$k_{(^3CBBP^*+PXT)} = k_d' \times \left(\frac{m}{P_{a,CBBP}} - \frac{0.68 \times S_a \times k_{(^1O_2+PXT)}}{k_{q,^1O_2}} \right) \quad (9)$$

where $P_{a,CBBP}$ is the photon flux absorbed by CBBP, $k_d' = 6 \times 10^5$ s^{-1} is the deactivation rate constant of $^3CBBP^*$ in aerated solution, 0.68 is the

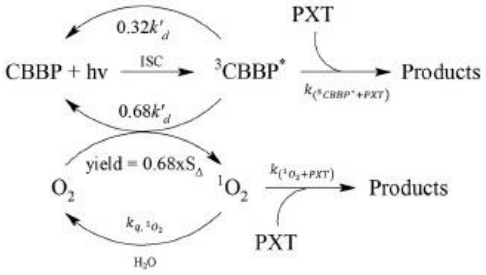

Scheme 2. Simplified scheme showing the possible reactions taking place in the irradiated solutions, used for the determination of the second-order rate constant of the reaction between PXT and ^{3}CBBP*.

fraction of ^{3}CBBP* that reacts with dissolved triplet O_2 (the remaining fraction of ^{3}CBBP* is likely deactivated by internal conversion), $S_\Delta = 0.46$ is the yield of $^1O_2$ upon reaction between ^{3}CBBP* and O_2, and $k_{q,^1O2} = 2.5 \times 10^5\ s^{-1}$ is the $^1O_2$ quenching rate constant by collision with water molecules (Scheme 2). Finally, m (in s^{-1} units) is the slope of the line R vs. [S].

In our case, PXT was irradiated under the UVA black lamp (see Fig. S-3 for the lamp spectral photon flux density spectrum, $p°(\lambda)$). Under these experimental conditions, the photon flux absorbed by CBBP was $P_{a,CBBP} = \int_\lambda p°(\lambda) \times [1 - 10^{-\varepsilon_{CBBP}(\lambda) \times b \times [CBBP]}] = (1.1 \pm 0.1) \times 10^{-8}$ Einstein $L^{-1}\ s^{-1}$ ($b = 0.4$ cm and [CBBP] = 70 μmol L^{-1}). Note that PXT is not able to absorb radiation in the wavelength range emitted by the lamp (Fig. 1a), thus radiation absorption by PXT was not taken into account in the calculation of $P_{a,CBBP}$. Moreover, the lack of UVA absorption by PXT also prevented its direct photolysis under UVA irradiation. Fig. 3a shows the dependence of the PXT degradation rate on the added [PXT] (from 5 to 20 μmol L^{-1}). The linear fit of the experimental data ($R^2 = 0.98$) gave $m = (8.33 \pm 0.26) \times 10^{-5}\ s^{-1}$, from which $k_{(^3CBBP^*+PXT)} = (4.5 \pm 0.6) \times 10^9\ L\ mol^{-1}\ s^{-1}$ was calculated.

From the above data, the triplet-sensitised reaction of PXT looks very fast. However, several previous works have shown that the transformation reactions, sensitised by ^{3}CDOM* and ^{3}CDOM* proxies, of some water pollutants such as anilines and sulfonamides are inhibited by the antioxidant moieties of DOM (AODOM) (Canonica and Laubscher, 2008; Carena et al., 2019; Leresche et al., 2016; Vione et al., 2018; Wenk et al., 2011; Wenk and Canonica, 2012). In particular, ^{3}CDOM* can partially oxidise xenobiotics through electron transfer (Davis et al., 2018; Li et al., 2015; Wang et al., 2015), producing radicals that can be reduced back to the parent compounds by AODOM (Eqs. (10), (11)) (Wenk and Canonica, 2012). At the laboratory scale AODOM is well represented by phenol (PhOH), because PhOH resembles the anti-oxidant phenolic moieties that are very common in AODOM. Moreover, PhOH is conveniently water-soluble and it is oxidized to poorly reactive phenoxy radicals (Carena et al., 2019; Leresche et al., 2016; Vione et al., 2018; Wenk and Canonica, 2012).

$$S + {}^3CDOM*/{}^3CBBP* \rightarrow S^{\bullet+} + CDOM^{\bullet-}/CBBP^{\bullet-} \quad (10)$$

$$S^{\bullet+} + AODOM/PhOH \rightarrow S + AODOM^{\bullet+}/(PhO^{\bullet} + H^+) \quad (11)$$

$$S^{\bullet+} \rightarrow \text{oxidation products} \quad (12)$$

If the back-reduction process induced by PhOH is operational, the actual (corrected) value of the second-order rate constant for the reaction of S with ^{3}CBBP* should be $k_{(^3CBBP^*+S)}^{corr} = \Psi \times k_{(^3CBBP^*+S)}$ (Vione et al., 2018), where $\Psi < 1$. Because the degradation rate of S by ^{3}CBBP* is $R = k_{(^3CBBP^*+S)}^{corr} \times [S] \times [^3CBBP^*]$, one has $R = \Psi \times R^0$, where $R^0 = k_{(^3CBBP^*+S)} \times [S] \times [^3CBBP^*]$ is the transformation rate of S measured in the absence of PhOH. The correction factor Ψ takes into account the back-reduction, as $\Psi = (1 + [PhOH]/[PhOH]_{1/2})^{-1}$, where $[PhOH]_{1/2}$ is the phenol concentration that halves the value of R^0 (Wenk and Canonica, 2012).

$$R = \frac{R^0}{1 + \frac{[PhOH]}{[PhOH]_{1/2}}} \quad (13)$$

Fig. 3b shows that the degradation rate of PXT induced by ^{3}CBBP* decreases with increasing phenol concentration, which suggests that the back-reduction process is operational with PXT. The fit of Fig. 3b data with Eq. (13) yielded $[PhOH]_{1/2} = 1.46 \pm 0.25$ μmol L^{-1}.

3.1.5. Photochemical model for surface water (SW)

The photochemical fate of PXT in sunlit SW was modelled by means of the APEX software (*Aqueous Photochemistry of Environmentally-occurring Xenobiotics*) (Bodrato and Vione, 2014; Vione, 2020). The model takes into account the photoreactivity parameters of water pollutants (in the present case PXT, the photochemical parameters of

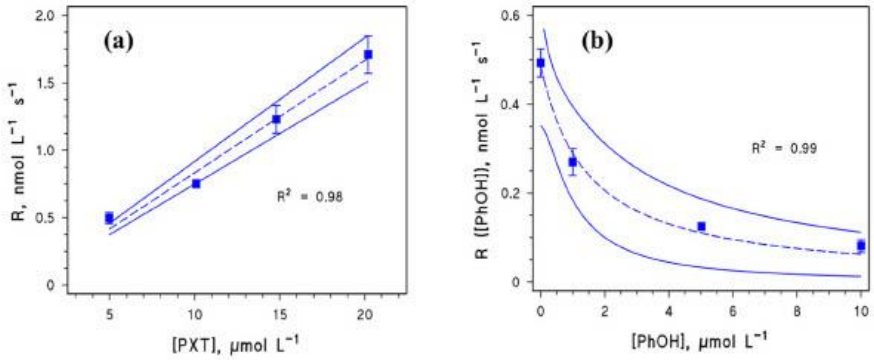

Fig. 3. (a) Rate of PXT degradation by ^{3}CBBP*, as a function of the added PXT concentration. (b) Dependence of the degradation rate of PXT (initial concentration 5 μmol L^{-1}) induced by ^{3}CBBP*, on the concentration of added phenol (PhOH). Experimental data were fitted with (a) Eq. (9) and (b) Eq. (13) (dashed lines). The associated 95% confidence bands (solid lines) and R^2 values are also reported, which both represent the goodness of the fit.

Table 1
Second-order reaction rate constants with the main PPRIs, and UVB quantum yield of paroxetine (PXT) direct photolysis. The second-order rate constant of the reaction PXT + $CO_3^{\bullet-}$ was taken from Wols et al. (2014), while ^{3}CDOM* is here represented by ^{3}CBBP*.

Compound	Φ (UVB)	$k_{(PXT+PPRI)}$, L mol^{-1} s^{-1}			
		HO$^\bullet$	$CO_3^{\bullet-}$	$^1O_2$	^{3}CDOM*
PXT	$(4.0 \pm 0.3) \times 10^{-2}$	$(1.7 \pm 0.5) \times 10^{10}$	$(4.2 \pm 0.9) \times 10^{8}$	$(1.3 \pm 0.2) \times 10^{8}$	$\psi \times (4.5 \pm 0.6) \times 10^{9}$ $[PhOH]_{1/2} = 1.46$ μmol L^{-1}

which are listed in Table 1), sunlight irradiance, as well as the chemical composition and depth of the water body. PXT phototransformation was modelled in environmental scenarios that differed for both water depth and chemical composition (Fig. 4). In particular, the dissolved organic carbon (DOC, which quantifies the (C)DOM content), nitrate concentration and water depth were chosen as master variables of the model. Depth was set at either 0.5 m (Fig. 4a, c) or 5 m (Fig. 4b, d) to represent a shallow river (or the upper layer of a lake) and a lake epilimnion, respectively. The back-reduction process was considered in the model, by converting the value of $[PhOH]_{1/2}$ (μmol L^{-1}) into a quantity that is more representative of SW ($DOC_{1/2}$, mg$_C$ L^{-1}), through the relationship $DOC_{1/2} = \beta \times [PhOH]_{1/2}$ (Leresche et al., 2016; Vione et al., 2018). In particular, the conversion factor β was set at 0.4 or 0.9 when, respectively, Suwannee River fulvic acids (SRFA) or Pony Lake fulvic acids (PLFA) were used as model AODOM. These β values have been reported for the back-reduction of a N-centred radical produced through ^{3}CDOM*-sensitised oxidation of *N*,*N*-dimethyl-4-cyanoaniline (Leresche et al., 2016). Furthermore, the previous relationship has been found to hold as well for the basic form of sulfadiazine, which would be oxidized to a N-centred radical by the triplet states of DOM (Tentscher et al., 2013; Vione et al., 2018). Because also the N atom of the piperidine ring of PXT may be potentially oxidized by ^{3}CDOM*, forming an aminyl radical that may react with AODOM via back-reduction, we can expect that the previous equation can apply for PXT as well. Therefore, the rate constant between PXT and ^{3}CDOM* was corrected as per $k_{(^3CDOM^* + PXT)}^{corr} = \Psi \times k_{(^3CBBP^* + PXT)}^{corr}$, with $\Psi = (1 + DOC/DOC_{1/2})^{-1}$ and $DOC_{1/2}$ as per the above discussion.

The pseudo-first order photodegradation rate constant of PXT (k'_{PXT}) is strongly dependent on the DOC value (Fig. 4a, b). This is likely due to the key roles played by $CO_3^{\bullet-}$ and HO$^\bullet$ in the overall phototransformation (Vione et al., 2014). The reaction of PXT with $CO_3^{\bullet-}$ and HO$^\bullet$ prevails at low DOC, where scavenging of the two radical species by DOM is still limited. The reverse happens at high DOC, where both $CO_3^{\bullet-}$ and HO$^\bullet$ are very efficiently consumed by DOM.

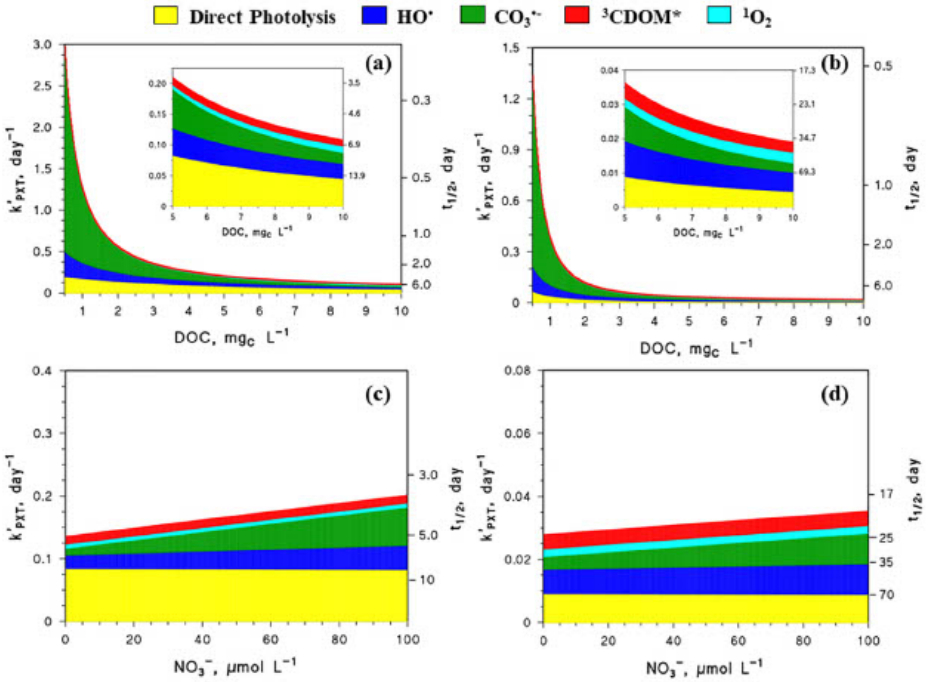

Fig. 4. Pseudo-first order rate constants (left axis) and half-life times (right axis) of PXT photodegradation, as a function of DOC (with constant 100 μmol L^{-1} NO_3^-) and nitrate content (with constant 5 mg$_C$ L^{-1} DOC). PXT phototransformation was modelled in a surface-water column, with depth values of 0.5 m (a), (c) and 5 m (b), (d). Other water chemistry parameters were: pH 8.0, alkalinity 1.0 mmol L^{-1}, and $[NO_3^-] = 1.0$ μmol L^{-1} (a), (b) or 0.1 μmol L^{-1} (c), (d). Concerning PXT degradation by back-reduction, SRFA was used in the model as AODOM proxy. The phototransformation kinetics is referred to mid-latitude irradiation conditions during mid-July. The color code depicts the fractions of PXT phototransformation accounted for by the different processes. The inserts in panels (a), (b) show a focus on the k'_{PXT} and $t_{1/2}$ profiles for 5 < DOC <10 mg$_C$ L^{-1}.

Compared to the DOC, nitrate plays a less important role in the photodegradation kinetics of PXT (Fig. 4c, d). The increase of k'_{PXT} with increasing $[NO_3^-]$ is mostly due to the enhancement of photodegradation by $CO_3^{\bullet-}$, while degradation by $HO^\bullet$ is poorly dependent on nitrate. The most likely reason for the latter finding is that, in the presence of 5 $mg_C\ L^{-1}$ DOC, CDOM would out-compete nitrate in $HO^\bullet$ generation.

The direct photolysis of PXT gets slower as the DOC increases, because of competition for irradiance between PXT and CDOM. In contrast, a variation of $[NO_3^-]$ does not affect the direct photolysis kinetics significantly, because NO_3^- is a minor radiation absorber. Interestingly, the reactions with $^3CDOM^*$ and $^1O_2$ play a secondary role in PXT photodegradation. The former process is depressed by back-reduction, while PXT is poorly reactive with $^1O_2$. Concerning the inhibition by back-reduction, the overall PXT degradation is not significantly affected by the type of AODOM considered in the model, either SRFA (Fig. 4) or PLFA (Fig. S-4).

Looking at the photochemical half-life times, our findings suggest that PXT is degraded fast by both direct photolysis and indirect photochemistry. Therefore, photochemical reactions are potentially important degradation pathways for PXT in SW. Lifetimes range from a few days or less in shallow waters ($d = 0.5$ m), which are well illuminated by sunlight, up to 20–30 days in deeper waters ($d = 5$ m) at high DOC.

Photochemical lifetimes (annual mean values) of PXT were assessed for Slovenian lakes and watercourses in 2018 (Fig. 5, and Chapter 3 of SM). These values were obtained with modelling tools, based on data about the chemical composition of Slovenian water bodies that were provided by (https://www.arso.gov.si/vode/). A detailed description of the modelling procedure is reported in a recently published paper (Carena et al., 2021). It is seen that photochemical reactions potentially play a key role in the environmental fate of PXT, as the drug's lifetime was <2 days in the majority (~ 60%) of the investigated water bodies, including our sampling sites. Additionally, $CO_3^{\bullet-}$ radicals and the direct photolysis should have been the main PXT phototransformation pathways, accounting for, respectively, ~ 55% and ~30% of the overall PXT photodegradation (note that many Slovenian surface waters flow in karst regions, Garmo et al., 2014, providing them with pH and inorganic carbon conditions that are particularly favourable to the occurrence of $CO_3^{\bullet-}$). The remaining fraction of PXT photodegradation was mainly due to reaction with $HO^\bullet$ radicals, while the reactivity with $^3CDOM^*$ and $^1O_2$ was negligible.

3.2. Validation of the analytical methods

The HPLC-DAD method was linear in the range of 10^{-6} - 10^{-4} mol L^{-1} PXT ($R^2 = 0.9995$), with method repeatability of 1.6%. Validation parameters of the UHPLC-Qtrap method for PXT are reported in SM, Table S-3. Because we observed that the metabolite PC partially degraded during sample preparation, we succeeded to qualitatively determine its occurrence but its quantification was not possible.

3.3. Detection, identification and formation of TPs

Our workflow first followed the screening of the 53 candidates from our suspect list, resulting in TP-210, which has already been reported in the literature (Kwon and Armbrust, 2004; Šakić et al., 2013). Moreover, an additional three candidates from the predicted suspects were detected (TP-192, TP-226, TP-328).

The MZmine analysis of the LC-MS data gave rise to a list of 908 features. After application of our filtering criteria (remove duplicates, retention time < 7.1 min, $100 < m/z < 500$), we were left with 453 features. In order to extract possible TP candidates, we compared blanks and control samples (withdrawn at the beginning of the experiment) with the corresponding irradiated samples using scatter plots. An example is Fig. S-5, which compares a scatter plot of a control sample with that of a sample withdrawn after 180 min of irradiation, both in the

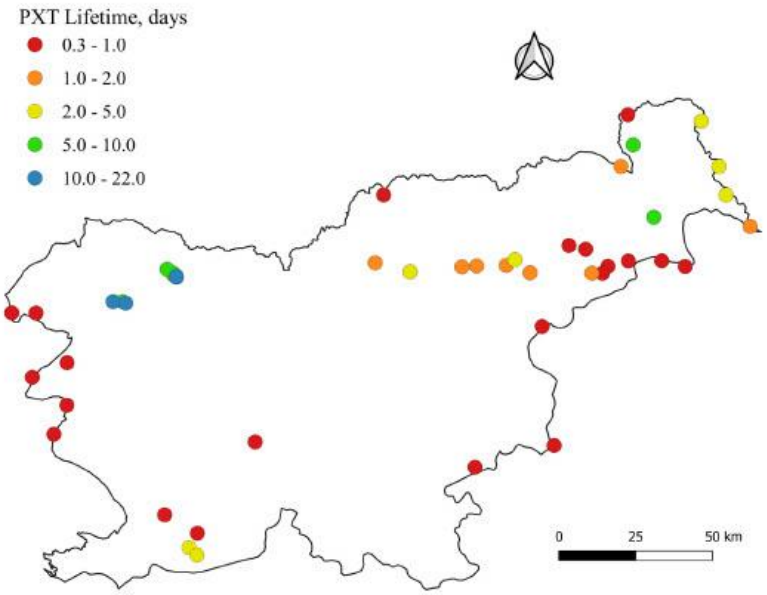

Fig. 5. PXT photochemical lifetime map in Slovenian water bodies, referred to the year 2018. The results are annual mean values for a standard water depth of 20 cm. The map was made by means of the QGIS software (QGIS, 2020).

presence of $NaNO_3$. The ions that are placed above the chosen significance level are more abundant in the sample irradiated for 180 min, and thus represent potential TP candidates. This acquired list of potential TPs was also checked manually. For each of the candidates, MS/MS spectra were obtained and nine of them were identified as TPs of PXT.

All the identified TPs were detected with the positive electrospray ionisation mode, while no newly formed TPs were observed in negative ionisation mode. The accurate masses of the protonated molecules and MS/MS fragmentation patterns were the basis for TP identification. The level of confidence for each identified TP was assigned based on the system suggested by Schymanski et al. (2014). When no other structure fitted the experimental information, a level of confidence 2b was assigned to the TP. If the exact location of a functional group was unknown, a level of confidence of 3 was assigned. The level of confidence 4 was assigned if we determined the elemental formula of the TP, but were unable to propose any possible structure. The isotope ratio score was obtained with the MZmine "Predict molecular formula" tool. The diagnostic information for PXT and its identified TPs can be found in Table 2, and the process of assigning chemical structures to the detected TPs, including their MS/MS spectra can be found in the SM, Chapter 2.2.

Table 2
Summary of the diagnostic data on the identified TPs: compound ID, RT, measured mass of $[M + H]^+$, mass error [ppm] and proposed elemental formula, RDBE, isotope ratio score [%], the diagnostic product ion mass with the corresponding mass error [ppm] and elemental composition of fragment ions.

Compound ID	RT [min]	Measured mass $[M + H]^+$	Error [ppm]	Elemental formula: $[M + H]^+$	RDBE	Isotope ratio score [%]	Confidence level	Diagnostic production mass	Error [ppm]	Elemental composition of fragment ions
PXT	3.52	330.1521	4.8	$C_{19}H_{21}FNO_3$	10	96	L1	192.1200	5.7	$C_{12}H_{15}FN$
								178.1046	7.9	$C_{11}H_{13}FN$
								163.0935	7.4	$C_{11}H_{12}F$
								151.0412	−6.6	$C_8H_7O_3$
								135.0628	13.3	C_9H_8F
								123.0610	−3.3	C_8H_8F
								109.0457	2.8	C_7H_6F
TP-192	1.49	192.1402	7.3	$C_{12}H_{18}NO$	5	/	L2b	174.1306	13.2	$C_{12}H_{16}N$
								145.1001	−11.0	$C_{11}H_{13}$
								130.0804	16.1	$C_{10}H_{10}$
								117.0718	16.4	C_9H_9
								105.0736	35.4	C_8H_9
								91.0552	10.7	C_7H_7
TP-210	1.80	210.1305	4.5	$C_{12}H_{17}FNO$	5	96	L2b	192.1194	2.6	$C_{12}H_{15}FN$
								163.0934	6.7	$C_{11}H_{12}F$
								135.0616	4.4	C_9H_8F
								123.0627	13.8	C_8H_8F
								109.0465	10.1	C_7H_6F
TP-226	2.26	226.1276	4.9	$C_{12}H_{17}FNO_2$	5	/	L3	208.1110	−13.5	$C_{12}H_{15}FNO$
								178.1050	10.1	$C_{11}H_{13}FN$
								163.0926	1.8	$C_{11}H_{12}F$
								135.0624	10.4	C_9H_8F
								109.0432	20.2	C_7H_6F
TP-238	2.27	238.1261	7.6	$C_{13}H_{17}FNO_2$	6	/	L3	163.0930	4.3	$C_{11}H_{12}F$
								135.0584	−19.2	C_9H_8F
								123.0623	3.3	C_7H_6F
								109.0457	2.8	C_7H_6F
TP-296	2.33	296.1411	−13.5	$C_{19}H_{19}FNO$	11	/	L4	278.1243	−34.8	$C_{19}H_{17}FN$
								252.1472	35.3	$C_{17}H_{18}NO$
								210.1341	24.7	$C_{12}H_{17}FNO$
								192.1232	23.9	$C_{12}H_{15}FN$
								163.0955	19.6	$C_{11}H_{12}F$
								135.0637	20.0	C_9H_8F
								123.0640	24.3	C_7H_6F
TP-328	2.37	328.1561	3.7	$C_{19}H_{22}NO_4$	10	/	L2b	310.1545	34.5	$C_{19}H_{20}NO_3$
								298.1441	−0.7	$C_{18}H_{20}NO_3$
								270.1505	4.1	$C_{17}H_{20}NO_2$
								241.0918	22	$C_{15}H_{13}O_3$
								218.1202	9.6	$C_{13}H_{16}NO_2$
TP-350	2.51	350.1404	0	$C_{18}H_{21}FNO_5$	9	97	L3	332.1350	17.3	$C_{18}H_{19}FNO_4$
								306.1531	8.5	$C_{17}H_{21}FNO_3$
								210.1322	10.9	$C_{12}H_{17}FNO$
								192.1214	13.3	$C_{12}H_{15}FN$
								190.1045	9.7	$C_{12}H_{13}FN$
								163.0949	13.0	$C_{11}H_{12}F$
								135.0634	15.9	C_9H_8F
								123.0636	17.7	C_8H_8F
TP-364	3.99	364.1135	6.8	$C_{19}H_{20}ClFNO_3$	10	/	L3	192.1206	8.8	$C_{12}H_{15}FN$
								190.1032	2.9	$C_{12}H_{13}FN$
								178.1026	−3.4	$C_{11}H_{13}FN$
								151.0408	−9.3	$C_8H_7O_3$
								135.0637	20.0	C_9H_8F
								123.0636	7.3	C_7H_6F
								109.0460	5.5	C_7H_6F
TP-375	3.49	375.1364	3.5	$C_{19}H_{20}FN_2O_5$	11	92	L3	192.1212	12.0	$C_{12}H_{15}FN$
								178.1042	5.6	$C_{11}H_{13}FN$
								163.0933	6.1	$C_{11}H_{12}F$
								135.0630	14.8	C_9H_8F
								123.0626	13.0	C_8H_8F
								109.0467	11.9	C_7H_6F

Fig. S-18 shows the formation profiles of the TPs, which served as the basis for constructing the degradation pathway (Fig. 6). TP-192 was formed during direct photolysis and in the reactions involving hydroxyl and carbonate radicals (Fig. S-18: a, b, c, f). According to the TP formation profiles in Fig. S-18 and in line with its chemical structure, TP-192 results from the cleavage of fluorine from TP-210. A TP with $[M+H]^+$ 192 was also observed by Kwon and Armbrust (2004) during their photodegradation experiments, but the structure of the dehydrated form of TP-210 was suggested based on the MS spectra obtained with a low resolution instrument. TP-210, which has also been

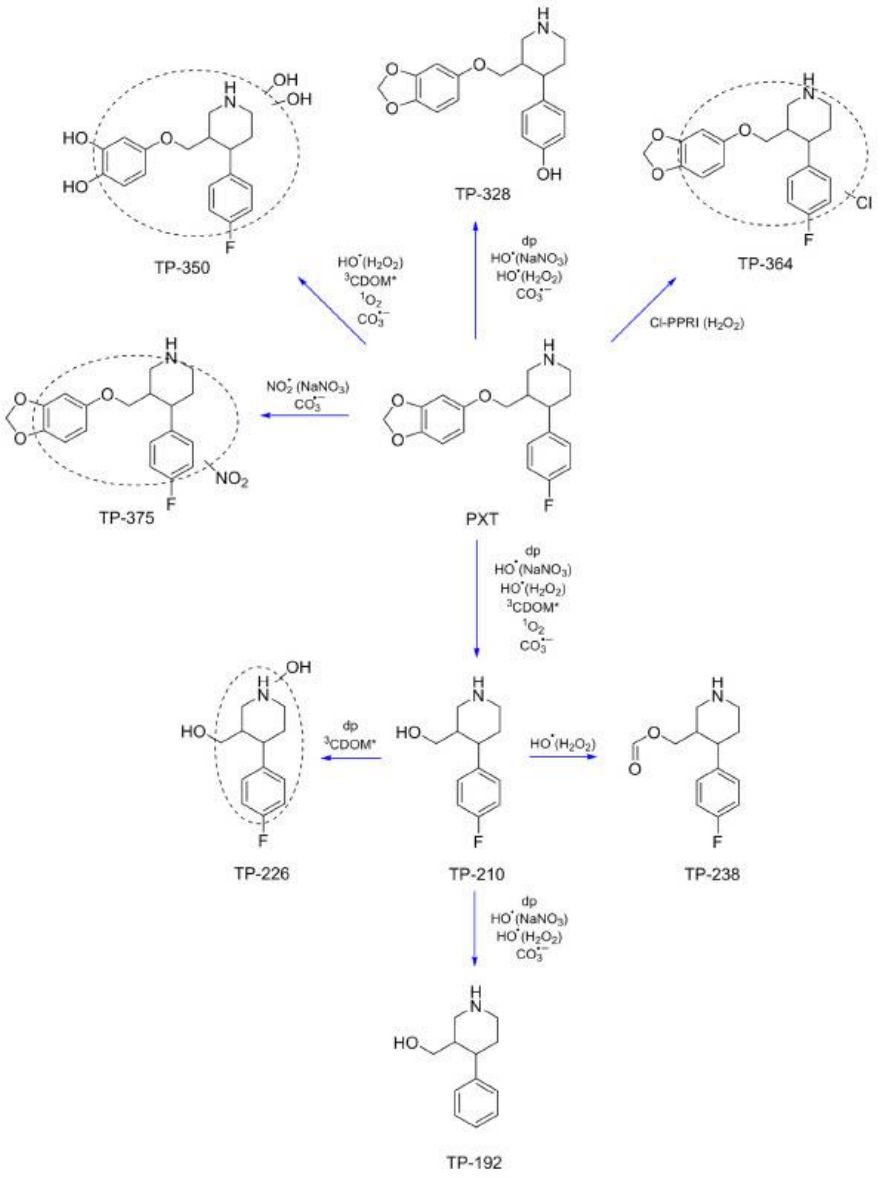

Fig. 6. Proposed photodegradation pathway of PXT including the main photochemical pathways. dp – direct photolysis.

identified as a photoproduct by Kwon and Armbrust (2004) and Šakić et al. (2013) was formed during all of our experiments, and it was one of the most abundant TPs of PXT. In contrast, TP-226 (Fig. S-18: a, d) and TP-238 (Fig. S-18: c) were formed only under certain conditions and on a smaller scale, and they likely originate from hydroxylation and formylation of TP-210. As we were not able to suggest an exact structure for TP-296, we excluded it from the predicted pathway. All the remaining TPs (TP-328, TP-350, TP-364 and TP-375) are formed from the parent molecule. While hydroxylation (TP-350, Fig. S-18: c, d, e, f) and oxidative deflourination (TP-328, Fig. S-18: a, b, c, f) are known photoreactions (Gornik et al., 2020; Hörsing et al., 2012; Kosjek et al., 2013), chlorination and nitration are less common. However, nitration has been reported as the result of biotransformation (Kosjek et al., 2008). TP-375 in our experiments was formed specifically because of the presence of nitrates in the irradiated solution (Fig. S-18: b, f), which yield the nitrating agent $^{\bullet}NO_2$ upon UV photolysis (Mack and Bolton, 1999; Vione et al., 2011):

$$NO_3^- + h\nu + H^+ \leftrightarrows [^{\bullet}NO_2 + HO^{\bullet}]_{cage} \quad (14)$$

$$[^{\bullet}NO_2 + HO^{\bullet}]_{cage} \rightarrow NO_3^- + H^+ \quad (15)$$

$$[^{\bullet}NO_2 + HO^{\bullet}]_{cage} \rightarrow {}^{\bullet}NO_2 + HO^{\bullet} \quad (16)$$

$$[^{\bullet}NO_2 + HO^{\bullet}]_{cage} \rightarrow HOONO \quad (17)$$

$$HOONO \rightarrow NO_3^- + H^+ \quad (18)$$

$$HOONO \rightarrow {}^{\bullet}NO_2 + HO^{\bullet} \quad (19)$$

Most reported nitrate levels in SW are below the limit of 50 mg L^{-1}, assigned in the Nitrates Directive (European Commission, 2019), while during the irradiation experiments we used a nitrate concentration that was more than ten-fold higher. Hence, the formation of TP-375 in SW is possible albeit this TP would be less abundant as compared to our experiments. The formation of TP-364 is even less probable in freshwaters. The only possible source of Cl in our experiments was the PXT reference standard itself, which is sold in the HCl salt form. The combination of UVB light, H_2O_2 and chloride probably resulted in the formation of chlorine reactive species (Vione et al., 2005) that effectively chlorinated the parent compound (Fig. S-18: c).

The occurrence of the identified TPs as well as that of PXT was assessed in three Slovenian river-water samples, but PXT concentrations were below the LOQ and no TPs were detected in any sample (-Chapter 4.4 of SM). This finding, together with results reported in Fig. 5, might suggest that photoreactions taking place in Slovenian SWs can efficiently degrade both PXT and its TPs.

4. Conclusions

- Direct photolysis and reaction with $HO^{\bullet}$ radicals should be the main reactions that induce degradation of PXT in most SWs. Carbonate radicals can play an important role in PXT transformation as well, in particular at low DOC values and in the presence of high pH and inorganic carbon. PXT lifetime ranges from a few days up to a month, depending on the DOC and the water depth.
- Short lifetimes in shallow water bodies make photochemistry an important dissipation pathway for PXT in these environments.
- Reaction with $^3CDOM^*$ should be a minor degradation pathway, mostly because of the occurrence of back-reduction reactions induced by antioxidants species, which inhibit PXT degradation.
- We identified seven new TPs for PXT, and suggested benzodioxol-cleaved PXT (TP-210) as the main TP formed during photodegradation.
- The photochemical modelling of Slovenian water bodies suggests that fast photodegradation could explain why we were unable to determine either PXT, its metabolite PC or any of the identified TPs in the sampled SWs.

Slovenia is a freshwater-rich country, with high precipitation and, consequently, high dilution factors. Natural attenuation is also very likely because of very well-preserved ecosystems, with more than half of the country covered with forests and a relatively low population density. Therefore, it would be intriguing to apply the same methodology in countries that face water scarcity, high population density and a higher degree of industrialisation.

CRediT authorship contribution statement

Tjasa Gornik: Investigation; Methodology; Data curation; Formal analysis; Writing - original draft. **Luca Carena:** Methodology; Formal analysis; Photochemical modelling; Writing - review & editing. **Tina Kosjek:** Conceptualization; Funding acquisition; Supervision; Validation; Writing - review & editing. **Davide Vione:** Conceptualization; Funding acquisition; Supervision; Validation; Writing - review & editing.

Declaration of competing interest

The authors declare that they have no known competing financial interests or personal relationships that could have appeared to influence the work reported in this paper.

Acknowledgements

The authors acknowledge financial support from the Slovenian Research Agency (research core funding No. P1-0143) and projects J1-6744 (Development of Molecularly Imprinted Polymers and their application in environmental and bio-analysis) and BI-IT-18-20-005 (Photochemical fate and treatment of pharmaceutical contaminants in drinking water). L.C. acknowledges Compagnia di San Paolo (Torino, Italy) for financially supporting his PhD fellowship. We thank Mr. Dušan Žigon (Jožef Stefan Institute) for his support in sampling campaign and HR-MS analyses, and Mr. M. Marafante (Dept. of Chemistry, University of Torino) for his help in photochemical mapping. Personnel exchange between the University of Torino and the Jožef Stefan Institute was financially supported by the bilateral cooperation agreement between Italy and Slovenia (project BI-IT-18-20-005).

Appendix A. Supplementary data

Further experimental details, method validation parameters, mass spectra of the detected intermediates, details of the photochemical modelling of slovenian surface waters. Supplementary data to this article can be found online at https://doi.org/10.1016/j.scitotenv.2021.145380.

References

Arnnok, P., Singh, R.R., Burakham, R., Pérez-Fuentetaja, A., Aga, D.S., 2017. Selective uptake and bioaccumulation of antidepressants in fish from effluent-impacted Niagara River. Environ. Sci. Technol. 51, 10652–10662. https://doi.org/10.1021/acs.est.7b02912.

Arnold, W.A., Oueis, Y., O'Connor, M., Rinaman, J.E., Taggart, M.G., McCarthy, R.E., Foster, K.A., Latch, D.E., 2017. QSARs for phenols and phenolates: oxidation potential as a predictor of reaction rate constants with photochemically produced oxidants. Environ Sci Process Impacts 19, 324–338. https://doi.org/10.1039/c6em00580h.

Berto, S., Carena, L., Chiavazza, E., Marletti, M., Fin, A., Giacomino, A., Malandrino, M., Barolo, C., Prenesti, E., Vione, D., 2018. Off-line and real-time monitoring of acetaminophen photodegradation by an electrochemical sensor. Chemosphere 204, 556–562. https://doi.org/10.1016/j.chemosphere.2018.03.069.

Bodrato, M., Vione, D., 2014. APEX (aqueous photochemistry of environmentally occurring Xenobiotics): a free software tool to predict the kinetics of photochemical processes. Environ Sci Process Impacts 16, 732–740. https://doi.org/10.1039/c3em00541k.

Buxton, G.V., Greenstock, C.L., Helman, P.W., Ross, A.B., 1988. Critical review of rate constants for reactions of hydrated electrons, hydrogen atoms and hydroxyl radicals

(•OH/•O⁻) in aqueous solution. J. Phys. Chem. Ref. Data 17, 513–886. https://doi.org/10.1063/1.555805.
Canonica, S., 2007. Oxidation of aquatic organic contaminants induced by excited triplet states. Chimia 61, 641–644. https://doi.org/10.2533/chimia.2007.641 Chimia.
Canonica, S., Laubscher, H.U., 2008. Inhibitory effect of dissolved organic matter on triplet-induced oxidation of aquatic contaminants. Photochem. Photobiol. Sci. 7, 547–551. https://doi.org/10.1039/b719982a.
Canonica, S., Kohn, T., Mac, M., Real, F.J., Wirz, J., von Gunten, U., 2005. Photosensitizer method to determine rate constants for the reaction of carbonate radical with organic compounds. Environ. Sci. Technol. 39, 9182–9188. https://doi.org/10.1021/es051236b.
Carena, L., Minella, M., Barsotti, F., Brigante, M., Milan, M., Ferrero, A., Berto, S., Minero, C., Vione, D., 2017. Phototransformation of the herbicide propanil in paddy field water. Environ. Sci. Technol. 51, 2695–2704. https://doi.org/10.1021/acs.est.6b05053.
Carena, L., Proto, M., Minella, M., Ghigo, G., Giovannoli, C., Brigante, M., Mailhot, G., Maurino, V., Minero, C., Vione, D., 2018. Evidence of an important role of photochemistry in the attenuation of the secondary contaminant 3,4-Dichloroaniline in Paddy water. Environ. Sci. Technol. 52, 6334–6342. https://doi.org/10.1021/acs.est.8b00710.
Carena, L., Puscasu, C.G., Comis, S., Sarakha, M., Vione, D., 2019. Environmental photodegradation of emerging contaminants: a re-examination of the importance of triplet-sensitised processes, based on the use of 4-carboxybenzophenone as proxy for the chromophoric dissolved organic matter. Chemosphere 237, 124476. https://doi.org/10.1016/j.chemosphere.2019.124476.
Carena, L., Comis, S., Vione, D., 2021. Geographical and temporal assessment of the photochemical decontamination potential of river waters from agrochemicals: a first application to the Piedmont region (NW Italy). Chemosphere 263, 127921. https://doi.org/10.1016/j.chemosphere.2020.127921.
Challis, J.K., Hanson, M.L., Friesen, K.J., Wong, C.S., 2014. A critical assessment of the photodegradation of pharmaceuticals in aquatic environments: defining our current understanding and identifying knowledge gaps. Environ Sci Process Impacts 16, 672–696. https://doi.org/10.1039/c3em00515h.
Cunningham, V.L., Constable, D.J.C., Hannah, R.E., 2004. Environmental risk assessment of paroxetine. Environ. Sci. Technol. 38, 3351–3359. https://doi.org/10.1021/es035119x.
Davis, C.A., McNeill, K., Janssen, E.M.L., 2018. Non-singlet oxygen kinetic solvent isotope effects in aquatic photochemistry. Environ. Sci. Technol. 52, 9908–9916. https://doi.org/10.1021/acs.est.8b01512.
Demchenko, A.P., Tomin, V.I., Chou, P., 2017. Breaking the kasha rule for more efficient photochemistry. Chem. Rev. 117, 13353–13381. https://doi.org/10.1021/acs.chemrev.7b00110.
European Commission, 2019. Nitrates - Water Pollution - Environment [WWW Document]. URL https://ec.europa.eu/environment/water/water-nitrates/index_en.html (accessed 4.10.20).
Fong, P.P., 2001. Antidepressants in aquatic organisms: a wide range of effects. In: Daughton, C.G., Jones-Lepp, T.L. (Eds.), Pharmaceuticals and Care Products in the Environment. American Chemical Society, Washington, DC, pp. 264–281 https://doi.org/10.1021/bk-2001-0791.ch015.
Fuentes, A., Pineda, M., Venkata, K., 2018. Comprehension of top 200 prescribed drugs in the US as a resource for pharmacy teaching, training and practice. Pharmacy 6, 43. https://doi.org/10.3390/pharmacy6020043.
Galhavy, E.S., Ram, K., Anastasio, C., 2010. Chemistry 2-Nitrobenzaldehyde as a chemical actinometer for solution and ice photochemistry. J. Photochem. Photobiol. Chem. 209, 186–192. https://doi.org/10.1016/j.jphotochem.2009.11.013.
Garmo, Ø.A., Skjelkvåle, B.L., de Wit, H.A., Colombo, L., Curtis, C., Fölster, J., Hoffmann, A., Hruška, J., Høgåsen, T., Jeffries, D.S., Keller, W.B., Krám, P., Majer, V., Monteith, D.T., Paterson, A.M., Rogora, M., Rzychon, D., Steingruber, S., Stoddard, J.L., Vuorenmaa, J., Worsztynowicz, A., 2014. Trends in surface water chemistry in acidified areas in Europe and North America from 1990 to 2008. Water Air Soil Pollut. 225, 1880. https://doi.org/10.1007/s11270-014-1880-6.
Gornik, T., Vozic, A., Heath, E., Trontelj, J., Roskar, R., Zigon, D., Vione, D., Kosjek, T., 2020. Determination and photodegradation of sertraline residues in aqueous environment. Environ. Pollut. 256, 113431. https://doi.org/10.1016/j.envpol.2019.113431.
Henry, T.B., Kwon, J.-W., Armbrust, K.L., Black, M.C., 2004. Acute and chronic toxicity of five selective serotonin reuptake inhibitors in Ceriodaphnia dubia. Environ. Toxicol. Chem. 23, 2229–2233.
Hiemke, C., Härtter, S., 2000. Pharmacokinetics of selective serotonin reuptake inhibitors. Pharmacol. Ther. 85, 11–28. https://doi.org/10.1016/S0163-7258(99)00048-0.
Hörsing, M., Kosjek, T., Andersen, H.R., Heath, E., Ledin, A., 2012. Fate of citalopram during water treatment with O3, ClO2, UV and fenton oxidation. Chemosphere 89, 129–135. https://doi.org/10.1016/j.chemosphere.2012.05.024.
Klančar, A., Trontelj, J., Roškar, R., 2018. Development of a multi-residue method for monitoring 44 pharmaceuticals in slovene surface water by SPE-LC-MS/MS. Water Air Soil Pollut. 229, 192. https://doi.org/10.1007/s11270-018-3845-7.
Kosjek, T., Žigon, D., Kralj, B., Heath, E., 2008. The use of quadrupole-time-of-flight mass spectrometer for the elucidation of diclofenac biotransformation products in wastewater. J. Chromatogr. A 1215, 57–63. https://doi.org/10.1016/j.chroma.2008.10.111.
Kosjek, T., Perko, S., Žigon, D., Heath, E., 2013. Fluorouracil in the environment: analysis, occurrence, degradation and transformation. J. Chromatogr. A 1290, 62–72. https://doi.org/10.1016/j.chroma.2013.03.046.
Kwon, J.-W., Armbrust, K.L., 2004. Hydrolysis and photolysis of paroxetine, a selective serotonin reuptake inhibitor, in aqueous solutions. Environ. Toxicol. Chem. 23, 1394–1399.
Leresche, F., Von Gunten, U., Canonica, S., 2016. Probing the photosensitizing and inhibitory effects of dissolved organic matter by using N,N-dimethyl-4-cyanoaniline (DMABN). Environ. Sci. Technol. 50, 10997–11007. https://doi.org/10.1021/acs.est.6b02868.
Li, Y., Wei, X., Chen, J., Xie, H., Zhang, Y. Nan, 2015. Photodegradation mechanism of sulfonamides with excited triplet state dissolved organic matter: a case of sulfadiazine with 4-carboxybenzophenone as a proxy. J. Hazard. Mater. 290, 9–15. https://doi.org/10.1016/j.jhazmat.2015.02.040.
Mack, J., Bolton, J.R., 1999. Photochemistry of nitrite and nitrate in aqueous solution: a review. J. Photochem. Photobiol. Chem. 128, 1–13. https://doi.org/10.1016/S1010-6030(99)00155-0.
Matsunaga, N., Nunoya, K., Okada, M., Ogawa, M., Tamai, I., 2013. Evaluation of hepatic disposition of paroxetine using sandwich-cultured rat and human hepatocytes. Drug Metab. Dispos. 41, 735–743. https://doi.org/10.1124/dmd.112.049817.
McDermott, S., 2018. HSE Prescriptions for Antidepressants and Anxiety Medications Up by Two Thirds since 2009 [WWW Document]. TheJournal.ie. URL https://www.thejournal.ie/ireland-antidepressant-anxiety-medicine-prescriptions-4157452-Aug2018/ (accessed 3.26.20).
McNeill, K., Canonica, S., 2016. Triplet state dissolved organic matter in aquatic photochemistry: reaction mechanisms, substrate scope, and photophysical properties. Environ Sci Process Impacts 18, 1381–1399. https://doi.org/10.1039/C6EM00408C.
Minella, M., Giannakis, S., Mazzavillani, A., Maurino, V., Minero, C., Vione, D., 2017. Phototransformation of Acesulfame K in surface waters: Comparison of two techniques for the measurement of the second-order rate constants of indirect photodegradation, and modelling of photoreaction kinetics. Chemosphere 186, 185–192.
Minella, M., Rapa, L., Carena, L., Pazzi, M., Maurino, V., Minero, C., Brigante, M., Vione, D., 2018. An experimental methodology to measure the reaction rate constants of processes sensitised by the triplet state of 4-carboxybenzophenone as a proxy of the triplet states of chromophoric dissolved organic matter, under steady-state irradiation conditions. Environ Sci Process Impacts 20, 1007–1019. https://doi.org/10.1039/c8em00155c.
Mole, R.A., Brooks, B.W., 2019. Global scanning of selective serotonin reuptake inhibitors: occurrence, wastewater treatment and hazards in aquatic systems. Environ. Pollut. 250, 1019–1031. https://doi.org/10.1016/j.envpol.2019.04.118.
Myers, O.D., Sumner, S.J., Li, S., Barnes, S., Du, X., 2017. One step forward for reducing false positive and false negative compound identifications from mass spectrometry metabolomics data: new algorithms for constructing extracted ion chromatograms and detecting chromatographic peaks. Anal. Chem. 89, 8696–8703. https://doi.org/10.1021/acs.analchem.7b00947.
Radjenovic, J., Petrovic, M., Barceló, D., 2007a. Analysis of pharmaceuticals in wastewater and removal using a membrane bioreactor. Anal. Bioanal. Chem. 387, 1365–1377. https://doi.org/10.1007/s00216-006-0883-6.
Radjenović, J., Petrović, M., Barceló, D., Petrović, M., 2007b. Advanced mass spectrometric methods applied to the study of fate and removal of pharmaceuticals in wastewater treatment. TrAC Trends Anal. Chem. 26, 1132–1144. https://doi.org/10.1016/j.trac.2007.10.002.
Rosario-ortiz, F.L., Canonica, S., 2016. Probe compounds to assess the photochemical activity of dissolved organic matter. Environ. Sci. Technol. 50, 12532–12547. https://doi.org/10.1021/acs.est.6b02776.
Šakić, D., Achrainer, F., Vrček, V., Zipse, H., 2013. The chemical fate of paroxetine metabolites. Dehydration of radicals derived from 4-(4-fluorophenyl)-3-(hydroxymethyl) piperidine. Org. Biomol. Chem. 11, 4232. https://doi.org/10.1039/c3ob40219c.
Santoke, H., Cooper, W.J., 2017. Environmental photochemical fate of selected pharmaceutical compounds in natural and reconstituted Suwannee River water: role of reactive species in indirect photolysis. Sci. Total Environ. 580, 626–631. https://doi.org/10.1016/j.scitotenv.2016.12.008.
Schultz, M.M., Furlong, E.T., Kolpin, D.W., Werner, S.L., Schoenfuss, H.L., Barber, L.B., Blazer, V.S., Norris, D.O., Vajda, A.M., 2010. Antidepressant pharmaceuticals in two US effluent-impacted streams: occurrence and fate in water and sediment, and selective uptake in fish neural tissue. Environ. Sci. Technol. 44, 1918–1925.
Schymanski, E.L., Jeon, J., Gulde, R., Fenner, K., Ruff, M., Singer, H.P., Hollender, J., 2014. Identifying small molecules via high resolution mass spectrometry: communicating confidence. Environ. Sci. Technol. 48, 2097–2098. https://doi.org/10.1021/es5002105.
Silva, L.J.G., Pereira, A.M.P.T., Meisel, L.M., Lino, C.M., Pena, A., 2015. Reviewing the serotonin reuptake inhibitors (SSRIs) footprint in the aquatic biota: uptake, bioaccumulation and ecotoxicology. Environ. Pollut. 197, 127–143. https://doi.org/10.1016/j.envpol.2014.12.002.
Tentscher, P.R., Eustis, S.N., McNeill, K., Arey, J.S., 2013. Aqueous oxidation of sulfonamide antibiotics: aromatic nucleophilic substitution of an aniline radical cation. Chem. - A Eur. J. 19, 11216–11223. https://doi.org/10.1002/chem.201204005.
Turro, N.J., Ramamurthy, V., Cherry, W., Farneth, W., 1978. The effect of wavelength on organic photoreactions in solution. Reactions from Upper Excited States. Chem. Rev. 78, 125–145. https://doi.org/10.1021/cr60312a003.
US Environmental Protection Agency, 2016. Final Report, the Environmental Occurrence, Fate, and Ecotoxicity of Selective Serotonin Reuptake Inhibitors (SSRIs) in Aquatic Environments, Research Project Database, NCER | ORD | US EPA [WWW Document]. URL https://cfpub.epa.gov/ncer_abstracts/index.cfm/fuseaction/display.highlight/abstract/1755/report/F.
Vasskog, T., Berger, U., Samuelsen, P.-J., Kallenborn, R., Jensen, E., 2006. Selective serotonin reuptake inhibitors in sewage influents and effluents from Tromsø, Norway. J. Chromatogr. A 1115, 187–195. https://doi.org/10.1016/j.chroma.2006.02.091.
Vasskog, T., Anderssen, T., Pedersen-Bjergaard, S., Kallenborn, R., Jensen, E., 2008. Occurrence of selective serotonin reuptake inhibitors in sewage and receiving waters at Spitsbergen and in Norway. J. Chromatogr. A 1185, 194–205. https://doi.org/10.1016/j.chroma.2008.01.053.
Vay, M., Majewsky, M., Mikus, G., 2018. Isotopically labelled paroxetine standard allows for definite structure elucidation of the paroxetine tandem mass spectrum. Rapid Commun. Mass Spectrom. 32, 1311–1312. https://doi.org/10.1002/rcm.8178.

Vione, D., 2020. A critical view of the application of the APEX software (aqueous photochemistry of environmentally-occurring Xenobiotics) to predict photoreaction kinetics in surface freshwaters. Molecules 25, 9. https://doi.org/10.3390/molecules25010009.
Vione, D., Maurino, V., Minero, C., Calza, P., Pelizzetti, E., 2005. Phenol chlorination and photochlorination in the presence of chloride ions in homogeneous aqueous solution. Environ. Sci. Technol. 39, 5065–5075.
Vione, D., Sur, B., Dutta, B.K., Maurino, V., Minero, C., 2011. On the effect of 2-propanol on phenol photonitration upon nitrate photolysis. J. Photochem. Photobiol. A: Chem. 224, 68–70.
Vione, D., Minella, M., Maurino, V., Minero, C., 2014. Indirect photochemistry in sunlit surface waters: photoinduced production of reactive transient species. Chem.-Eur. J. 20, 10590–10606.
Vione, D., Fabbri, D., Minella, M., Canonica, S., 2018. Effects of the antioxidant moieties of dissolved organic matter on triplet-sensitized phototransformation processes: implications for the photochemical modeling of sulfadiazine. Water Res. 128, 38–48. https://doi.org/10.1016/j.watres.2017.10.020.
von Sonntag, C., Schuchmann, H.-P., 1991. The elucidation of peroxyl radical reactions in aqueous solution with the help of radiation-chemical methods. Angew Chem Int Ed Engl 30, 1229–1253. https://doi.org/10.1002/anie.199112291.
Wang, S., Song, X., Hao, C., Gao, Z., Chen, J., Qiu, J., 2015. Elucidating triplet-sensitized photolysis mechanisms of sulfadiazine and metal ions effects by quantum chemical calculations. Chemosphere 122, 62–69. https://doi.org/10.1016/j.chemosphere.2014.11.007.
Wenk, J., Canonica, S., 2012. Phenolic antioxidants inhibit the triplet-induced transformation of anilines and sulfonamide antibiotics in aqueous solution. Environ. Sci. Technol. 46, 5455–5462. https://doi.org/10.1021/es300485u.
Wenk, J., Von Gunten, U., Canonica, S., 2011. Effect of dissolved organic matter on the transformation of contaminants induced by excited triplet states and the hydroxyl radical. Environ. Sci. Technol. 45, 1334–1340. https://doi.org/10.1021/es202028w.
Wilkinson, F., Helman, W.P., Ross, A.B., 1995. Rate Constants for the Decay and Reactions of the Lowest Electronically Excited Singlet State of Molecular Oxygen in Solution. An Expanded and Revised Compilation. J. Phys. Chem. Ref. Data 24, 663. https://doi.org/10.1063/1.555965.
Willett, K.L., Hites, R.A., 2000. Chemical actinometry: using o-nitrobenzaldehyde to measure light intensity in photochemical experiments. J. Chem. Educ. 77, 900–902. https://doi.org/10.1021/ed077p900.
Wojnárovits, L., Tóth, T., Takács, E., 2020. Rate constants of carbonate radical anion reactions with molecules of environmental interest in aqueous solution: a review. Sci. Total Environ. 717, 137219. https://doi.org/10.1016/j.scitotenv.2020.137219.
Wols, B.A., Harmsen, D.J.H., Beerendonk, E.F., Hofman-caris, C.H.M., 2014. Predicting pharmaceutical degradation by UV (LP)/H2O2 processes: a kinetic model. Chem. Eng. J. 255, 334–343. https://doi.org/10.1016/j.cej.2014.05.088.
Wu, C., Witter, J.D., Spongberg, A.L., Czajkowski, K.P., 2009. Occurrence of selected pharmaceuticals in an agricultural landscape, western Lake Erie basin. Water Res. 43, 3407–3416. https://doi.org/10.1016/j.watres.2009.05.014.
Zhao, S.X., Dalvie, D.K., Kelly, J.M., Soglia, J.R., Frederick, K.S., Smith, E.B., Obach, R.S., Kalgutkar, A.S., 2007. NADPH-dependent covalent binding of [^3H]paroxetine to human liver microsomes and S-9 fractions: identification of an electrophilic quinone metabolite of paroxetine. Chem. Res. Toxicol. 20, 1649–1657. https://doi.org/10.1021/tx700132x.

3.1.3 Biotransformation study of antidepressant sertraline and its removal during biological wastewater treatment

The paper "Biotransformation study of antidepressant sertraline and its removal during biological wastewater treatment" by T. Gornik, A. Kovačič, E. Heath, J. Hollender and T. Kosjek was published in *Water Research* in August 2020. I led and performed most of the experimental work, method optimization and validation, data analysis, data interpretation and manuscript writing under supervision of Assoc Prof Dr T. Kosjek and Prof Dr E. Heath and Prof Dr J. Hollender. The measurements on the UHPLC coupled with a hybrid quadrupole-orbital trap were performed at the Eawag, Swiss Federal Institute of Aquatic Science and Technology in Switzerland, by Assoc Prof Dr T. Kosjek.

Based on available information, the behavior of SER in the environment is of concern. Hence, this study aimed to fill a clear knowledge gap on SER removal during biological WW treatment. It included laboratory-scale batch biodegradation and sorption experiments and flow-through pilot wastewater treatment bioreactors that helped determine the leading mechanisms and extent of SER removal. Sorption of the drug prevailed, eliminating 90 % of SER in the b atch experiments. However, biodegradation also occurred, resulting in the formation of TPs. The structures of 10 TPs were suggested, including the known metabolites NS, sertraline ketone and TP hydroxy-sertraline. The flow-through bioreactors confirmed the high removal percentages for sertraline during biological treatment at 94 %. In order to support laboratory findings, the influents and effluents of two WWTPs and untreated wastewater from a psychiatric hospital were sampled. Eight previously identified TPs were detected in WW, while removal efficiencies were 81 % and 77 %.

The results of this study provided addressed three aims of this thesis. Namely, 1) investigation of the biodegradation of SER and identification of TPs, 2) determination of SER and PXT residues in SW and SER residues in WW samples and 3) assessment of removal efficiency of SER during biological treatment.

This paper is the first to study SER behavior during WW treatment extensively. It highlights sorption as the primary removal mechanism, investigates the mechanism of its biodegradation and identifies seven new TPs, confirming their presence also in actual WW. The TPs determination in sampled sewage hospital WW also established that limited biotransformation already occurs in the sewage system before reaching the WWTP. Consequently, it provides vital information for further research on SER recalcitrance and ecotoxicity.

Water Research 181 (2020) 115864

Contents lists available at ScienceDirect

Water Research

journal homepage: www.elsevier.com/locate/watres

Biotransformation study of antidepressant sertraline and its removal during biological wastewater treatment

Tjasa Gornik [a, b], Ana Kovacic [a, b], Ester Heath [a, b], Juliane Hollender [c, d], Tina Kosjek [a, b, *]

[a] Jozef Stefan Institute, Department of Environmental Sciences, Jamova 39, Ljubljana, Slovenia
[b] Jozef Stefan International Postgraduate School, Jamova 39, Ljubljana, Slovenia
[c] Eawag, Swiss Federal Institute of Aquatic Science and Technology, 8600, Dübendorf, Switzerland
[d] Institute of Biogeochemistry and Pollutant Dynamics, ETH Zürich, 8092, Zürich, Switzerland

ARTICLE INFO

Article history:
Received 11 February 2020
Received in revised form
19 April 2020
Accepted 21 April 2020
Available online 18 May 2020

Keywords:
Mass spectrometry
Identification
Degradation
Sorption
Transformation product
Activated sludge

ABSTRACT

Sertraline is one of the most commonly prescribed antidepressants in the last few years. Therefore, it is not surprising that it is regularly detected in wastewaters, surface waters, sediments, biosolids and biota. Effluents from wastewater treatment plants are the main contributors to its presence in the environment. The presented study aims to elucidate the processes involved in its removal, concentrating mainly on sorption and biodegradation during wastewater treatment.

We performed our laboratory scale experiments in two sets of experiments: 1) batch biodegradation and sorption experiments and 2) flow-through laboratory scale pilot wastewater treatment bioreactors. The batch experiments revealed that sorption to activated sludge was the leading removal process, eliminating up to 90% of sertraline present in the batches. Biodegradation was however the secondary removal process, influenced by the presence of alternative easily biodegradable carbon sources. We postulated chemical structures of ten detected biotransformation products. Among these, we propose the previously recognized metabolite norsertraline, sertraline ketone and hydroxy-sertraline. All the remaining biotransformation products are herein reported for the first time.

The removal efficiency of approximately 94% was determined after the treatment in the flow-through bioreactors. To support our findings, we sampled influents and effluents from two wastewater treatment plants and untreated wastewater from a psychiatric hospital. Removal efficiencies of 81% and 77% were determined, and along with the parent compound sertraline, the presence of eight transformation products was confirmed in the actual wastewaters.

1. Introduction

Pharmaceuticals in the environment have been one of the most discussed topics in environmental sciences in the last few decades. Examining the occurrence, behavior and toxicity of these compounds is essential in order to determine the risk arising from the exposure and to put an appropriate legislation in place (Rowsell et al., 2010). One of the main factors influencing the occurrence of a contaminant in the environment is wastewater (WW) treatment. For micropollutants, such as pharmaceuticals, secondary biological treatment is on average 30% more efficient than primary WW treatments. The main mechanisms of removal during secondary treatment are sorption and biodegradation. Nonetheless, the existing treatment techniques are only partially successful in removing them (Choubert et al., 2011). Consequently, the discharge from wastewater treatment plants (WWTPs) is often the main source of contamination for receiving waters (Luo et al., 2014).

As the focus of our study, we chose the antidepressant sertraline (SER). It belongs to the selective serotonin reuptake inhibitor (SSRI) class and is reported as the 14th on the list of top 200 drugs prescribed in the USA (Fuentes et al., 2018). The occurrence of SER in both WW and surface waters (SW) has been reported several times, in the range of a few ng L^{-1} and up to 200 ng L^{-1}, whereas its highest concentrations at almost 1 μg L^{-1} were reported for two WWTP effluents discharging into the east-branch of the Niagara river located in the USA (Arnnok et al., 2017; Golovko et al., 2014; Gornik et al., 2020; Nagarnaik et al., 2011; Yuan et al., 2013). The reported concentrations are not expected to cause lethal acute toxic

* Corresponding author. Jozef Stefan Institute, Jamova 39, 1000, Ljubljana, Slovenia.
E-mail address: tina.kosjek@ijs.si (T. Kosjek).

https://doi.org/10.1016/j.watres.2020.115864
0043-1354/

effects on aquatic organisms. However, based on toxicity predictions and hazard assessments by Ortiz de Garcia et al. (2013), Kuzmanović et al. (2016), Osorio et al. (2016) and Mole and Brooks (2019) the sub-lethal concentrations of SER will likely cause chronic toxic effects on organisms in the sampled rivers. Studies by Minguez et al. (2015), Vaclavik et al. (2020) and Gómez-Canela et al. (2019) have confirmed this hypothesis, reporting that through influencing biochemical processes (e.g., neurotransmitter concentrations, enzymatic activity) SER causes behavior changes, such as suppression of the escape reflex, decreased food consumption or increased swimming activity. Further, several sources report on SER bioaccumulation in aquatic organisms including invertebrates (e.g., mollusks, crustaceans), fish and water beetles (de Solla et al., 2016; Grabicova et al., 2017, 2015). Boström et al. (2017) reported that the bioaccumulation factors decrease with higher trophic level. In addition to SER, its most abundant metabolite norsertraline (NS) has been shown to bioaccumulate in fish tissue, where Arnnok et al. (2017) showed that the metabolism from SER to NS can also take place in the fish.

While the toxicity and occurrence have been extensively studied, there is a lack of data on SER biodegradation and biotransformation, apart from the Final report on the environmental occurrence, fate, and ecotoxicity of SSRIs in aquatic environments, by the Environmental Protection Agency (EPA) USA site (US EPA, 2001–2007), where no biodegradation was observed within the test period. Few papers however reported on removal efficiencies in WWTPs, but the outcomes were very inconsistent, varying from only a few percent to almost 100% elimination, without any further results on the actual mechanism responsible for the removal (Golovko et al., 2014; Lajeunesse et al., 2008, 2012; Schlüsener et al., 2015; Silva et al., 2014).

To fill in these gaps, the objectives of our study were as follows: 1) to assess the biodegradability of SER, 2) to identify potential transformation products (TPs) formed during this process, and 3) to determine its removal efficiency during WW treatment. We set up a batch biodegradation experiment in order to study the biodegradation kinetics and biotransformation. To determine SER removal efficiency we simulated WW treatment on previously designed laboratory-scale pilot wastewater treatment bioreactors (PWTB) (Kosjek et al., 2007). The findings obtained by these two experiments were then compared to the behavior of SER at two Slovenian WWTPs with activated sludge (AS) biodegradation as the secondary treatment.

2. Materials and methods

The list of standards, reagents and chemicals, together with the description of standard solution preparation, can be found in the Supplementary material (SM), Chapter 1.

2.1. Biodegradation experiments

We studied biotransformation of SER by a modified Zahn-Wellens test (Kosjek et al., 2013), whereas the removal was investigated by simulating secondary WW treatment in PWTB.

2.1.1. Batch biodegradation and sorption experiments

Batch biodegradation tests were carried out in 0.5 L glass bottles. During the experiment, they were kept in the dark and aerated with an aquarium pump (see Table 1). SER was added at the concentration of 1 mg L^{-1}. Series A, B, C, D and BL contained 10 mL of AS obtained from the Slovenian WWTP. 330 mL of nutrient rich medium was added into A, B and BL, while mineral rich medium without an added carbon source was added to C and D (for the composition of nutrient and mineral rich medium see SM, Tables S–3). Batch E and F contained deionized water without the addition of AS. The biological activity was inhibited in batches B, D and E by adding 2% formaldehyde. These three series were employed as controls to the batches A, C and E, respectively, to account for possible abiotic degradation. BL served as the control of matrix and was prepared without the addition of SER. The ambient temperature was kept at 23 °C and pH was monitored at each sampling event. Biomass concentration was determined at the beginning of the experiment in three separately prepared flasks, containing 10 mL of AS and 390 mL of deionized water. Two 50-mL parallels of the homogenized sample were taken from each flask ($n = 6$) and filtered through GF-2 filters, that were beforehand dried to constant weight at 105 °C. After filtering, the filters with biomass were again dried at 105 °C and weighted. From the difference in masses we calculated the concentration of biomass. After the closure of the experiment the biomass concentration was again determined following the same procedure for each sample flask (A-F, BL) in two 50-mL parallels.

4-mL samples for determination of biodegradation were withdrawn from each flask in approximately 24-h intervals, during an incubation period of nine days. The first sample was withdrawn after 15 min post spiking, when, to assure homogeneous concentration of SER, we intensively stirred the flask's content.

To account for a possible influence of the formaldehyde on SER sorption to AS or to glass surfaces we performed an additional sorption experiment, as demonstrated in Table 1. The medium used was ultrapure water with the addition of 10 mL of AS. In the first series the AS was left intact (G), while in the second set it was again inhibited by adding 2% formaldehyde (H), and in the third by autoclaving the AS beforehand (I). J and K series correspond with controls E and F, respectively (Table 1). SER concentration was again monitored by withdrawing the first sample at 15 min post spiking, and then after 0.5, 1, 4, 8, 24 and 48 h.

2.1.2. PWTB

The benchtop PWTBs simulate the biological treatment applied at most WWTPs. A detailed description of the bioreactors and their configuration is given by Kosjek et al. (2007). Each bioreactor contained 4 L of wetted volume including AS obtained from the Slovenian municipal WWTP A. Three flow-through bioreactors were used: BR1, BR2 and BR0. To the influents of BR1 and BR2 SER was added at the concentration of 1 μg L^{-1}, while BR0 served as the control reactor, which was operated at the same conditions, but without SER addition. The daily feed rate was 2 L at hydraulic retention time of 48 h. The adaptation period after the addition of AS to each bioreactor was one month. After this period, sampling of the bioreactors' influents and effluents was performed monthly for six months. Effluents were sampled 48 h after influent sampling. Parameters such as pH, temperature and dissolved oxygen were measured on each sampling occasion in each compartment (anoxic, aerated and settling tank). Biomass concentration, NO_3–N, NH_4–N and chemical oxygen demand were measured at the beginning of the experiment and after three and six months. Additional information on how the parameters were measured can be found in SM, Chapter 3 on PWTB.

2.2. Occurrence in Slovenian WWs

We sampled WWs from two Slovenian WWTPs with the capacity of 149.000 and 360.000 population equivalents for the WWTP A and B, respectively. Both WWTPs receive municipal, industrial and hospital WWs. They both apply a combination of mechanical and biological treatment with an anaerobic stabilization of sludge. The 24-h composite samples of influents and effluents were sampled on two respective days in August 2019. In

Table 1
The constituents of each series in the batch biodegradation and sorption experiment.

Sample	AS [mL]	Nutrient rich medium [mL]	Mineral rich medium [mL]	DIW [mL]	FDH [mL]	SER standard addition [μL]	Total volume [mL]
Biodegradation experiment							
SER-A/1	10	330	0	60	0	400	400
SER-A/2	10	330	0	60	0	400	400
SER-B	10	330	0	0	60	400	400
SER-C/1	10	0	330	60	0	400	400
SER-C/2	10	0	330	60	0	400	400
SER-D	10	0	330	0	60	400	400
SER-E	0	0	0	340	60	400	400
SER-F	0	0	0	400	0	400	400
BL	10	330	0	60	0	/	400
Adsorption experiment							
SER-G/1	10	0	0	390	0	400	400
SER-G/2	10	0	0	390	0	400	400
SER-H/1	10	0	0	330	60	400	400
SER-H/2	10	0	0	330	60	400	400
SER-I/1	10[a]	0	0	390	0	400	400
SER-I/2	10[a]	0	0	390	0	400	400
SER-J	0	0	0	340	60	400	400
SER-K	0	0	0	400	0	400	400

[a] autoclaved.

addition to the WWTPs, a 6-h composite sample from a Slovenian psychiatric hospital was sampled from the hospital sewer in order to determine the occurrence of the parent compound and metabolites before entering the treatment system.

2.3. Sample preparation and instrumental analysis

The purpose of the batch biodegradation experiment (2.1.1) was the identification of the formed TPs, which was done using the high performance liquid chromatograph (Ultimate 3000, Dionex) coupled to QExactive Plus hybrid quadrupole-orbital trap™ (Thermo Scientific) high resolution mass spectrometer (HPLC-QExactive). Samples were processed by filtering 0.5 mL of each sample through 0.2 μm syringe filters and addition of 20 μL of deuterated SER hydrochloride ($SERD_3$) and ^{13}C labeled norsertraline (NS $^{13}C_6$) internal standards (IS) at the final concentration of 200 ng L^{-1}. The samples were kept frozen at −20 °C until analysis.

SER quantification in the PWTB samples (2.1.2) was determined by gas chromatography coupled to mass spectrometry (GC-MS; 7890B/5977A, Agilent Technologies) following the instrumental method applied in Gornik et al. (2020). The sample preparation was adapted and slightly modified from the method applied to SW, also found in Gornik et al. (2020). The main differences can be found in the washing step, one-step elution and additional derivatization step detailed in the Supplementary material, Chapter 1.3.

Trace-level analyses of SER, NS, sertraline ketone (SEK), and semi-quantitative analyses of the TPs identified in PWTB effluents (2.1.2) and actual WW (2.2) samples were performed using a Shimadzu Nexera X2 ultra-high performance liquid chromatograph (UHPLC) coupled to Sciex hybrid quadrupole-linear ion trap mass spectrometry analyzer (Qtrap) 4500. Samples were prepared following the method for SW in Gornik et al. (2020).

The exact procedures and operating conditions for all three methods are stated in SM, Chapters 1.3, 1.4 and Tables S−1.

2.4. Analytical method validation

The performance of the quantification methods was evaluated by estimating linearity, trueness, repeatability, sensitivity, matrix effect and extraction recovery. The information on the determination of the validation parameters can be found in SM, Chapter 1.5.

2.5. Detection and identification of transformation products

We did the screening and the identification of TPs following two workflows. The first one was done in XCalibur™ ver. 3.0 software by adding suspects either already identified in the literature (De Vane et al., 2002; Gornik et al., 2020; Jakimska, A. et al., 2014; Li et al., 2013; Shen et al., 2011), predicted by the Eawag-BBD Pathway Prediction System (EAWAG, BBD Pathway Prediction System) or generated from parent compounds using possible modifications that were applied for at least three generations as described in Stravs et al. (2017).

In the second workflow we used the open-source software packages MZmine (version 2.37) and R (version 3.5.2) in order to screen for possible TPs in a nontargeted way (R Core Team, 2011). First, differential analysis was performed for a set of samples based on LC-MS data with MZmine software. The peaks were detected using the exact mass algorithm, followed by a chromatogram building. The chromatographs were deconvoluted by the wavelets (Automated Data Analysis Pipeline (ADAP)) algorithm (Myers et al., 2017) and deisotoped with the isotopic peaks grouper algorithm with a *m/z* tolerance 0.015 mu or 25 ppm, retention time (RT) tolerance of 0.2 min and the lowest *m/z* value as the representative isotope. The peaks were aligned using the Random Sample Consensus (RANSAC) algorithm. Gap filling was performed based on the same RT and *m/z* range gap with *m/z* tolerance of 0.015 mu or 25 ppm. The results were filtered by removing duplicates and *m/z* below 100 and over 600. The obtained data was processed further using R (Vervliet, 2018). A student t-test was employed in order to obtain statistically significant features between the samples and their controls (fold change > 10 and p-value < 0.05). The elemental formula of the selected *m/z* values was predicted in MZmine with the "Predict molecular formula" tool and compared with the prediction obtained by XCalibur™. The tentative structures were proposed based on the mass shift compared to the parent compound, the suggested elemental formula and MS/MS fragmentation. The criteria applied to the identification of TPs were based on 1) maximum error of 10 ppm between the measured and theoretical mass of the (de)protonated molecule and its product ions; 2) isotopic pattern score over 70%, where available; 3) DBE value; 4) absence of the TPs in the blanks, biologically inhibited control samples and in samples withdrawn at the onset of the biodegradation experiment.

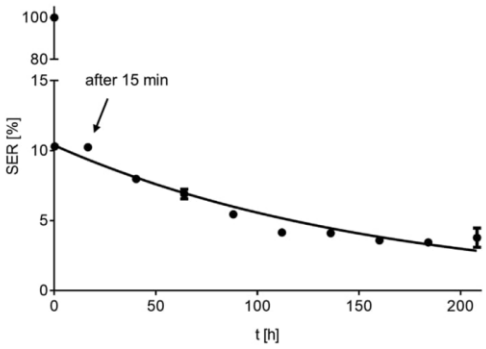

Fig. 1. Degradation of SER in mineral rich medium (C). The 90% decrease of SER took place during the first 15 min post spiking.

The chemical structures and transformations were drawn in ChemDraw Ultra 12.0.2 (Perkin Elmer). The raw data of the potential candidates was examined and processed manually in XCalibur ™.

3. Results and discussion

3.1. Biodegradation kinetics and sorption experiments

For the batch biodegradation experiment, we prepared nine flasks, of which two series (A and C) served as biodegradation test samples, whereas, B, D, E, F and the blank served as the controls. Series A and C were run in parallels. Compared to the initially spiked, i.e. "expected initial concentration" we observed a significant decline of 74% and 90% SER in the nutrient-rich (A) and mineral-rich medium (C) already at the first sample withdrawal, which took place 15 min post the addition of SER into the flasks (Fig. 1). In the C series, the level of SER decreased further, until only 3.8% of the initial concentration remained in the flask after nine days. Conversely, we noted only a slight further decrease in the A series. We assume that AS in nutrient rich medium had superior growing conditions and utilized easily biodegradable nutrients, which in turn slowed down the biodegradation of SER. In series C however, SER was the only available carbon source and was therefore consumed more rapidly. Its biodegradation followed pseudo-first kinetics (Fig. 1), with the half-life of 4.6 days. In the absence of AS (series E and F) or when AS was inhibited (series B and D), hardly any degradation was observed, with RSDs below 15% during the nine-day experiment.

To investigate further the reason for the initial decline of SER in series A and C, we studied its sorption. For this purpose we compared the untreated AS (series G), formaldehyde inhibited AS (series H), and previously autoclaved AS (series I). It was shown that only 19% of the initially spiked SER was left after 15 min in series G. A similar drop to 26% of the initial concentration was observed in series I, while there was no change in SER concentration in series H. SER concentration decreased for an additional 5–10% during the next 24 h in the batches G and I. This finding indicates that sorption to AS was responsible for the initial drastic decline in concentration of SER, whereas formaldehyde (series H) prevented this process. The result was in agreement with articles reporting high sorption coefficients and constants with soils, sediments and activated sludge (Silva et al., 2015; Hörsing et al., 2011).

An alternative mechanism for elimination of aliphatic amines with pK_a 7–10 is ion trapping in protozoa, as suggested by Gulde et al. (2018). This mechanism has also been reported for the structurally related SSRI antidepressant, citalopram. The ion trapping occurs due to the pH difference between the relatively neutral outside environment and the acidic conditions of vesicles present in eukaryotic cells of the protozoa. This difference allows the amines to diffuse into the vesicles in their neutral form, while their diffusion back from the vesicles is strongly inhibited by their positive charge. In order to either confirm or refute this potential mechanism, additional experiments are needed by specifically inhibiting protozoa (Gulde et al., 2018).

The biodegradation experiment started with 0.57 ± 0.01 g L^{-1} of biomass and ended with a similar concentration of 0.46 ± 0.15 g L^{-1}. It was shown that the pH remained constant during the experiment in all batches. As illustrated in the SM (Figure S-1), pH ranged between 6.6 and 8 in the batches A, C, F and BL. The addition of formaldehyde however reduced the pH, resulting in the average pH of 4.2 in the batches B and D, whereas in the batch E, which was not buffered by the AS and mineral nutrient medium, the pH was about one additional unit lower (pH 3.1). Pharmaceutical drug stability stress tests (Singh and Bakshi, 2000; Walash et al., 2011) and study by Lam et al. (2004) have shown that SER was highly hydrolytically stable. Accordingly, we observed no increase in the degradation of SER under acidic conditions in the batches B, D and E.

3.2. Detection, identification and formation of BTPs

The TPs were detected only in series C or A, meaning that they were the result of biodegradation and are therefore from now on referred to as biotransformation products (BTPs). All BTPs were detected in positive ionization mode, while we found no newly formed compounds in the negative, neither did we find any adduct ions to imply their presence in the biodegradation mixtures. The diagnostic information on SER and its nine BTPs can be found in Table 2. A level of confidence proposed by Schymanski et al. (2014) was assigned to each BTP based on available reference standards, previous references, MS, MS/MS spectra and possibility of existing isomers. The isotope ratio score was determined using MZmine's "Predict molecular formula" tool. Their MS/MS spectra, together with the tentative chemical structures are illustrated in Figure S-2. The chromatograms are reported in Figure S-3.

The parent compound SER eluted from the column at 12.6 min, with the protonated molecule $[M+H]^+$ 306.08 corresponding to the elemental formula of $C_{17}H_{17}Cl_2N$. Its MS/MS spectrum shows ion fragment ions at *m/z* 275.04 formed by the loss of CH_3NH_2, *m/z* 158.98 by the further loss of the tetralin ring, *m/z* 129.07 representing the protonated dihydronaphtalene and *m/z* 91.05 the protonated toluene.

The fragment ions observed in the MS/MS spectra of BTP-292 (NS), BTP-320b, BTP-334 and BTP-406 correspond to those found in the SER MS/MS spectrum (*m/z* 275.04, 158.98, 129.07, 91.05). The identity of BTP-292 ($[M+H]^+$ 292.07, $C_{16}H_{15}Cl_2N$) being the demethylated SER or NS was confirmed by the reference standard. To assign the structure to the remaining three BTPs, we took into account that their fragment ion at *m/z* 275 stayed intact, implying that the transformation likely occurred on the amine group. Based on the elemental formulae of BTP-320b ($[M+H]^+$ 320.06, $C_{17}H_{15}Cl_2NO$) and BTP-334 ($[M+H]^+$ 334.08, $C_{18}H_{17}Cl_2NO$) their structures correspond to formamide and acetamide moiety bound to NS, respectively. According to the addition of $C_4H_4O_3$ to the elemental formula of SER ($C_{17}H_{17}Cl_2N$), we propose that the BTP-406 ($[M+H]^+$ 406.10) is the product of N-succinylation.

BTP-158 ($[M+H]^+$ 158.10, $C_{11}H_{11}N$) is tentatively formed by the loss of dichlorophenyl ring from SER. The only identified fragment

Table 2
Summary of the diagnostic data on the identified BTPs: compound ID, RT, measured mass of $[M+H]^+$, mass error [ppm] and proposed elemental formula, DBE, isotope ratio score [%], the diagnostic product ion mass with the corresponding mass error [ppm] and elemental composition of fragment ions.

Compound ID	RT [min]	Measured mass $[M+H]^+$	Error [ppm]	Elemental formula	DBE	Isotope ratio score [%]	Confidence level	Diagnostic product ion mass	Error [ppm]	Elemental composition of fragment ions
SER	12.61	306.08089	−0.63	$C_{17}H_{17}Cl_2N$	9	70	L1	275.03681	−7.53	$C_{16}H_{13}Cl_2^+$
								158.97613	−0.94	$C_7H_5Cl_2^+$
								129.07017	2.25	$C_{10}H_9^+$
								91.05424	0.11	$C_7H_7^+$
TP-158	11.58	158.09645	0.13	$C_{11}H_{11}N$	7	N	L2b	143.07312	1.19	$C_{10}H_9N^+$
TP-176	9.06	176.10703	0.23	$C_{11}H_{13}NO$	6	N	L3	158.09648	0.32	$C_{11}H_{12}N^+$
								143.07327	2.24	$C_{10}H_9N^+$
TP-292 (NS)	12.87	292.06526	−0.58	$C_{16}H_{15}Cl_2N$	9	80	L1	275.03864	−0.87	$C_{16}H_{13}Cl_2^+$
								158.97621	−0.44	$C_7H_5Cl_2^+$
								129.06996	0.62	$C_{10}H_9^+$
								91.05437	1.54	$C_7H_7^+$
TP-320a	13.98	320.06016	−0.59	$C_{17}H_{15}Cl_2NO$	10	N	L3	302.04861	−3.87	$C_{17}H_{14}Cl_2N^+$
								238.05482	1.85	$C_{16}H_{11}Cl^{\bullet+}$
TP-320b	15.20	320.06024	−0.33	$C_{17}H_{15}Cl_2NO$	10	N	L2b	275.03888	0	$C_{16}H_{13}Cl_2^+$
								158.97635	0.44	$C_7H_5Cl_2^+$
								129.07001	1.08	$C_{10}H_9^+$
								91.05418	−0.55	$C_7H_7^+$
TP-322	10.61	322.07572	−0.87	$C_{17}H_{17}Cl_2NO$	9	79	L3	291.03354	−0.89	$C_{16}H_{13}Cl_2O^+$
								273.02286	−1.36	$C_{16}H_{11}Cl_2^+$
								238.05411	−1.13	$C_{16}H_{11}Cl^{\bullet+}$
TP-334	15.40	334.07570	−0.9	$C_{18}H_{17}Cl_2NO$	10	81	L2b	275.03848	−1.45	$C_{16}H_{13}Cl_2^+$
								158.97612	−1.01	$C_7H_5Cl_2^+$
								129.06976	−0.93	$C_{10}H_9^+$
								91.05405	−1.98	$C_7H_7^+$
TP-350	13.10	350.07076	−0.43	$C_{18}H_{17}Cl_2NO_2$	10	N	L3	273.02255	−2.49	$C_{16}H_{11}Cl_2^+$
								238.05453	0.63	$C_{16}H_{11}Cl^{\bullet+}$
TP-406	15.30	406.09700	−0.32	$C_{21}H_{21}Cl_2NO_3$	11	77	L3	275.03873	−0.55	$C_{16}H_{13}Cl_2^+$
								158.97661	2.08	$C_7H_5Cl_2^+$
								129.06990	0.15	$C_{10}H_9^+$
								91.05408	−1.65	$C_7H_7^+$

ion at *m/z* 143.07 indicates the loss of the methyl group. This fragment ion was previously observed in the MS spectra of SER imine, identified as protonated radical ion of naphthalene-1(2H)-imine (Gornik et al., 2020). The suggested structure of BTP-176 ($[M+H]^+$ 176.11) with the elemental formula of $C_{11}H_{13}NO$ is hydroxylated BTP-158, justified by the diagnostic ions *m/z* 158.10 that indicates the cleavage of H_2O, and the previously mentioned *m/z* 143.07.

BTP-320a ($[M+H]^+$ 320.06) is an isomer of BTP-320b, both differing in their retention times (RT) and MS/MS spectra. By the loss of H_2O the fragment ion at *m/z* 302.05 can be observed. Further fragmentation leads to the *m/z* 238.05 corresponding to the radical cation of chlorophenyl-dihydronaphthalene. The fragment ion has been reported before by Jakimska et al. (2014) and Gornik et al. (2020) in the MS/MS spectra of hydroxy-SER, SER imine and SEK. A double bond is formed, which argues in favor of the hydroxyl group located in the cyclohex-2-enamine system. BTP-322 and BTP-350 also have the fragment ion at *m/z* 238.05 in their spectra, indicating that the transformations took place at the same potential locations. The elemental formula $C_{17}H_{17}Cl_2NO$ of BTP-322 ($[M+H]^+$ 322.08) suggests that an additional oxygen was added to SER, and based on its fragmentation pattern (*m/z* 291.03, 273.02, 238.05), exact mass and cross-confirmation of the RT it was concluded that this compound is the product of SER hydroxylation. This compound was previously identified as the product of solar photodegradation by Gornik et al. (2020), and degradation in soil by Li et al. (2013). The elemental formula $C_{18}H_{17}Cl_2NO_2$ and fragmentation ions *m/z* 273.02 and *m/z* 238.05 in the spectra of BTP-350 ($[M+H]^+$ 350.07) suggest that in this case hydroxylation occurred on BTP-334.

Sertraline ketone (TP-291, SEK) was determined following targeted identification using UHPLC-Qtrap. Its identification was based on three MRM transitions including *m/z* 291 > 145, *m/z* 291 > 238 and *m/z* 291 > 117 in ratios and the RT at 5.12 min, all matching with the SEK reference standard. Therefore, the level of confidence 1 was assigned to this compound. There could be several possible reasons why SEK was not detected in the QExactive measurements. The most plausible reason is that the method sensitivity was too low to detect it.

Fig. 2 shows the kinetic profiles of the BTPs formed by biodegradation of SER by AS in the nutrient rich medium. The duration of the experiment is plotted against the ratio between the area under curve (AUC) of each BTP versus $SERD_3$ or NS $^{13}C_6$, which were used as IS. NS $^{13}C_6$ was used as the IS for studying the kinetics of NS and SEK, whereas $SERD_3$ was used for all remaining BTPs. Based on the identified structures and their kinetic profiles we also propose a breakdown mechanism, as depicted in Fig. 2.

The level of BTP-291 or SEK (Fig. 2, A) increased from the beginning of the experiment, but reached a plateau on the second day, after which another rise was observed at the end of the experiment. SEK could either have formed directly from SER as suggested by Jakimska et al. (2014) or from NS, as suggested by Shen et al. (2011), so the breakdown pathway in Fig. 3 is constructed accordingly.

The levels of BTP-292 or NS increased fast to the maximum on the second day and then decreased till day seven, whereafter the compound was not detected in the mixture anymore (Fig. 2, B). BTP-334 gradually increased from day one, but it did not reach the plateau during the time of the experiment. A much milder increase was observed for the compound BTP-350, starting from day three, though its levels remained substantially lower in comparison with the first two compounds (provided that the ionization levels of the three BTPs are comparable). Based on these data we constructed the pathway in the breakdown scheme (Fig. 3), postulating that SER is first demethylated to form NS, which is followed by the acetylation to BTP-334 and hydroxylation to BTP-350.

The levels of BTP-322 (Fig. 2, C) gradually increased from day

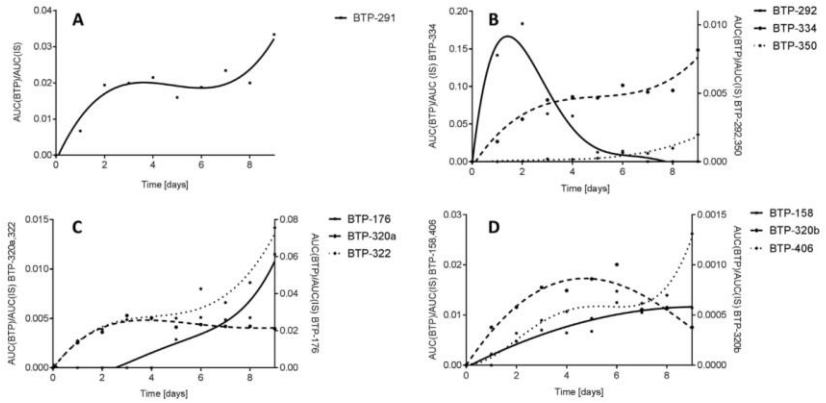

Fig. 2. Kinetic profiles of BTPs: A: BTP-291 (SEK) kinetics was studied by UHPLC-Qtrap and is therefore depicted in a separate plot; B: kinetic profiles for BTP-292 (NS), BTP-334, BTP-350; C: kinetic profiles for BTP-176, BTP-320a, BTP-322; d: kinetic profiles for BTP-158, BTP-320b and BTP-406.

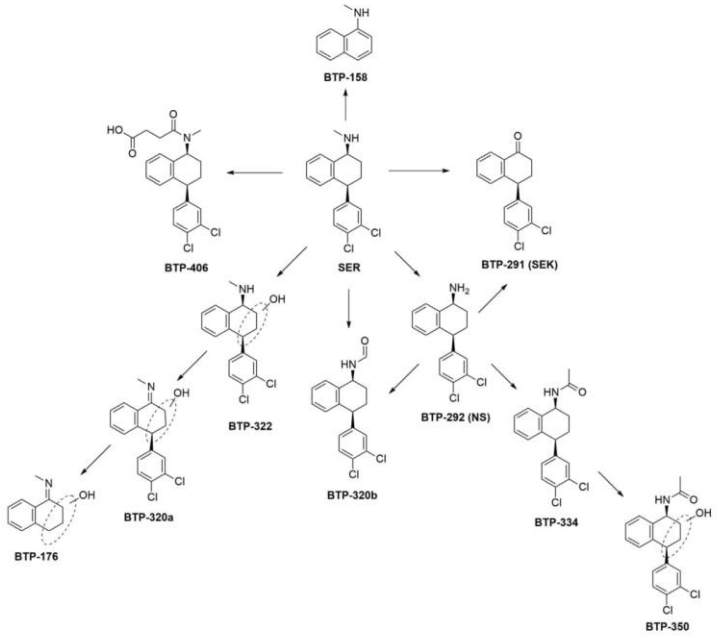

Fig. 3. The proposed scheme of SER biotransformation based on identified BTPs.

one to nine, probably by hydroxylation of SER, while the levels of BTP-320a increased accordingly, then reached a plateau after the day three, possibly due to its further transformation into BTP-176. BTP-176 was not detected until day four, then its concentration started to increase and kept this trend until the end of the experiment. It is hypothesized that TP-320a was formed from BTP-322 by dehydrogenation (Gornik et al., 2020; Shen et al., 2011) and BTP-176 after the cleavage of the dichlorophenyl ring from BTP-320a.

Fig. 2 (D) shows how BTP-158 slowly increased from the

beginning of the biodegradation experiment, reaching a plateau after six days. The exact mechanism of BTP-158 formation could not be predicted based on the available data, nevertheless it probably includes the cleavage of the dichlorophenyl ring, also observed in the formation of BTP-176.

Further, we hypothesize that BTP-320b (Fig. 2, D) was formed either directly from SER after α-C-oxidation or from N-formylation of NS. Similarly, we suggest BTP-406 is formed by N-succinylation of SER. Both reaction pathways have been shown on several examples of amine-containing micropollutants investigated in the study by Gulde et al. (2016).

3.3. Validation of the analytical methods

The validation details for the quantification methods are reported in SM, Tables S–2 in Chapter 1.5.

3.4. Occurrence and removal in WW

3.4.1. Removal in PWTB

SM (Tables S–4) reports on physicochemical WW quality parameters determined in the influents and effluents of the control bioreactor and two test bioreactors, which were run at 1 μg L^{-1} of SER spiked in the influent. The conditions in PWTB were kept as stable as possible by controlling the external influences, but since the biomass is a lively system, the changes of biomass concentration through the six-month period could not be avoided. The second problem that we encountered, was keeping the anoxic conditions in the non-aerated compartments of the bioreactors. Since the return flow from the oxic into the anoxic compartment is strong, and because the concentrations of dissolved oxygen in the oxic compartment is high, it was not possible to keep the low oxygen levels in the anoxic part, as it was earlier discussed in Kosjek et al. (2007). As the result, the BTPs formed in our experiments were the products of aerobic biotransformation only. As shown in SM Tables S–4 the levels of N–NH_4 are substantially lower than 10 mg L^{-1} and chemical oxygen demand concentrations are lower than 100 mg L^{-1} in the effluents of all three bioreactors. Hence, the quality of WW treated in PWTB meets the national requirements (Official Gazette of the Republic of Slovenia, 2007) for the discharge of WW.

Despite somewhat varying physicochemical parameters measured in the PWTBs, the removal efficiency of SER remained sufficiently high and reasonably constant; i.e. 95.0 ± 2.4% for BR1 and 93.3 ± 2.2% for BR2. Along with the SER removal studies, we followed the formation of BTPs in PWTB effluents. NS was present in concentrations of 3.6 ± 2.9 ng L^{-1} and 5.6 ± 2.7 ng L^{-1} in BR1 and BR2, respectively. SEK was determined at 0.6 ± 0.2 ng L^{-1} in BR1, and at 0.7 ± 0.1 ng L^{-1} in BR2. Other BTPs, including BTP-176, BTP-320b, BTP-322, BTP-334 and BTP-406 were also detected in the BR1 and BR2 effluents.

3.4.2. WW samples

Table 3 reports on concentrations or qualitative determinations of SER and its BTPs in WWs obtained from psychiatric hospital and from two WWTPs.

The WW sampled in the hospital sewage system revealed the presence of SER at 549 ng L^{-1}, NS at 139 ng L^{-1} and SEK at 13 ng L^{-1}. In addition, BTP-176, BTP-320b, BTP-322 and BTP-334 were detected. NS and SEK can be formed by human metabolism as well as by biotransformation of SER, so they can be formed by either of the two processes. Namely, it is assumed that limited biotransformation can already take place in the sewage waters before they reach WWTPs. This also explains the presence of four other BTPs found in the hospital WW.

The concentrations of SER at the influents of WWTP A and B were remarkably similar, at 114 ng L^{-1} in A, and at 119 ng L^{-1} in the WWTP B. In the effluents, the concentrations of SER after 24 h were determined at 26 ng L^{-1} in WWTP A and 23 ng L^{-1} in the WWTP B. This corresponded to the removal of 77% at WWTP A and 81% at WWTP B. The removal determined in WWTPs was less than 15% lower compared to the removal of SER in the PWTBs. One possible reason for this difference could be the fact that the leading removal process, sorption, is a non-specific process. Since there are several compounds present in real WW that also bind to the available AS, the altogether capacity is lower. Other reasons for higher removal in the PWTB can involve the controlled conditions, the adaptation of the biomass and constant influent concentration of SER. The removal efficiencies of SER were also similar to the ones reported by Golovko et al. (2014) at 81% and Schlüsener et al. (2015) at 82 ± 2%. In both cases, comparable conditions to ours were applied, where 24-h composite samples were taken from WWTPs, where the secondary biological treatment took place. Subedi and Kannan et al. (2015) also reported a similar removal efficiency, stating that most of the mass load of SER had been removed by the sorption during primary treatment. On the other hand, Lajeunesse et al. (2012) reported lower removals ranging from 25 to 48%. Most papers report only on occurrence of SER in WW, not mentioning its BTPs.

The levels of NS in the effluents were 5.5 ng L^{-1} and 9.0 ng L^{-1} in WWTP A and B, respectively. In the influents, the concentrations of NS were markedly higher, i.e. 88 ng L^{-1} in WWTP A and 79 ng L^{-1} in WWTP B. The main source of NS in the influent is most likely human metabolism of SER, while the drop in NS concentration was 94% at WWTP A and 89% at WWTP B. Since our batch and PWTB experiments indicated that NS formed during biological treatment, we cannot label the change in the concentrations as removal of NS, however, it is apparent that more of NS is removed than formed during the treatment. Literature indicated a smaller drop in NS concentrations during WW treatment, e.g., 35 ± 7% determined by Schlüsener et al. (2015), and 17–28% by Lajeunesse et al. (2012), but this could be explained by the variability of several processes involved (i.e., sorption, biodegradation and formation).

As shown in Table 3, SEK was below LOQ in all four WWTP samples. The remaining BTPs were either absent in both influent

Table 3
Occurrence of SER and its BTPs in WWs. H – hospital WW, A, B – WWTPs, inf – influent, eff – effluent, D – detected, ND – not detected, AUC_{inf} – ratio between the area in the corresponding influent *vs.* effluent, normalized to internal standard.

Samples	SER [ng L^{-1}]	NS [ng L^{-1}]	SEK [ng L^{-1}]	BTP-176	BTP-320b	BTP-322	BTP-334	BTP-350	BTP-406
H	549 ± 24	139 ± 9	13 ± 1	D	D	D	D	ND	ND
A-inf	114 ± 8	88 ± 10	< LOQ[a]	D	ND	D	D	ND	ND
A-eff	26 ± 0.3	5.5 ± 0.1	< LOQ	D (0.7AUC_{inf})	D	D (0.3AUC_{inf})	D (1.6AUC_{inf})	D	D
B-inf	119 ± 4	79 ± 5	< LOQ	ND	ND	D	D	D	ND
B-eff	23 ± 0.1	9 ± 1	< LOQ	ND	D	D (0.2AUC_{inf})	D (2.4AUC_{inf})	D (2AUC_{inf})	D

[a] LOQ for SEK is 1 ng L^{-1}

and effluent (i.e. BTP-176 in WWTP B), or present only in the effluents, but not in the influents (BTP-350 in WWTPA, BTP-320b, BTP-406 in both WWTPs). BTP-334 (WWTP A and B) and BTP-350 (WWTP B) were found in the influents and effluents, with the ratios between the normalized area in the influent and area in the effluent over 1. Having detected them in the influents, BTP-334 and BTP-350 were apparently formed before the WWTP treatment took place, and since they have never been recognized as SER metabolites, we suppose that biotransformation occurred already before the compounds actually entered the WWTPs. Interestingly, the ratio under 1 was observed for BTP-176 (in WWTP A) and BTP-322 (in WWTP A and B). Both BTPs were also already found in the psychiatric hospital sewage, in addition to BTP-334, which supports the hypothesis that biotransformation can already take place before the compound actually enters a WWTP.

4. Conclusions

- This study investigated the transformation of SER during biodegradation. The formation of ten BTPs was reported, including the previously identified NS, SEK and BTP-322, while the formation of seven BTPs was reported for the first time. The presence of eight of the identified BTPs was confirmed in actual WWs from hospital or WWTPs. Occurrence of BTP-158 and BTP-320a could not be excluded considering their instability during sample preparation and analysis.
- SER is a partially biodegradable pharmaceutical. The degradation is faster with SER being the sole substrate. In contrast with its biodegradability, its sorption rate is fast, and is considered the principal mechanism responsible for the removal of SER.
- The elimination in PWTBs and in two investigated WWTPs was relatively high (>77%), which was presumably on account of its sorption to the AS, being the leading removal process.

The results of the study provide further understanding into the mechanism of SER transformation and removal in the environment. In the future, determining the concentrations of SER present in AS would provide better understanding of processes and mechanisms involved in SER elimination from WW. The data is also relevant in cases, where AS is additionally processed and used as fertilizer or disposed to landfills. Further investigations should also involve the toxicity of the newly formed BTPs.

Declaration of competing interest

The authors declare that they have no known competing financial interests or personal relationships that could have appeared to influence the work reported in this paper.

Acknowledgements

The authors acknowledge the financial support from the Slovenian Research Agency (research core funding No. P1-0143) and project J1-6744 (Development of Molecularly Imprinted Polymers and their application in environmental and bio-analysis). We thank Mrs. Birgit Beck (Eawag) for her support in the LC-QExactive analyses and Psychiatric hospital Vojnik for providing wastewater samples.

Appendix A. Supplementary data

Supplementary data to this article can be found online at https://doi.org/10.1016/j.watres.2020.115864.

References

Arnnok, P., Singh, R.R., Burakham, R., Pérez-Fuentetaja, A., Aga, D.S., 2017. Selective uptake and bioaccumulation of antidepressants in fish from effluent-impacted Niagara river. Environ. Sci. Technol. 51, 10652–10662. https://doi.org/10.1021/acs.est.7b02912.

Boström, M.L., Ugge, G., Jönsson, J.Å., Berglund, O., 2017. Bioaccumulation and trophodynamics of the antidepressants sertraline and fluoxetine in laboratory-constructed, 3-level aquatic food chains: trophodynamics of 2 SSRIs in 2 tree-level food chains. Environ. Toxicol. Chem. 36, 1029–1037. https://doi.org/10.1002/etc.3637.

Choubert, J.M., Martin Ruel, S., Esperanza, M., Budzinski, H., Miège, C., Lagarrigue, C., Coquery, M., 2011. Limiting the emissions of micro-pollutants: what efficiency can we expect from wastewater treatment plants? Water Sci. Technol. 63, 57–65. https://doi.org/10.2166/wst.2011.009.

De Vane, C.L., Liston, H.L., Markowitz, J.S., 2002. Clinical pharmacokinetics of sertraline. Clin. Pharmacokinet. 41, 1247–1266.

de Solla, S.R., Gilroy, É.A.M., Klinck, J.S., King, L.E., McInnis, R., Struger, J., Backus, S.M., Gillis, P.L., 2016. Bioaccumulation of pharmaceuticals and personal care products in the unionid mussel Lasmigona costata in a river receiving wastewater effluent. Chemosphere 146, 486–496. https://doi.org/10.1016/j.chemosphere.2015.12.022.

EAWAG. BBD pathway prediction system. WWW Document. http://eawag-bbd.ethz.ch/predict/. accessed 2.6.2020.

Fuentes, A., Pineda, M., Venkata, K., 2018. Comprehension of top 200 prescribed drugs in the US as a resource for pharmacy teaching, training and practice. Pharmacy 6, 43. https://doi.org/10.3390/pharmacy6020043.

Golovko, O., Kumar, V., Fedorova, G., Randak, T., Grabic, R., 2014. Seasonal changes in antibiotics, antidepressants/psychiatric drugs, antihistamines and lipid regulators in a wastewater treatment plant. Chemosphere 111, 418–426. https://doi.org/10.1016/j.chemosphere.2014.03.132.

Gómez-Canela, C., Rovira García, X., Martínez-Jerónimo, F., Marcé, R.M., Barata, C., 2019. Analysis of neurotransmitters in Daphnia magna affected by neuroactive pharmaceuticals using liquid chromatography-high resolution mass spectrometry. Environ. Pollut. 254, 113029. https://doi.org/10.1016/j.envpol.2019.113029.

Gornik, T., Vozic, A., Heath, E., Trontelj, J., Roskar, R., Zigon, D., Vione, D., Kosjek, T., 2020. Determination and photodegradation of sertraline residues in aqueous environment. Environ. Pollut. 256, 113431. https://doi.org/10.1016/j.envpol.2019.113431.

Grabicova, K., Grabic, R., Blaha, M., Kumar, V., Cerveny, D., Fedorova, G., Randak, T., 2015. Presence of pharmaceuticals in benthic fauna living in a small stream affected by effluent from a municipal sewage treatment plant. Water Res. 72, 145–153. https://doi.org/10.1016/j.watres.2014.09.018.

Grabicova, K., Grabic, R., Fedorova, G., Fick, J., Cerveny, D., Kolarova, J., Turek, J., Zlabek, V., Randak, T., 2017. Bioaccumulation of psychoactive pharmaceuticals in fish in an effluent dominated stream. Water Res. 124, 654–662. https://doi.org/10.1016/j.watres.2017.08.018.

Gulde, R., Anliker, S., Kohler, H.-P.E., Fenner, K., 2018. Ion trapping of amines in Protozoa: a novel removal mechanism for micropollutants in activated sludge. Environ. Sci. Technol. 52, 52–60. https://doi.org/10.1021/acs.est.7b03556.

Gulde, R., Meier, U., Schymanski, E.L., Kohler, H.-P.E., Helbling, D.E., Derrer, S., Rentsch, D., Fenner, K., 2016. Systematic exploration of biotransformation reactions of amine-containing micropollutants in activated sludge. Environ. Sci. Technol. 50, 2908–2920. https://doi.org/10.1021/acs.est.5b05186.

Hörsing, M., Ledin, A., Grabic, R., Fick, J., Tysklind, M., la Cour Jansen, J., Andersen, H.R., 2011. Determination of sorption of seventy-five pharmaceuticalsin sewage sludge. Water Res. 45, 4470–4482. https://doi.org/10.1016/j.watres.2011.05.033.

Jakimska, A., Kaszynska, M., Nagórski, P., Kot Wasik, A., Namieśnik, J., 2014. Environmental fate of two psychiatric drugs, diazepam and sertraline: phototransformation and investigation of their photoproducts in natural waters. J. Chromatogr. Separ. Tech. 5 https://doi.org/10.4172/2157-7064.1000253.

Kosjek, T., Heath, E., Kompare, B., 2007. Removal of pharmaceutical residues in a pilot wastewater treatment plant. Anal. Bioanal. Chem. 387, 1379–1387. https://doi.org/10.1007/s00216-006-0969-1.

Kosjek, T., Perko, S., Žigon, D., Heath, E., 2013. Fluorouracil in the environment : analysis, occurrence, degradation and transformation. J. Chromatogr., A 1290, 62–72. https://doi.org/10.1016/j.chroma.2013.03.046.

Kuzmanović, M., López-Doval, J.C., De Castro-Català, N., Guasch, H., Petrović, M., Muñoz, I., Ginebreda, A., Barceló, D., 2016. Ecotoxicological risk assessment of chemical pollution in four Iberian river basins and its relationship with the aquatic macroinvertebrate community status. Sci. Total Environ. 540, 324–333. https://doi.org/10.1016/j.scitotenv.2015.06.112.

Lajeunesse, A., Gagnon, C., Sauvé, S., 2008. Determination of basic antidepressants and their *N* -desmethyl metabolites in raw sewage and wastewater using solid-phase extraction and liquid Chromatography–Tandem mass spectrometry. Anal. Chem. 80, 5325–5333. https://doi.org/10.1021/ac800162q.

Lajeunesse, A., Smyth, S.A., Barclay, K., Sauvé, S., Gagnon, C., 2012. Distribution of antidepressant residues in wastewater and biosolids following different treatment processes by municipal wastewater treatment plants in Canada. Water Res. 46, 5600–5612. https://doi.org/10.1016/j.watres.2012.07.042.

Lam, M.W., Young, C.J., Brain, R.A., Johnson, D.J., Hanson, M.A., Wilson, C.J., Richards, S.M., Solomon, K.R., Mabury, S.A., 2004. Aquatic persistence of eight

pharmaceuticals in a microcosm study. Environ. Toxicol. Chem. 23, 1431–1440.
Li, H., Sumarah, M.W., Topp, E., 2013. Persistence and dissipation pathways of the antidepressant sertraline in agricultural soils. Sci. Total Environ. 452–453, 296–301. https://doi.org/10.1016/j.scitotenv.2013.02.080.
Luo, Y., Guo, W., Ngo, H.H., Nghiem, L.D., Hai, F.I., Zhang, J., Liang, S., Wang, X.C., 2014. A review on the occurrence of micropollutants in the aquatic environment and their fate and removal during wastewater treatment. Sci. Total Environ. 473–474, 619–641. https://doi.org/10.1016/j.scitotenv.2013.12.065.
Minguez, L., Ballandonne, C., Rakotomalala, C., Dubreule, C., Kientz-Bouchart, V., Halm-Lemeille, M.-P., 2015. Transgenerational effects of two antidepressants (sertraline and venlafaxine) on *Daphnia magna* life history traits. Environ. Sci. Technol. 49, 1148–1155. https://doi.org/10.1021/es504808g.
Mole, R.A., Brooks, B.W., 2019. Global scanning of selective serotonin reuptake inhibitors: occurrence, wastewater treatment and hazards in aquatic systems. Environ. Pollut. 250, 1019–1031. https://doi.org/10.1016/j.envpol.2019.04.118.
Myers, O.D., Sumner, S.J., Li, S., Barnes, S., Du, X., 2017. One step forward for reducing false positive and false negative compound identifications from mass spectrometry metabolomics data: new algorithms for constructing extracted ion chromatograms and detecting chromatographic peaks. Anal. Chem. 89, 8696–8703. https://doi.org/10.1021/acs.analchem.7b00947.
Nagarnaik, P., Batt, A., Boulanger, B., 2011. Source characterization of nervous system active pharmaceutical ingredients in healthcare facility wastewaters. J. Environ. Manag. 92, 872–877. https://doi.org/10.1016/j.jenvman.2010.10.058.
Official gazette of the republic of Slovenia: 45 [WWW Document], n.d. . pisrs. http://pisrs.si/Pis.web/pregledPredpisa?id=URED4442. accessed 1.21.2020.
Ortiz de García, S., Pinto, G.P., García-Encina, P.A., Mata, R.I., 2013. Ranking of concern, based on environmental indexes, for pharmaceutical and personal care products: an application to the Spanish case. J. Environ. Manag. 129, 384–397. https://doi.org/10.1016/j.jenvman.2013.06.035.
Osorio, V., Larrañaga, A., Aceña, J., Pérez, S., Barceló, D., 2016. Concentration and risk of pharmaceuticals in freshwater systems are related to the population density and the livestock units in Iberian Rivers. Sci. Total Environ. 540, 267–277. https://doi.org/10.1016/j.scitotenv.2015.06.143.
R Core Team, 2011. R: A Language and Environment for Statistical Computing. R Foundation for Statistical Computing, Vienna, Austria. WWW Document. https://www.r-project.org/. accessed 8.7.2019.
Rowsell, V.F., Tangney, P., Hunt, C., Voulvoulis, N., 2010. Estimating levels of micropollutants in municipal wastewater. Water, Air, Soil Pollut. 206, 357–368. https://doi.org/10.1007/s11270-009-0112-y.
Schlüsener, M.P., Hardenbicker, P., Nilson, E., Schulz, M., Viergutz, C., Ternes, T.A., 2015. Occurrence of venlafaxine, other antidepressants and selected metabolites in the Rhine catchment in the face of climate change. Environ. Pollut. 196, 247–256. https://doi.org/10.1016/j.envpol.2014.09.019.
Schymanski, E.L., Jeon, J., Gulde, R., Fenner, K., Ruff, M., Singer, H.P., Hollender, J., 2014. Identifying small molecules via high resolution mass spectrometry: communicating confidence. Environ. Sci. Technol. 48, 2097–2098. https://doi.org/10.1021/es5002105.
Shen, L.Q., Beach, E.S., Xiang, Y., Tshudy, D.J., Khanina, N., Horwitz, C.P., Bier, M.E., Collins, T.J., 2011. Rapid, biomimetic degradation in water of the persistent drug sertraline by TAML catalysts and hydrogen peroxide. Environ. Sci. Technol. 45, 7882–7887. https://doi.org/10.1021/es201392k.
Silva, L.J.G., Meisel, L.M., Lino, C.M., Pena, A., 2014. Profiling serotonin reuptake inhibitors (SSRIs) in the environment: trends in analytical methodologies. Crit. Rev. Anal. Chem. 44, 41–67. https://doi.org/10.1080/10408347.2013.827966.
Silva, L.J.G., Pereira, A.M.P.T., Meisel, L.M., Lino, C.M., Pena, A., 2015. Reviewing the serotonin reuptake inhibitors (SSRIs) footprint in the aquatic biota: uptake, bioaccumulation and ecotoxicology. Environ. Pollut. 197, 127–143. https://doi.org/10.1016/j.envpol.2014.12.002.
Singh, S., Bakshi, M., 2000. Guidance on Conduct of Stress Tests to Determine Inherent Stability of Drugs. Pharmaceutical Technology On-Line, pp. 1–14.
Stravs, M.A., Pomati, F., Hollender, J., 2017. Exploring micropollutant biotransformation in three freshwater phytoplankton species. Environ. Sci. Process. Impacts 19, 822–832. https://doi.org/10.1039/C7EM00100B.
Subedi, B., Kannan, K., 2015. Occurrence and fate of select psychoactive pharmaceuticals and antihypertensives in two wastewater treatment plants in New York State, USA. Sci. Total Environ. 514, 273–280. https://doi.org/10.1016/j.scitotenv.2015.01.098.
US Environmental Protection Agency, 2001-2007. Final report: the environmental occurrence, fate, and ecotoxicity of selective serotonin reuptake inhibitors (SSRIs) in aquatic environments, research project database. NCER | ORD | US EPA [WWW Document]. https://cfpub.epa.gov/ncer_abstracts/index.cfm/fuseaction/display.highlight/abstract/1755/report/F. accessed 3.7.2016.
Vaclavik, J., Sehonova, P., Hodkovicova, N., Vecerkova, L., Blahova, J., Franc, A., Marsalek, P., Mares, J., Tichy, F., Svobodova, Z., Faggio, C., 2020. The effect of foodborne sertraline on rainbow trout (Oncorhynchus mykiss). Sci. Total Environ. 708, 135082. https://doi.org/10.1016/j.scitotenv.2019.135082.
Vervliet, P., 2018. invitRo. WWW Document. https://zenodo.org/record/1253277#.XUq4tPZuLcs. accessed 8.7.2019.
Walash, M.I., Belal, F.F., El-Enany, N.M., Elmansi, H., 2011. Development and validation of stability indicating method for determination of sertraline following ICH guidlines and its determination in pharmaceuticals and biological fluids. Chem. Cent. J. 5, 61. https://doi.org/10.1186/1752-153X-5-61.
Yuan, S., Jiang, X., Xia, X., Zhang, H., Zheng, S., 2013. Detection, occurrence and fate of 22 psychiatric pharmaceuticals in psychiatric hospital and municipal wastewater treatment plants in Beijing, China. Chemosphere 90, 2520–2525. https://doi.org/10.1016/j.chemosphere.2012.10.089.

3.2 Application of MIPs in SSRI Environmental Analysis and Treatment

3.2.1 Preparation of molecularly imprinted copoly(acrylic acid-divinylbenzene) for extraction of environmentally relevant sertraline residues

The paper "Preparation of molecularly imprinted copoly(acrylic acid-divinylbenzene) for extraction of environmentally relevant sertraline residues" by A. Koler, T. Gornik, T. Kosjek, K. Jeřabek and P. Krajnc was published in *Reactive and Functional Polymers* in October 2018. Dr A. Koler designed and synthesized the polymers, performed chemical and physical characterization studies, and wrote most of the manuscript. I was responsible for developing and optimizing the analytical method for determining the recognition parameters of the synthesized material and writing the corresponding part of the manuscript. All work was supervised by Assoc Prof Dr T. Kosjek and Prof Dr P. Krajnc, with valuable input from Prof Dr K. Jeřabek.

The paper focused on synthesizing SER imprinted MIPs and their application as sorbent material during SPE of SER and its metabolites and TPs NS and sertraline ketone to improve existing analytical methods. The MIPs were prepared following two different polymerization approaches: in solvent or bulk polymerization and by two-stage polymerization. The former types of polymers continued to leach SER even after thorough washing and were therefore deemed inappropriate materials for SPE of SER from environmental samples. However, the high cross-reactivity toward NS and sertraline ketone make them potential sorbents for extracting SER-related compounds, such as metabolites, TPs and other antidepressants. Conversely, in the two-stage polymerized MIPs, the removal of SER below the method's LOQ was successful. In addition, these MIPs also showed increased selectivity towards SER compared to the NIP. However, unfortunately, the cross-reactivity toward NS and sertraline was lower than in solvent-synthesized polymers.

This work addresses the thesis aim of synthesizing and evaluating MIPs used as SPE sorbents, and hence it provides valuable information for improving analytical methods using specialized materials. It also highlights the possibility of using such materials for extracting compounds structurally related to the imprinted template, such as metabolites and TPs. Additionally, it researches the influence of an alternative two-stage polymerization to minimize the leaching of the template used during synthesis.

Reactive and Functional Polymers 131 (2018) 378–383

Contents lists available at ScienceDirect

Reactive and Functional Polymers

journal homepage: www.elsevier.com/locate/react

Preparation of molecularly imprinted copoly(acrylic acid-divinylbenzene) for extraction of environmentally relevant sertraline residues

Amadeja Koler[a], Tjaša Gornik[b,c], Tina Kosjek[b,c,*], Karel Ječabek[d], Peter Krajnc[a,**]

[a] University of Maribor, Faculty of Chemistry and Chemical Engineering, PolyOrgLab, Smetanova 17, SI-2000 Maribor, Slovenia
[b] Jožef Stefan Institute, Department of Environmental Sciences, Jamova cesta 39, SI-1000 Ljubljana, Slovenia
[c] Jožef Stefan International Postgraduate School, Jamova cesta 39, SI-1000 Ljubljana, Slovenia
[d] Institute of Chemical Process Fundamentals of the Czech Academy of Sciences, Rozvojova 2/135, CZ-165 02 Prague, Czech Republic

ARTICLE INFO

Keywords:
Molecularly imprinted polymers
Sertraline
Porous polymers
Two-stage polymerisation
Extraction

ABSTRACT

Aiming to improve the sensitivity and specificity of environmental analysis of sertraline residues, we investigated the use of molecularly imprinted polymers (MIPs) as the solid phase extraction sorbents for rebinding of the parent drug, its metabolite norsertaline and its transformation product (TP) sertraline ketone. MIPs were synthesized using the antidepressant sertraline as the target, where two polymerisation approaches were used: polymerisation in solvent and two-stage polymerisation. Leaching of sertraline from the imprinted material presented a major problem in case of MIPs polymerised in solvent. On the contrary, by synthetizing MIPs with the two-stage polymerisation approach, sertraline was removed to below the limit of quantification (LOQ). Two MIPs were selected that showed the best binding characteristics during the solid phase extraction rebinding experiments: one was prepared by polymerisation in solvent and another one by two-stage polymerisation. The former bound norsertraline and sertraline ketone in a high binding ratio compared to its non-imprinted analogue, while the latter had the highest imprinting factor for sertraline. Based on the proved cross-selectivity of MIPs, we propose their use in enrichment, purification and isolation of transformation products, including novel compounds that have before not been recognised.

1. Introduction

At the preparation of molecularly imprinted polymers (MIPs), target molecules are reversibly bound to a functional monomer and copolymerised with a crosslinker to provide an artificial recognition site inside a rigid polymer network in order to achieve increased affinity and selectivity [1–3]. The target molecule is removed after the polymerisation and leaves an imprint for its future rebinding. Due to their special properties MIPs have found many applications, e.g. in sensors [4,5], drug delivery [6], extraction of contaminants from water [7] and food [8], tissue engineering, etc. [9]. Covalent [10] or non-covalent [11] interactions between a target molecule and a functional monomer play a major role in a successful imprinting approach. Among them, non-covalent interactions such as ionic interactions, hydrogen bonds and hydrophobic interactions are favourable for the preparation of MIPs, because their kinetics of rebinding of a target molecule is faster, as compared to the rebinding kinetics in case of covalent interactions.

Preservation of the target molecule imprint after its removal requires high rigidity of the polymer matrix and hence, its accessibility cannot depend on polymer swelling. Useful polymer imprints must be located on the walls of "true" pores of the polymer backbone. Typically, phase separation during the polymerisation of monomers in the presence of a suitable solvent (porogen) is used for the creation of porous morphology. In the majority of such preparations, the phase separation is proceeded by macrosyneresis mechanism when solid polymer precipitates within the continuous liquid phase. In the resulting "cauliflower" morphology with pores formed by spaces between clusters of particles, high surface area can be achieved only at the cost of very narrow pores. Recently, the group of Jeřabekin Prague identified conditions at which the phase separation during polymerisation is proceeded by a microsyneretic mechanism, a separation of nanodroplets of the porogenic liquid within the continuous polymeric phase [12]. This resulted in a foam-like morphology, which offers a high surface area in relatively wide pores in the mesopore size range, where pore walls are formed by a highly crosslinked polymer matrix. For MIPs, such morphology seems to be advantageous.

* Corresponding author at: Jožef Stefan Institute, Dept. Envir. Sci., Jamova cesta 39, SI-1000 Ljubljana, Slovenia
** Corresponding author.
E-mail addresses: tina.kosjek@ijs.si (T. Kosjek), peter.krajnc@um.si (P. Krajnc).

https://doi.org/10.1016/j.reactfunctpolym.2018.08.016
Received 7 June 2018; Received in revised form 4 August 2018; Accepted 27 August 2018
Available online 28 August 2018
1381-5148/

The choice of the right functional monomer for the interaction with a target molecule is crucial in molecule imprinting technique [13]. Commonly, methacrylic acid (MAA) is used as a functional monomer in the non-covalent molecular imprinting approach because of hydrogen bonding and ionic interactions with amines [14]. Structurally similar acrylic acid (AA) is also used. AA in absence of a methyl group undergoes auto-accelerated polymerisation which causes the differences in polymer morphology and recognition between molecularly imprinted poly(MAA) and poly(AA) [15].

As our target compound, we chose sertraline (SER), a pharmaceutical compound that belongs to the class of selective serotonin reuptake inhibitors (SSRIs). Its presence in environmental waters and other environmental compartments, such as sediments, sewage sludge, biosolids, fish and invertebrate tissues, has been confirmed in several studies and ranges over 100 ng/L in wastewaters, and up to a few μg/g in tissue and sewage sludge [16–21]. Furthermore, this emerging contaminant also shows the potential for accumulation [22,23] and toxic effects already at μg/L levels in invertebrates. In the latest studies from the groups of Kuzmanović and Osorio, SER was shown to be the one mostly responsible for exceeding the chronic risk threshold in the river basin of Llobregat [24,25]. Its metabolite norsertraline (norSER) has also been found in the abovementioned compartments at comparable concentrations. Furthermore, SER transformation products including sertraline ketone (SEK) were reported to be potentially persistent in water [26,27]. The chemical structures of SER, norSER and SEK are illustrated in Fig. 1.

The need for an effective monitoring of SER residues, including the parent compound, its metabolites and TPs at the environmental levels is growing. This kind of studies face the ever-present constraint of target analysis, which is limited to the group of predetermined analytes, thus often overlooking pharmaceutical TPs, in particular those that have never before been recognised in the science. On the other hand, the nontarget analysis is generally too indistinct to tackle this particular question. Due to the low concentrations of SER residues and due to complexity of the environmental matrices, a sample preparation step, such as solid phase extraction (SPE) is needed. Commercial sorbents are available and show varying success with extraction of samples containing SER and norSER [17,18,28–32]. The idea is to overcome the abovementioned limitations by using novel MIP sorbents to extract, enrich and isolate the TPs. In this view, the fundamental hypothesis of the presented research is that "The characteristics of the MIP sorbents to selectively bind a target analyte along with its structural analogues may be exploited for concurrent isolation of the parent compound, its metabolites and TPs." To our knowledge the MIPs have to date not been used for this purpose.

Not many examples of SER imprinted polymers can be found in the literature. One is a potentiometric sensor, prepared from MIP that consisted of MAA as the functional monomer and ethylene glycol dimethacrylate as the crosslinker, while sertraline hydrochloride (SER*HCl) was used as the target molecule [33]. Potential response to SER was determined, where the high selectivity towards the target compound was proven. Khalilian et al. grafted the MIP on SiO_2/graphene oxide using a sol-gel method to overcome difficulties with the removal of the target molecule [34]. The polymeric adsorbents were again made of MAA (functional polymer) and ethylene glycol dimethacrylate (crosslinker), and were used in dispersed SPE for determination of SER in biological samples of urine and plasma achieving recoveries above 92%.

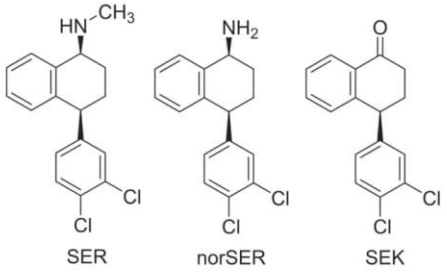

Fig. 1. Chemical structures of SER and its residues, norSER and SEK.

In the present report we describe a novel method of preparation of SER imprinted porous polymer using AA and divinylbenzene (DVB) as monomers and its performance in a designed environment. The overall aim of this study is the development of MIP to be used for enrichment of SER residues from aqueous environment in order to support the environmental fate and treatment studies.

2. Materials and methods

Materials

SER*HCl for MIP synthesis ((1*S*,4*S*)-4-(3,4-dichlorophenyl)-*N*-methyl-1,2,3,4-tetrahydronaphthalen-1-amine hydrochloride, 98% min.) was purchased from Fox-Chemicals GmbH, Pfinztal, Germany, whereas SER*HCl reference standard was obtained at Sigma-Aldrich (European Pharmacopeia Reference Standard, Sigma-Aldrich, St. Louis, MO, USA). Other internal and reference standards were sertraline-D_3 hydrochloride (SER-D_3*HCl, 99.8%) and norsertraline-$^{13}C_6$ hydrochloride (norSER-$^{13}C_6$*HCl, 99.1%), both obtained from Cerilliant (Sigma-Aldrich), norSER*HCl (99.1%, LGC, Teddington, UK), 4-(3,4-dichlorophenyl)-3,4-dihydronaphthalen-1(2H)-one (SEK, 98%, TCI, Tokyo, Japan) and 1-(2,6-Dichlorophenyl)-2-indolinone (DPI, Chemosyntha NV, Meulebeke, Belgium). DVB (80%, composed of 80% of DVB and 20% of ethylvinylbenzene, Sigma Aldrich) was purified by passing through a layer of aluminium oxide (Al_2O_3, Sigma Aldrich) to remove the inhibitors. Other chemicals involved in MIP synthesis were AA (anhydrous, 99%, Sigma Aldrich), α,α′-azobisisobutyronitrile (AIBN, Sigma Aldrich), potassium peroxodisulfate (Sigma Aldrich), toluene (≥99,8%, Carlo Erba, Milano, Italy), tetrahydrofurane (THF, ≥99,8%, Fischer Scientific, Loughborough, UK), methanol (MeOH, for analysis, Carlo Erba), sodium hydroxide (Merck, St. Louis, MO, USA) and hydrochloric acid (37%, Sigma Aldrich).

The solvents and reagents used for chemical analysis were pyridine (Py, 99.8%, Acros Organics, Geel, Belgium), dichloromethane (DCM, p.a., J.T. Baker, Deventer, Netherlands), ethyl acetate (EtAc, p.a., J.T. Baker), methanol (MeOH, p.a., J.T. Baker), acetonitrile (ACN, p.a., J.T. Baker), hydrochloric acid (HCl, p.a., J.T. Baker,), acetanhydride (99%, Sigma-Aldrich) and triethylamine (99.5%, Sigma-Aldrich). All aqueous standard and working solutions were prepared by using MilliQ (18.2 MΩ.cm, Millipore).

2.1. Methods

2.1.1. Preparation of sertraline imprinted poly(divynilbenzene-co-acrylic acid) using polymerisation in solvent

AA, DVB, SER*HCl (various amounts, see Table 1), AIBN (1 wt% to the mass of monomers AA and DVB combined), 90 mL of THF and 10 mL of deionised water were placed into a round bottom flask equipped with a magnetic stirrer and stirred for 1 h at room temperature. The content of the flask was transferred into a polypropylene mold and polymerised for 24 h at 80 °C (hot air). Polymers were purified by Soxhlet extraction for 24 h with water and for 24 h with ethanol and then air dried.

The resulting material was ground and sieved to obtain particles smaller than 200 μm. These polymer samples are in Table 1 annotated as A or Ai (polymerisation in solvent; A without the target molecule and Ai with the target molecule).

Table 1
Compositions and BET surface area of MIP samples.

Sample	m (DVB) [g]	Degree of crosslinking[a]	m (AA) [g]	m (SER) [g]	n (AA/DVB)	n (AA/SER)	BET area [m^2/g]
Ai1	8241	57	1,760	1,500	1:2,59	5:1	401
Ai2	9026	66	0,977	0,821	1:5,09	5:1	402
Ai3	9492	73	0,525	0,43	1:10	5:1	659
Bi1	1452	NA[b]	0,161	0,137	1:5	5:1	342
Bi2	1592	NA[b]	0,176	0,149	1:5	5:1	420

[a] Calculated as follows: $\frac{\text{n crosslinker} \times 0,80}{\text{n monomer} \times \text{n crosslinker}} \times 100 = \text{degree of crosslinking (\%)}$.
[b] Not applicable (two stage polymerisation).

2.1.2. Preparation of sertraline imprinted poly(divynilbenzene-co-acrylic acid) using a two-stage polymerisation procedure

DVB, toluene (various amounts; Bi1: DVB:toluene = 1:1 mL, Bi2: DVB:toluene = 1:3 mL) and AIBN were added into a round bottom flask (see Table 1 for amounts) and were stirred for 1 h at room temperature, transferred into polypropylene molds and polymerised for 24 h at 60 °C (hot air). Prepared monoliths were ground and sieved to get particles smaller than 200 μm, washed with 20 mL of toluene, 20 mL of toluene/methanol (1/1, v/v) and 20 mL of methanol, and then air-dried for 24 h. Dried materials were reswollen subsequently in THF, THF/water (1/1, v/v) and water. AA, SER*HCl, potassium peroxodisulfate (1 w.% in regards to the mass of AA and polyDVB) and 5 mL of water were added (see Table 1 for amounts). Mixture was stirred at 70 °C for 24 h and then washed with water (5 × 50 mL) and air dried. The samples obtained by two-stage polymerisation procedure are annotated as B or Bi (two-stage polymerisation; B without the target molecule and Bi with the target molecule).

2.1.3. NIP (non imprinted polymer) preparation

Non imprinted poly(DVB-*co*-AA) polymers were prepared by the same procedure as MIPs however in the absence of SER*HCl.

2.1.4. Characterisation of polymers

Nitrogen adsorption/desorption measurements were done on Micromeritics TriStar II3020 porosimeter using Brunauer-Emmett-Teller (B.E.T) method for surface area determination.

Morphology of selected polymers in swollen state was characterized using inverse steric exclusion chromatography (ISEC). In these measurements the examined polymer was used as filling of a chromatographic column and elution volumes of solutes with known effective molecular size with THF as the mobile phase were measured. The effective solute molecular sizes covered range from 319 nm for polystyrene (M_W 9835 kDa) down to 0.55 nm for n-pentane. The swollen-state morphology was modelled as a set of discrete pore fractions, each with its characteristic dimension and volume. Mathematical treatment of experimental data consisted of fitting of the model fraction volumes to achieve the best agreement of the determined elution volumes of the standard solutes and values computed on the base of the model. Details of the ISEC experimental procedure and data treatment can be found elsewhere [35].

2.1.5. Removal of sertraline from molecularly imprinted polymers

Both MIP and NIP samples were washed alternately with 5 × 50 mL of 1 M NaOH and 5 × 50 mL of 1 M HCl. We repeated the 24 h Soxhlet extraction with three organic solvents of different polarities from lowest to highest: DCM, EtAc and MeOH.

2.1.6. Preparation and storage of standard solutions

Stock solutions of SER*HCl, norSER*HCl and SEK were prepared in ACN at concentrations 100 μg/mL and 5.0 μg/mL and were stored in the dark at 4 °C for 3 to 5 months. The stability of the stock solutions at the storage temperature was confirmed for the solvent and for the duration of storage. The internal standard DPI was also prepared in stock solution at the concentration of 10 μg/mL in ACN. SER-D_3*HCl and norSER-$^{13}C_6$*HCl were purchased as 100 μg/mL MeOH solutions and were stored at −20 °C as required in the Material safety data sheet (Cerilliant, n.d.).

2.1.7. Solid phase extraction method for the determination of imprinting factor and cross-selectivity

The sorbents (MIP and NIP) were packed into empty 3 mL SPE cartridges (30–50 mg). To determine the imprinting factor and cross-selectivity of the materials towards SER residues the target compound SER, its metabolite norSER and transformation product SEK were bound on MIP and its corresponding NIP. The sorbents were preconditioned with 3 mL of DCM, 3 mL of EtAc and 3 mL of MeOH and equilibrated with 3 mL of MilliQ water, then 200 mL test solutions of 10 μg/L SER, norSER or SEK were loaded on the tested MIP or NIP sorbent at a flow rate of 1–2 mL per minute. The sorbents were vacuum dried for 30 min. The compounds were eluted with 12 mL of the DCM/EtAc/MeOH (1/1/1, v/v/v) mixture, then the eluates were N_2 dried at 40 °C down to 0.5 mL, quantitatively transferred to 1.5-mL glass vials and blown down to dryness. The analytes were derivatized with a mixture of acetanhydride (15 μL) and pyridine (5 μL) at room temperature for 15 min. The samples were again N_2 dried at 40 °C and reconstituted in 0.5 mL of EtAc.

We assessed the imprinting effect by comparing the extraction performances of MIP and NIP at SER concentration of 10 μg/L and reported it as the imprinting factor: the ratio between the amount of SER bound to MIP and the amount bound to its corresponding NIP. In order to evaluate the cross-selectivity of MIPs, the binding ratios for its environmental residues (norSER and SEK) were also calculated.

2.1.8. Instrumental analysis

The quantification of the compounds was performed on a gas chromatograph coupled to mass selective detector, GC-MSD (7890B/5977A Agilent Technologies, USA). The oven temperature programme was 100 °C held for 2 min, 25 °C/min to 300 °C and held for 6 min. The total runtime was 16 min. We used a HP-5 ms Ultra Inert, 30 m long capillary column, with a 0.25 mm i.d. and 0.25 μm film thickness. Helium was the carrier gas with a flow rate of 1 mL/min. 1 μL samples were injected in splitless mode at the inlet temperature of 270 °C. The ionisation mode was electron impact (EI) at 70 eV.

3. Results and discussion

3.1. Preparation of molecularly imprinted poly(DVB-co-AA)

Firstly, polymerisation in solvent using 57 (Ai1), 67 (Ai2) and 73 (Ai3) mol. % of DVB (Table 1) as the crosslinker was performed to prepare samples of MIPs. High amounts of DVB lead to high rigidity of polymer chains, which is important for fixation of cavities and consequently polymer morphology and recognition (rebinding of SER). An improved recognition and rebinding of SER and its structurally similar compounds is expected when higher amounts of a crosslinker are used. AA was chosen as the functional monomer in order to form acid-base

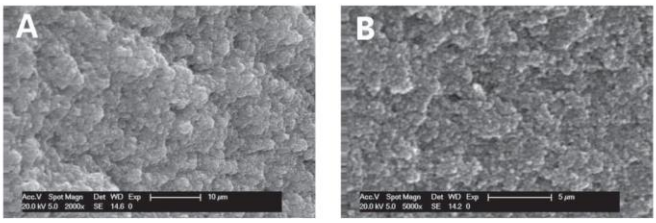

Fig. 2. Scanning electron microscopy images of samples A2 (left, Fig. 2a) and B2 (right, Fig. 2b), Bar on Fig. 2a is 10 µm, on Fig. 2b is 5 µm.

interaction with SER. Typically, in the presence of a porogenic solvent, porous polymer with a well-defined micro porosity and high specific surface area is formed [36]. It was reported that THF, toluene and 1,2-dichloroethane are good porogens for DVB-based polymers [12]. Furthermore, THF is a more polar solvent than toluene and 1,2-dichloroethane, and more miscible with AA [37]. With this rationale, a mixture of THF and water in volume ratio 90/10 was applied as the porogen. It is well known that solvation of polymer chains or swelling is the most efficient way to get access to reactive groups from the fluid phase to functional groups attached to the polymer [38]. Difference in polarity between DVB and AA forces the latter to polymerise mostly on the surface. Hence, it is expected to achieve a better accessibility of active functional groups.

As seen in Table 1, the resulting MIP samples all had high dry surface areas (401 m^2/g, 402 m^2/g and 659 m^2/g, for Ai1, Ai2 and Ai3, respectively), which is the consequence of a high degree of crosslinking and the use of THF/water as the porogenic solvent. It can be seen from the scanning electron microscope image (Fig. 2a) that a fine porous structure with a cauliflower-like morphology and pores in between the fused beads of polymer with approximate average diameters between 500 nm and 2 µm, is present.

With an aim of improving the accessibility of the imprinted reaction sites, we applied another method of polymerisation. Namely, to obtain a polymer with a higher concentration of acid functional groups positioned near the surface of the polymer, a two-stage polymerisation procedure was performed. Firstly, DVB alone was used as the monomer together with toluene as the porogen. Polymerising only DVB typically results in a substantial amount of free double bonds not consumed in the polymerisation [39]. So prepared polyDVB was further treated firstly with the swelling solvent (toluene) and then with AA and a radical initiator. AA was thus grafted (copolymerised) onto the swollen polyDVB in the second stage of this procedure.

Dry BET surface areas were comparable to solvent polymerisation samples, i.e. 342 m^2/g for Bi1 and 420 m^2/g for Bi2, respectively (see Table 1), and dependent on the initial concentration of porogen. No dramatic change in dry surface areas were found compared to solvent polymerised samples suggesting similar *meso* and micro porous structure, while the ratios of monomers (AA:DVB) had a significant impact on the SER binding in further experiments studying the imprinting effect. Furthermore, the investigation using scanning electron microscopy revealed similar morphology comparing to solvent polymerised samples, however significantly smaller macro pore size can be seen, with diameters in the range between 150 nm and 1 µm (Fig. 2b).

Samples Bi1 and Bi2 were further investigated for swollen state porosity using ISEC. It has been shown previously that elucidating surface area and pore size distribution data solely from gas adsorption/desorption on dry material, which is the case in using BET model, can yield in deceptive results as the polymers are actually used in wet conditions rather than dry [40].

It can be illustrated from the comparison of the dry-state surface area determination, which shows only a small difference between the values obtained for Bi1 and Bi2, in spite of 3-times greater volume of the porogenic solvent used in the first stage of the preparation of the sample Bi2 (see Table 1). In the swollen-state morphology evaluation by ISEC two types of the polymer porosity were distinguished – "true" pores modelled as cylindrical holes in the polymer matrix and porosity of swollen polymer gel depicted as spaces between randomly oriented rods representing polymer chains (Ogston model). Morphology parameters as determined by ISEC are shown in Table 2.

Table 2
Swollen-state morphology data as determined by ISEC.

Polymer sorbent		Bi1	Bi2
True pores	Pore volume [cm^3/g]	0.45	1.19
	Medium pore diameter [nm]	12.9	12.1
	Surface area [m^2/g]	144	401
Swollen polymer	Swollen gel volume [cm^3/g]	1.03	0.98
	Medium pore chain density [nm/nm^3]	0.5	0.6

ISEC results show true pore volumes and surfaces significantly more in accordance to the volume of toluene as the porogen used in the first stage of the polymer preparations, compared to nitrogen adsorption experiments on the dry samples. On the other hand, the detected volume of the swollen gel phase, probably formed by the grafted acrylic acid, is in both polymers quite similar, what corresponds with the similar amounts of the reagents used in the second preparation stage (see Table 1).

3.2. Imprinting effect and cross-selectivity study through solid phase extraction

Despite many efforts paid to the repeated washing of the polymers using a series of solvents of different strength and polarity, the complete removal of the target compound was unsuccessful for the MIPs prepared by the polymerisation in solvent (Ai). SER remained present in the leachate in the concentrations above instrumental limit of quantification (LOQ) (54.3 ng/mL). The continuous leaching may imply that there are some specific electrostatic interactions between the target

Table 3
Imprinting factor determined for SER and binding ratios for norSER and SEK for the MIP samples.

	MIP/NIP nr.	Polymerisation type	Imprinting factor/binding ratio
SER	Bi1/B1	two-stage	1.89
	Bi2/B2	two-stage	0.56
norSER	Ai1/A1	polymerisation in solvent	0.95
	Ai2/A2	polymerisation in solvent	1.62
	Ai3/A3	polymerisation in solvent	1.11
	Bi1/B1	two-stage	0.74
SEK	Ai1/A1	polymerisation in solvent	1.12
	Ai2/A2	polymerisation in solvent	2.14
	Ai3/A3	polymerisation in solvent	1.63
	Bi1/B1	two-stage	1.39

molecule and the polymer (acid-base interactions), which in turn make the detection of SER at environmental concentrations impossible. For this reason, we tested the polymers for the binding of the two SER residues, i.e. norSER and SEK. Table 3 reports the binding ratios.

In contrast to the MIPs prepared by polymerisation in solvent, we did not observe SER leaching from the two-stage polymerised Bi1 and Bi2 (i.e., the leaching concentration was below the instrumental LOQ). Therefore, we report the imprinting factor for SER, and cross-selectivity binding ratios for its metabolite and transformation product, norSER and SEK (Table 3).

Bi2 showed very poor rebinding of SER and was therefore not tested further, while we observed a promising amount of SER and SEK bound to Bi1. The grafted layer of AA imprinted with SER is in the sorbent Bi2 spread across a much wider surface area than in Bi1. It may promote higher mobility of the acrylic acid polymer chains, what could be responsible for erasing of the SER imprints evident in the low imprinting effect found for the Bi2 sorbent.

However, for norSER the imprinting effect in two-stage polymerised MIP was < 1 (Table 3), which suggests that nonspecific interactions between norSER and B1 outweighed specific plus nonspecific interactions between norSER and Bi1. The possible explanation for this is that the Bi1 polymer binds with specific electrostatic interactions to a single norSER enantiomer. In support to this justification is the fact that norSER reference standard was a racemic mixture [41], whereas SER standards we used for both imprinting and analysis were optically pure (1S, 4S).

Generally, the degree of crosslinking is highly important for mechanical stability of MIPs resulting in better fixation of cavities thus having an effect also on the ability of imprinting effect of the polymer support. Sample Ai1, with the lowest crosslinking degree (57%) within the series, had the lowest binding ratio for norSER and SEK among the MIPs polymerised in solvent, while sample Ai2 (67% crosslinked) had the highest binding ratio (Table 3). Sample Ai3 with the highest crosslinking degree (73%) again exhibited reduced binding ratio for norSER and SEK. This may be ascribed to the very high crosslinking resulting in cavity sites being inaccessible for the target molecule, while up to a certain value, this increase in the crosslinking degree has a positive effect on selectivity due to increased rigidity of polymer chains keeping the cavities in proper shape. The sample Ai3 also leached the smallest amount of SER (Fig. 2) among the polymers synthetized in solvent, but at the same time, the smallest amount of SER was added during the polymerisation (Table 1). Since the material was still leaching SER we should also keep in mind that not all of the possible binding sites have been successfully washed off, therefore, there is potential for an even higher binding ratio.

Among the synthesized MIPs, Bi1 is the only one that could potentially be used as an SPE sorbent for SER at the environmental levels. Still, experiments using more sensitive instrumental methods such as LC-MS/MS should confirm this finding. Other MIPs synthesized within this study either showed very poor imprinting effect (Bi2) or caused continuous leaching of the template molecule (Ai1, Ai2 and Ai3), so that the assessment of their imprinting effect was not possible. On the other hand, Ai2 was shown most promising for binding of the metabolite norSER and the transformation product SEK, which proves that there exists a cross-selectivity between SER and its structurally related compounds. This finding opens up several possibilities and potentials for using MIP Ai2 and its further development. One example is to use it as a sorbent for sensitive and matrix-free determination of SER residues in the environmental samples or for determination of the metabolite norSER in clinical samples. Just as importantly, this polymer may find its use in sensor technology for fast and easy on-site assessment of anthropogenic activities or for wastewater treatment and reuse.

4. Conclusions

Molecularly imprinted polymers aimed for rebinding of SER and its structurally related compounds were synthesized. The MIPs were prepared according to two polymerisation approaches, namely polymerisation in solvent and a two-stage polymerisation. We found that the latter, tailored polymerisation procedure improved the accessibility of MIP-induced cavities and was therefore the more effective polymerisation approach in regards to the improved imprinting effect of SER, since swelling of polyDVB in the first stage of polymerisation made unreacted vinyl groups more accessible for further binding of AA in the second stage. On the other hand, polymerisation in solvent resulted in an improved imprinting effect of structurally related compounds, i.e. norSER and SEK. The degree of crosslinking proved very important for fixation of cavities and consequently selectivity.

Since we confirmed the existence of cross-selectivity between SER and its environmental residues, our future attempt will be to use MIPs for extraction of other structurally related SER residues, in particular transformation products, which may appear in environment, but they have possibly not been recognised yet.

Acknowledgements

The authors acknowledge the financial support from the Slovenian Research Agency (research core funding No. P1-0143) and project J1-6744 (Development of Molecularly Imprinted Polymers and their application in environmental and bio-analysis). We wish to thank Dr. Jernej Iskra for his support in initiation of this study.

References

[1] P.A. Cormack, A.Z. Elorza, Molecularly imprinted polymers: synthesis and characterisation, J. Chromatogr. B 804 (2004) 173–182, https://doi.org/10.1016/j.jchromb.2004.02.013.
[2] K. Haupt, A.V. Linares, M. Bompart, B.T.S. Bui, Molecularly imprinted polymers, in: K. Haupt (Ed.), Mol. Imprinting, Springer Berlin Heidelberg, Berlin, Heidelberg, 2011, pp. 1–28.
[3] N.A. Samah, M.J. Sánchez-Martín, R.M. Sebastián, M. Valiente, M. López-Mesas, Molecularly imprinted polymer for the removal of diclofenac from water: synthesis and characterization, Sci. Total Environ. 631–632 (2018) 1534–1543, https://doi.org/10.1016/j.scitotenv.2018.03.087.
[4] G. Ertürk, B. Mattiasson, Molecular imprinting techniques used for the preparation of biosensors, Sensors 17 (2017) 288, https://doi.org/10.3390/s17020288.
[5] Y. Saylan, F. Yilmaz, E. Özgür, A. Derazshamshir, H. Yavuz, A. Denizli, Molecular imprinting of macromolecules for sensor applications, Sensors (Switzerland) 17 (2017), https://doi.org/10.3390/s17040898.
[6] P. Luliński, Molecularly imprinted polymers based drug delivery devices: a way to application in modern pharmacotherapy. A review, Mater. Sci. Eng. C 76 (2017) 1344–1353, https://doi.org/10.1016/j.msec.2017.02.138.
[7] O.M. Rodriguez-Narvaez, J.M. Peralta-Hernandez, A. Goonetilleke, E.R. Bandala, Treatment technologies for emerging contaminants in water: a review, Chem. Eng. J. 323 (2017) 361–380, https://doi.org/10.1016/j.cej.2017.04.106.
[8] A. Speltini, A. Scalabrini, F. Maraschi, M. Sturini, A. Profumo, Newest applications of molecularly imprinted polymers for extraction of contaminants from environmental and food matrices: a review, Anal. Chim. Acta 974 (2017) 1–26, https://doi.org/10.1016/j.aca.2017.04.042.
[9] M.I. Neves, M.E. Wechsler, M.E. Gomes, R.L. Reis, P.L. Granja, N.A. Peppas, Molecularly imprinted intelligent scaffolds for tissue engineering applications, Tissue Eng. Part B Rev. 23 (2017) 27–43, https://doi.org/10.1089/ten.teb.2016.0202.
[10] G. Wulff, Molecular imprinting in cross-linked materials with the aid of molecular templates— a way towards artificial antibodies, Angew. Chem. Int. Ed. Eng. 34 (1995) 1812–1832, https://doi.org/10.1002/anie.199518121.
[11] K. Mosbach, K. Haupt, Some new developments and challenges in non-covalent molecular imprinting technology, J. Mol. Recognit. 11 (1998) 62–68, https://doi.org/10.1002/(SICI)1099-1352(199812)11:1/6<62::AID-JMR391>3.0.CO;2-5.
[12] L. Hanková, L. Holub, K. Jeřábek, Formation of porous polymer morphology by microsyneresis during divinylbenzene polymerization, J. Polym. Sci. Part B Polym. Phys. 53 (2015) 774–781, https://doi.org/10.1002/polb.23693.
[13] A.G. Mayes, M.J. Whitcombe, Synthetic strategies for the generation of molecularly imprinted organic polymers, Adv. Drug Deliv. Rev. 57 (2005) 1742–1778, https://doi.org/10.1016/j.addr.2005.07.011.
[14] H. Zhang, Water-compatible molecularly imprinted polymers: Promising synthetic substitutes for biological receptors, Polymer (Guildf) 55 (2014) 699–714, https://doi.org/10.1016/j.polymer.2013.12.064.
[15] K. Golker, G.D. Olsson, I.A. Nicholls, The influence of a methyl substituent on molecularly imprinted polymer morphology and recognition – Acrylic acid versus methacrylic acid, Eur. Polym. J. 92 (2017) 137–149, https://doi.org/10.1016/j.eurpolymj.2017.04.043.
[16] A. Lajeunesse, S.A. Smyth, K. Barclay, S. Sauvé, C. Gagnon, Distribution of

antidepressant residues in wastewater and biosolids following different treatment processes by municipal wastewater treatment plants in Canada, Water Res. 46 (2012) 5600–5612, https://doi.org/10.1016/j.watres.2012.07.042.
[17] P. Nagarnaik, A. Batt, B. Boulanger, Source characterization of nervous system active pharmaceutical ingredients in healthcare facility wastewaters, J. Environ. Manag. 92 (2011) 872–877, https://doi.org/10.1016/j.jenvman.2010.10.058.
[18] B. Petrie, J. Youdan, R. Barden, B. Kasprzyk-Hordern, Multi-residue analysis of 90 emerging contaminants in liquid and solid environmental matrices by ultra-high-performance liquid chromatography tandem mass spectrometry, J. Chromatogr. A 1431 (2016) 64–78, https://doi.org/10.1016/j.chroma.2015.12.036.
[19] L. Sabourin, P. Duenk, S. Bonte-Gelok, M. Payne, D.R. Lapen, E. Topp, Uptake of pharmaceuticals, hormones and parabens into vegetables grown in soil fertilized with municipal biosolids, Sci. Total Environ. 431 (2012) 233–236, https://doi.org/10.1016/j.scitotenv.2012.05.017.
[20] B. Subedi, S. Lee, H.-B. Moon, K. Kannan, Psychoactive pharmaceuticals in sludge and their emission from wastewater treatment facilities in Korea, Environ. Sci. Technol. 47 (2013) 13321–13329, https://doi.org/10.1021/es404129r.
[21] S. Yuan, X. Jiang, X. Xia, H. Zhang, S. Zheng, Detection, occurrence and fate of 22 psychiatric pharmaceuticals in psychiatric hospital and municipal wastewater treatment plants in Beijing, China, Chemosphere 90 (2013) 2520–2525, https://doi.org/10.1016/j.chemosphere.2012.10.089.
[22] L. Minguez, C. Ballandonne, C. Rakotomalala, C. Dubreule, V. Kientz-Bouchart, M.P. Halm-Lemeille, Transgenerational effects of two antidepressants (sertraline and venlafaxine) on Daphnia magna life history traits, Environ. Sci. Technol. 49 (2015) 1148–1155, https://doi.org/10.1021/es504808g.
[23] A.P. Rodrigues, L.H.M.L.M. Santos, M.J. Ramalhosa, C. Delerue-Matos, L. Guimarães, Sertraline accumulation and effects in the estuarine decapod Carcinus maenas: importance of the history of exposure to chemical stress, J. Hazard. Mater. 283 (2015) 350–358, https://doi.org/10.1016/j.jhazmat.2014.08.035.
[24] M. Kuzmanović, J.C. López-Doval, N. De Castro-Català, H. Guasch, M. Petrović, I. Muñoz, A. Ginebreda, D. Barceló, Ecotoxicological risk assessment of chemical pollution in four Iberian river basins and its relationship with the aquatic macroinvertebrate community status, Sci. Total Environ. 540 (2016) 324–333, https://doi.org/10.1016/j.scitotenv.2015.06.112.
[25] V. Osorio, A. Larrañaga, J. Aceña, S. Pérez, D. Barceló, Concentration and risk of pharmaceuticals in freshwater systems are related to the population density and the livestock units in Iberian Rivers, Sci. Total Environ. 540 (2016) 267–277, https://doi.org/10.1016/j.scitotenv.2015.06.143.
[26] A. Jakimska, K.M. Śliwka, P. Nagórski, W.a. Kot, J. Namieśnik, Environmental fate of two psychiatric drugs, diazepam and sertraline: phototransformation and investigation of their photoproducts in natural waters, Chromatogr. Sep. Tech. 5 (2014) 1–12, https://doi.org/10.4172/2157-7064.1000253.
[27] L.Q. Shen, E.S. Beach, Y. Xiang, D.J. Tshudy, N. Khanina, C.P. Horwitz, M.E. Bier, T.J. Collins, Rapid, biomimetic degradation in water of the persistent drug sertraline by TAML catalysts and hydrogen peroxide, Environ. Sci. Technol. 45 (2011) 7882–7887, https://doi.org/10.1021/es201392k.
[28] O. Golovko, V. Kumar, G. Fedorova, T. Randak, R. Grabic, Seasonal changes in antibiotics, antidepressants/psychiatric drugs, antihistamines and lipid regulators in a wastewater treatment plant, Chemosphere 111 (2014) 418–426, https://doi.org/10.1016/j.chemosphere.2014.03.132.
[29] M. Huerta-Fontela, M.T. Galceran, F. Ventura, Occurrence and removal of pharmaceuticals and hormones through drinking water treatment, Water Res. 45 (2011) 1432–1442, https://doi.org/10.1016/j.watres.2010.10.036.
[30] M.S. Kostich, A.L. Batt, J.M. Lazorchak, Concentrations of prioritized pharmaceuticals in effluents from 50 large wastewater treatment plants in the US and implications for risk estimation, Environ. Pollut. 184 (2014) 354–359, https://doi.org/10.1016/j.envpol.2013.09.013.
[31] M.M. Schultz, E.T. Furlong, D.W. Kolpin, S.L. Werner, H.L. Schoenfuss, L.B. Barber, V.S. Blazer, D.O. Norris, A.M. Vajda, Antidepressant pharmaceuticals in two US effluent-impacted streams: occurrence and fate in water and sediment, and selective uptake in fish neural tissue, Environ. Sci. Technol. 44 (2010) 1918–1925.
[32] T. Vasskog, T. Anderssen, S. Pedersen-Bjergaard, R. Kallenborn, E. Jensen, Occurrence of selective serotonin reuptake inhibitors in sewage and receiving waters at Spitsbergen and in Norway, J. Chromatogr. A 1185 (2008) 194–205, https://doi.org/10.1016/j.chroma.2008.01.063.
[33] M. Arvand, M. Hashemi, Synthesis by precipitation polymerization of a molecularly imprinted polymer membrane for the potentiometric determination of sertraline in tablets and biological fluids, J. Braz. Chem. Soc. 23 (2012) 392–402, https://doi.org/10.1590/S0103-50532012000300004.
[34] F. Khalilian, F.K. Kermani, Selective dispersive solid phase extraction of Ser-traline using surface molecularly imprinted polymer grafted on SiO_2/graphene oxide, J. Chem. Heal. Risks 7 (2017).
[35] K. Jeřábek, Inverse steric exclusion chromatography as a tool for morphology characterization, ACS Symp. Ser. 635 (1996) 211–224, https://doi.org/10.1021/bk-1996-0635.ch012.
[36] M. Paljevac, P. Krajnc, L. Hanková, L. Holub, B. Le Droumaguet, D. Grande, K. Jeřábek, Two-step syneretic formation of highly porous morphology during co-polymerization of hydroxyethyl methacrylate and ethylene glycol dimethylacrylate, Mater. Today Commun. 7 (2016) 16–21, https://doi.org/10.1016/j.mtcomm.2016.02.004.
[37] P. Krajnc, D. Štefanec, I. Pulko, Acrylic acid "reversed" PolyHIPEs, Macromol. Rapid Commun. 26 (2005) 1289–1293, https://doi.org/10.1002/marc.200500353.
[38] S. Sterchele, P. Centomo, M. Zecca, L. Hanková, K. Jeřábek, Dry- and swollen-state morphology of novel high surface area polymers, Microporous Mesoporous Mater. 185 (2014) 26–29, https://doi.org/10.1016/j.micromeso.2013.10.005.
[39] U. Sevšek, J. Brus, K. Jeřabek, P. Krajnc, Post polymerisation hypercrosslinking of styrene/divinylbenzene poly(HIPE)s: Creating micropores within macroporous polymer, Polym. (United Kingdom). 55 (2014) 410–415, https://doi.org/10.1016/j.polymer.2013.09.026.
[40] K. Jeřábek, I. Pulko, K. Soukupova, D. Štefanec, P. Krajnc, Porogenic solvents influence on morphology of 4-vinylbenzyl chloride based PolyHIPEs, Macromolecules 41 (2008) 3543–3546, https://doi.org/10.1021/ma8002104.
[41] rac-Norsertraline Hydrochloride-CAS Number 91797-57-8, (n.d.).

3.2.2 Molecularly imprinted polymers for the removal of antidepressants from contaminated wastewater

The paper "Molecularly imprinted polymers for the removal of antidepressants from contaminated wastewater" by T. Gornik, S. Shinde, L. Lamovsek, M. Koblar, E. Heath, B. Sellergren and T. Kosjek was published in *Polymers* in December 2020. Part of the experimental work was performed at the Department of Biomedical Sciences and Biofilms-Research Center for Biointerfaces at the Faculty of Health and Society in Sweden. I was responsible for the conceptualization, experimental work, methodology, analysis, interpretation and writing of the manuscript under the supervision of Dr S. Shinde, Prof Dr B. Sellergren and Assoc Prof Dr T. Kosjek.

Considering that antidepressants are regularly detected in WW effluents and surface waters, it seems that existing WW treatments are not successful in removing them before they contaminate the environment. This study investigated the possibility of using imprinted polymers as sorbents to remove the most prescribed group of antidepressants, the SSRIs. The polymers were prepared via bulk polymerization using SER as the template. The composition of the polymeric mixture was optimized to obtain the best recognition characteristics for SER during batch rebinding experiments. The maximal observed capacity in water was 72.6 mg g^{-1}, with a maximum imprinting factor of 3.7. The MIPs were also cross-reactive towards other SSRIs, metabolites, and TP NS. However, no cross-reactivity was noted for the TP sertraline ketone, indicating that the amino group is needed for specific interactions. The steric hindrance of the amino group also played a crucial role in the binding ability of the MIP. While the goal in preparing a MIP is to have as much specific binding as possible, the results indicate that non-specific binding majorly contributes to the removal efficiency. In this case, non-specific binding was also considerably influenced by the salt concentration in the matrix. Lastly, the performance of the MIPs was compared to AC, where the MIPs were deemed superior when used in WW.

With this research, we strived to fulfill the aim of synthesizing and evaluating MIPs used as WW treatment technique. It is one of only a few studies that study in-depth the sample parameters and material characteristics influencing the binding during WW treatment with MIPs. Furthermore, we demonstrated that producing specialized materials can be a viable WW treatment option for specific hard-to-remove contaminants or even groups of such contaminants.

polymers

MDPI

Article

Molecularly Imprinted Polymers for the Removal of Antide-Pressants from Contaminated Wastewater

Tjasa Gornik [1,2], Sudhirkumar Shinde [3,4], Lea Lamovsek [5], Maja Koblar [2,6], Ester Heath [1,2], Börje Sellergren [3] and Tina Kosjek [1,2,*]

[1] Department of Environmental Sciences, Jozef Stefan Institute, Jamova 39, 1000 Ljubljana, Slovenia; tjasa.gornik@ijs.si (T.G.); ester.heath@ijs.si (E.H.)
[2] Jozef Stefan International Postgraduate School, Jamova 39, 1000 Ljubljana, Slovenia; maja.koblar@ijs.si
[3] Department of Biomedical Sciences and Biofilms-Research Center for Biointerfaces (BRCB), Faculty of Health and Society, Malmö University, 20506 Malmö, Sweden; sudhirshinde1@gmail.com (S.S.); borje.sellergren@mau.se (B.S.)
[4] School of Chemistry and Chemical Engineering, Queens University Belfast, Belfast BT9 5AG, UK
[5] Department of Biopharmacy and Pharmacokinetics, Faculty of Pharmacy, University of Ljubljana, Askerceva 7, 1000 Ljubljana, Slovenia; lealamovsek@gmail.com
[6] Center for Electron Microscopy and Microanalysis (CEMM), Jamova 39, 1000 Ljubljana, Slovenia
* Correspondence: tina.kosjek@ijs.si; Tel.: +386/1-477-3288

Abstract: Selective serotonin reuptake inhibitors (SSRIs) are a class of antidepressants regularly detected in the environment. This indicates that the existing wastewater treatment techniques are not successfully removing them beforehand. This study investigated the potential of molecularly imprinted polymers (MIPs) to serve as sorbents for removal of SSRIs in water treatment. Sertraline was chosen as the template for imprinting. We optimized the composition of MIPs in order to obtain materials with highest capacity, affinity, and selectivity for sertraline. We report the maximum capacity of MIP for sertraline in water at 72.6 mg g^{-1}, and the maximum imprinting factor at 3.7. The MIPs were cross-reactive towards other SSRIs and the metabolite norsertraline. They showed a stable performance in wastewater-relevant pH range between 6 and 8, and were reusable after a short washing cycle. Despite having a smaller surface area between 27.4 and 193.8 $m^2 \cdot g^{-1}$, as compared to that of the activated carbon at 1400 $m^2 \cdot g^{-1}$, their sorption capabilities in wastewaters were generally superior. The MIPs with higher surface area and pore volume that formed more non-specific interactions with the targets considerably contributed to the overall removal efficiency, which made them better suited for use in wastewater treatment.

Keywords: molecular imprinting; polymer; wastewater treatment; sertraline; cross-reactivity; SSRI; template; sorbent

Citation: Gornik, T.; Shinde, S.; Lamovsek, L.; Koblar, M.; Heath, E.; Sellergren, B.; Kosjek, T. Molecularly Imprinted Polymers for the Removal of Antide-Pressants from Contaminated Wastewater. *Polymers* **2020**, *13*, 120. https://doi.org/10.3390/polym13010120

Academic Editor: Marta Otero
Received: 24 November 2020
Accepted: 23 December 2020
Published: 30 December 2020

1. Introduction

The fast population growth, advances in industry, and increased agricultural activity have greatly influenced the environment. In order to continue with the current pace, we need solutions in environmental management, especially wastewater (WW) reuse. The development in the area of sample preparation and instrumentation has put the removal of trace-level emerging contaminants in the forefront of environmental research [1,2]. Among them, pharmaceuticals are a very problematic group, since they are particularly designed to have a pharmacological effect on humans or animals, thus potentially yielding adverse effects in living organisms [3] after they have entered the aquatic environment.

The selective serotonin reuptake inhibitors (SSRIs) are members of the most prescribed class of antidepressants in the USA and Europe [4–6]. They have been repeatedly detected in WW, surface waters, sediments, and aquatic organisms [7–12], and are thus part of different monitoring programs [13]. In aquatic organisms, SSRIs cause changes in biochemical processes, feeding behavior, survivorship behavior, growth, and potential changes in

their genetic material [7,14–17]. Hence, it is crucial to improve their removal from WW before they are introduced into the environment. Among the existing WW treatment techniques, advanced oxidation processes and biological treatment are most successful in removing SSRIs from WW [18,19]. While during the former, the leading process of removal is degradation, sorption to activated sludge seems to be responsible for the removal of the majority of SSRIs during biological treatment [19]. Hence, other adsorption-based treatment techniques have been considered. Among them, activated carbon (AC) is by far the most researched material for SSRI removal [20,21]. AC as a treatment technique is technologically simple, has relatively fast kinetics, and removes a high variety of contaminants. Its main disadvantages are a high initial investment, the non-selectivity of the process, and the need for frequent regeneration due to fouling, which is expensive, time-consuming, and results in the loss of material in each regeneration cycle [22,23]. Greener alternatives, such as using products of pyrolysis of primary and secondary paper mill sludge, spent coffee grounds, and pine bark have been reported [24,25]. However, there is a lack of literature investigating modified synthetic composite materials, such as carbon-based nanomaterials, different types of membranes, and other forms of modified polymers, which, however, present promising alternatives to achieve superior SSRI removal from WWs [19,26–29]. On the basis of this knowledge gap, we investigated molecularly imprinted polymers (MIPs) as an alternative sorption material to AC [23,30,31].

MIPs are polymers that have been imprinted by a chosen template during the polymerization step in order to create selective recognition sites and are therefore often referred to as artificial antibodies or synthetic receptors [32]. After the template is removed from the MIP, the same or similar molecule can be rebound. They have already been commercially used for solid-phase extraction (SPE) [33,34] and researched for several other applications, such as catalysis, chromatography, and drug delivery [35,36]. In the last few years, the number of studies considering MIPs for water treatment has increased. Thus far, they have been utilized to remove non-steroidal anti-inflammatory drugs, antibiotics, antimicrobials, endocrine-disrupting compounds, herbicides, phenols, and beta-blockers from contaminated WW [30,35,37–41]. The advantages of using MIPs for water treatment are their high selectivity and affinity for their targets. Hence, we expect to be able to regenerate the material after longer intervals compared to AC, since slower fouling rates are expected. Literature reports MIPs as mechanically and chemically stable, and thus they should withstand several regeneration cycles unchanged, making the treatment more cost-effective [35,38]. The main disadvantage of MIPs is, however, the initial investment into the production of the polymers. Among multiple polymerization procedures available today, we chose bulk polymerization as one of the simplest and cheapest one for MIP production [2].

The aim of this work was to develop a MIP that could be used for removal of not only our targeted template, but for the whole class of SSRIs. We evaluated the affinity, capacity, and selectivity of the synthetized MIPs for sertraline (SER) and chose the best performing materials. Further characterization included cross-reactivity towards other antidepressants fluoxetine (FLU), paroxetine (PXT), escitalopram (ESC), bupropion (BUP), two SER metabolites—norsertraline (NS) and sertraline ketone (SEK) [9,10,42], and structurally related compound bupivacaine (BUC) (Figure 1). Potential parameters influencing the removal were considered and the performance of the MIPs in WW was tested in order to evaluate their applicability for WW treatment. The composition of the polymers was confirmed using Fourier transform infrared spectroscopy (FTIR) and elemental analysis. Surface properties and pore volume were calculated on the basis of the obtained Brunauer–Emmett–Teller (BET) isotherms, and scanning electron microscopy images of materials were taken for morphological characterization.

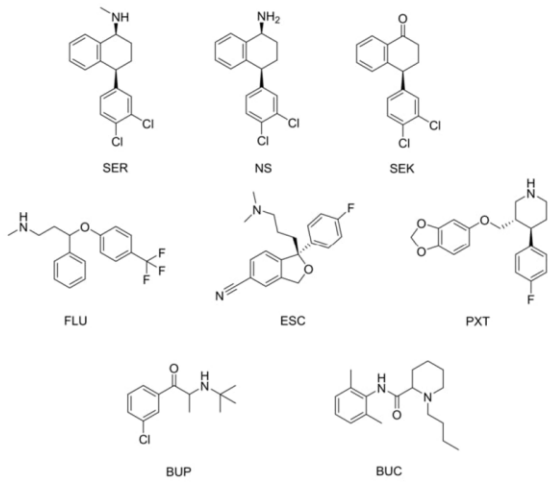

Figure 1. Chemical structures of the tested compounds.

2. Materials and Methods

The list of chemicals, materials, and the description of standard solution preparation and pre-preparation of the polymerization ingredients are reported in the Supplementary Material (SM) Section 1.

2.1. The Synthesis of MIP

The polymers were prepared via bulk radical polymerization with the ingredients in ratios specified in Table 1.

Table 1. Polymer compositions (molar ratio) and ingredients used for the synthesis of molecularly imprinted polymers (MIPs).

Material	Template	MAA	mMA	HEMA	EGDMA	Initiator (V-65)	Porogen
MIP1	SER×HCl (1)	4	/	/	20	1 wt % based on total monomers	$CHCl_3$
MIP2	SER×HCl (1)	4	8	/	12		$CHCl_3$
MIP3	SER×HCl (1)	4	/	8	12		$CHCl_3$
MIP4	SER (1)	4	/	/	20		MeOH
MIP5	SER (1)	4	/	/	20		$CHCl_3$
MIP6	SER (1)	4	/	/	20		ACN
MIP7	SER (1)	4	/	/	20		toluen
MIP8	SER (1)	4	8	/	12		$CHCl_3$
MIP9	SER (1)	4	8	/	12		ACN
MIP10	SER (1)	4	8	/	12		toluen
MIP11	SER (1)	4	/	8	12		$CHCl_3$
MIP12	SER (1)	4	/	8	12		ACN
MIP13	SER (1)	4	/	8	12		toluen

The mini-MIP library was synthesized by varying functional monomer, porogen, and the form of the template, as illustrated in the Table 1. The molar ratio between the template, functional monomer, and cross-linker was 1/4/20. In the case of mini-MIPs, 34.1 mg (0.1 mmol) of sertraline in HCl salt form (SER HCl) or 30.8 mg (0.1 mmol) free base sertraline (SER), 34 µL (0.4 mmol) methacrylic acid (MAA), and 380 µL (2 mmol) ethylene glycol dimethacrylate (EGDMA) was used. A total of 560 µL of porogen (either $CHCl_3$, methanol—MeOH,

or acetonitrile—ACN) was added, with the exception of anhydrous toluene, where 580 µL was needed due to solubility issues. For polymers prepared using two functional monomers, we changed the ratio to 1/4/8/12 for the template (30.8 mg SER, 0.1 mmol), functional monomer (34 µL MAA, 0.4 mmol), co-monomer (860 µL of methyl methacrylate (mMA) or 970 µL of 2-hydroxyethyl methacrylate (HEMA), 0.8 mmol), and 227 µL of the EGDMA cross-linker (1.2 mmol). We used 1 wt % of the initiator 2,2′-azobis(2,4-dimethyl valeronitrile) (V-65) for synthesis of polymers on the basis of total monomers.

The synthetic procedure was identical for all MIPs. The monomers and the template were first mixed and dissolved in the porogen solvent. Then cross-linker EGDMA was added and the solution was mixed again. Finally, the initiator V-65 was added. The solution was mixed, purged with N_2 for 10 min, and polymerized at 50 °C for 24 h in an oven. After 24 h, the polymerization was carried out for another 2 hours at 70 °C. The corresponding non-imprinted polymers (NIPs) were prepared following the identical procedures in the absence of the template.

Best-performing MIPs and their corresponding NIPs were later prepared in a 10 times larger quantity, maintaining the same polymer compositions and ingredients. The polymers were then crushed and sieved into 25–50 µm particle size. Both MIPs and NIPs underwent Soxhlet extraction in 10% of acetic acid in methanol for 96 h until no SER was detected by a high-performance liquid chromatograph coupled with a diode array detector (HPLC-DAD). The polymers were further washed with water and MeOH to remove the acetic acid, before drying them in the oven at 50 °C for 24 h. The dried polymers were used for further physical and analytical characterization.

2.2. Selection of the Material: Batch Rebinding

Batch rebinding tests were performed in both water and acetonitrile (ACN). A total of 5 mg of each MIP and the corresponding NIP was weighed and placed in 1.5 mL Eppendorf tubes containing 500 µL of the SER solution with increasing concentrations: 0.1, 0.4, 1.0, 2.0, 3.0, and 4.0 mM. We used SER × HCl for rebinding in water, and SER in the free base form for the rebinding in ACN. All the experiments were performed after the equilibrium had been reached, i.e., after 20 h (see Section 2.5). The suspension was centrifuged at 10,000 rpm for 15 min. The supernatant was diluted 10 times with the mixture of 50% ACN and 50% 20 mM phosphate buffer at pH 3.70 (mobile phase) and subsequently quantified by HPLC-DAD analysis. The levels of bound compounds to the MIP/NIP for each solvent mixture were estimated from plotted calibration curves. We plotted the data in the form of rebinding isotherms using the bi-Langmuir isotherm as the best fit ($R^2 > 0.90$). The capacity, affinity, and selectivity were calculated for each polymer. Capacity was reported as the mass of bound compound per gram of polymer. Affinity was determined as the distribution ratio (D), the ratio between the amount of SER bound to the polymer (B), and the remaining SER in the supernatant (F). The selectivity was calculated as the imprinting factor (IF), comparing the D of MIP to the D of its corresponding NIP. All the parameters were calculated at equilibrium at the highest added concentration of 4.0 mM. On the basis of the results in both ACN and water, we chose three best performing MIPs for further testing.

2.3. Reusability Experiments

Reusability of the chosen MIPs and NIPs was tested by repeating 4 times the batch rebinding of 0.1 mM SER in ultrapure water (UW) on the same material, while following any changes in the performance. Between the cycles, the polymers were washed with 1 mL 1% trifluoroacetic acid (TFA) in MeOH (30 min) and 1 mL of MeOH (15 min) in order to remove SER from polymers. Solvent-free polymers were obtained by drying in the oven for 1 h at 60 °C. The experiment was performed in 5 parallels.

2.4. Cross-Reactivity Experiments

The cross-reactivity of the 3 materials selected as described in Section 2.2 was evaluated by binding experiments for antidepressants and their structurally related compounds: NS,

SEK, FLU, ESC, PXT, BUP, and BUC. The cross-reactivity was assessed through selectivity factor (α), the capacity, and the difference in binding between MIP and NIP for each compound. A was calculated as the ratio between the D of SER and D of the tested compound.

The cross-reactivity experiments were performed separately for each compound in UW, applying the same conditions as for SER rebinding tests (see Section 2.2.). The experiments were performed at the concentration of 1 mM, which was selected on the basis of the maximal solubility of NS in UW. SEK binding was evaluated in ACN due to solubility limitation. The concentrations in the supernatant were again determined with the HPLC-DAD.

2.5. Time to Reach Equilibrium

The time to reach the equilibrium state was estimated in batch experiments in UW. A total of 5 mg of each chosen polymer and AC were shaken for 15 min, 30 min, 1 h, 4 h, 8 h and 20 h. The 0.5 mL solutions contained a mixture of SER and the compounds included in Section 2.4 (test mixture), each added at the final concentration of 0.1 mM. The removal percentage was determined by HPLC-DAD.

2.6. Binding in WW Matrix: Influence of pH, Salts, and Chemical Oxygen Demand

The behavior of the chosen polymers and AC was observed in WW matrix spiked with the test mixture, again at the final concentration of 0.1 mM. The binding experiments were performed in 3 different matrices: UW, artificial wastewater (WW1) [43], and actual wastewater (WW2) obtained from a Slovenian wastewater treatment plant (WWTP). The WW was filtered (see SM, Section 1.1) before spiking in order to remove particulates and microorganisms that could have influenced the removal. The pH of the WWs was measured using the pH electrode by Wissenschaftlich-Technische Werkstätten GmbH (Weilheim, Germany) and the chemical oxygen demand (COD) was determined on a spectrophotometer using Hach reagents for water analysis, LCK 314 and 514.

We researched the influence of 2 parameters most often reported to influence the binding: pH and the presence of salt ions [44–46]. Since the reported pH of WW is between 6 and 8, the performance of the polymers was tested by batch tests in 50 mM phosphate buffer solutions with pH adjusted to 6.0, 7.0, or 8.0 with either a 2 mM HCl or 1 mM NaOH solution. The influence of salt ions was observed by comparing the binding in UW and in NaCl solutions at the concentrations of 0.1 M and 1.0 M.

2.7. Upscale Experiment

In order to observe the performance of the materials on a larger scale and at lower concentration of substrate, we packed the material into SPE cartridges by separately weighing 50 mg of MIP, NIP, or AC. MIPs and NIPs were sedimented beforehand in a mixture of MeOH and water (v/v = 80/20) four-times for 1.5 h to avoid the loss of material through the frit. For the same reason, AC mesh size 100–400 was used.

The materials were first washed with 5 mL of MeOH and 5 mL of UW water. Then, the cartridges were stacked on top of Oasis HLB cartridges in order to bind the remainder of the unbound compounds. The method used for Oasis HLB conditioning, equilibration, loading, and elution was adapted from our article on photodegradation of SER [9].

A total of 50 mL of WW2 spiked with the mixture of compounds at concentrations of 0.4 µM was loaded at the flow rate of 2 mL min^{-1} on to each material. The solution then flowed directly onto the Oasis HLB cartridge. After loading, the Oasis HLB cartridges were dried for 30 min and then eluted with 3 × 0.6 mL of triethylamine in MeOH. The elution solvent was evaporated, and the extracts were redissolved in 0.5 mL the HPLC mobile phase and filtered through 0.45 µm syringe filters before the HPLC measurements.

2.8. Leaching Evaluation

To examine the applicability of developed MIPs as SPE extraction materials, we checked the potential leaching of the template from the MIP. As reported under the upscale experiment (Section 2.7), 50 mg of each MIP was packed in the SPE column, conditioned, loaded,

and eluted with 5 mL 1% TFA in MeOH. The extract was dried under nitrogen at 40 °C and the amount of leaching was quantified with a Nexera X2 ultra high performance liquid chromatograph (UHPLC, Schimadzu, Kyoto, Japan) coupled to the hybrid quadrupole-linear ion trap mass spectrometry analyzer QTRAP 4500 (Sciex, Framingham, MA, USA) following the method developed by Gornik et al., (2020a) [9].

2.9. Chemical and Morphological Characterization

Fourier transform infrared (FTIR) spectroscopy was performed on IRAffinity-1S (Schimadzu, Kyoto, Japan).

Elemental analysis was performed on a 2400, Series II, CHNS/O Analyzer (Perkin-Elmer, Waltham, MA, USA).

BET surface area analysis was performed with Porozimeter TriStar II (Micromeritics, Norcross, GA, USA).

The morphological characteristics were observed using a scanning electron microscope (SEM). The images were recorded with JSM-7600F (JEOL Ltd., Tokyo, Japan).

2.10. HPLC Measurements

For the determination of SER, NS, SEK, FLU, ESC, PXT, BUP, and BUC in the solutions, we utilized an HPLC-DAD (1260 Infinity Agilent Technologies, Santa Clara, CA, USA). For separation, we applied the column Zorbax Eclipse C-18 column (150 mm × 4.6 mm, 5 μm) (Agilent Technologies, Santa Clara, CA, USA). The injection volume was 10 μL or 20 μL, depending on the tested concentration range. The mobile phases were (A) ACN and (B) 20 mM phosphate buffer at pH 3.70. The gradient started with 70% B for 2 min, decreased to 61% in 13 min, then increased back to 70% B in 0.1 min and was kept as so for 1.5 min. The flow rate was 1 mL·min^{-1}. The retention times of the compounds were 3.27 min for BUP, 4.04 min for BUC, 6.20 min for ESC, 8.52 min for PXT, 11.95 min for NS, 12.65 min for FLU, and 13.04 min for SER. SEK was determined with a separate method at flow 2 mL·min^{-1}, isocratic elution at 70% A and 30% B. Other parameters coincided with the previous method. SEK eluted at 3.80 min.

3. Results and Discussion

All experiments with the exception of the reusability experiments (n = 5) were performed in duplicate. The inter-day repeatability reported as the relative standard deviation (RSD) for experiments performed in UW was <5% and in WW < 6%.

3.1. MIP Synthesis, Selection, and Reusability

We optimized the polymer composition to tune recognition properties of the material. The initiator (V-65) and cross-linker (EGDMA) were kept constant for all polymerization experiments, while different porogens and co-monomers were added in order to obtain water compatibility, increase capacity, and improve selectivity. The behavior of MIPs compared to their corresponding NIPs was evaluated in batch rebinding experiments performed in water and ACN at different concentrations to generate binding isotherms and calculate the capacity, affinity, and IF. The data we obtained during ACN rebinding experiments enabled us to quantify the binding on the basis only of specific interactions, such as hydrogen bonding, with the minimal non-specific hydrophobic effect [47], while our prime goal was recognition of the investigated compounds in water.

EGDMA in combination with MAA in different porogen solvents is one of the most commonly reported compositions of MIPs to date [30,48,49], including those in MIPs imprinted with SER [50,51]. Unlike in the literature [50,51], we observed no imprinting in MIPs where SER was used in its salt form (MIPs 1–3 in Table 1). Adding the extracted free base form of SER, on the other hand, resulted in successful imprinting. As shown in Figures 2 and 3, we observed higher capacities and affinities in water compared to those in ACN for most tested MIPs, except for MIP11 and MIP12. However, compared to ACN, the Ifs in water were lower in all the cases, indicating loss of selectivity in water. This can be justified

by the hydrophobic effect established in polar solvents such as water, and disrupting the formation of hydrogen bonds. In order to improve the recognition abilities in water, we tested the influence of adding co-monomers mMA or HEMA (see examples MIP8–MIP13 in Table 1). Here, the ratios between monomers and cross-linker we applied were based on the results from Dirion et al., (2003). HEMA was chosen on the basis of the reports on improved Ifs in water [47,48], while the mMA was selected as its more non-polar alternative. MIPs with the mMA added into the polymerization mixture (MIP8, MIP9, and MIP10) had a similar IF in ACN, as compared to MIPs 5–7, which were prepared by MAA only (Table 1). However, the Ifs in water were slightly higher for all three materials (Figure 3). The capacities and affinities of MIP8, MIP9, and MIP10 in ACN were higher, yet lower or comparable in water. Compared to MIPs 5–7, adding HEMA as a co-monomer (MIP11, MIP12, and MIP13) did not improve the capacity or affinity of the MIPs in ACN. Additionally, both parameters were noticeably lower in UW. The considerable improvement was, however, observed in IF; the highest was that of MIP13. This high IF is in agreement with the results of Dirion et al., (2013).

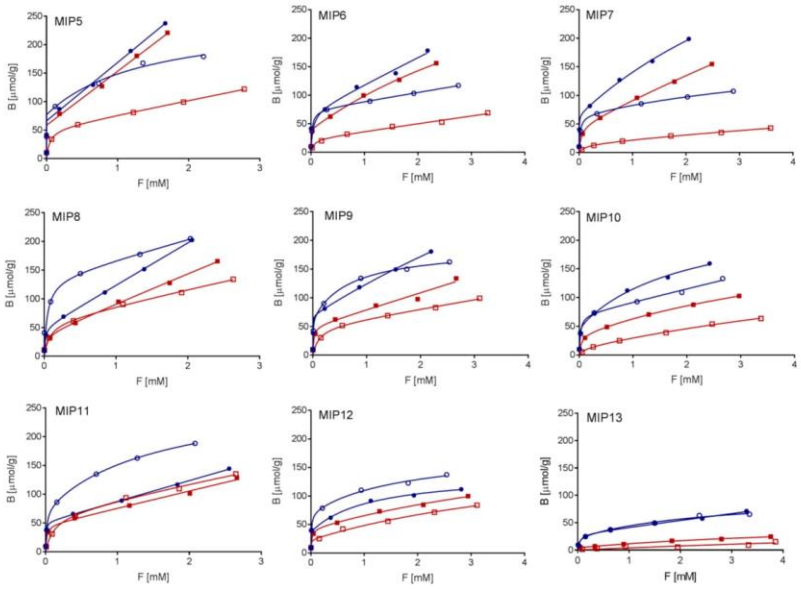

Figure 2. Rebinding isotherms for MIP (blue symbols) and non-imprinted polymer (NIP; red symbols) combinations 5–13 in ultrapure water (UW; full symbols) and acetonitrile (ACN; empty symbols).

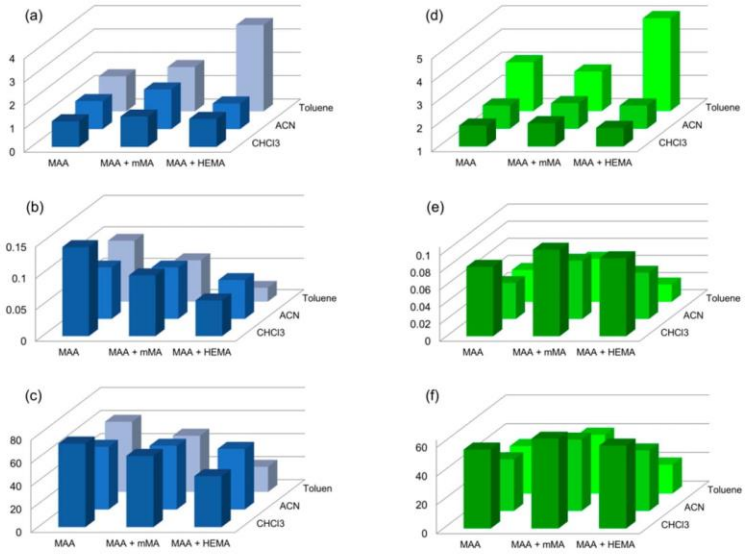

Figure 3. (**a**) The selectivity (imprinting factor, IF), (**b**) the affinity ($L \cdot g^{-1}$), and (**c**) the capacity ($mg \cdot g^{-1}$) of the MIPs in UW in blue. (**d**) The selectivity (IF), (**e**) the affinity ($L \cdot g^{-1}$), and (**f**) the capacity ($mg \cdot g^{-1}$) of the MIPs in ACN in green.

As seen in Table 1 and Figure 3, the porogen severely influenced the selectivity, capacity, and affinity of the MIPs. This happens as it affects the stability of the "pre-polymerization complex" (i.e., interactions between functional monomers and the template in the chosen porogen), which plays a crucial role in the imprinting effect. If the porogen disrupts hydrogen bonds between the template and monomers, no specific binding is observed, as can be seen in the case of MeOH (MIP4). On the contrary, using a more non-polar aprotic porogen, the pre-polymerization complex is stabilized, resulting in higher IF, which we showed in MIPs 7, 10, and 13 synthetized in toluene, as compared to those synthetized in ACN (MIPs 6, 9, 12) or $CHCl_3$ (MIPs 5, 8, 11) (Table 1, Figure 3a,d) [47].

Determining rebinding characteristics allowed us to select three most promising materials for further testing. In terms of capacity and affinity in water, the material MIP5 was chosen. MIP13 was chosen for its highest IF. Lastly, MIP9 was chosen because it combines satisfactory selectivity, capacity, and affinity in both water and ACN. The chosen polymers were reusable, with the maximum observed decrease in the capacity for SER in four consecutive rebinding experiments being only 2%.

3.2. *Cross-Reactivity*

We determined the cross-reactivity of three selected MIPs for the following antidepressants and structurally related compounds (Figure 1): BUC, BUP, ESC, PXT, NS, SEK, and FLU. While SEK, the metabolite of SER, was also initially included, it however showed very poor binding in ACN and no observed selectivity for any of the three MIPs. Its binding will therefore be based on non-specific interactions only. As for its poor solubility in water, it was thus excluded from further testing.

The results of cross-reactivity tests are selectivity factors (α) reported in Table 2. In general, α for each compound were comparable between the three selected MIPs, with the exception of BUP in MIP13. Here, the factor α 3.29, as compared to 9.60 and 9.76 for MIP5 and MIP9, respectively, indicated more cross-reactivity of MIP13 towards BUP. As reported in Table 2, for NS the selectivity factor was below 1, indicating better

binding as compared to SER, which is reasoned by the absence of the methyl group in the chemical structure (Figure 1). Among the SSRI compounds, FLU and PXT had the factors slightly above 1, meaning comparable binding, while the factor for ESC varied between 2.7 and 2.9. The fact that ESC was the only SSRI with a tertiary amine in the structure, together with the favorable α for NS, suggests the impact of steric hindrance of the hydrogen bond-forming amino group on cross-reactivity. The size of the binding site seemed to be of lesser importance, considering that PXT and FLU are larger molecules as compared to SER and NS. BUC and BUP showed higher α in all three MIPs, which is justified by them being less structurally related to the SSRI group. Additionally, their amino groups are also sterically more hindered (tert-butyl group and tertiary amine).

Table 2. The capacity and selectivity factor of MIP5, MIP9, and MIP13 and the difference in binding of each compound between MIP and the corresponding NIP at 1 mM concentration of each tested analyte.

	MIP5			MIP9			MIP13		
Compound	**Capacity ($mg \cdot g^{-1}$)**	**Selectivity Factor (α)**	**% (MIP-NIP)**	**Capacity ($mg \cdot g^{-1}$)**	**Selectivity Factor (α)**	**% (MIP-NIP)**	**Capacity ($mg \cdot g^{-1}$)**	**Selectivity Factor (α)**	**% (MIP-NIP)**
SER	26.6 ± 0.6	1.0	8.4	24.4 ± 0.4	1.0	17.4	11.0 ± 0.3	1.0	25.6
NS	26.3 ± 0.3	0.8	7.2	23.1 ± 0.4	1.0	17.1	13.0 ± 0.1	0.7	33.5
FLU	25.3 ± 0.6	1.3	4.9	22.4 ± 0.4	1.2	16.2	10.3 ± 0.2	1.1	25.3
ESC	20.3 ± 0.5	2.9	4.7	18.8 ± 0.6	2.7	14.8	5.5 ± 0.2	2.8	10.8
PXT	27.3 ± 0.1	1.0	3.4	26.3 ± 0.4	1.0	16.8	11.3 ± 0.1	1.1	25.0
BUP	7.9 ± 0.1	9.6	2.2	6.5 ± 0.3	9.8	8.0	3.5 ± 0.3	3.3	12.3
BUC	10.3 ± 0.3	8.7	9.4	9.7 ± 0.3	7.0	9.4	2.2 ± 0.4	7.0	6.1

In general, the capacities of the three MIPs for SSRIs followed the same pattern as in SER binding. The highest capacity was observed in MIP5, closely followed by MIP9, and with more than half-lower capacities observed in MIP13 (Figure S1). Furthermore, we compared the binding to the corresponding NIPs. The difference between MIP and NIP was the largest in the case of MIP/NIP13 and the lowest in MIP/NIP5 (Table 2).

3.3. Time to Reach the Equilibrium

The time to reach equilibrium was tested for the chosen polymers and AC. A 0.1 mM test mixture was added. Figure S2 illustrates that for AC, the equilibrium was reached within 1 h; in cases of MIP5 and MIP9, the equilibrium was reached in 4 h; and for MIP13, in 20 h. For the NIPs, similar times to reach the equilibrium were shown as for their corresponding MIPs. As also depicted from Figure 4, AC non-selectively bound all the available compounds until their concentrations in the solvent reached below the limit of quantification (LOQ ≈ 0.001 mM).

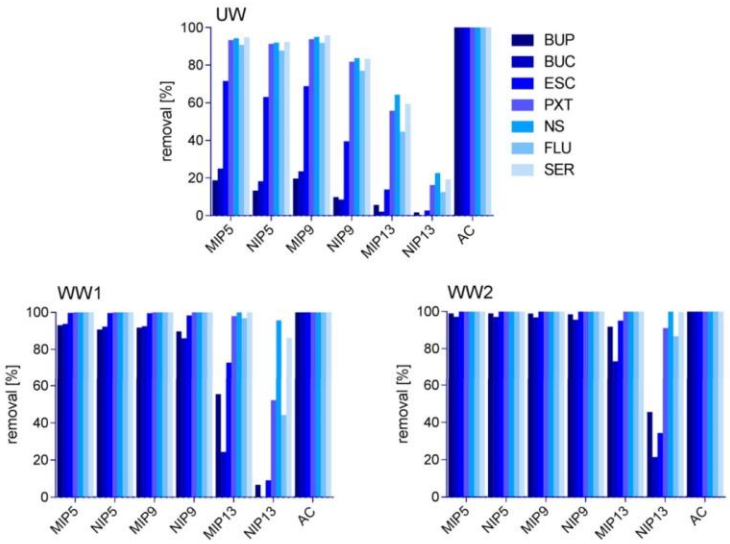

Figure 4. The impact of matrices (UW, artificial wastewater (WW1), and actual wastewater (WW2)) on the performance of MIPs, NIPs, and AC in the batch rebinding test.

3.4. Effect of WW Matrix

With the underlying objective to remove pharmaceuticals from WWs, we tested the capacity of MIPs to bind them. This way, we evaluated the ability of MIPs to be applied as sorbents in WW treatment systems. Aiming to get closer to the conditions during WW treatment, we employed the pH adjusted to 6–8 and simulated actual WW matrix composition. By comparing the results between the binding of BUP, BUC, ESC, PXT, NS, FLU and SER in UW, WW1, and WW2, we observed large differences in the removals of the test compounds (Figure 4), whereas AC removed all the tested compounds in any matrix to below LOQ concentrations (0.001 mM). In contrast with our expectations, as shown in Figure 4, the removal efficiencies of MIPs were lowest in UW and highest in the most complex matrix, WW2. In line with the trends shown in the capacity experiments, MIP5 and MIP9 showed best performance, closely followed by NIP5, NIP9, MIP13, and finally NIP13. By investigating the reason for such behavior, we determined the pH and COD of each inspected matrix. The pH values of UW, WW1, and WW2 were approximately 7, 7.2, and 8.2, respectively, whereas we measured COD at <15 $mg \cdot L^{-1}$ for WW1 (LOQ of the test) and 379 $mg \cdot L^{-1}$ for WW2. On the contrary, the literature reports either no change (up to 690 $mg \cdot L^{-1}$ COD) or a slight decrease in adsorption of their chosen templates to their MIPs at high COD values (over 800 $mg \cdot L^{-1}$) [52–55]. The MIPs in these cases used similar reagents to those in our synthesis, i.e., MAA and EGDMA, albeit in different ratios, and employed DCM or ACN as porogens and 2,2′-azobisisobutyronitrile (AIBN) as the initiator [52–55]. Hence, we did not expect the higher COD values to be the cause behind the increased removal.

In order to deeper investigate the reasons behind the positive impact of matrix complexity on the removal of pharmaceuticals, we performed the rebinding experiments at different pH values and salt concentrations. Here, the imprinted and non-imprinted polymers showed similar trends, with the most notable differences for MIP and NIP13, as portrayed in Figure 5. The pH in the range of 6 to 8 had almost no influence on the bind-

ing with differences below 1%. The only exception was NIP13, with differences between pH 6 and pH 8 ranging up to 7.8%. On the other hand, the increasing salt concentration improved the removal of pharmaceuticals. This finding was further supported by the improved binding found during the pH tests, which were performed in phosphate buffer, as compared to the binding in UW. Our results are consistent with the findings of Kempe and Kempe (2010), where elevated concentrations of salts had a significant influence on the removal of penicillin G from solution and followed the Hofmeister series. As seen in Kempe and Kempe (2010), the higher removal was of non-specific nature, observed in both MIP and NIP [46]. The kosmotropic ions seem to promote the formation of stable interactions between the polymers and tested compounds. Since phosphate ions are more kosmotropic than chloride ions, this would also explain the larger effect in the buffer solutions, despite their lower concentrations [56].

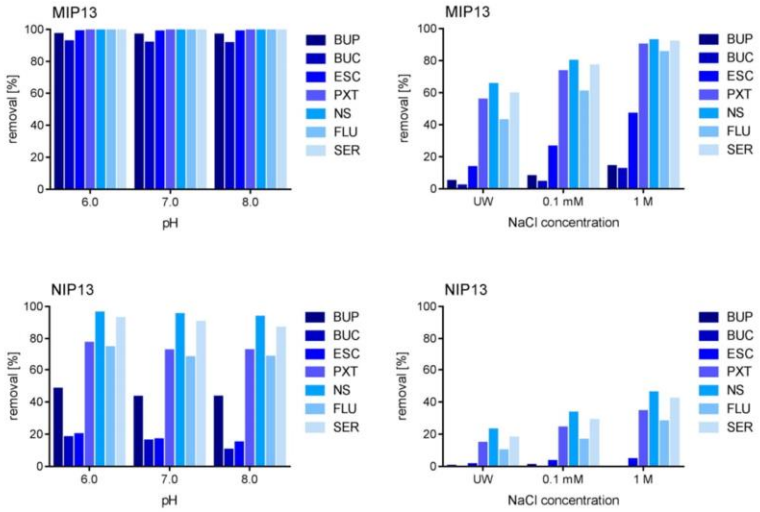

Figure 5. The effect of pH and presence of salt ions in MIP13 and NIP13.

3.5. Upscale Experiment

The performance of the materials was evaluated as the difference between the initial concentration and the remainder extracted by Oasis HLB SPE. This way, we avoided underestimating the performance of AC, since completely eluting compounds off the AC is a known difficulty [23]. The results on the performance of selected materials in the upscale experiment are shown in Figure 6. The main difference from the batch (mini-MIP) experiments is the less efficient binding to AC (Figure 6). The two main reasons behind this may involve the shorter contact time between the material and WW, or lower capacity of the material due to the non-specific binding of other matrix components. Since in the batch experiment AC showed shortest time to reach equilibrium, the latter is more probable. Furthermore, several reports showed AC performance deteriorating with an increase of matrix complexity (e.g., COD, total dissolved solids) [23,55].

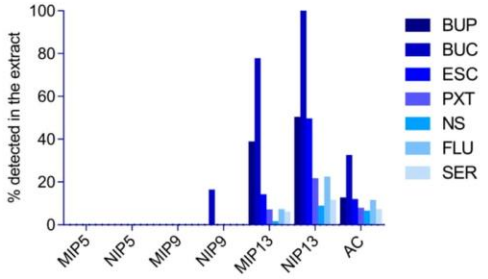

Figure 6. The remainder of compounds detected in the Oasis HLB extracts in the upscale experiment.

In the Oasis HLB extracts from MIP5, NIP5, and MIP9, none of the investigated pharmaceuticals were detected. On the contrary, as expected, their highest remainder was determined in the Oasis HLB extracts from NIP13, again implying its lowest binding capacity.

While non-specific rebinding is not desired in MIPs that are used, for example, in sample preparation or chromatography, we show here that this phenomenon is favorable in WW treatment. As Le Noir et al., (2007) pointed out, it only becomes a problem if it causes lower capacity and affinity of the selective binding [39]. MIP5 and MIP9 both showed higher capacities compared to MIP13, and even NIP5 and NIP9 performed better under tested conditions. This means that a larger amount of MIP13 would have to be used to achieve the competitive removal efficiencies. However, specific interactions of MIPs will likely play a more important role at higher volumes and more complex matrices. At the same time, we show that the NIPs, which are based on non-specific binding only, are less negatively affected by matrix, as compared to AC, and along with their easy recyclability they could therefore pose a less expensive alternative for the removal of pharmaceuticals.

3.6. Leaching

As an alternative to sorption in WW treatment, we also considered the developed MIPs for SPE extraction of environmental samples. As for our hypothesis, MIP could be employed as an SPE sorbent in order to selectively extract targeted compounds, thus reducing the suppressing effect of matrix interferences in further liquid chromatography coupled to mass spectrometry (LC–MS) analysis. Such sorbents may potentially be employed in a highly sensitive analytical method for an ultra-trace level determination of contaminants in WW [57]. MIPs have previously been used for SPE several times [58–61]. However, given the fact that the template in polymerization (SER) is also the analyte in the LC–MS method, the MIP sorbent would have to pass the "leaching test", which means that it would have to show a negligible leaching and thus avoid interfering with the assessment of trace-level analytes in the subsequent LC–MS analysis. Leaching of SER from the material was tested on UHPLC-QTRAP, applying the instrumental method developed by Gornik et al., (2020a) [9]. By using 5 mL of 1% TFA in MeOH, we eluted up to 3.5 µg of SER from the MIPs. Alternative methods for template removal, such as microwave or ultrasound-assisted extraction, heating under pressure, or even the use of another acid during Soxhlet extraction, could have lessened the leaching from the MIPs. On the other hand, the more extreme conditions could also have damaged or distorted the imprinted cavities and thus decreased the selectivity, affinity, and capacity of the MIPs [62,63]. Furthermore, the synthesis of MIPs and the subsequent washing procedures triggered the formation of SER transformation products (NS, SEK, hydroxyl-SER) [9], which in turn leached off the materials, thus interfering the environmental analysis. Unfortunately, this makes the material inappropriate for the determination of SER residues including its metabolites and transformation products at trace levels. Finding an appropriate dummy template that would substitute SER and produce a MIP cross-reactive towards SSRI could be a viable

solution to such a problem [35]. Nonetheless, the synthetized material can still be applied to SPE of the remaining tested pharmaceuticals (Figure 1).

3.7. Characterization

The FTIR spectra for the chosen MIP/NIP pairs 5, 9, and 13 can be found in Figure 7. The broad band visible at approximately 3500 cm^{-1} corresponds with the stretching vibration of the hydroxyl group from MAAs COOH group. The stretch bands around 2950 cm^{-1} in all the spectra are part of the C–H vibration present in MAA, mMA, HEMA, and EGDMA. The band around 1720 cm^{-1} represents the vibration from the carboxylic C=O group that can be associated with the C=O groups from MAA, mMA, and EGDMA. The 1250 and 1140 cm^{-1} stretch bands contributed to the stretching of C–O also present in all three compounds. The stretch bands corresponded with the polymerized material. Since the composition of the synthetized materials did not vary strongly, the resulting FTIR spectra were accordingly similar.

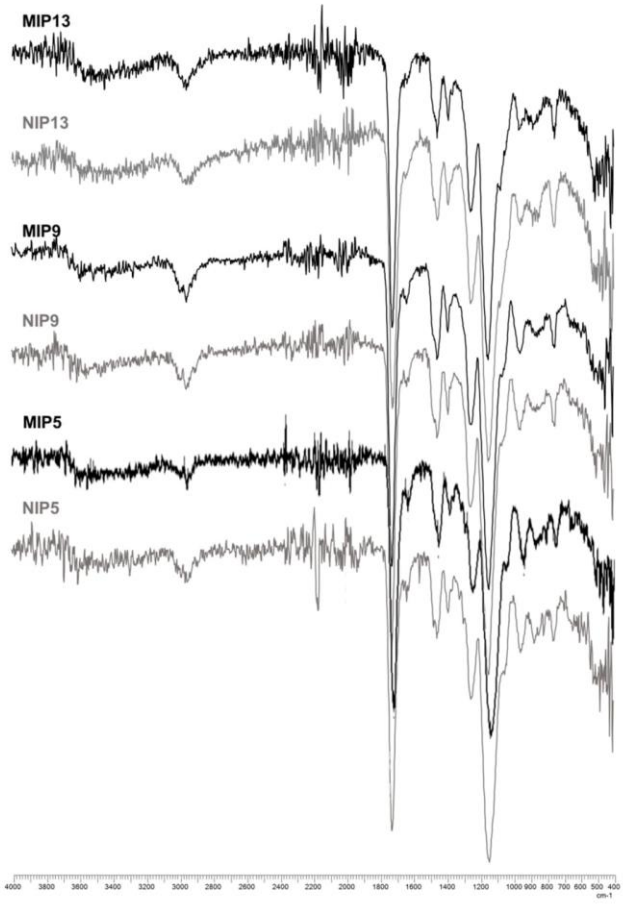

Figure 7. The FTIR spectra of MIPs and NIPs 5, 9, and 13.

The results of the elemental analysis of the MIP and NIP pairs 5, 9, and 13 are reported in Table 3. The results are in accordance with the expected values of the synthetized material. With this measurement, we confirmed that the added reagents reacted in the expected ratio.

Table 3. Results of the elemental analysis for MIPs and NIPs 5, 9, and 13.

MIP 5	**% C**	**% H**	**NIP 5**	**% C**	**% H**
Theoretical	60.21	7.11	Theoretical	60.21	7.11
Actual	59.56	7.81	Actual	59.68	8
Deviation	0.65	−0.7	Deviation	0.53	−0.89
MIP 9	**% C**	**% H**	**NIP 9**	**% C**	**% H**
Theoretical	59.99	7.28	Theoretical	59.99	7.28
Actual	59.55	8.18	Actual	60.2	8.25
Deviation	0.44	−0.9	Deviation	−0.21	−0.97
MIP 13	**% C**	**% H**	**NIP 13**	**% C**	**% H**
Theoretical	59.27	7.23	Theoretical	59.27	7.23
Actual	57.00	7.60	Actual	58.03	8.17
Deviation	2.27	−0.37	Deviation	1.24	−0.94

The BET surface area, pore size, and pore volume of the MIPs and NIPs are reported in Table 4. As expected, the larger the surface area and pore volume of the tested polymers, the higher the reported capacity and affinity. All three parameters were comparable between MIP and NIP pairs 5 and 9, with BET surface areas for MIP/NIP 5 in the 200 $m^2 \cdot g^{-1}$ range and MIP/NIP 9 at the 100 $m^2 \cdot g^{-1}$ range. However, NIP13 exhibited a more than five times lower BET surface area and pore volume compared to its corresponding MIP (Table 4). A similar difference was observed in MIP and NIP pairs using HEMA as the copolymer in toluene in the research by Dirion et al., (2003). They reported that stronger swelling was observed for the NIPs and similar elution times measured for void markers (acetone or MeOH) in their chromatographic evaluations of the polymers. This indicated a smaller difference between the MIP and NIP in their swollen state.

Table 4. Brunauer–Emmett–Teller (BET) surface area of MIPs and NIPs 5, 9, and 13.

Material	**BET Area ($m^2 \cdot g^{-1}$)**	**Pore Size (nm)**	**Pore Volume ($cm^3 \cdot g^{-1}$)**
MIP5	193.8	7.7	0.374061
NIP5	262.1	7.2	0.470623
MIP9	136.0	10.3	0.349167
NIP9	125.7	9.6	0.300946
MIP13	27.4	7.6	0.051835
NIP13	5.5	6.6	0.009074

The SEM images of the surface of our polymers in Figure 8 support the surface area and pore volume measurements. While the morphology of MIP5/NIP5 and MIP9/NIP9 were comparable, the surfaces of MIP13 and NIP13 were dissimilar. These differences in the morphology between MIP and NIP 13 indicate that care should be taken when NIPs are used for the evaluation of MIP selectivity. Comparing a material imprinted with a completely different compound or the determination of α between the template and other compounds can offer more information [35,48].

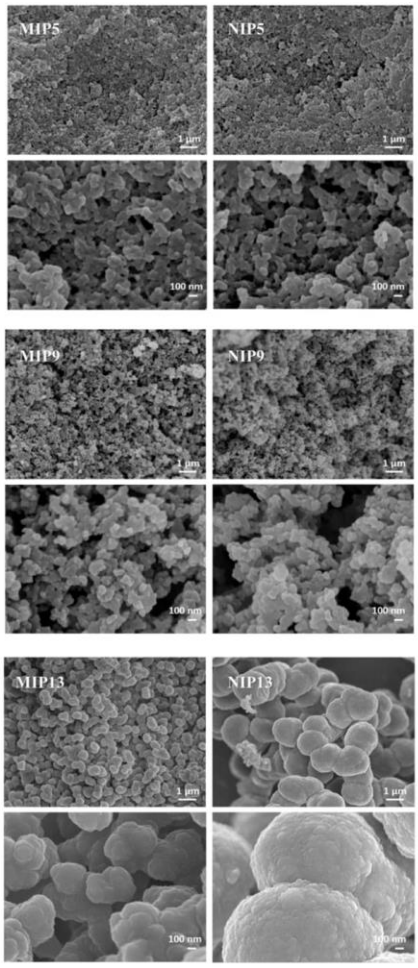

Figure 8. SEM images of MIPs and NIPs 5, 9, and 13.

Compared to AC with a surface area of 1400 $m^2 \cdot g^{-1}$ [64], the surface areas of MIPs and NIPs were 5 to 253 times lower. Nevertheless, some of them showed superior binding characteristics in WW.

4. Conclusions

This study investigated the ability of MIPs imprinted with the free base form of SER to remove SSRIs and their metabolites. The functional monomers and porogens revealed a strong impact on the capacity, affinity, and selectivity of the synthetized MIPs. The three selected MIPs showed cross-reactivity towards the SSRIs and the metabolite norsertraline, whereas they bound a lesser amount of the competitors BUP and BUC. Further, the loss of selectivity towards the metabolite SEK was probably due to the loss of the amino group, which was thus

found crucial for selective binding to the MIP. The performance of both the imprinted and non-imprinted materials was strongly influenced by the presence of salt ions, which improved their performance in WW. The performance of MIPs was stable throughout WW-relevant pH range 6–8. Compared to AC, the synthetized polymers had at least five times lower surface area and required a longer equilibration time. This slower mass transfer was particularly evident when selective binding was the main driving force behind the removal, as observed in MIP13. However, the capacity in WW for two out of the three tested MIPs surpassed that of AC, and thus both the non-specific and specific interactions showed an important role for the removal from WW. The surface area calculated from the BET isotherm for the MIPs correlated with a higher removal and more non-specific interactions. The advantage of the MIPs is also their reusability that, together with the lower number of regeneration cycles needed due to slower fouling, will cut the costs of the treatment. Unfortunately, the MIPs were found inappropriate for SPE of samples containing trace levels of SER due to continuous leaching of the template and its degradation products. Future work should include a large-scale experiment confirming the advantages of the synthetized material for the removal of SSRIs from WW.

Supplementary Materials: The following are available online at https://www.mdpi.com/2073-4360/13/1/120/s1: List of standards, chemicals, and materials; Standard solution preparation; Pre-preparation of the ingredients. Figure S1: Cross-reactivity of MIP5, MIP9, and MIP13 in UW. Figure S2: Time to reach the equilibrium for MIP5, MIP9, MIP13, and activated carbon (AC).

Author Contributions: Conceptualization, T.G., S.S., B.S. and T.K.; methodology, T.G., S.S., B.S. and T.K.; analysis and investigation, T.G., L.L., M.K. and S.S.; writing—original draft preparation, T.G.; writing—review and editing, S.S., B.S., T.K. and E.H.; supervision, B.S. and T.K.; project administration, B.S. and T.K.; funding acquisition, B.S., E.H. and T.K. All authors have read and agreed to the published version of the manuscript.

Funding: The authors acknowledge the financial support from the Slovenian Research Agency (research core funding no. P1-0143) and project J1-6744 (Development of Molecularly Imprinted Polymers and their application in environmental and bio-analysis). This work was supported by a STSM Grant from the NEREUS COST Action ES1403 and the Erasmus plus program.

Acknowledgments: Special thanks go to Amadeja Koler from the University of Maribor, Faculty of Chemistry and Chemical Engineering, PolyOrgLab, Maribor, Slovenia, for the work on chemical characterization of the polymers.

Conflicts of Interest: The authors declare no conflict of interest.

References

1. Radjenović, J.; Petrović, M.; Barceló, D. Fate and distribution of pharmaceuticals in wastewater and sewage sludge of the conventional activated sludge (CAS) and advanced membrane bioreactor (MBR) treatment. *Water Res.* **2009**, *43*, 831–841. [CrossRef] [PubMed]
2. Sarpong, K.A.; Xu, W.; Huang, W.; Yang, W. The Development of Molecularly Imprinted Polymers in the Clean-Up of Water Pollutants: A Review. *Am. J. Anal. Chem.* **2019**, *10*, 202–226. [CrossRef]
3. Gómez-Oliván, L.M. *The Handbook of Environmental Chemistry*; Springer International Publishing: Cham, Switzerland, 2019; Volume 66.
4. Bauer, M.; Monz, B.U.; Montejo, A.L.; Quail, D.; Dantchev, N.; Demyttenaere, K.; Garcia-Cebrian, A.; Grassi, L.; Perahia, D.G.; Reed, C.; et al. Prescribing patterns of antidepressants in Europe: Results from the Factors Influencing Depression Endpoints Research (FINDER) study. *Eur. Psychiatry* **2008**, *23*, 66–73. [CrossRef] [PubMed]
5. Fuentes, A.V.; Pineda, M.D.; Venkata, K.C.N. Comprehension of Top 200 Prescribed Drugs in the US as a Resource for Pharmacy Teaching, Training and Practice. *Pharmacy* **2018**, *6*, 43. [CrossRef]
6. NIJZ Poraba Ambulantno Predpisanih Zdravil v Sloveniji v Letu 2019. Available online: https://www.nijz.si/sites/www.nijz.si/files/publikacije-datoteke/publikacija_220520_koncno_0.pdf (accessed on 22 November 2020).
7. Arnnok, P.; Singh, R.R.; Burakham, R.; Pérez-Fuentetaja, A.; Aga, D.S. Selective Uptake and Bioaccumulation of Antidepressants in Fish from Effluent-Impacted Niagara River. *Environ. Sci. Technol.* **2017**, *51*, 10652–10662. [CrossRef]
8. Bergersen, O.; Hanssen, K.Ø.; Vasskog, T. Anaerobic treatment of sewage sludge containing selective serotonin reuptake inhibitors. *Bioresour. Technol.* **2012**, *117*, 325–332. [CrossRef]

9. Gornik, T.; Vozic, A.; Heath, E.; Trontelj, J.; Roskar, R.; Zigon, D.; Vione, D.; Kosjek, T. Determination and photodegradation of sertraline residues in aqueous environment. *Environ. Pollut.* **2020**, *256*, 113431. [CrossRef]
10. Gornik, T.; Kovacic, A.; Heath, E.; Hollender, J.; Kosjek, T. Biotransformation study of antidepressant sertraline and its removal during biological wastewater treatment. *Water Res.* **2020**, *181*, 115864. [CrossRef]
11. Mole, R.A.; Brooks, B. Global scanning of selective serotonin reuptake inhibitors: Occurrence, wastewater treatment and hazards in aquatic systems. *Environ. Pollut.* **2019**, *250*, 1019–1031. [CrossRef]
12. Schultz, M.M.; Furlong, E.T.; Kolpin, D.W.; Werner, S.L.; Schoenfuss, H.L.; Barber, L.B.; Blazer, V.S.; Norris, D.O.; Vajda, A.M. Antidepressant Pharmaceuticals in Two U.S. Effluent-Impacted Streams: Occurrence and Fate in Water and Sediment, and Selective Uptake in Fish Neural Tissue. *Environ. Sci. Technol.* **2010**, *44*, 1918–1925. [CrossRef]
13. OECD. Pharmaceutical Residues in Freshwater: Hazards and Policy Responses-Policy Highlights. In *OECD Studies on Water*; OECD Publishing: Paris, France, 2019; Volume 2019.
14. Park, J.-W.; Heah, T.P.; Gouffon, J.S.; Henry, T.; Sayler, G.S. Global gene expression in larval zebrafish (Danio rerio) exposed to selective serotonin reuptake inhibitors (fluoxetine and sertraline) reveals unique expression profiles and potential biomarkers of exposure. *Environ. Pollut.* **2012**, *167*, 163–170. [CrossRef] [PubMed]
15. Vaclavik, J.; Sehonova, P.; Hodkovicova, N.; Vecerkova, L.; Blahova, J.; Franc, A.; Marsalek, P.; Mares, J.; Tichy, F.; Svobodova, Z.; et al. The effect of foodborne sertraline on rainbow trout (Oncorhynchus mykiss). *Sci. Total. Environ.* **2020**, *708*, 135082. [CrossRef]
16. Xie, Z.; Lu, G.; Li, S.; Nie, Y.; Ma, B.; Liu, J. Behavioral and biochemical responses in freshwater fish Carassius auratus exposed to sertraline. *Chemosphere* **2015**, *135*, 146–155. [CrossRef] [PubMed]
17. Silva, L.J.; Pereira, A.M.; Meisel, L.M.; Lino, C.; Pena, A. Reviewing the serotonin reuptake inhibitors (SSRIs) footprint in the aquatic biota: Uptake, bioaccumulation and ecotoxicology. *Environ. Pollut.* **2015**, *197*, 127–143. [CrossRef] [PubMed]
18. Salgado, R.; Marques, R.; Noronha, J.; Mexia, J.; Carvalho, G.; Oehmen, A.; Reis, M. Assessing the diurnal variability of pharmaceutical and personal care products in a full-scale activated sludge plant. *Environ. Pollut.* **2011**, *159*, 2359–2367. [CrossRef] [PubMed]
19. Cao, J.; Fu, B.; Zhang, T.; Wu, Y.; Zhou, Z.; Zhao, J.; Yang, E.; Qian, T.; Luo, J. Fate of typical endocrine active compounds in full-scale wastewater treatment plants: Distribution, removal efficiency and potential risks. *Bioresour. Technol.* **2020**, *310*, 123436. [CrossRef]
20. Ek, M.; Baresel, C.; Magnér, J.; Bergström, R.; Harding, M. Activated carbon for the removal of pharmaceutical residues from treated wastewater. *Water Sci. Technol.* **2014**, *69*, 2372–2380. [CrossRef]
21. Guillossou, R.; Le Roux, J.; Mailler, R.; Vulliet, E.; Morlay, C.; Nauleau, F.; Gasperi, J.; Rocher, V. Organic micropollutants in a large wastewater treatment plant: What are the benefits of an advanced treatment by activated carbon adsorption in comparison to conventional treatment? *Chemosphere* **2019**, *218*, 1050–1060. [CrossRef]
22. Kårelid, V.; Larsson, G.; Björlenius, B. Pilot-scale removal of pharmaceuticals in municipal wastewater: Comparison of granular and powdered activated carbon treatment at three wastewater treatment plants. *J. Environ. Manag.* **2017**, *193*, 491–502. [CrossRef]
23. Crini, G.; Lichtfouse, E. Advantages and disadvantages of techniques used for wastewater treatment. *Environ. Chem. Lett.* **2019**, *17*, 145–155. [CrossRef]
24. Silva, B.; Martins, M.; Rosca, M.; Rocha, V.; Lago, A.; Neves, I.C.; Tavares, T. Waste-based biosorbents as cost-effective alternatives to commercial adsorbents for the retention of fluoxetine from water. *Sep. Purif. Technol.* **2020**, *235*, 116139. [CrossRef]
25. Jaria, G.; Calisto, V.; Gil, M.V.; Otero, M.; Esteves, V.I. Removal of fluoxetine from water by adsorbent materials produced from paper mill sludge. *J. Colloid Interface Sci.* **2015**, *448*, 32–40. [CrossRef] [PubMed]
26. Ebrahimi, F.; Orooji, Y.; Alizadeh, A. Applying Membrane Distillation for the Recovery of Nitrate from Saline Water Using PVDF Membranes Modified as Superhydrophobic Membranes. *Polymers* **2020**, *12*, 2774. [CrossRef] [PubMed]
27. Orooji, Y.; Jaleh, B.; Homayouni, F.; Fakhri, P.; Kashfi, M.; Torkamany, M.J.; Yousefi, A.A. Laser Ablation-Assisted Synthesis of Poly (Vinylidene Fluoride)/Au Nanocomposites: Crystalline Phase and Micromechanical Finite Element Analysis. *Polymers* **2020**, *12*, 2630. [CrossRef] [PubMed]
28. Mashile, G.P.; Dimpe, K.M.; Nomngongo, P.N. A Biodegradable Magnetic Nanocomposite as a Superabsorbent for the Simultaneous Removal of Selected Fluoroquinolones from Environmental Water Matrices: Isotherm, Kinetics, Thermodynamic Studies and Cost Analysis. *Polymers* **2020**, *12*, 1102. [CrossRef] [PubMed]
29. Awual, R. A novel facial composite adsorbent for enhanced copper(II) detection and removal from wastewater. *Chem. Eng. J.* **2015**, *266*, 368–375. [CrossRef]
30. Cantarella, M.; Carroccio, S.C.; Dattilo, S.; Avolio, R.; Castaldo, R.; Puglisi, C.; Privitera, V. Molecularly imprinted polymer for selective adsorption of diclofenac from contaminated water. *Chem. Eng. J.* **2019**, *367*, 180–188. [CrossRef]
31. Qiu, L.; Jaria, G.; Gil, M.; Feng, J.; Dai, Y.; Esteves, V.I.; Otero, M.A.; Calisto, V. Core−Shell Molecularly Imprinted Polymers on Magnetic Yeast for the Removal of Sulfamethoxazole from Water. *Polymers* **2020**, *12*, 1385. [CrossRef]
32. Sellergren, B. *Molecularly Imprinted Polymers: Man-Made Mimics of Antibodies and Their Application in Analytical Chemistry*; Elsevier: Amsterdam, The Netherlands, 2000.
33. Affinisep Affinimip. Available online: https://www.affinisep.com/spe-kits-applications/spe-kit-for-sample-preparation/affinimip-spe-selectives-mip-spe-cartridges (accessed on 3 August 2020).

34. SupelMIP® SPE, Supelco. Available online: https://www.sigmaaldrich.com/analytical-chromatography/sample-preparation/spe/supelmip.html (accessed on 3 August 2020).
35. Mattiasson, B.; Ye, L. *Molecularly Imprinted Polymers in Biotechnology (Advances in Biochemical Engineering/Biotechnology)*; Springer International Publishing: Cham, Switzerland, 2015; Volume 150.
36. Sellergren, B.; Allender, C.J. Molecularly imprinted polymers: A bridge to advanced drug delivery. *Adv. Drug Deliv. Rev.* **2005**, *57*, 1733–1741. [CrossRef]
37. Altintas, Z.; Chianella, I.; Da Ponte, G.; Paulussen, S.; Gaeta, S.; Tothill, I. Development of functionalized nanostructured polymeric membranes for water purification. *Chem. Eng. J.* **2016**, *300*, 358–366. [CrossRef]
38. An, F.-Q.; Li, H.-F.; Guo, X.-D.; Hu, T.-P.; Gao, B.; Gao, J.-F. Design of novel "imprinting synchronized with crosslinking" surface imprinted technique and its application for selectively removing phenols from aqueous solution. *Eur. Polym. J.* **2019**, *112*, 273–282. [CrossRef]
39. Le Noir, M.; Lepeuple, A.-S.; Guieysse, B.; Mattiasson, B. Selective removal of 17β-estradiol at trace concentration using a molecularly imprinted polymer. *Water Res.* **2007**, *41*, 2825–2831. [CrossRef] [PubMed]
40. Lu, Y.C.; Mao, J.H.; Zhang, W.; Wang, C.; Cao, M.; Wang, X.D.; Wang, K.Y.; Xiong, X. A novel strategy for selective removal and rapid collection of triclosan from aquatic environment using magnetic molecularly imprinted nano−polymers. *Chemosphere* **2020**, *238*, 124640. [CrossRef] [PubMed]
41. Tan, F.; Sun, D.; Gao, J.; Zhao, Q.; Wang, X.; Teng, F.; Quan, X.; Chen, J. Preparation of molecularly imprinted polymer nanoparticles for selective removal of fluoroquinolone antibiotics in aqueous solution. *J. Hazard. Mater.* **2013**, 750–757. [CrossRef]
42. DeVane, C.L.; Liston, H.L.; Markowitz, J.S.; De Vane, C.L. Clinical Pharmacokinetics of Sertraline. *Clin. Pharmacokinet.* **2002**, *41*, 1247–1266. [CrossRef]
43. Kosjek, T.; Heath, E.; Kompare, B. Removal of pharmaceutical residues in a pilot wastewater treatment plant. *Anal. Bioanal. Chem.* **2007**, *387*, 1379–1387. [CrossRef]
44. Abdouss, M.; Asadi, E.; Azodi-Deilami, S.; Beik-Mohammadi, N.; Aslanzadeh, S.A. Development and characterization of molecularly imprinted polymers for controlled release of citalopram. *J. Mater. Sci. Mater. Electron.* **2011**, *22*, 2273–2281. [CrossRef]
45. Chapuis, F.; Mullot, J.-U.; Pichon, V.; Tuffal, G.; Hennion, M.-C. Molecularly imprinted polymers for the clean-up of a basic drug from environmental and biological samples. *J. Chromatogr. A* **2006**, *1135*, 127–134. [CrossRef]
46. Kempe, H.; Kempe, M. Influence of salt ions on binding to molecularly imprinted polymers. *Anal. Bioanal. Chem.* **2009**, *396*, 1599–1606. [CrossRef]
47. Horemans, F.; Weustenraed, A.; Spivak, D.A.; Cleij, T.J. Towards water compatible MIPs for sensing in aqueous media. *J. Mol. Recognit.* **2012**, *25*, 344–351. [CrossRef]
48. Dirion, B.; Cobb, Z.; Schillinger, E.; Andersson, A.L.I.; Sellergren, B. Water-Compatible Molecularly Imprinted Polymers Obtained via High-Throughput Synthesis and Experimental Design. *J. Am. Chem. Soc.* **2003**, *125*, 15101–15109. [CrossRef] [PubMed]
49. Yan, H.; Row, K.H. Characteristic and Synthetic Approach of Molecularly Imprinted Polymer. *Int. J. Mol. Sci.* **2006**, *7*, 155–178. [CrossRef]
50. Arvand, M.; Hashemi, M. Synthesis by precipitation polymerization of a molecularly imprinted polymer membrane for the potentiometric determination of sertraline in tablets and biological fluids. *J. Braz. Chem. Soc.* **2012**, *23*, 392–402. [CrossRef]
51. Khalilian, F.; Kermani, F.K. Selective Dispersive Solid Phase Extraction of Ser-Traline Using Surface Molecu-larly Imprinted Polymer Grafted on SiO_2/Graphene Oxide. *J. Chem. Health Risks* **2017**, *7*, 49–60.
52. Krupadam, R.J.; Patel, G.P.; Balasubramanian, R. Removal of cyanotoxins from surface water resources using reusable molecularly imprinted polymer adsorbents. *Environ. Sci. Pollut. Res.* **2011**, *19*, 1841–1851. [CrossRef]
53. Krupadam, R.J.; Khan, M.S.; Wate, S.R. Removal of probable human carcinogenic polycyclic aromatic hydrocarbons from contaminated water using molecularly imprinted polymer. *Water Res.* **2010**, *44*, 681–688. [CrossRef]
54. Krupadam, R.J.; Bhagat, B.; Wate, S.R.; Bodhe, G.L.; Sellergren, B.; Anjaneyulu, Y. Fluorescence Spectrophotometer Analysis of Polycyclic Aromatic Hydrocarbons in Environmental Samples Based on Solid Phase Extraction Using Molecularly Imprinted Polymer. *Environ. Sci. Technol.* **2009**, *43*, 2871–2877. [CrossRef]
55. Murray, A.; Örmeci, B. Application of molecularly imprinted and non-imprinted polymers for removal of emerging contaminants in water and wastewater treatment: A review. *Environ. Sci. Pollut. Res.* **2012**, *19*, 3820–3830. [CrossRef]
56. Tadeo, X.; López-Méndez, B.; Castaño, D.; Trigueros, T.; Millet, O. Protein Stabilization and the Hofmeister Effect: The Role of Hydrophobic Solvation. *Biophys. J.* **2009**, *97*, 2595–2603. [CrossRef]
57. Zhou, W.; Yang, S.; Wang, P.G. Matrix effects and application of matrix effect factor. *Bioanalysis* **2017**, *9*, 1839–1844. [CrossRef]
58. Azizi, A.; Bottaro, C.S. A critical review of molecularly imprinted polymers for the analysis of organic pollutants in environmental water samples. *J. Chromatogr. A* **2020**, *1614*, 460603. [CrossRef] [PubMed]
59. Martín-Esteban, A.; Sellergren, B. 2.17-Molecularly Imprinted Polymers. In *Comprehensive Sampling and Sample Preparation*; Pawliszyn, J., Ed.; Academic Press: Oxford, UK, 2012; pp. 331–344.
60. Sellergren, B.; Lanza, F. *Techniques and Instrumentation in Analytical Chemistry*; Elsevier: Amsterdam, The Netherlands, 2001; Volume 23, pp. 355–375.
61. Turiel, E.; Esteban, A.M. 8-Molecularly imprinted polymers. In *Solid-Phase Extraction*; Poole, C.F., Ed.; Elsevier: Amsterdam, The Netherlands, 2020; pp. 215–233.

62. Ellwanger, A.; Karlsson, L.; Owens, P.K.; Berggren, C.; Crecenzi, C.; Ensing, K.; Bayoudh, S.; Cormack, P.A.; Sherrington, D.; Sellergren, B. Evaluation of methods aimed at complete removal of template from molecularly imprinted polymers. *Analyst* **2001**, *126*, 784–792. [CrossRef] [PubMed]
63. Lorenzo, R.A.; Carro, A.; Alvarez-Lorenzo, C.; Concheiro, A. To Remove or Not to Remove? The Challenge of Extracting the Template to Make the Cavities Available in Molecularly Imprinted Polymers (MIPs). *Int. J. Mol. Sci.* **2011**, *12*, 4327–4347. [CrossRef] [PubMed]
64. Activated Charcoal C3345. Available online: https://www.sigmaaldrich.com/catalog/product/sigald/c3345 (accessed on 8 September 2020).

Chapter 4

Conclusions and Future Perspective

This thesis provides knowledge on the behavior and fate of SSRI antidepressants during water treatment and in the environment that was missing from the existing literature. Furthermore, using SSRI as model compounds, we demonstrated that specialized materials such as MIPs hold great potential as sorbents for SPE or as an alternative form of WW treatment for contaminants. The scientific contributions of this thesis are presented in five scientific papers published in SCI international journals and presented as oral and poster presentations at national and international conferences (see appendix). The significant achievements and conclusions of this thesis are:

1) Developed, optimized and validated analytical methods for quantifying nine common SSRIs, where we would like to underline less studied SSRI, SER and PXT, and the identification of their TPs employing different techniques (HPLC-UV, GC-MS, UHPLC-MS/MS, UHPLC-HRMS). The methods were applied to different aqueous matrices (WW effluent, WW influent, artificial WW, hospital sewage, SW).

2) SER and PXT breakdown during sunlight exposure in SW was researched. A well-thought-out experimental design using photosensitizers and scavengers enabled the collection of a sufficient amount of data to model it successfully with APEX software, additionally considering different depths and compositions of SW. Thus, clarification is provided on the photochemistry and kinetics involved in SER and PXT degradation. The experimental design can be applied again to other compounds. In addition, the identities of their phototransformation products formed during laboratory-scale experiments were tentatively suggested, and their degradation pathways were proposed. SER degradation behavior was additionally observed in sunlight-irradiated samples of actual SW. Based on these results, the first hypothesis, H1: Photodegradation is the main degradation pathway of SER and PXT in SW, can be accepted. Also, during sunlight irradiation, TPs were shown to form.

3) The removal of SER during biological treatment was thoroughly examined. Adsorption to activated sludge was the leading removal process, while biodegradation occurred to a certain extent. Chemical structures for the determined biotransformation products and the most probable degradation pathway were suggested. The removal efficiencies determined were high, ranging from 77 % to >90 % in actual WWTP and laboratory-scale experiments, respectively. Nevertheless, SER and its TPs were still detected in the WW effluent, thus

supporting the second hypothesis H2: SER is only partially biodegradable. TPs are formed during SER biodegradation.

4) Actual composite samples of WW and SW samples from Slovenian rivers, WWTPs and hospital sewage were collected and analyzed. The results supported only part of hypothesis H3: SER and PXT, and their residues are present in Slovenian SW and WW. SER and its residues (metabolites and TPs) were determined in WW and SW samples, whereas no PXT or its residues were detected in Slovenian SW.

5) MIPs were synthesized and evaluated for the application as sorbents used in SPE to improve the sample preparation step. With bulk polymerization, successfully imprinted polymers with good recognition characteristics for SER and its metabolites/TPs were obtained, partially confirming hypothesis H4: Besides the original template compound, MIPs can rebind structurally related analogues, metabolites and TPs. However, continuous leaching of the imprinted SER from the material meant they could not be used to analyze environmental samples containing trace amounts of SER. With two-stage polymerization, we obtained MIPs with more binding sites on the surface of the polymer. No leaching of the template was detected with the analytical method applied, making it an appropriate sorbent for SPE and confirming hypothesis H5: MIPs can be used as sorbents for SPE of SER and its residues.

6) Another set of MIPs was prepared via bulk polymerization to assess their performance in WW treatment. The ingredients used in the polymerization were varied to obtain the best possible recognition abilities for SER. The produced material was cross-reactive towards other antidepressants and their TPs (PXT, FLU, ESC, NS), supporting hypothesis H4. The crucial characteristics were the surface area of the MIP, contact time with the sample, salt concentration in the matrix and the structure of the analyte, especially the amino group. The polymers were reusable, and when comparing the removal efficiency between AC and our chosen MIPs at higher volumes of WW, the polymers performed better despite their lower surface areas enabling hypothesis H6: MIPs can be utilized for the removal of SSRI and its residues from WW, to be accepted.

Since the consumption of antidepressants is on the rise with no indication that this trend will change [2], future work should focus on the impact of rising consumption on their environmental occurrence. However, the occurrence of the parent compounds should not be the only area of interest for future research. Now that the data on the potentially formed TPs is available, their presence in the environment should be equally researched. Not only that, some recent studies are suggesting that they could be more toxic than their parent compounds [139]. Hence, studying their ecotoxicity and possible interactions with other contaminants will be crucial for estimating if any SSRIs and their TPs need to be included in official monitoring programs or regulated.

Models and predictions, as seen herein for phototransformation of SER and PXT, can offer guidance on future work. Hence, in the future they will in all likelihood enter the foreground of environmental research [77], [270]. Further development, optimization and harmonization of similar models predicting the behavior of contaminants in the environment will become essential tools that will enable better environmental resource management in the future.

Another direction that future work should take is to find alternative treatment options that will enable the mineralization of both parent compounds and TPs. Awareness of the behavior of SSRIs, their metabolites and TPs, for example, the tendencies to adsorb and

photodegrade, can allude to which techniques to investigate first. While the currently studied AC and AOP are both excellent choices, the rising presence of SSRIs reported in different compartments of the environment indicates that it is an issue that urgently needs to be addressed. More innovative techniques and materials, such as MIPs, are welcome options and this thesis only scratched the surface of the possibilities of applying molecular imprinting to WW treatment. Several other polymerization techniques and approaches are available, giving the material characteristics that would improve the recognition properties of chosen analytes and make them easier to use (*e.g.*, particle size and magnetic properties). Of course, the balance between the efficiency of the treatment, reusability and regeneration of such materials and investment costs should be carefully considered. Such options, however, are not only needed for antidepressants but all contaminants of emerging concern where reported concentrations are reaching critical levels.

References

[1] "Medicinal Products Act," *pisrs*, 2014. http://pisrs.si/Pis.web/pregledPredpisa?id=ZAKO6295 (accessed Aug. 21, 2022).

[2] OECD, *Health at a Glance 2021: OECD Indicators*. OECD, 2021. doi: 10.1787/ae3016b9-en.

[3] T. aus der Beek *et al.*, "Pharmaceuticals in the environment-Global occurrences and perspectives: Pharmaceuticals in the global environment," *Environ. Toxicol. Chem.*, vol. 35, no. 4, Art. no. 4, Apr. 2016, doi: 10.1002/etc.3339.

[4] OECD, *Pharmaceutical Residues in Freshwater : Hazards and Policy Responses*, vol. 2019. Paris: OECD Publishing, 2019. Accessed: Mar. 27, 2020. [Online]. Available: ../env-2019-2329-en/index.html

[5] E. E. Burns, L. J. Carter, J. Snape, J. Thomas-Oates, and A. B. A. Boxall, "Application of prioritization approaches to optimize environmental monitoring and testing of pharmaceuticals," *J. Toxicol. Environ. Health Part B*, vol. 21, no. 3, pp. 115–141, Apr. 2018, doi: 10.1080/10937404.2018.1465873.

[6] "Central Slovenian Drug Database," 2020. http://www.cbz.si/cbz/bazazdr2.nsf/Search/$searchForm?SearchView (accessed May 13, 2020).

[7] N. C. for T. Research, "Drug Induced Liver Injury Rank (DILIrank) Dataset," *FDA*, May 2019, Accessed: Apr. 30, 2020. [Online]. Available: https://www.fda.gov/science-research/liver-toxicity-knowledge-base-ltkb/drug-induced-liver-injury-rank-dilirank-dataset

[8] "Etoperidone." https://www.drugbank.ca/drugs/DB09194 (accessed May 13, 2020).

[9] L. J. G. Silva, C. M. Lino, L. M. Meisel, and A. Pena, "Selective serotonin re-uptake inhibitors (SSRIs) in the aquatic environment: An ecopharmacovigilance approach," *Sci. Total Environ.*, vol. 437, pp. 185–195, Oct. 2012, doi: 10.1016/j.scitotenv.2012.08.021.

[10] A. Fuentes, M. Pineda, and K. Venkata, "Comprehension of Top 200 Prescribed Drugs in the US as a Resource for Pharmacy Teaching, Training and Practice," *Pharmacy*, vol. 6, no. 2, Art. no. 2, May 2018, doi: 10.3390/pharmacy6020043.

[11] S. McDermott, "HSE prescriptions for antidepressants and anxiety medications up by two thirds since 2009," *TheJournal.ie*, 2018. https://www.thejournal.ie/ireland-antidepressant-anxiety-medicine-prescriptions-4157452-Aug2018/ (accessed Mar. 26, 2020).

[12] G. Trifirò *et al.*, "A nationwide prospective study on prescribing pattern of antidepressant drugs in Italian primary care," *Eur J Clin Pharmacol*, vol. 69, pp. 227–236, 2013.

[13] M. Bourin, P. Chue, and Y. Guillon, "Paroxetine: A Review," *CNS Drug Rev.*, vol. 7, no. 1, pp. 25–47, Jun. 2006, doi: 10.1111/j.1527-3458.2001.tb00189.x.

[14] N. Diaz-Camal, J. D. Cardoso-Vera, H. Islas-Flores, L. M. Gómez-Oliván, and A. Mejía-García, "Consumption and ocurrence of antidepressants (SSRIs) in pre- and post-COVID-19 pandemic, their environmental impact and innovative removal methods: A review," *Sci. Total Environ.*, vol. 829, p. 154656, Jul. 2022, doi: 10.1016/j.scitotenv.2022.154656.

[15] C. Hiemke and S. Härtter, "Pharmacokinetics of selective serotonin reuptake inhibitors," *Pharmacol. Ther.*, vol. 85, no. 1, pp. 11–28, Jan. 2000, doi: 10.1016/S0163-7258(99)00048-0.

[16] J. M. Grohol, P. D. Founder, and E.-C. L. updated: 15 D. 2019 ~ 3 min read, "Top 25 Psychiatric Medications for 2018," Dec. 15, 2019. //psychcentral.com/blog/top-25-psychiatric-medications-for-2018/ (accessed Mar. 25, 2020).

[17] "ClinCalc DrugStats Database: The Top 200 Drugs of 2019," 2021. https://clincalc.com/DrugStats/ (accessed Nov. 15, 2021).

[18] NIJZ, "Poraba ambulantno predpisanih zdravil v Sloveniji v letu 2020," NIJZ, 2020.

[19] PubChem, "PubChem." https://pubchem.ncbi.nlm.nih.gov/ (accessed Oct. 31, 2022).

[20] "CAS Common Chemistry." https://commonchemistry.cas.org/ (accessed Oct. 31, 2022).

[21] A. C. Altamura, A. R. Moro, and M. Percudani, "Clinical Pharmacokinetics of Fluoxetine," *Clin. Pharmacokinet.*, vol. 26, no. 3, Art. no. 3, Mar. 1994, doi: 10.2165/00003088-199426030-00004.

[22] "Home - electronic medicines compendium (emc)," 2020. https://www.medicines.org.uk/emc/ (accessed May 15, 2020).

[23] A. C. Altamura, A. R. Moro, and M. Percudani, "Clinical Pharmacokinetics of Fluoxetine:," *Clin. Pharmacokinet.*, vol. 26, no. 3, pp. 201–214, Mar. 1994, doi: 10.2165/00003088-199426030-00004.

[24] P. Baumann, D. F. Zullino, and C. B. Eap, "Enantiomers' potential in psychopharmacology—a critical analysis with special emphasis on the antidepressant escitalopram," *Eur. Neuropsychopharmacol.*, p. 12, 2002.

[25] C. L. DeVane, H. L. Liston, and J. S. Markowitz, "Clinical Pharmacokinetics of Sertraline," *Clin. Pharmacokinet.*, vol. 41, no. 15, Art. no. 15, 2002, doi: 10.2165/00003088-200241150-00002.

[26] H. Overmars, P. M. Scherpenisse, and L. C. Post, "Fluvoxamine maleate: metabolism in man," *Eur. J. Drug Metab. Pharmacokinet.*, vol. 8, no. 3, pp. 269–280, Jul. 1983, doi: 10.1007/BF03188757.

[27] N. Rao, "The Clinical Pharmacokinetics of Escitalopram," *Clin Pharmacokinet*, p. 10, 2007.

[28] B. Rochat, M. Kosel, G. Boss, B. Testa, M. Gillet, and P. Baumann, "Stereoselective Biotransformation of the Selective Serotonin Reuptake Inhibitor Citalopram and Its

Demethylated Metabolites by Monoamine Oxidases in Human Liver," *Biochem. Pharmacol.*, vol. 56, no. 1, pp. 15–23, Jul. 1998, doi: 10.1016/S0006-2952(98)00008-2.

[29] K. Sangkuhl, T. E. Klein, and R. B. Altman, "PharmGKB summary: citalopram pharmacokinetics pathway," *Pharmacogenet. Genomics*, vol. 21, no. 11, pp. 769–772, Nov. 2011, doi: 10.1097/FPC.0b013e328346063f.

[30] J. van Harten, "Overview of the Pharmacokinetics of Fluvoxamine," *Clin. Pharmacokinet.*, vol. 29, no. Supplement 1, Art. no. Supplement 1, 1995, doi: 10.2165/00003088-199500291-00003.

[31] "Electronic medicines compendium: Fluoxetine - SmPC," 2019. https://www.medicines.org.uk/emc/product/6013/smpc (accessed May 13, 2020).

[32] "Central Slovenian Drug Database: Citalopram SmPC," 2019. http://www.cbz.si/cbz/bazazdr2.nsf/o/E9BF511B8BC29C0FC12579C2003F5044/$File/s-023015.pdf (accessed May 15, 2020).

[33] "Electronic medicines compendium: Citalopram - SmPC," 2019. https://www.medicines.org.uk/emc/product/992/smpc (accessed May 15, 2020).

[34] J. Waugh and K. L. Goa, "Escitalopram: A Review of its Use in the Management of Major Depressive and Anxiety Disorders," *CNS Drugs*, vol. 17, no. 5, pp. 343–362, 2003, doi: 10.2165/00023210-200317050-00004.

[35] "Electronic medicines compendium: Escitalopram - SmPC," 2020. https://www.medicines.org.uk/emc/product/7718/smpc#PHARMACOLOGICAL_PROPS (accessed May 15, 2020).

[36] "Electronic medicines compendium: Paroxetine - SmPC," 2019. https://www.medicines.org.uk/emc/product/4168/smpc#PHARMACOKINETIC_PROPS (accessed May 15, 2020).

[37] J. Jornil, K. G. Jensen, F. Larsen, and K. Linnet, "Identification of Cytochrome P450 Isoforms Involved in the Metabolism of Paroxetine and Estimation of Their Importance for Human Paroxetine Metabolism Using a Population-Based Simulator," *Drug Metab. Dispos.*, vol. 38, no. 3, Art. no. 3, Mar. 2010, doi: 10.1124/dmd.109.030551.

[38] "Electronic medicines compendium: Sertraline - SmPC," 2018. https://www.medicines.org.uk/emc/product/2835/smpc (accessed May 14, 2020).

[39] "Electronic medicines compendium: Fluvoxamine - SmPC," 2019. https://www.medicines.org.uk/emc/product/6603/smpc (accessed May 14, 2020).

[40] J. van Harten, "Overview of the Pharmacokinetics of Fluvoxamine:," *Clin. Pharmacokinet.*, vol. 29, no. Supplement 1, pp. 1–9, 1995, doi: 10.2165/00003088-199500291-00003.

[41] K. Demeestere, M. Petrović, M. Gros, J. Dewulf, H. Van Langenhove, and D. Barceló, "Trace analysis of antidepressants in environmental waters by molecularly imprinted polymer-based solid-phase extraction followed by ultra-performance liquid chromatography coupled to triple quadrupole mass spectrometry," *Anal. Bioanal. Chem.*, vol. 396, no. 2, pp. 825–837, Jan. 2010, doi: 10.1007/s00216-009-3270-2.

[42] K. H. Langford and K. V. Thomas, "Determination of pharmaceutical compounds in hospital effluents and their contribution to wastewater treatment works,"

Environ. Int., vol. 35, no. 5, pp. 766–770, Jul. 2009, doi: 10.1016/j.envint.2009.02.007.

[43] S. Mompelat, B. Le Bot, and O. Thomas, "Occurrence and fate of pharmaceutical products and by-products, from resource to drinking water," *Environ. Int.*, vol. 35, no. 5, pp. 803–814, Jul. 2009, doi: 10.1016/j.envint.2008.10.008.

[44] OECD, *Pharmaceutical Residues in Freshwater: Hazards and Policy Responses - Policy Highlights*, vol. 2019. Paris: OECD Publishing, 2019.

[45] "Council Directive 91/271/EEC," 1991. https://eur-lex.europa.eu/legal-content/EN/TXT/HTML/?uri=CELEX:31991L0271&from=EN (accessed Aug. 11, 2020).

[46] "Council Directive 91/271/EEC." 2014.

[47] "Directive 2000/60/EC," *Official Journal L 327, 22/12/2000 P. 0001 - 0073*, 2000. https://eur-lex.europa.eu/legal-content/EN/TXT/HTML/?uri=CELEX:32000L0060&from=EN (accessed Aug. 11, 2020).

[48] EMA, "Guideline on the Environmental risk assessment of medicinal products for human use," 2006.

[49] Joint Research Centre, "Development of the first Watch List under the Environmental Quality Standards Directive," 2015. Accessed: Aug. 11, 2020. [Online]. Available: https://publications.jrc.ec.europa.eu/repository/bitstream/JRC95018/lbna27142enn.pdf

[50] L. O'Connor, "First Watch List for emerging water pollutants," *EU Science Hub - European Commission*, Jul. 31, 2015. https://ec.europa.eu/jrc/en/news/first-watch-list-emerging-water-pollutants (accessed Aug. 11, 2020).

[51] J. Hollender *et al.*, "High resolution mass spectrometry-based non-target screening can support regulatory environmental monitoring and chemicals management," *Environ. Sci. Eur.*, vol. 31, no. 1, Art. no. 1, Dec. 2019, doi: 10.1186/s12302-019-0225-x.

[52] Joint Research Centre, "Review of the 1st Watch List under the Water Framework Directive and recommendations for the 2nd Watch List," Apr. 2018. Accessed: Aug. 11, 2020. [Online]. Available: https://publications.jrc.ec.europa.eu/repository/bitstream/JRC111198/wl_report_jrc_2018_04_26_final_online.pdf

[53] G. Mulhern, "Updated surface water Watch List adopted by the Commission," *EU Science Hub - European Commission*, Jul. 03, 2018. https://ec.europa.eu/jrc/en/science-update/updated-surface-water-watch-list-adopted-commission (accessed Apr. 17, 2020).

[54] L. Gomez Cortes *et al.*, *Selection of substances for the 3rd Watch List under the Water Framework Directive*. 2020. Accessed: May 01, 2022. [Online]. Available: https://op.europa.eu/publication/manifestation_identifier/PUB_KJNA30297ENN

[55] R. A. Mole and B. W. Brooks, "Global scanning of selective serotonin reuptake inhibitors: occurrence, wastewater treatment and hazards in aquatic systems,"

Environ. Pollut., vol. 250, pp. 1019–1031, Jul. 2019, doi: 10.1016/j.envpol.2019.04.118.

[56] A. M. Christensen, S. Faaborg-Andersen, I. Flemming, and A. Baun, "Mixture and single-substance toxicity of selective serotonin reuptake inhibitors toward algae and crustaceans," *Environ. Toxicol. Chem.*, vol. 26, no. 1, pp. 85–91, 2007.

[57] J.-W. Kwon and K. L. Armbrust, "Aqueous Solubility, n-Octanol–Water Partition Coefficient, and Sorption of Five Selective Serotonin Reuptake Inhibitors to Sediments and Soils," *Bull. Environ. Contam. Toxicol.*, vol. 81, no. 2, pp. 128–135, Aug. 2008, doi: 10.1007/s00128-008-9401-1.

[58] P. Arnnok, R. R. Singh, R. Burakham, A. Pérez-Fuentetaja, and D. S. Aga, "Selective Uptake and Bioaccumulation of Antidepressants in Fish from Effluent-Impacted Niagara River," *Environ. Sci. Technol.*, vol. 51, no. 18, Art. no. 18, Sep. 2017, doi: 10.1021/acs.est.7b02912.

[59] M. P. Schlüsener, P. Hardenbicker, E. Nilson, M. Schulz, C. Viergutz, and T. A. Ternes, "Occurrence of venlafaxine, other antidepressants and selected metabolites in the Rhine catchment in the face of climate change," *Environ. Pollut.*, vol. 196, pp. 247–256, Jan. 2015, doi: 10.1016/j.envpol.2014.09.019.

[60] R. Loos *et al.*, "EU-wide monitoring survey on emerging polar organic contaminants in wastewater treatment plant effluents," *Water Res.*, vol. 47, no. 17, Art. no. 17, Nov. 2013, doi: 10.1016/j.watres.2013.08.024.

[61] R. C. Pivetta, C. Rodrigues-Silva, A. R. Ribeiro, and S. Rath, "Tracking the occurrence of psychotropic pharmaceuticals in Brazilian wastewater treatment plants and surface water, with assessment of environmental risks," *Sci. Total Environ.*, vol. 727, p. 138661, Jul. 2020, doi: 10.1016/j.scitotenv.2020.138661.

[62] R. Salgado *et al.*, "Assessing the diurnal variability of pharmaceutical and personal care products in a full-scale activated sludge plant," *Environ. Pollut.*, vol. 159, no. 10, pp. 2359–2367, Oct. 2011, doi: 10.1016/j.envpol.2011.07.004.

[63] W. Peysson and E. Vulliet, "Determination of 136 pharmaceuticals and hormones in sewage sludge using quick, easy, cheap, effective, rugged and safe extraction followed by analysis with liquid chromatography–time-of-flight-mass spectrometry," *J. Chromatogr. A*, vol. 1290, pp. 46–61, May 2013, doi: 10.1016/j.chroma.2013.03.057.

[64] A. Lajeunesse, S. A. Smyth, K. Barclay, S. Sauvé, and C. Gagnon, "Distribution of antidepressant residues in wastewater and biosolids following different treatment processes by municipal wastewater treatment plants in Canada," *Water Res.*, vol. 46, no. 17, pp. 5600–5612, Nov. 2012, doi: 10.1016/j.watres.2012.07.042.

[65] B. Subedi, S. Lee, H.-B. Moon, and K. Kannan, "Psychoactive Pharmaceuticals in Sludge and Their Emission from Wastewater Treatment Facilities in Korea," *Environ. Sci. Technol.*, vol. 47, no. 23, pp. 13321–13329, Dec. 2013, doi: 10.1021/es404129r.

[66] B. D. Blair, J. P. Crago, C. J. Hedman, and R. D. Klaper, "Pharmaceuticals and personal care products found in the Great Lakes above concentrations of environmental concern," *Chemosphere*, vol. 93, no. 9, pp. 2116–2123, Nov. 2013, doi: 10.1016/j.chemosphere.2013.07.057.

[67] M. M. Schultz *et al.*, "Antidepressant pharmaceuticals in two US effluent-impacted streams: occurrence and fate in water and sediment, and selective uptake in fish neural tissue," *Environ. Sci. Technol.*, vol. 44, no. 6, pp. 1918–1925, 2010.

[68] US Environmental Protection Agency, "Final Report, The Environmental Occurrence, Fate, and Ecotoxicity of Selective Serotonin Reuptake Inhibitors (SSRIs) in Aquatic Environments, Research Project Database, NCER | ORD | US EPA," Mar. 07, 2016. https://cfpub.epa.gov/ncer_abstracts/index.cfm/fuseaction/display.highlight/abstract/1755/report/F (accessed Mar. 07, 2016).

[69] L. J. G. Silva, A. M. P. T. Pereira, L. M. Meisel, C. M. Lino, and A. Pena, "Reviewing the serotonin reuptake inhibitors (SSRIs) footprint in the aquatic biota: Uptake, bioaccumulation and ecotoxicology," *Environ. Pollut.*, vol. 197, pp. 127–143, Feb. 2015, doi: 10.1016/j.envpol.2014.12.002.

[70] B. W. Brooks *et al.*, "Determination of select antidepressants in fish from an effluent-dominated stream," *Environ. Toxicol. Chem.*, vol. 24, no. 2, pp. 464–469, 2005.

[71] S. Chu and C. D. Metcalfe, "Analysis of paroxetine, fluoxetine and norfluoxetine in fish tissues using pressurized liquid extraction, mixed mode solid phase extraction cleanup and liquid chromatography–tandem mass spectrometry," *J. Chromatogr. A*, vol. 1163, no. 1–2, pp. 112–118, Sep. 2007, doi: 10.1016/j.chroma.2007.06.014.

[72] J. Gelsleichter and N. J. Szabo, "Uptake of human pharmaceuticals in bull sharks (Carcharhinus leucas) inhabiting a wastewater-impacted river," *Sci. Total Environ.*, vol. 456–457, pp. 196–201, Jul. 2013, doi: 10.1016/j.scitotenv.2013.03.078.

[73] C. D. Metcalfe *et al.*, "Antidepressants and their metabolites in municipal wastewater, and downstream exposure in an urban watershed," *Environ. Toxicol. Chem.*, vol. 29, no. 1, pp. 79–89, Jan. 2010, doi: 10.1002/etc.27.

[74] A. J. Ramirez, M. A. Mottaleb, B. W. Brooks, and C. K. Chambliss, "Analysis of Pharmaceuticals in Fish Using Liquid Chromatography-Tandem Mass Spectrometry," *Anal. Chem.*, vol. 79, no. 8, pp. 3155–3163, Apr. 2007, doi: 10.1021/ac062215i.

[75] A. J. Ramirez *et al.*, "Occurrence of pharmaceuticals and personal care products in fish: results of a national pilot study in the United States," *Environ. Toxicol. Chem.*, vol. 28, no. 12, pp. 2587–2597, 2009.

[76] M. Petrovic, M. Petrovic, and D. Barceló, "LC-MS for identifying photodegradation products of pharmaceuticals in the environment," *TrAC Trends Anal. Chem.*, vol. 26, no. 6, Art. no. 6, Jun. 2007, doi: 10.1016/j.trac.2007.02.010.

[77] D. Vione and L. Carena, "The Possible Production of Harmful Intermediates Is the 'Dark Side' Of the Environmental Photochemistry of Contaminants (Potentially Adverse Effects, And Many Knowledge Gaps)," *Environ. Sci. Technol.*, vol. 54, no. 9, Art. no. 9, May 2020, doi: 10.1021/acs.est.0c01049.

[78] P. Klimaszyk and P. Rzymski, "Water and Aquatic Fauna on Drugs: What are the Impacts of Pharmaceutical Pollution?," in *Water Management and the Environment: Case Studies*, vol. 86, M. Zelenakova, Ed. Cham: Springer International Publishing, 2018, pp. 255–278. doi: 10.1007/978-3-319-79014-5_12.

[79] B. Silva, F. Costa, I. C. Neves, and T. Tavares, *Psychiatric Pharmaceuticals as Emerging Contaminants in Wastewater*. Cham: Springer International Publishing, 2015. doi: 10.1007/978-3-319-20493-2.

[80] J. Cao *et al.*, "Fate of typical endocrine active compounds in full-scale wastewater treatment plants: Distribution, removal efficiency and potential risks," *Bioresour. Technol.*, vol. 310, p. 123436, Aug. 2020, doi: 10.1016/j.biortech.2020.123436.

[81] M. Huerta-Fontela, M. T. Galceran, and F. Ventura, "Occurrence and removal of pharmaceuticals and hormones through drinking water treatment," *Water Res.*, vol. 45, no. 3, pp. 1432–1442, Jan. 2011, doi: 10.1016/j.watres.2010.10.036.

[82] R. Gulde *et al.*, "Systematic Exploration of Biotransformation Reactions of Amine-Containing Micropollutants in Activated Sludge," *Environ. Sci. Technol.*, vol. 50, no. 6, Art. no. 6, Mar. 2016, doi: 10.1021/acs.est.5b05186.

[83] R. Salgado, R. Marques, J. P. Noronha, G. Carvalho, A. Oehmen, and M. A. M. Reis, "Assessing the removal of pharmaceuticals and personal care products in a full-scale activated sludge plant," *Environ. Sci. Pollut. Res.*, vol. 19, no. 5, Art. no. 5, Jun. 2012, doi: 10.1007/s11356-011-0693-z.

[84] Y. F. Velázquez and P. M. Nacheva, "Biodegradability of fluoxetine, mefenamic acid, and metoprolol using different microbial consortiums," *Environ. Sci. Pollut. Res.*, vol. 24, no. 7, Art. no. 7, Mar. 2017, doi: 10.1007/s11356-017-8413-y.

[85] V. G. Beretsou, A. K. Psoma, P. Gago-Ferrero, R. Aalizadeh, K. Fenner, and N. S. Thomaidis, "Identification of biotransformation products of citalopram formed in activated sludge," *Water Res.*, vol. 103, pp. 205–214, Oct. 2016, doi: 10.1016/j.watres.2016.07.029.

[86] M. E. Casas *et al.*, "Biodegradation of pharmaceuticals in hospital wastewater by staged Moving Bed Biofilm Reactors (MBBR)," *Water Res.*, vol. 83, pp. 293–302, Oct. 2015, doi: 10.1016/j.watres.2015.06.042.

[87] M. Escolà Casas *et al.*, "Biodegradation of pharmaceuticals in hospital wastewater by a hybrid biofilm and activated sludge system (Hybas)," *Sci. Total Environ.*, vol. 530–531, pp. 383–392, Oct. 2015, doi: 10.1016/j.scitotenv.2015.05.099.

[88] V. L. Cunningham, D. J. C. Constable, and R. E. Hannah, "Environmental Risk Assessment of Paroxetine," *Environ. Sci. Technol.*, vol. 38, no. 12, Art. no. 12, Jun. 2004, doi: 10.1021/es035119x.

[89] M. Ek, C. Baresel, J. Magnér, R. Bergström, and M. Harding, "Activated carbon for the removal of pharmaceutical residues from treated wastewater," *Water Sci. Technol.*, vol. 69, no. 11, pp. 2372–2380, Jun. 2014, doi: 10.2166/wst.2014.172.

[90] R. Guillossou *et al.*, "Organic micropollutants in a large wastewater treatment plant: What are the benefits of an advanced treatment by activated carbon adsorption in comparison to conventional treatment?," *Chemosphere*, vol. 218, pp. 1050–1060, Mar. 2019, doi: 10.1016/j.chemosphere.2018.11.182.

[91] G. Crini and E. Lichtfouse, "Advantages and disadvantages of techniques used for wastewater treatment," *Environ. Chem. Lett.*, vol. 17, no. 1, pp. 145–155, Mar. 2019, doi: 10.1007/s10311-018-0785-9.

[92] V. Calisto, C. I. A. Ferreira, S. M. Santos, M. V. Gil, M. Otero, and V. I. Esteves, "Production of adsorbents by pyrolysis of paper mill sludge and application on the

removal of citalopram from water," *Bioresour. Technol.*, vol. 166, pp. 335–344, Aug. 2014, doi: 10.1016/j.biortech.2014.05.047.

[93] V. Calisto, G. Jaria, C. P. Silva, C. I. A. Ferreira, M. Otero, and V. I. Esteves, "Single and multi-component adsorption of psychiatric pharmaceuticals onto alternative and commercial carbons," *J. Environ. Manage.*, vol. 192, pp. 15–24, May 2017, doi: 10.1016/j.jenvman.2017.01.029.

[94] G. Jaria, V. Calisto, M. V. Gil, M. Otero, and V. I. Esteves, "Removal of fluoxetine from water by adsorbent materials produced from paper mill sludge," *J. Colloid Interface Sci.*, vol. 448, pp. 32–40, Jun. 2015, doi: 10.1016/j.jcis.2015.02.002.

[95] B. Silva *et al.*, "Waste-based biosorbents as cost-effective alternatives to commercial adsorbents for the retention of fluoxetine from water," *Sep. Purif. Technol.*, vol. 235, p. 116139, Mar. 2020, doi: 10.1016/j.seppur.2019.116139.

[96] S. Miralles-Cuevas, I. Oller, A. Agüera, M. Llorca, J. A. Sánchez Pérez, and S. Malato, "Combination of nanofiltration and ozonation for the remediation of real municipal wastewater effluents: Acute and chronic toxicity assessment," *J. Hazard. Mater.*, vol. 323, pp. 442–451, Feb. 2017, doi: 10.1016/j.jhazmat.2016.03.013.

[97] A. Aghaeinejad-Meybodi, A. Ebadi, S. Shafiei, A. R. Khataee, and M. Rostampour, "Modeling and optimization of antidepressant drug Fluoxetine removal in aqueous media by ozone/H2O2 process: Comparison of central composite design and artificial neural network approaches," *J. Taiwan Inst. Chem. Eng.*, vol. 48, pp. 40–48, Mar. 2015, doi: 10.1016/j.jtice.2014.10.022.

[98] A. Aghaeinejad-Meybodi, A. Ebadi, S. Shafiei, A. Khataee, and A. D. Kiadehi, "Degradation of Fluoxetine using catalytic ozonation in aqueous media in the presence of nano-γ-alumina catalyst: Experimental, modeling and optimization study," *Sep. Purif. Technol.*, vol. 211, pp. 551–563, Mar. 2019, doi: 10.1016/j.seppur.2018.10.020.

[99] M. Bourgin *et al.*, "Evaluation of a full-scale wastewater treatment plant upgraded with ozonation and biological post-treatments: Abatement of micropollutants, formation of transformation products and oxidation by-products," *Water Res.*, vol. 129, pp. 486–498, Feb. 2018, doi: 10.1016/j.watres.2017.10.036.

[100] M. Hörsing, T. Kosjek, H. R. Andersen, E. Heath, and A. Ledin, "Fate of citalopram during water treatment with O3, ClO2, UV and fenton oxidation," *Chemosphere*, vol. 89, no. 2, Art. no. 2, Sep. 2012, doi: 10.1016/j.chemosphere.2012.05.024.

[101] A. Lajeunesse, M. Blais, B. Barbeau, S. Sauvé, and C. Gagnon, "Ozone oxidation of antidepressants in wastewater-treatment evaluation and characterization of new by-products by LC-QToFMS," *Chem Cent J*, vol. 7, no. 1, p. 15, 2013.

[102] F. Méndez-Arriaga *et al.*, "Photooxidation of the antidepressant drug Fluoxetine (Prozac®) in aqueous media by hybrid catalytic/ozonation processes," *Water Res.*, vol. 45, no. 9, Art. no. 9, Apr. 2011, doi: 10.1016/j.watres.2011.02.030.

[103] N. F. F. Moreira *et al.*, "Photocatalytic ozonation of urban wastewater and surface water using immobilized TiO2 with LEDs: Micropollutants, antibiotic resistance genes and estrogenic activity," *Water Res.*, vol. 94, pp. 10–22, May 2016, doi: 10.1016/j.watres.2016.02.003.

[104] Y. Zhao *et al.*, "Ozonation of antidepressant fluoxetine and its metabolite product norfluoxetine: Kinetics, intermediates and toxicity," *Chem. Eng. J.*, vol. 316, pp. 951–963, May 2017, doi: 10.1016/j.cej.2017.02.032.

[105] G. A. Zoumpouli, F. Siqueira Souza, B. Petrie, L. A. Féris, B. Kasprzyk-Hordern, and J. Wenk, "Simultaneous ozonation of 90 organic micropollutants including illicit drugs and their metabolites in different water matrices," *Environ. Sci. Water Res. Technol.*, p. 10.1039.D0EW00260G, 2020, doi: 10.1039/D0EW00260G.

[106] J. A. de L. Perini, B. C. e Silva, A. L. Tonetti, and R. F. P. Nogueira, "Photo-Fenton degradation of the pharmaceuticals ciprofloxacin and fluoxetine after anaerobic pre-treatment of hospital effluent," *Environ. Sci. Pollut. Res.*, vol. 24, no. 7, pp. 6233–6240, Mar. 2017, doi: 10.1007/s11356-016-7416-4.

[107] G. Pliego *et al.*, "Complete degradation of the persistent anti-depressant sertraline in aqueous solution by solar photo-Fenton oxidation: Complete degradation of sertraline by solar photo-Fenton," *J. Chem. Technol. Biotechnol.*, vol. 89, no. 6, pp. 814–818, Jun. 2014, doi: 10.1002/jctb.4314.

[108] J. L. Rodríguez-Gil *et al.*, "Heterogeneous photo-Fenton treatment for the reduction of pharmaceutical contamination in Madrid rivers and ecotoxicological evaluation by a miniaturized fern spores bioassay," *Chemosphere*, vol. 80, no. 4, pp. 381–388, Jun. 2010, doi: 10.1016/j.chemosphere.2010.04.045.

[109] Y. Li *et al.*, "Life cycle assessment of advanced wastewater treatment processes: Involving 126 pharmaceuticals and personal care products in life cycle inventory," *J. Environ. Manage.*, vol. 238, pp. 442–450, May 2019, doi: 10.1016/j.jenvman.2019.01.118.

[110] T. Vasskog, U. Berger, P.-J. Samuelsen, R. Kallenborn, and E. Jensen, "Selective serotonin reuptake inhibitors in sewage influents and effluents from Tromsø, Norway," *J. Chromatogr. A*, vol. 1115, no. 1–2, pp. 187–195, May 2006, doi: 10.1016/j.chroma.2006.02.091.

[111] T. Vasskog, T. Anderssen, S. Pedersen-Bjergaard, R. Kallenborn, and E. Jensen, "Occurrence of selective serotonin reuptake inhibitors in sewage and receiving waters at Spitsbergen and in Norway," *J. Chromatogr. A*, vol. 1185, no. 2, pp. 194–205, Mar. 2008, doi: 10.1016/j.chroma.2008.01.063.

[112] L. J. G. Silva, A. M. P. T. Pereira, L. M. Meisel, C. M. Lino, and A. Pena, "A one-year follow-up analysis of antidepressants in Portuguese wastewaters: Occurrence and fate, seasonal influence, and risk assessment," *Sci. Total Environ.*, vol. 490, pp. 279–287, Aug. 2014, doi: 10.1016/j.scitotenv.2014.04.131.

[113] H. Ejhed *et al.*, "The effect of hydraulic retention time in onsite wastewater treatment and removal of pharmaceuticals, hormones and phenolic utility substances," *Sci. Total Environ.*, vol. 618, pp. 250–261, Mar. 2018, doi: 10.1016/j.scitotenv.2017.11.011.

[114] O. Golovko, V. Kumar, G. Fedorova, T. Randak, and R. Grabic, "Seasonal changes in antibiotics, antidepressants/psychiatric drugs, antihistamines and lipid regulators in a wastewater treatment plant," *Chemosphere*, vol. 111, pp. 418–426, Sep. 2014, doi: 10.1016/j.chemosphere.2014.03.132.

[115] L. F. Angeles *et al.*, "Assessing pharmaceutical removal and reduction in toxicity provided by advanced wastewater treatment systems," *Environ. Sci. Water Res. Technol.*, vol. 6, no. 1, Art. no. 1, 2020, doi: 10.1039/C9EW00559E.

[116] "Eurostat - Data Explorer." http://appsso.eurostat.ec.europa.eu/nui/submitViewTableAction.do (accessed Oct. 16, 2022).

[117] "Water statistics." https://ec.europa.eu/eurostat/statistics-explained/index.php?title=Water_statistics (accessed Oct. 16, 2022).

[118] O. US EPA, "Basic Information about Biosolids." https://www.epa.gov/biosolids/basic-information-about-biosolids (accessed Oct. 16, 2022).

[119] R. Kodešová *et al.*, "Soil influences on uptake and transfer of pharmaceuticals from sewage sludge amended soils to spinach," *J. Environ. Manage.*, vol. 250, p. 109407, Nov. 2019, doi: 10.1016/j.jenvman.2019.109407.

[120] O. Bergersen, K. Ø. Hanssen, and T. Vasskog, "Anaerobic treatment of sewage sludge containing selective serotonin reuptake inhibitors," *Bioresour. Technol.*, vol. 117, pp. 325–332, Aug. 2012, doi: 10.1016/j.biortech.2012.04.086.

[121] O. Bergersen, K. Ø. Hanssen, and T. Vasskog, "Aerobic treatment of selective serotonin reuptake inhibitors in landfill leachate," *Environ. Sci. Eur.*, vol. 27, no. 1, Art. no. 1, Jan. 2015, doi: 10.1186/s12302-014-0035-0.

[122] T. Vasskog, O. Bergersen, T. Anderssen, E. Jensen, and T. Eggen, "Depletion of selective serotonin reuptake inhibitors during sewage sludge composting," *Waste Manag.*, vol. 29, no. 11, Art. no. 11, Nov. 2009, doi: 10.1016/j.wasman.2009.06.010.

[123] J.-W. Kwon and K. L. Armbrust, "Laboratory persistence and fate of fluoxetine in aquatic environments," *Environ. Toxicol. Chem.*, vol. 25, no. 10, pp. 2561–2568, 2006.

[124] W. A. Arnold and K. McNeill, "Chapter 3.2 Transformation of pharmaceuticals in the environment: Photolysis and other abiotic processes," in *Comprehensive Analytical Chemistry*, vol. 50, Elsevier, 2007, pp. 361–385. Accessed: Feb. 11, 2016. [Online]. Available: http://linkinghub.elsevier.com/retrieve/pii/S0166526X07500115

[125] E. De Laurentiis *et al.*, "Assessing the photochemical transformation pathways of acetaminophen relevant to surface waters: Transformation kinetics, intermediates, and modelling," *Water Res.*, vol. 53, pp. 235–248, Apr. 2014, doi: 10.1016/j.watres.2014.01.016.

[126] D. Vione, "Photochemical Reactions in Sunlit Surface Waters," in *Applied Photochemistry*, vol. 92, G. Bergamini and S. Silvi, Eds. Cham: Springer International Publishing, 2016, pp. 343–376. Accessed: Aug. 30, 2016. [Online]. Available: http://link.springer.com/10.1007/978-3-319-31671-0_7

[127] D. Vione and P. Calza, "Chapter 1. Introduction," in *Comprehensive Series in Photochemical & Photobiological Sciences*, P. Calza and D. Vione, Eds. Cambridge: Royal Society of Chemistry, 2015, pp. 1–15. Accessed: Aug. 30, 2016. [Online]. Available: http://ebook.rsc.org/?DOI=10.1039/9781782622154-00001

[128] L. Perez-Caballero, S. Torres-Sanchez, L. Bravo, J. A. Mico, and E. Berrocoso, "Fluoxetine: a case history of its discovery and preclinical development," *Expert Opin. Drug Discov.*, vol. 9, no. 5, pp. 567–578, May 2014, doi: 10.1517/17460441.2014.907790.

[129] M. W. Lam, C. J. Young, and S. A. Mabury, "Aqueous Photochemical Reaction Kinetics and Transformations of Fluoxetine," *Environ. Sci. Technol.*, vol. 39, no. 2, Art. no. 2, Jan. 2005, doi: 10.1021/es0494757.

[130] B. A. Wols, D. J. H. Harmsen, E. F. Beerendonk, and C. H. M. Hofman-Caris, "Predicting pharmaceutical degradation by UV (LP)/H2O2 processes: A kinetic model," *Chem. Eng. J.*, vol. 255, pp. 334–343, Nov. 2014, doi: 10.1016/j.cej.2014.05.088.

[131] L. Yin, R. Ma, B. Wang, H. Yuan, and G. Yu, "The degradation and persistence of five pharmaceuticals in an artificial climate incubator during a one year period," *RSC Adv.*, vol. 7, no. 14, Art. no. 14, 2017, doi: 10.1039/C6RA28351A.

[132] O. US EPA, "Series 835 - Fate, Transport and Transformation Test Guidelines," May 28, 2015. https://www.epa.gov/test-guidelines-pesticides-and-toxic-substances/series-835-fate-transport-and-transformation-test (accessed Oct. 16, 2022).

[133] J.-W. Kwon and K. L. Armbrust, "Degradation of citalopram by simulated sunlight," *Environ. Toxicol. Chem.*, vol. 24, no. 7, pp. 1618–1623, 2005.

[134] R. A. Osawa, A. P. Carvalho, O. C. Monteiro, M. C. Oliveira, and M. H. Florêncio, "Transformation products of citalopram: Identification, wastewater analysis and in silico toxicological assessment," *Chemosphere*, vol. 217, pp. 858–868, Feb. 2019, doi: 10.1016/j.chemosphere.2018.11.027.

[135] M. Sharma, P. R. Jawa, R. S. Gill, and G. Bansal, "Citalopram Hydrobromide: degradation product characterization and a validated stability-indicating LC-UV method," *J. Braz. Chem. Soc.*, vol. 22, no. 5, pp. 836–848, May 2011, doi: 10.1590/S0103-50532011000500005.

[136] J.-W. Kwon and K. L. Armbrust, "Hydrolysis and photolysis of paroxetine, a selective serotonin reuptake inhibitor, in aqueous solutions," *Environ. Toxicol. Chem.*, vol. 23, no. 6, pp. 1394–1399, 2004.

[137] H. Santoke and W. J. Cooper, "Environmental photochemical fate of selected pharmaceutical compounds in natural and reconstituted Suwannee River water: Role of reactive species in indirect photolysis," *Sci. Total Environ.*, vol. 580, pp. 626–631, Feb. 2017, doi: 10.1016/j.scitotenv.2016.12.008.

[138] D. Šakić, F. Achrainer, V. Vrček, and H. Zipse, "The chemical fate of paroxetine metabolites. Dehydration of radicals derived from 4-(4-fluorophenyl)-3-(hydroxymethyl)piperidine," *Org. Biomol. Chem.*, vol. 11, no. 25, p. 4232, 2013, doi: 10.1039/c3ob40219c.

[139] P. Calza *et al.*, "Study of the photoinduced transformations of sertraline in aqueous media," *Sci. Total Environ.*, vol. 756, p. 143805, Feb. 2021, doi: 10.1016/j.scitotenv.2020.143805.

[140] Jakimska, A., Kaszynska M., Kot Wasik A., and Mamieśnik J., "Environmental Fate of Two Psychiatric Drugs, Diazepam and Sertraline: Phototransformation and

Investigation of their Photoproducts in Natural Waters," *J. Chromatogr. Sep. Tech.*, vol. 05, no. 06, 2014, doi: 10.4172/2157-7064.1000253.

[141] J.-W. Kwon and K. L. Armbrust, "Photo-isomerization of fluvoxamine in aqueous solutions," *J. Pharm. Biomed. Anal.*, vol. 37, no. 4, pp. 643–648, Apr. 2005, doi: 10.1016/j.jpba.2004.09.057.

[142] R. M. Baena-Nogueras, E. González-Mazo, and P. A. Lara-Martín, "Degradation kinetics of pharmaceuticals and personal care products in surface waters: photolysis vs biodegradation," *Sci. Total Environ.*, vol. 590–591, pp. 643–654, Jul. 2017, doi: 10.1016/j.scitotenv.2017.03.015.

[143] M. J. Benotti and B. J. Brownawell, "Microbial degradation of pharmaceuticals in estuarine and coastal seawater," *Environ. Pollut.*, vol. 157, no. 3, pp. 994–1002, Mar. 2009, doi: 10.1016/j.envpol.2008.10.009.

[144] A. P. Rodrigues, L. H. M. L. M. Santos, M. J. Ramalhosa, C. Delerue-Matos, and L. Guimarães, "Sertraline accumulation and effects in the estuarine decapod Carcinus maenas : Importance of the history of exposure to chemical stress," *J. Hazard. Mater.*, vol. 283, pp. 350–358, Feb. 2015, doi: 10.1016/j.jhazmat.2014.08.035.

[145] Y. Nakamura, H. Yamamoto, J. Sekizawa, T. Kondo, N. Hirai, and N. Tatarazako, "The effects of pH on fluoxetine in Japanese medaka (Oryzias latipes): Acute toxicity in fish larvae and bioaccumulation in juvenile fish," *Chemosphere*, vol. 70, no. 5, Art. no. 5, Jan. 2008, doi: 10.1016/j.chemosphere.2007.06.089.

[146] T. W. Valenti, P. Perez-Hurtado, C. K. Chambliss, and B. W. Brooks, "Aquatic toxicity of sertraline to Pimephales promelas at environmentally relevant surface water pH," *Environ. Toxicol. Chem.*, vol. 28, no. 12, pp. 2685–2694, 2009.

[147] M. L. Boström, G. Ugge, J. Å. Jönsson, and O. Berglund, "Bioaccumulation and trophodynamics of the antidepressants sertraline and fluoxetine in laboratory-constructed, 3-level aquatic food chains: Trophodynamics of 2 SSRIs in 2 tree-level food chains," *Environ. Toxicol. Chem.*, vol. 36, no. 4, pp. 1029–1037, Apr. 2017, doi: 10.1002/etc.3637.

[148] M. C. Bossus, Y. Z. Guler, S. J. Short, E. R. Morrison, and A. T. Ford, "Behavioural and transcriptional changes in the amphipod Echinogammarus marinus exposed to two antidepressants, fluoxetine and sertraline," *Aquat. Toxicol.*, vol. 151, pp. 46–56, Jun. 2014, doi: 10.1016/j.aquatox.2013.11.025.

[149] N. Kreke and D. R. Dietrich, "Physiological Endpoints for Potential SSRI Interactions in Fish," *Crit. Rev. Toxicol.*, vol. 38, no. 3, pp. 215–247, Jan. 2008, doi: 10.1080/10408440801891057.

[150] D. Caminada, C. Escher, and K. Fent, "Cytotoxicity of pharmaceuticals found in aquatic systems: Comparison of PLHC-1 and RTG-2 fish cell lines," *Aquat. Toxicol.*, vol. 79, no. 2, pp. 114–123, Aug. 2006, doi: 10.1016/j.aquatox.2006.05.010.

[151] C. Castillo-Zacarías *et al.*, "Antidepressant drugs as emerging contaminants: Occurrence in urban and non-urban waters and analytical methods for their detection," *Sci. Total Environ.*, vol. 757, p. 143722, Feb. 2021, doi: 10.1016/j.scitotenv.2020.143722.

[152] B. R. Eisenreich, S. Greene, and A. Szalda-Petree, "Of fish and mirrors: Fluoxetine disrupts aggression and learning for social rewards," *Physiol. Behav.*, vol. 173, pp. 258–262, May 2017, doi: 10.1016/j.physbeh.2017.02.021.

[153] N. Estévez-Calvar, L. Canesi, M. Montagna, M. Faimali, V. Piazza, and F. Garaventa, "Adverse effects of the SSRI antidepressant sertraline on early life stages of marine invertebrates," *Mar. Environ. Res.*, vol. 128, pp. 88–97, Jul. 2017, doi: 10.1016/j.marenvres.2016.05.021.

[154] P. P. Fong and N. Molnar, "Antidepressants cause foot detachment from substrate in five species of marine snail," *Mar. Environ. Res.*, vol. 84, pp. 24–30, Mar. 2013, doi: 10.1016/j.marenvres.2012.11.004.

[155] T. B. Henry, J.-W. Kwon, K. L. Armbrust, and M. C. Black, "Acute and chronic toxicity of five selective serotonin reuptake inhibitors in Ceriodaphnia dubia," *Environ. Toxicol. Chem.*, vol. 23, no. 9, pp. 2229–2233, 2004.

[156] T. B. Henry and M. C. Black, "MIXTURE AND SINGLE-SUBSTANCE ACUTE TOXICITY OF SELECTIVE SEROTONIN REUPTAKE INHIBITORS IN CERIODAPHNIA DUBIA," *Environ. Toxicol. Chem.*, vol. 26, no. 8, Art. no. 8, 2007, doi: 10.1897/06-265R.1.

[157] D. J. Johnson, H. Sanderson, R. A. Brain, C. J. Wilson, and K. R. Solomon, "Toxicity and hazard of selective serotonin reuptake inhibitor antidepressants fluoxetine, fluvoxamine, and sertraline to algae," *Ecotoxicol. Environ. Saf.*, vol. 67, no. 1, pp. 128–139, May 2007, doi: 10.1016/j.ecoenv.2006.03.016.

[158] K. Lamichhane, S. N. Garcia, D. B. Huggett, D. L. DeAngelis, and T. W. La Point, "Exposures to a selective serotonin reuptake inhibitor (SSRI), sertraline hydrochloride, over multiple generations: Changes in life history traits in Ceriodaphnia dubia," *Ecotoxicol. Environ. Saf.*, vol. 101, pp. 124–130, Mar. 2014, doi: 10.1016/j.ecoenv.2013.11.026.

[159] E. Minagh, R. Hernan, K. O'Rourke, F. M. Lyng, and M. Davoren, "Aquatic ecotoxicity of the selective serotonin reuptake inhibitor sertraline hydrochloride in a battery of freshwater test species," *Ecotoxicol. Environ. Saf.*, vol. 72, no. 2, pp. 434–440, Feb. 2009, doi: 10.1016/j.ecoenv.2008.05.002.

[160] L. Minguez, R. Bureau, and M.-P. Halm-Lemeille, "Joint effects of nine antidepressants on Raphidocelis subcapitata and Skeletonema marinoi : A matter of amine functional groups," *Aquat. Toxicol.*, vol. 196, pp. 117–123, Mar. 2018, doi: 10.1016/j.aquatox.2018.01.015.

[161] G. Nałęcz-Jawecki, M. Wawryniuk, J. Giebułtowicz, A. Olkowski, and A. Drobniewska, "Influence of Selected Antidepressants on the Ciliated Protozoan Spirostomum ambiguum: Toxicity, Bioaccumulation, and Biotransformation Products," *Molecules*, vol. 25, no. 7, p. 1476, Mar. 2020, doi: 10.3390/molecules25071476.

[162] S. M. Richards and S. E. Cole, "A toxicity and hazard assessment of fourteen pharmaceuticals to Xenopus laevis larvae," *Ecotoxicology*, vol. 15, no. 8, pp. 647–656, Nov. 2006, doi: 10.1007/s10646-006-0102-4.

[163] P. Sehonova, Z. Svobodova, P. Dolezelova, P. Vosmerova, and C. Faggio, "Effects of waterborne antidepressants on non-target animals living in the aquatic

environment: A review," *Sci. Total Environ.*, vol. 631–632, pp. 789–794, Aug. 2018, doi: 10.1016/j.scitotenv.2018.03.076.

[164] D. B. D. Simmons, E. S. McCallum, S. Balshine, B. Chandramouli, J. Cosgrove, and J. P. Sherry, "Reduced anxiety is associated with the accumulation of six serotonin reuptake inhibitors in wastewater treatment effluent exposed goldfish Carassius auratus," *Sci. Rep.*, vol. 7, no. 1, p. 17001, Dec. 2017, doi: 10.1038/s41598-017-15989-z.

[165] J. Vaclavik *et al.*, "The effect of foodborne sertraline on rainbow trout (Oncorhynchus mykiss)," *Sci. Total Environ.*, vol. 708, p. 135082, Mar. 2020, doi: 10.1016/j.scitotenv.2019.135082.

[166] B. Vrana *et al.*, "Passive sampling techniques for monitoring pollutants in water," *TrAC Trends Anal. Chem.*, vol. 24, no. 10, Art. no. 10, Nov. 2005, doi: 10.1016/j.trac.2005.06.006.

[167] Y. Jeong, A. Schäffer, and K. Smith, "A comparison of equilibrium and kinetic passive sampling for the monitoring of aquatic organic contaminants in German rivers," *Water Res.*, vol. 145, pp. 248–258, Nov. 2018, doi: 10.1016/j.watres.2018.08.016.

[168] M. Ibáñez *et al.*, "UHPLC-QTOF MS screening of pharmaceuticals and their metabolites in treated wastewater samples from Athens," *J. Hazard. Mater.*, vol. 323, pp. 26–35, Feb. 2017, doi: 10.1016/j.jhazmat.2016.03.078.

[169] O. Koba *et al.*, "Transport of pharmaceuticals and their metabolites between water and sediments as a further potential exposure for aquatic organisms," *J. Hazard. Mater.*, vol. 342, pp. 401–407, Jan. 2018, doi: 10.1016/j.jhazmat.2017.08.039.

[170] M. S. Kostich, A. L. Batt, and J. M. Lazorchak, "Concentrations of prioritized pharmaceuticals in effluents from 50 large wastewater treatment plants in the US and implications for risk estimation," *Environ. Pollut.*, vol. 184, pp. 354–359, Jan. 2014, doi: 10.1016/j.envpol.2013.09.013.

[171] A. Lajeunesse, S. A. Smyth, K. Barclay, S. Sauvé, and C. Gagnon, "Distribution of antidepressant residues in wastewater and biosolids following different treatment processes by municipal wastewater treatment plants in Canada," *Water Res.*, vol. 46, no. 17, Art. no. 17, Nov. 2012, doi: 10.1016/j.watres.2012.07.042.

[172] C. D. Metcalfe *et al.*, "Antidepressants and their metabolites in municipal wastewater, and downstream exposure in an urban watershed," *Environ. Toxicol. Chem.*, vol. 29, no. 1, Art. no. 1, Jan. 2010, doi: 10.1002/etc.27.

[173] P. Nagarnaik, A. Batt, and B. Boulanger, "Source characterization of nervous system active pharmaceutical ingredients in healthcare facility wastewaters," *J. Environ. Manage.*, vol. 92, no. 3, Art. no. 3, Mar. 2011, doi: 10.1016/j.jenvman.2010.10.058.

[174] M. M. Schultz *et al.*, "Antidepressant pharmaceuticals in two US effluent-impacted streams: occurrence and fate in water and sediment, and selective uptake in fish neural tissue," *Environ. Sci. Technol.*, vol. 44, no. 6, Art. no. 6, 2010.

[175] T. Vasskog, U. Berger, P.-J. Samuelsen, R. Kallenborn, and E. Jensen, "Selective serotonin reuptake inhibitors in sewage influents and effluents from Tromsø,

Norway," *J. Chromatogr. A*, vol. 1115, no. 1–2, Art. no. 1–2, May 2006, doi: 10.1016/j.chroma.2006.02.091.

[176] T. Vasskog, T. Anderssen, S. Pedersen-Bjergaard, R. Kallenborn, and E. Jensen, "Occurrence of selective serotonin reuptake inhibitors in sewage and receiving waters at Spitsbergen and in Norway," *J. Chromatogr. A*, vol. 1185, no. 2, Art. no. 2, Mar. 2008, doi: 10.1016/j.chroma.2008.01.063.

[177] R. López-Serna, M. Petrović, and D. Barceló, "Development of a fast instrumental method for the analysis of pharmaceuticals in environmental and wastewaters based on ultra high performance liquid chromatography (UHPLC)–tandem mass spectrometry (MS/MS)," *Chemosphere*, vol. 85, no. 8, pp. 1390–1399, Nov. 2011, doi: 10.1016/j.chemosphere.2011.07.071.

[178] E. E. Burns, L. J. Carter, D. W. Kolpin, J. Thomas-Oates, and A. B. A. Boxall, "Temporal and spatial variation in pharmaceutical concentrations in an urban river system," *Water Res.*, vol. 137, pp. 72–85, Jun. 2018, doi: 10.1016/j.watres.2018.02.066.

[179] E. T. Furlong, M. C. Noriega, C. J. Kanagy, L. K. Kanagy, L. J. Coffey, and M. R. Burkhardt, *Determination of Human-Use Pharmaceuticals in Filtered Water by Direct Aqueous Injection–High-Performance Liquid Chromatography/Tandem Mass SpectrometryTechniques and Methods*, vol. Book 5, Laboratory Analysis. 2014.

[180] L. J. G. Silva, L. M. Meisel, C. M. Lino, and A. Pena, "Profiling Serotonin Reuptake Inhibitors (SSRIs) in the Environment: Trends in Analytical Methodologies," *Crit. Rev. Anal. Chem.*, vol. 44, no. 1, Art. no. 1, Jan. 2014, doi: 10.1080/10408347.2013.827966.

[181] E. M. Melchor-Martínez *et al.*, "Antidepressants surveillance in wastewater: Overview extraction and detection," *Case Stud. Chem. Environ. Eng.*, vol. 3, p. 100074, Jun. 2021, doi: 10.1016/j.cscee.2020.100074.

[182] L. J. G. Silva, C. M. Lino, L. M. Meisel, and A. Pena, "Selective serotonin re-uptake inhibitors (SSRIs) in the aquatic environment: An ecopharmacovigilance approach," *Sci. Total Environ.*, vol. 437, pp. 185–195, Oct. 2012, doi: 10.1016/j.scitotenv.2012.08.021.

[183] S. Yuan, X. Jiang, X. Xia, H. Zhang, and S. Zheng, "Detection, occurrence and fate of 22 psychiatric pharmaceuticals in psychiatric hospital and municipal wastewater treatment plants in Beijing, China," *Chemosphere*, vol. 90, no. 10, Art. no. 10, Mar. 2013, doi: 10.1016/j.chemosphere.2012.10.089.

[184] T. Kosjek and E. Heath, "Tools for evaluating selective serotonin re-uptake inhibitor residues as environmental contaminants," *TrAC Trends Anal. Chem.*, vol. 29, no. 8, pp. 832–847, Sep. 2010, doi: 10.1016/j.trac.2010.04.012.

[185] J. T. Althakafy, C. Kulsing, M. R. Grace, and P. J. Marriott, "Liquid chromatography – quadrupole Orbitrap mass spectrometry method for selected pharmaceuticals in water samples," *J. Chromatogr. A*, vol. 1515, pp. 164–171, Sep. 2017, doi: 10.1016/j.chroma.2017.08.003.

[186] P. Gago-Ferrero, A. Krettek, S. Fischer, K. Wiberg, and L. Ahrens, "Suspect Screening and Regulatory Databases: A Powerful Combination To Identify

Emerging Micropollutants," *Environ. Sci. Technol.*, vol. 52, no. 12, Art. no. 12, Jun. 2018, doi: 10.1021/acs.est.7b06598.

[187] O. Golovko, A.-L. Rehrl, S. Köhler, and L. Ahrens, "Organic micropollutants in water and sediment from Lake Mälaren, Sweden," *Chemosphere*, vol. 258, p. 127293, Nov. 2020, doi: 10.1016/j.chemosphere.2020.127293.

[188] A. D. McEachran *et al.*, "Comparison of emerging contaminants in receiving waters downstream of a conventional wastewater treatment plant and a forest-water reuse system," *Environ. Sci. Pollut. Res.*, vol. 25, no. 13, Art. no. 13, May 2018, doi: 10.1007/s11356-018-1505-5.

[189] J. Pablo Lamas, C. Salgado-Petinal, C. García-Jares, M. Llompart, R. Cela, and M. Gómez, "Solid-phase microextraction–gas chromatography–mass spectrometry for the analysis of selective serotonin reuptake inhibitors in environmental water," *J. Chromatogr. A*, vol. 1046, no. 1–2, pp. 241–247, Aug. 2004, doi: 10.1016/j.chroma.2004.06.099.

[190] M. Behpour, S. Nojavan, S. Asadi, and A. Shokri, "Combination of gel-electromembrane extraction with switchable hydrophilicity solvent-based homogeneous liquid-liquid microextraction followed by gas chromatography for the extraction and determination of antidepressants in human serum, breast milk and wastewater," *J. Chromatogr. A*, vol. 1621, p. 461041, Jun. 2020, doi: 10.1016/j.chroma.2020.461041.

[191] K. Demeestere, M. Petrović, M. Gros, J. Dewulf, H. Van Langenhove, and D. Barceló, "Trace analysis of antidepressants in environmental waters by molecularly imprinted polymer-based solid-phase extraction followed by ultra-performance liquid chromatography coupled to triple quadrupole mass spectrometry," *Anal. Bioanal. Chem.*, vol. 396, no. 2, Art. no. 2, Jan. 2010, doi: 10.1007/s00216-009-3270-2.

[192] S. Chu and C. D. Metcalfe, "Analysis of paroxetine, fluoxetine and norfluoxetine in fish tissues using pressurized liquid extraction, mixed mode solid phase extraction cleanup and liquid chromatography–tandem mass spectrometry," *J. Chromatogr. A*, vol. 1163, no. 1–2, Art. no. 1–2, Sep. 2007, doi: 10.1016/j.chroma.2007.06.014.

[193] J.-W. Kwon and K. L. Armbrust, "Laboratory persistence and fate of fluoxetine in aquatic environments," *Environ. Toxicol. Chem.*, vol. 25, no. 10, Art. no. 10, 2006.

[194] H. Runnqvist, S. A. Bak, M. Hansen, B. Styrishave, B. Halling-Sørensen, and E. Björklund, "Determination of pharmaceuticals in environmental and biological matrices using pressurised liquid extraction—Are we developing sound extraction methods?," *J. Chromatogr. A*, vol. 1217, no. 16, pp. 2447–2470, Apr. 2010, doi: 10.1016/j.chroma.2010.02.046.

[195] C. Wu, J. D. Witter, A. L. Spongberg, and K. P. Czajkowski, "Occurrence of selected pharmaceuticals in an agricultural landscape, western Lake Erie basin," *Water Res.*, vol. 43, no. 14, Art. no. 14, Aug. 2009, doi: 10.1016/j.watres.2009.05.014.

[196] J. Giebułtowicz and G. Nałęcz-Jawecki, "Occurrence of antidepressant residues in the sewage-impacted Vistula and Utrata rivers and in tap water in Warsaw (Poland)," *Ecotoxicol. Environ. Saf.*, vol. 104, pp. 103–109, Jun. 2014, doi: 10.1016/j.ecoenv.2014.02.020.

[197] O. Golovko, V. Kumar, G. Fedorova, T. Randak, and R. Grabic, "Seasonal changes in antibiotics, antidepressants/psychiatric drugs, antihistamines and lipid regulators in a wastewater treatment plant," *Chemosphere*, vol. 111, pp. 418–426, Sep. 2014, doi: 10.1016/j.chemosphere.2014.03.132.

[198] M. Krauss, H. Singer, and J. Hollender, "LC–high resolution MS in environmental analysis: from target screening to the identification of unknowns," *Anal. Bioanal. Chem.*, vol. 397, no. 3, Art. no. 3, Jun. 2010, doi: 10.1007/s00216-010-3608-9.

[199] K. Mee Kim, B. Hwa Jung, M. Ho Choi, J. Soo Woo, K.-J. Paeng, and B. Chul Chung, "Rapid and sensitive determination of sertraline in human plasma using gas chromatography–mass spectrometry," *J. Chromatogr. B*, vol. 769, no. 2, pp. 333–339, Apr. 2002, doi: 10.1016/S1570-0232(02)00027-2.

[200] P. Arnnok, R. R. Singh, R. Burakham, A. Pérez-Fuentetaja, and D. S. Aga, "Selective Uptake and Bioaccumulation of Antidepressants in Fish from Effluent-Impacted Niagara River," *Environ. Sci. Technol.*, vol. 51, no. 18, Art. no. 18, Sep. 2017, doi: 10.1021/acs.est.7b02912.

[201] A. L. Batt, M. S. Kostich, and J. M. Lazorchak, "Analysis of Ecologically Relevant Pharmaceuticals in Wastewater and Surface Water Using Selective Solid-Phase Extraction and UPLC−MS/MS," *Anal. Chem.*, vol. 80, no. 13, Art. no. 13, Jul. 2008, doi: 10.1021/ac800066n.

[202] Y. Choi, J.-H. Lee, K. Kim, H. Mun, N. Park, and J. Jeon, "Identification, quantification, and prioritization of new emerging pollutants in domestic and industrial effluents, Korea: Application of LC-HRMS based suspect and non-target screening," *J. Hazard. Mater.*, vol. 402, p. 123706, Jan. 2021, doi: 10.1016/j.jhazmat.2020.123706.

[203] I. González-Mariño *et al.*, "Multi-residue determination of psychoactive pharmaceuticals, illicit drugs and related metabolites in wastewater by ultra-high performance liquid chromatography-tandem mass spectrometry," *J. Chromatogr. A*, vol. 1569, pp. 91–100, Sep. 2018, doi: 10.1016/j.chroma.2018.07.045.

[204] A. Lajeunesse, C. Gagnon, and S. Sauvé, "Determination of Basic Antidepressants and Their *N*-Desmethyl Metabolites in Raw Sewage and Wastewater Using Solid-Phase Extraction and Liquid Chromatography−Tandem Mass Spectrometry," *Anal. Chem.*, vol. 80, no. 14, Art. no. 14, Jul. 2008, doi: 10.1021/ac800162q.

[205] K. H. Langford and K. V. Thomas, "Determination of pharmaceutical compounds in hospital effluents and their contribution to wastewater treatment works," *Environ. Int.*, vol. 35, no. 5, Art. no. 5, Jul. 2009, doi: 10.1016/j.envint.2009.02.007.

[206] A. J. Ramirez, M. A. Mottaleb, B. W. Brooks, and C. K. Chambliss, "Analysis of Pharmaceuticals in Fish Using Liquid Chromatography-Tandem Mass Spectrometry," *Anal. Chem.*, vol. 79, no. 8, Art. no. 8, Apr. 2007, doi: 10.1021/ac062215i.

[207] M. M. Schultz and E. T. Furlong, "Trace Analysis of Antidepressant Pharmaceuticals and Their Select Degradates in Aquatic Matrixes by LC/ESI/MS/MS," *Anal. Chem.*, vol. 80, no. 5, Art. no. 5, Mar. 2008, doi: 10.1021/ac702154e.

[208] A. Macherone, "The Future of GC/Q-TOF in Environmental Analysis," in *Comprehensive Analytical Chemistry*, vol. 61, Elsevier, 2013, pp. 471–490. doi: 10.1016/B978-0-444-62623-3.00020-4.

[209] E. L. Schymanski *et al.*, "Identifying Small Molecules via High Resolution Mass Spectrometry: Communicating Confidence," *Environ. Sci. Technol.*, vol. 48, no. 4, Art. no. 4, Feb. 2014, doi: 10.1021/es5002105.

[210] B. J. Vanderford, R. A. Pearson, D. J. Rexing, and S. A. Snyder, "Analysis of Endocrine Disruptors, Pharmaceuticals, and Personal Care Products in Water Using Liquid Chromatography/Tandem Mass Spectrometry," *Anal. Chem.*, vol. 75, no. 22, pp. 6265–6274, Nov. 2003, doi: 10.1021/ac034210g.

[211] F. Hernández, J. V. Sancho, M. Ibáñez, E. Abad, T. Portolés, and L. Mattioli, "Current use of high-resolution mass spectrometry in the environmental sciences," *Anal. Bioanal. Chem.*, vol. 403, no. 5, Art. no. 5, May 2012, doi: 10.1007/s00216-012-5844-7.

[212] C. Baduel, J. F. Mueller, H. Tsai, and M. J. Gomez Ramos, "Development of sample extraction and clean-up strategies for target and non-target analysis of environmental contaminants in biological matrices," *J. Chromatogr. A*, vol. 1426, pp. 33–47, Dec. 2015, doi: 10.1016/j.chroma.2015.11.040.

[213] P. Gago-Ferrero *et al.*, "Wide-scope target screening of >2000 emerging contaminants in wastewater samples with UPLC-Q-ToF-HRMS/MS and smart evaluation of its performance through the validation of 195 selected representative analytes," *J. Hazard. Mater.*, vol. 387, p. 121712, Apr. 2020, doi: 10.1016/j.jhazmat.2019.121712.

[214] M. Petrovic and D. Barcelo, "LC-MS for identifying photodegradation products of pharmaceuticals in the environment," *TrAC Trends Anal. Chem.*, vol. 26, no. 6, pp. 486–493, Jun. 2007, doi: 10.1016/j.trac.2007.02.010.

[215] C. Veenaas and P. Haglund, "Methodology for non-target screening of sewage sludge using comprehensive two-dimensional gas chromatography coupled to high-resolution mass spectrometry," *Anal. Bioanal. Chem.*, vol. 409, no. 20, pp. 4867–4883, Aug. 2017, doi: 10.1007/s00216-017-0429-0.

[216] L. Malm, E. Palm, A. Souihi, M. Plassmann, J. Liigand, and A. Kruve, "Guide to Semi-Quantitative Non-Targeted Screening Using LC/ESI/HRMS," *Molecules*, vol. 26, no. 12, p. 3524, Jun. 2021, doi: 10.3390/molecules26123524.

[217] JCGM: BIPM, IEC, IFCC, ILAC, ISO, IUPAC, IUPAP and OIML, "International vocabulary of metrology – Basic and general concepts and associated terms (VIM)," Geneva, Switzerland, 2008. Accessed: May 11, 2016. [Online]. Available: http://digilib.uin-suka.ac.id/10881/

[218] S. Tavazzi *et al.*, *Water framework directive watch list method analytical method for determination of compounds selected for the first surface water watch list.* Luxembourg: Publications Office, 2016. Accessed: Aug. 22, 2016. [Online]. Available: http://bookshop.europa.eu/uri?target=EUB:NOTICE:LBNA27813:EN:HTML

[219] I. Taverniers, M. De Loose, and E. Van Bockstaele, "Trends in quality in the analytical laboratory. II. Analytical method validation and quality assurance,"

TrAC Trends Anal. Chem., vol. 23, no. 8, Art. no. 8, Sep. 2004, doi: 10.1016/j.trac.2004.04.001.

[220] A. M. Almeida, M. M. Castel-Branco, and A. C. Falcão, "Linear regression for calibration lines revisited: weighting schemes for bioanalytical methods," *J. Chromatogr. B*, vol. 774, no. 2, Art. no. 2, Jul. 2002, doi: 10.1016/S1570-0232(02)00244-1.

[221] ICH Expert Working Group, "Validation of analytical procedures: text and methodology," *Q2 R1*, vol. 1, 2005, Accessed: Jan. 08, 2016. [Online]. Available: http://somatek.com/content/uploads/2014/06/sk140605h.pdf

[222] B. Mattiasson and L. Ye, *Molecularly Imprinted Polymers in Biotechnology*, vol. 150. Cham: Springer International Publishing, 2015. doi: 10.1007/978-3-319-20729-2.

[223] M. Yan and O. Ramström, Eds., *Molecularly imprinted materials: science and technology*. New York: Marcel Dekker, 2005.

[224] Y. C. Lu *et al.*, "A novel strategy for selective removal and rapid collection of triclosan from aquatic environment using magnetic molecularly imprinted nano−polymers," *Chemosphere*, vol. 238, p. 124640, Jan. 2020, doi: 10.1016/j.chemosphere.2019.124640.

[225] J. O. Mahony, K. Nolan, M. R. Smyth, and B. Mizaikoff, "Molecularly imprinted polymers—potential and challenges in analytical chemistry," *Anal. Chim. Acta*, vol. 534, no. 1, pp. 31–39, Apr. 2005, doi: 10.1016/j.aca.2004.07.043.

[226] M. Komiyama, Ed., *Molecular imprinting: from fundamentals to applications*. Weinheim: Wiley-VCH, 2003.

[227] H. Yan and K. H. Row, "Characteristic and synthetic approach of molecularly imprinted polymer," *Int. J. Mol. Sci.*, vol. 7, no. 5, pp. 155–178, 2006.

[228] P. A. G. Cormack and A. Z. Elorza, "Molecularly imprinted polymers: synthesis and characterisation," *J. Chromatogr. B*, vol. 804, no. 1, pp. 173–182, May 2004, doi: 10.1016/j.jchromb.2004.02.013.

[229] F. Horemans, A. Weustenraed, D. Spivak, and T. J. Cleij, "Towards water compatible MIPs for sensing in aqueous media: TOWARDS WATER COMPATIBLE MIPS FOR SENSING IN AQUEOUS MEDIA," *J. Mol. Recognit.*, vol. 25, no. 6, pp. 344–351, Jun. 2012, doi: 10.1002/jmr.2191.

[230] G. Vasapollo *et al.*, "Molecularly Imprinted Polymers: Present and Future Prospective," *Int. J. Mol. Sci.*, vol. 12, no. 12, pp. 5908–5945, Sep. 2011, doi: 10.3390/ijms12095908.

[231] Bo Mattiasson and Lei Ye, "Molecularly Imprinted Polymers in Biotechnology - Google Books," *Adv Biochem EnginBiothechnol*, vol. 2015, pp. 54–68.

[232] A. Kloskowski, M. Pilarczyk, A. Przyjazny, and J. Namieśnik, "Progress in Development of Molecularly Imprinted Polymers as Sorbents for Sample Preparation," *Crit. Rev. Anal. Chem.*, vol. 39, no. 1, pp. 43–58, Feb. 2009, doi: 10.1080/10408340802570223.

[233] D. Spivak, "Optimization, evaluation, and characterization of molecularly imprinted polymers," *Adv. Drug Deliv. Rev.*, vol. 57, no. 12, pp. 1779–1794, Dec. 2005, doi: 10.1016/j.addr.2005.07.012.

[234] B. Dirion, Z. Cobb, E. Schillinger, L. I. Andersson, and B. Sellergren, "Water-Compatible Molecularly Imprinted Polymers Obtained via High-Throughput Synthesis and Experimental Design," *J. Am. Chem. Soc.*, vol. 125, no. 49, pp. 15101–15109, Dec. 2003, doi: 10.1021/ja0355473.

[235] Z. Dorkó, A. Szakolczai, T. Verbić, and G. Horvai, "Binding capacity of molecularly imprinted polymers and their nonimprinted analogs: Sample Preparation," *J. Sep. Sci.*, vol. 38, no. 24, pp. 4240–4247, Dec. 2015, doi: 10.1002/jssc.201500874.

[236] F. Chapuis, J.-U. Mullot, V. Pichon, G. Tuffal, and M.-C. Hennion, "Molecularly imprinted polymers for the clean-up of a basic drug from environmental and biological samples," *J. Chromatogr. A*, vol. 1135, no. 2, pp. 127–134, Dec. 2006, doi: 10.1016/j.chroma.2006.09.076.

[237] H. Kempe, A. Parareda Pujolràs, and M. Kempe, "Molecularly Imprinted Polymer Nanocarriers for Sustained Release of Erythromycin," *Pharm. Res.*, vol. 32, no. 2, Art. no. 2, Feb. 2015, doi: 10.1007/s11095-014-1468-2.

[238] M. Cantarella *et al.*, "Molecularly imprinted polymer for selective adsorption of diclofenac from contaminated water," *Chem. Eng. J.*, vol. 367, pp. 180–188, Jul. 2019, doi: 10.1016/j.cej.2019.02.146.

[239] M. C. Blanco-López, M. J. Lobo-Castañón, A. J. Miranda-Ordieres, and P. Tuñón-Blanco, "Electrochemical sensors based on molecularly imprinted polymers," *TrAC Trends Anal. Chem.*, vol. 23, no. 1, pp. 36–48, Jan. 2004, doi: 10.1016/S0165-9936(04)00102-5.

[240] Z. Cobb, B. Sellergren, and L. I. Andersson, "Water-compatible molecularly imprinted polymers for efficient direct injection on-line solid-phase extraction of ropivacaine and bupivacaine from human plasma," *The Analyst*, vol. 132, no. 12, p. 1262, 2007, doi: 10.1039/b711116a.

[241] R. Gutiérrez-Climente, A. Gómez-Caballero, M. Halhalli, B. Sellergren, M. A. Goicolea, and R. J. Barrio, "Iniferter-mediated grafting of molecularly imprinted polymers on porous silica beads for the enantiomeric resolution of drugs: INIFERTER-MEDIATED GRAFTING OF MIP ON POROUS SILICA BEADS," *J. Mol. Recognit.*, vol. 29, no. 3, pp. 106–114, Mar. 2016, doi: 10.1002/jmr.2443.

[242] K. Haupt, "Peer reviewed: molecularly imprinted polymers: the next generation," *Anal. Chem.*, vol. 75, no. 17, pp. 376-A, 2003.

[243] M. Le Noir, A.-S. Lepeuple, B. Guieysse, and B. Mattiasson, "Selective removal of 17β-estradiol at trace concentration using a molecularly imprinted polymer," *Water Res.*, vol. 41, no. 12, pp. 2825–2831, Jun. 2007, doi: 10.1016/j.watres.2007.03.023.

[244] R. Ansell, "Molecularly imprinted polymers for the enantioseparation of chiral drugs," *Adv. Drug Deliv. Rev.*, vol. 57, no. 12, pp. 1809–1835, Dec. 2005, doi: 10.1016/j.addr.2005.07.014.

[245] W.-C. Lee, C.-H. Cheng, H.-H. Pan, T.-H. Chung, and C.-C. Hwang, "Chromatographic characterization of molecularly imprinted polymers," *Anal. Bioanal. Chem.*, vol. 390, no. 4, pp. 1101–1109, Feb. 2008, doi: 10.1007/s00216-007-1765-2.

[246] V. Pichon and F. Chapuis-Hugon, "Role of molecularly imprinted polymers for selective determination of environmental pollutants—A review," *Anal. Chim. Acta*, vol. 622, no. 1–2, pp. 48–61, Aug. 2008, doi: 10.1016/j.aca.2008.05.057.

[247] S. A. Piletsky, S. Subrahmanyam, and A. P. Turner, "Application of molecularly imprinted polymers in sensors for the environment and biotechnology," *Sens. Rev.*, vol. 21, no. 4, pp. 292–296, 2001.

[248] AFFINISEP, "AFFINIMIP," 2020. https://www.affinisep.com/spe-kits-applications/spe-kit-for-sample-preparation/affinimip-spe-selectives-mip-spe-cartridges/ (accessed Aug. 03, 2020).

[249] Supelco, "SupelMIP® SPE," *Sigma-Aldrich*, 2020. https://www.sigmaaldrich.com/analytical-chromatography/sample-preparation/spe/supelmip.html (accessed Aug. 03, 2020).

[250] A. Azizi and C. S. Bottaro, "A critical review of molecularly imprinted polymers for the analysis of organic pollutants in environmental water samples," *J. Chromatogr. A*, vol. 1614, p. 460603, Mar. 2020, doi: 10.1016/j.chroma.2019.460603.

[251] K. A. Sarpong, W. Xu, W. Huang, and W. Yang, "The Development of Molecularly Imprinted Polymers in the Clean-Up of Water Pollutants: A Review," *Am. J. Anal. Chem.*, vol. 10, no. 05, Art. no. 05, 2019, doi: 10.4236/ajac.2019.105017.

[252] M. Le Noir, F. M. Plieva, and B. Mattiasson, "Removal of endocrine-disrupting compounds from water using macroporous molecularly imprinted cryogels in a moving-bed reactor," *J. Sep. Sci.*, vol. 32, no. 9, pp. 1471–1479, May 2009, doi: 10.1002/jssc.200800670.

[253] K. K. M. S. da Silva, V. B. Boralli, C. Wisniewski, and E. C. Figueiredo, "On-Line Restricted Access Molecularly Imprinted Solid-Phase Extraction of Selective Serotonin Reuptake Inhibitors Directly from Untreated Human Plasma Samples Followed by HPLC-UV Analysis," *J. Anal. Toxicol.*, vol. 40, no. 2, pp. 108–116, Mar. 2016, doi: 10.1093/jat/bkv121.

[254] T. Alizadeh and S. Azizi, "Graphene/graphite paste electrode incorporated with molecularly imprinted polymer nanoparticles as a novel sensor for differential pulse voltammetry determination of fluoxetine," *Biosens. Bioelectron.*, vol. 81, pp. 198–206, Jul. 2016, doi: 10.1016/j.bios.2016.02.052.

[255] A. Barati, E. Kazemi, S. Dadfarnia, and A. M. Haji Shabani, "Synthesis/characterization of molecular imprinted polymer based on magnetic chitosan/graphene oxide for selective separation/preconcentration of fluoxetine from environmental and biological samples," *J. Ind. Eng. Chem.*, vol. 46, pp. 212–221, Feb. 2017, doi: 10.1016/j.jiec.2016.10.033.

[256] A. Nezhadali, Z. Es'haghi, and A. Khatibi, "Selective extraction of progesterone hormones from environmental and biological samples using a polypyrrole molecularly imprinted polymer and determination by gas chromatography," *Anal Methods*, vol. 8, no. 8, pp. 1813–1827, 2016, doi: 10.1039/C5AY02174J.

[257] A. D. Hudson *et al.*, "Synthesis of Optimized Molecularly Imprinted Polymers for the Isolation and Detection of Antidepressants via HPLC," *Biomimetics*, vol. 4, no. 1, p. 18, Feb. 2019, doi: 10.3390/biomimetics4010018.

[258] S. S. M. Hassan, A. H. Kamel, A. E.-G. E. Amr, H. M. Hashem, and E. M. A. Bary, "Imprinted Polymeric Beads-Based Screen-Printed Potentiometric Platforms Modified with Multi-Walled Carbon Nanotubes (MWCNTs) for Selective Recognition of Fluoxetine," *Nanomaterials*, vol. 10, no. 3, p. 572, Mar. 2020, doi: 10.3390/nano10030572.

[259] M. Abdouss, E. Asadi, S. Azodi-Deilami, N. Beik-mohammadi, and S. A. Aslanzadeh, "Development and characterization of molecularly imprinted polymers for controlled release of citalopram," *J. Mater. Sci. Mater. Med.*, vol. 22, no. 10, Art. no. 10, Oct. 2011, doi: 10.1007/s10856-011-4395-3.

[260] M. Abdouss, S. Azodi-Deilami, E. Asadi, and Z. Shariatinia, "Synthesis of molecularly imprinted polymer as a sorbent for solid phase extraction of citalopram from human serum and urine," *J. Mater. Sci. Mater. Med.*, vol. 23, no. 6, pp. 1543–1552, Jun. 2012, doi: 10.1007/s10856-012-4623-5.

[261] A. Gomez-Caballero, A. Guerreiro, K. Karim, S. Piletsky, M. A. Goicolea, and R. J. Barrio, "Chiral imprinted polymers as enantiospecific coatings of stir bar sorptive extraction devices," *Biosens. Bioelectron.*, vol. 28, no. 1, pp. 25–32, Oct. 2011, doi: 10.1016/j.bios.2011.06.048.

[262] N. Unceta *et al.*, "Enantioselective extraction of (+)-(S)-citalopram and its main metabolites using a tailor-made stir bar chiral imprinted polymer for their LC-ESI-MS/MS quantitation in urine samples," *Talanta*, vol. 116, pp. 448–453, Nov. 2013, doi: 10.1016/j.talanta.2013.07.004.

[263] R. Gutiérrez-Climente, A. Gómez-Caballero, N. Unceta, M. Aránzazu Goicolea, and R. J. Barrio, "A new potentiometric sensor based on chiral imprinted nanoparticles for the discrimination of the enantiomers of the antidepressant citalopram," *Electrochimica Acta*, vol. 196, pp. 496–504, Apr. 2016, doi: 10.1016/j.electacta.2016.03.010.

[264] R. Gutierrez-Climente *et al.*, "Molecularly imprinted nanoparticles grafted to porous silica as chiral selectors in liquid chromatography," *J. Chromatogr. A*, vol. 1508, pp. 53–64, Jul. 2017, doi: 10.1016/j.chroma.2017.05.066.

[265] M. Arvand and M. Hashemi, "Synthesis by precipitation polymerization of a molecularly imprinted polymer membrane for the potentiometric determination of sertraline in tablets and biological fluids," *J. Braz. Chem. Soc.*, vol. 23, no. 3, pp. 392–402, 2012.

[266] F. Khalilian and F. K. Kermani, "Selective Dispersive Solid Phase Extraction of Sertraline Using Surface Molecularly Imprinted Polymer Grafted on SiO2/Graphene Oxide," *J. Chem. Health Risks*, vol. 7, no. 1, 2017, Accessed: Oct. 05, 2017. [Online]. Available: http://www.jchr.org/index.php/JCHR/article/view/724

[267] R. Khosrokhavar, A. Motaharian, M. R. Milani Hosseini, and S. Mohammadsadegh, "Screen-printed carbon electrode (SPCE) modified by molecularly imprinted polymer (MIP) nanoparticles and graphene nanosheets for determination of sertraline antidepressant drug," *Microchem. J.*, vol. 159, p. 105348, Dec. 2020, doi: 10.1016/j.microc.2020.105348.

[268] Z. M. Torbati, A. Nezhadali, and M. Mojarrab, "Synthesis of molecularly imprinted polypyrrole for extraction and determination of fluvoxamine in serum sample using multivariable optimization methods," p. 6, 2017.

[269] M. Soleimani, A. P. Daryasari, and P. Joshani, "Molecularly Imprinted Polymer Nanoparticles for Selective Solid Phase Extraction of Fluvoxamine in Human Urine and Plasma," *J. Chromatogr. Sci.*, vol. 58, no. 3, pp. 274–279, Apr. 2020, doi: 10.1093/chromsci/bmz092.

[270] X. Tong *et al.*, "Source, fate, transport and modelling of selected emerging contaminants in the aquatic environment: Current status and future perspectives," *Water Res.*, vol. 217, p. 118418, Jun. 2022, doi: 10.1016/j.watres.2022.118418.

Bibliography

Publications Related to the Thesis

Journal Articles

Gornik, T., Carena, L., Kosjek, T., & Vione, D. (2021). Phototransformation study of the antidepressant paroxetine in surface waters. Science of The Total Environment, 774, 145380. https://doi.org/10.1016/j.scitotenv.2021.145380

Gornik, T., Kovacic, A., Heath, E., Hollender, J., & Kosjek, T. (2020). Biotransformation study of antidepressant sertraline and its removal during biological wastewater treatment. Water Research, 181, 115864. https://doi.org/10.1016/j.watres.2020.115864

Gornik, T., Shinde, S., Lamovsek, L., Koblar, M., Heath, E., Sellergren, B., & Kosjek, T. (2020). Molecularly Imprinted Polymers for the Removal of Antidepressants from Contaminated Wastewater. Polymers, 13(1), 120. https://doi.org/10.3390/polym13010120

Gornik, T., Vozic, A., Heath, E., Trontelj, J., Roskar, R., Zigon, D., Vione, D., & Kosjek, T. (2020). Determination and photodegradation of sertraline residues in aqueous environment. Environmental Pollution, 256, 113431. https://doi.org/10.1016/j.envpol.2019.113431

Koler, A., Gornik, T., Kosjek, T., Jeřabek, K., & Krajnc, P. (2018). Preparation of molecularly imprinted copoly(acrylic acid-divinylbenzene) for extraction of environmentally relevant sertraline residues. Reactive and Functional Polymers, 131, 378–383. https://doi.org/10.1016/j.reactfunctpolym.2018.08.016

Conference Papers

Kosjek, T., Gornik, T., Trontelj, J., Roškar, R. (2019) What happens to sertraline when it leaves the human body?. In Proceedings: *Researchers day (Dan za raziskovalce)*, Ljubljana, Slovenia

Gornik, T., Shinde, S., Kosjek, T., Heat E., Sellergren, B. (2019) Application of molecularly imprinted polymers imprinted with sertraline in wastewater treatment and reuse. In Book of Abstracts: *Graduate Student Symposium on Molecular Imprinting 2019*, Berlin, Germany

Gornik, T., Shinde, S., Kosjek, T., Heat E., Sellergren, B. (2018). Molecularly imprinted polymer based solid phase extraction of sertraline and its transformation products. In Proceedings book: *3rd Caparica Christmas Conference on Sample Treatment*, Caparica, Portugal: Bioscope group.

Koler, A., Jeřábek, K., Gornik, T., Kosjek, T., Krajnc, P. (2018) Extraction of sertraline by molecularly imprinted porous copoly(acrylic acid-divinylbenzene) prepared by

two-stage polymerisation. In Abstract booklet: *Biomimetic polymers by rational design, imprinting and conjugation*, Como, Italy: EUPOC.

Gornik, T., Shinde, S., Kosjek, T., Heat E., Sellergren, B. (2018) Synthesis and evaluation of molecularly imprinted polymers for the detection and removal of sertraline in aqueous matrices. In Proceedings: *MASSTWIN Workshop on Mass spectrometry in support of the environment, food, and health interaction and disease*, Antwerp, Belgium

Gornik, T., Shinde, S., Kosjek, T., Heat E., Sellergren, B. (2018) Molecularly imprinted polymers as solid phase extraction sorbents for the determination of sertraline and its analogues in aqueous matrices. In Proceedings: Dežman, Miha (ed.), et al., *10th Jožef Stefan International Postgraduate School Students' Conference and 12th Young Researchers' Day*, Piran, Slovenia. Ljubljana.

Koler, A., Gornik, T., Kosjek, T., Krajnc, P. (2017) Sertraline imprinted porous poly(acrylic acid-co-divinylbenzene). In Abstracts accepted for presentation: *Danube Vltava Sava Polymer Meeting*, Vienna, Austria.

Gornik, T., Krajnc, A., Brcar, T., Heath, E., Trontelj, J., Roškar, R., Kosjek, T. (2017) Simulating environmental photodegradation of sertraline in aqueous environment. In Proceedings: Pavlin, Majda (ed.), et al., *9th Jožef Stefan International Postgraduate School Students' Conference and 11th Young researchers' Day*, Ljubljana, Slovenija.

Gornik, T., Krajnc, A., Brcar, T., Heath, E., Trontelj, J., Roškar, R., Kosjek, T. (2016) Simulation of environmental photodegradation of sertraline. In Proceedings: Zupančič Justin, Maja (ed.). *Pharmacologically active substances in wastewater: optimisation of analytical methods and removal processes, Closure Conference of the Project LIFE PharmDegrade*, Ljubljana, Slovenia.

Koler, A., Kosjek, T., Jeřábek, K., Gornik, T., Krajnc, P. (2016) Molecular Imprinted Poly(Acrylic Acid) For Removal Of Sertraline. In Proceedings: Mlakar, Damir (ed.). *1st AARC PhD Students Conference on Environment and Sustainable Energy*, Maribor, Slovenia.

Gornik, T., Krajnc, A., Koler, A., Turnšek, M., Heath, E., Iskra, J., Krajnc, P., Jeřábek, K., Kosjek, T. (2016) Implementing molecularly imprinted polymer (MIP) in the analytical method for determining sertraline residues in aqueous environment. In Proceedings: Pavlin, Majda (ed.). *8th Jožef Stefan International Postgraduate School Students' Conference*, Ljubljana, Slovenia.

Other Publications

Kosjek, T., Krajnc, A., Gornik, T., Zigon, D., Groselj, A., Sersa, G., & Cemazar, M. (2016). Identification and quantification of bleomycin in serum and tumor tissue by liquid chromatography coupled to high resolution mass spectrometry. Talanta, 160, 164–171. https://doi.org/10.1016/j.talanta.2016.06.062

Kovačič, A., Gys, C., Gulin, M. R., Gornik, T., Kosjek, T., Heath, D., Covaci, A., & Heath, E. (2021). Kinetics and biotransformation products of bisphenol F and S during aerobic degradation with activated sludge. Journal of Hazardous Materials, 404, 124079. https://doi.org/10.1016/j.jhazmat.2020.124079

Biography

Education and research activities:

- 2020 – Present: Lek d.d., Ljubljana: Scientist
- 2018 – 2020: Jožef Stefan Institute, Ljubljana: assistant
- 2015 – 2020: Jožef Stefan International Postgraduate School, Ljubljana: PhD student of Ecotechnology
- 2009 – 2015: University of Ljubljana, Faculty of Pharmacy, Ljubljana: master student
- 2014 – 2015: National Institute of Chemistry, Ljubljana: student laboratory assistant at the Analytical Chemistry Laboratory
- 2012 – 2014: University of Ljubljana, Faculty of Pharmacy, Ljubljana, Slovenia: student researcher at the Department of Pharmaceutical Chemistry

Foreign work and study experience:

- 2019: Dipartimento di Chimica, Universitá di Torino, Torino, Italy; bilateral agreement
- 2017: Malmö University, Malmö, Sweden; COST STSM and Erasmus Plus Internship
- 2014 – 2015: Complutense University of Madrid, Madrid, Spain; Erasmus Plus Internship

Awards:

- 2018: Excellent poster presentation award at the 3rd International Caparica Christmas Conference on Sample Treatment
- 2018: One of the best overall contributions awarded by the commission at the 10th Jožef Stefan International Postgraduate School Students' Conference and 12th Young researchers' Day
- 2016: Best paper award according to the votes from active participants at the 8th Jožef Stefan International Postgraduate School Students' Conference

Fellowships and scholarships:

- 2017: COST NEREUS ES1403: Short-Term Scientific Mission
- 2014, 2017: Erasmus Plus Internship scholarship
- 2005 – 2015: Zois scholarship

Research projects:

- P1-0143 (Program Group): Cycling of nutrients and contaminants in the environment, mass balances and modelling of environmental processes, and risk analysis
- J1-6744: Development of molecularly imprinted polymers and their application in environmental and bio-analysis

- BI-IT-18-20-005, bilateral agreement: Photochemical fate and treatment of pharmaceutical contaminants in drinking water